# CORROSION EVALUATION OF NOVEL COATINGS FOR STEEL COMPONENTS OF HIGHWAY BRIDGES

FINAL REPORT
Project BDV29 977-02
(800002608)

Submitted To:

FDOT Research Center
605 Suwannee Street
Tallahassee, FL 32399

Project Manager:
Dale DeFord, Ph.D.
Florida Department of Transportation, State Materials Office
5007 NE 39th Avenue
Gainesville, FL 32609

Submitted By:

Kingsley Lau
Florida International University
10555 W. Flagler Street
Miami, FL 33174

March 2015

Prepared by:
Md Ahsan Sabbir
Saiada Fuadi Fancy

and Kingsley Lau

DISCLAIMER

The opinions, findings, and conclusions expressed in this publication are those of the authors and not necessarily those of the State of Florida Department of Transportation

## APPROXIMATE CONVERSIONS TO SI UNITS

| SYMBOL | WHEN YOU KNOW | MULTIPLY BY | TO FIND | SYMBOL |
|---|---|---|---|---|
| | | **LENGTH** | | |
| **in** | inches | 25.4 | millimeters | mm |
| **mils** | mils | 25.4 | micrometers | µm |
| **ft** | feet | 0.305 | meters | m |
| **yd** | yards | 0.914 | meters | m |
| **mi** | miles | 1.61 | kilometers | km |

| SYMBOL | WHEN YOU KNOW | MULTIPLY BY | TO FIND | SYMBOL |
|---|---|---|---|---|
| | | **AREA** | | |
| **$in^2$** | squareinches | 645.2 | square millimeters | $mm^2$ |
| **$ft^2$** | squarefeet | 0.093 | square meters | $m^2$ |
| **$yd^2$** | square yard | 0.836 | square meters | $m^2$ |
| **ac** | acres | 0.405 | hectares | ha |
| **$mi^2$** | square miles | 2.59 | square kilometers | $km^2$ |

| SYMBOL | WHEN YOU KNOW | MULTIPLY BY | TO FIND | SYMBOL |
|---|---|---|---|---|
| | | **VOLUME** | | |
| **fl oz** | fluid ounces | 29.57 | milliliters | mL |
| **gal** | gallons | 3.785 | liters | L |
| **$ft^3$** | cubic feet | 0.028 | cubic meters | $m^3$ |
| **$yd^3$** | cubic yards | 0.765 | cubic meters | $m^3$ |
| NOTE: volumes greater than 1000 L shall be shown in $m^3$ | | | | |

| SYMBOL | WHEN YOU KNOW | MULTIPLY BY | TO FIND | SYMBOL |
|---|---|---|---|---|
| | | **MASS** | | |
| **oz** | ounces | 28.35 | grams | g |
| **lb** | pounds | 0.454 | kilograms | kg |
| **T** | short tons (2000 lb) | 0.907 | megagrams (or "metric ton") | Mg (or "t") |

| SYMBOL | WHEN YOU KNOW | MULTIPLY BY | TO FIND | SYMBOL |
|---|---|---|---|---|
| | | **TEMPERATURE (exact degrees)** | | |
| **°F** | Fahrenheit | 5 (F-32)/9<br>or (F-32)/1.8 | Celsius | °C |

| SYMBOL | WHEN YOU KNOW | MULTIPLY BY | TO FIND | SYMBOL |
|---|---|---|---|---|
| **ILLUMINATION** | | | | |
| **fc** | foot-candles | 10.76 | lux | lx |
| **fl** | foot-Lamberts | 3.426 | candela/$m^2$ | $cd/m^2$ |

| SYMBOL | WHEN YOU KNOW | MULTIPLY BY | TO FIND | SYMBOL |
|---|---|---|---|---|
| **FORCE and PRESSURE or STRESS** | | | | |
| **lbf** | poundforce | 4.45 | newtons | N |
| **$lbf/in^2$** | poundforce per square inch | 6.89 | kilopascals | kPa |

## APPROXIMATE CONVERSIONS TO SI UNITS

| SYMBOL | WHEN YOU KNOW | MULTIPLY BY | TO FIND | SYMBOL |
|---|---|---|---|---|
| **LENGTH** | | | | |
| **mm** | millimeters | 0.039 | inches | in |
| **µm** | micrometers | 0.039 | mils | mils |
| **m** | meters | 3.28 | feet | ft |
| **m** | meters | 1.09 | yards | yd |
| **km** | kilometers | 0.621 | miles | mi |

| SYMBOL | WHEN YOU KNOW | MULTIPLY BY | TO FIND | SYMBOL |
|---|---|---|---|---|
| **AREA** | | | | |
| **$mm^2$** | square millimeters | 0.0016 | square inches | $in^2$ |
| **$m^2$** | square meters | 10.764 | square feet | $ft^2$ |
| **$m^2$** | square meters | 1.195 | square yards | $yd^2$ |
| **ha** | hectares | 2.47 | acres | ac |
| **$km^2$** | square kilometers | 0.386 | square miles | $mi^2$ |

| SYMBOL | WHEN YOU KNOW | MULTIPLY BY | TO FIND | SYMBOL |
|---|---|---|---|---|
| **VOLUME** | | | | |
| **mL** | milliliters | 0.034 | fluid ounces | fl oz |
| **L** | liters | 0.264 | gallons | gal |
| **$m^3$** | cubic meters | 35.314 | cubic feet | $ft^3$ |
| **$m^3$** | cubic meters | 1.307 | cubic yards | $yd^3$ |

| SYMBOL | WHEN YOU KNOW | MULTIPLY BY | TO FIND | SYMBOL |
|---|---|---|---|---|
| **MASS** | | | | |
| **g** | grams | 0.035 | ounces | oz |
| **kg** | kilograms | 2.202 | pounds | lb |
| **Mg (or "t")** | megagrams (or "metric ton") | 1.103 | short tons (2000 lb) | T |

| SYMBOL | WHEN YOU KNOW | MULTIPLY BY | TO FIND | SYMBOL |
|---|---|---|---|---|
| **TEMPERATURE (exact degrees)** | | | | |
| **ºC** | Celsius | 1.8C+32 | Fahrenheit | ºF |

| SYMBOL | WHEN YOU KNOW | MULTIPLY BY | TO FIND | SYMBOL |
|---|---|---|---|---|
| **ILLUMINATION** | | | | |
| **lx** | lux | 0.0929 | foot-candles | fc |
| **cd/m²** | candela/m² | 0.2919 | foot-Lamberts | fl |

| SYMBOL | WHEN YOU KNOW | MULTIPLY BY | TO FIND | SYMBOL |
|---|---|---|---|---|
| **FORCE and PRESSURE or STRESS** | | | | |
| **N** | newtons | 0.225 | poundforce | lbf |
| **kPa** | kilopascals | 0.145 | poundforce per square inch | lbf/in² |

| 1. Report No.<br>BDV29 977-02 | 2. Government Accession No. | 3. Recipient's Catalog No. |
|---|---|---|
| 4. Title and Subtitle<br>CORROSION EVALUATION OF NOVEL COATINGS FOR STEEL COMPONENTS OF HIGHWAY BRIDGES | | 5. Report Date<br>December 31, 2014 |
| | | 6. Performing Organization Code |
| 7. Author(s)<br>Kingsley Lau and Md Ahsan Sabbir | | 8. Performing Organization Report No. |
| 9. Performing Organization Name and Address<br>Florida International University<br>10555 W. Flagler St.<br>Miami, FL 33174 | | 10. Work Unit No. (TRAIS) |
| | | 11. Contract or Grant No. |
| 12. Sponsoring Agency Name and Address<br>Florida Department of Transportation<br>605 Suwannee St. MS 30<br>Tallahassee, FL 32399 | | 13. Type of Report and Period Covered<br>March 9, 2013-March 30, 2015 |
| | | 14. Sponsoring Agency Code |

15. Supplementary Notes

16. Abstract

The Florida Department of Transportation (FDOT) had expressed interest in gauging the available coating technologies that may have suitable applications for steel components in highway bridges. The motivation was to possibly identify coating systems that would provide corrosion durability of steel components in highway bridges and reduce costs associated with regular inspection and maintenance of the coating systems. Chemically bonded phosphate ceramics (CBPC) and the thermal diffusion galvanizing (TDG) process have been identified for further testing due to growing interest in the systems for possible corrosion mitigation, the lack of sufficient data to determine their effectiveness for corrosion protection of steel structures, and their commercial availability.

An issue for further evaluation of long term durability and corrosion protection by CBPC coatings is the degree of deterioration of the ceramic coating in aggressive environments. Initial testing showed that the material was not durable in highly alkaline solutions (pH 13), and in exposure conditions that cycle between frequent high moisture contents and drying conditions. The rather short-term outdoor exposures investigated so far have produced some promising results, but the significant extent of undercoating surface oxidation that was observed may compromise long-term durability. The intermediate alloy layer was not consistently identified and its role in corrosion mitigation has not been elucidated.

Although no severe steel corrosion was observed for TDG in outdoor exposure, degradation of the topcoat, when present, and subsequent consumption of the TDG would result in a shorter service life of the coating for corrosion mitigation. Variations in quality of the topcoats resulted in variations in coating performance. The findings suggest that sufficient application of the TDG and robust topcoats are required for long-term durability.

| 17. Key Word<br>Corrosion, Coatings, Degradation, Ceramic, Galvanizing | 18. Distribution Statement | | |
|---|---|---|---|
| 19. Security Classif. (of this report)<br>unclassified | 20. Security Classif. (of this page)<br>unclassified | 21. No. of Pages<br>199 | 22. Price |

**TABLE OF CONTENTS**

## LIST OF FIGURES

## LIST OF TABLES

## EXECUTIVE SUMMARY

New coating materials, application technology, and substrate surface treatment requirements and techniques have introduced a myriad of commercially available coating systems. The Florida Department of Transportation (FDOT) had expressed interest in gauging the available coating technologies not currently being regularly used for civil infrastructure, but that may have suitable applications for steel components in highway bridges. The motivation of this interest was to identify coating systems that could provide corrosion durability of steel components in highway bridges, and reduce costs associated with regular inspection and maintenance of the coating systems and steel bridge components in Florida. Two coatings of interest were chemically bonded phosphate ceramic coating (CBPC) and thermal diffusion galvanized coating (TDG). These coating systems have been selected for further testing due to growing interest in corrosion mitigation systems, the scarcity of information on detailing application and performance of these coatings on highway bridges, and their current commercial availability. Of major interest was the performance of these coatings in alkaline environments representative to Florida exposures of reinforced concrete structures.

Not all the coating materials tested were recommended for the application and the exposure environments tested. Furthermore, the materials used in testing were expected to be prepared and coated by the respective manufacturers in accordance to their best practices, but significant sample variability and defects were observed. As with any test program with producer-provided test materials, the findings described here are based solely on the results for the coated samples in the conditions received from the producers. The findings from this study were meant to be preliminary to provide indicators of major material incompatibility with environments relevant to highway bridges.

Preliminary findings indicate that further evaluation of long-term durability and corrosion protection provided by CBPC coatings is needed to address the deterioration of the ceramic coating. This coating exhibited very poor compatibility with alkaline solutions of pH 13, which could be produced in hydrating concrete pore water. High available moisture contents and exposures where wetting and drying conditions are prevalent could also cause early degradation of the coating. Atmospheric exposure can cause some coating degradation, but early observations indicate that this rate can be reduced. The rather short-term outdoor exposures gave some promising results, but the significant extent of undercoating surface oxidation that was observed may compromise long-term durability. After 5800 hours in salt-fog exposure, rust bleed-out through the coating occurred. The protective intermediate alloy layer was not consistently identified and its role in corrosion mitigation has not been elucidated.

Although no severe steel corrosion was observed for TDG in outdoor exposure, degradation of the topcoat when present and subsequent consumption of the TDG would result in shorter service life of the coating. Variations in topcoats resulted in varying coating performance. Electrochemical testing of TDG in neutral pH chloride and chloride-free solutions indicated a decrease in corrosion rates with time. The decrease in corrosion rates indicates a progressive passivation of the exposed surface. Significant deterioration of the topcoat and oxidation of the TDG was apparent in some outdoor exposure cases, which indicates that significant zinc consumption can occur quickly in ambient conditions. Furthermore, salt-fog testing showed that wet conditions with the presence of chlorides would cause severe surface oxidation, indicating that appropriate topcoats are needed in very aggressive environments. The findings suggest that sufficient application of the TDG and robust topcoats are required for long-term durability.

# CHAPTER ONE: INTRODUCTION

## 1.1. BACKGROUND

Corrosion of steel components and subsequent loss of structural integrity is a concern for highway bridge owners. In the US, recent estimates indicated that there are approximately 200,000 steel bridges and ~240,000 prestressed and reinforced concrete bridges, of which ~15% were considered structurally deficient due to corrosion [Materials Performance, 2002]. Of the estimated $8.3 billion cost of corrosion in highway bridges, half a billion dollars is spent for maintenance of painting on steel bridges. Coating systems for corrosion protection of steel bridges have significantly changed in the past couple decades due to advances in technology, changes in environmental and health regulations, and differences in costs.

New coating materials, application technology, and substrate surface treatment requirements and techniques have introduced a myriad of commercially available coating systems. Environmental protection regulations have made some older functional coating systems obsolete and costs associated with coating removal, containment, coating application, and maintenance have further spurred need to develop effective and cost-efficient coating systems that also meet or exceed health and environmental regulations. Novel coating formulations continue to be introduced and have been examined for use in other industries such as automotive and defense and may have effective application for steel components in highway bridges.

The Florida Department of Transportation (FDOT) has expressed interest in gauging the available coating technologies not currently being regularly used for civil infrastructure but that may have suitable applications for steel components in highway bridges. Among those include bonded phosphate coatings for corrosion mitigation. The motivation of this interest is to identify coating systems that would provide corrosion durability of steel components in highway bridges and reduce costs associated with regular inspection and maintenance of the coating systems and steel bridge components in Florida bridges.

The long-term effectiveness of coating systems is of major importance. Not only should the coating system provide adequate corrosion control and meet environmental and health regulation, but degradation of the coating should be minimized so that costly remediation, including coating removal, surface preparation and reapplication, can also be minimized. The installation costs of the coating system and whether or not the coating can be applied in shop or in the field are important factors for consideration, as is ease of future surface preparation and repair paint application if needed.

In a 1997 Federal Highway Administration (FHWA) study tour for bridge maintenance coatings [Bernecki et al., 1997], it was identified that a large portion of US steel bridges

still had coatings with lead-containing paints that were utilized until the 1970s. Approximately 80-90% of the 200,000 steel bridges in the US were coated with lead or other heavy metals [Myers et al., 2010]. Increasing maintenance costs were due to the need for appropriate containment for paint removal and to satisfy enhanced environmental regulations on heavy metals and solvents. Because of the high maintenance costs to remove old coatings, application of overcoating systems such as moisture-cured urethane, calcium sulfonate alkyd, epoxy mastic, epoxy/polyurethane, and waterborne acrylic systems have been used by some transportation departments [Myers et al., 2010].

The use of zinc-rich primers such as in three-coat systems as well as thermal spray metal coatings were among coating systems adopted to replace lead-based paints. Vinyl coating systems were specified by some bridge owners but health and environmental concerns of high volatile organic compound, VOC, levels associated with that coating has also been a concern [Chang et al. 1999]. The current state of practice for paint coatings involves multiple coating layers typically comprising of a metal primer coating applied to a blast cleaned steel substrate followed by an intermediate and topcoat [Kline, 2009]. Metallic coatings utilize methods of thermal spraying or hot-dip galvanizing.

## 1.2. FDOT STRUCTURAL STEEL COATING SYSTEMS

FDOT specifications are outlined in Section 560 ‘Coating New Structural Steel’ and Section 975 ‘Structural Coating Materials’ in the FDOT Standard Specifications for Road and Bridge Construction [FDOT 2013a]. Preventative maintenance of steel superstructure and bearings are described in the FDOT Bridge Maintenance and Repair Handbook. General structural coating materials requirements prescribe non-hazardous coatings and coating systems to produce a visually uniform, adherent coating upon curing. Minimum performance requirements for coating test panels are listed in Table 1.1.

Table 1.1. FDOT Coating Performance Requirements (after FDOT 2013a)

| Laboratory Testing | | |
|---|---|---|
| Property | Test Method | Requirement |
| Slip Coefficient | AASHTO R-31 | Min Class B (primer only) |
| Salt Fog Resistance | AASHTO R-31 | Blister Size = 10<br>Avg Rust Creep at the Scribe ≤0.1 inches |
| Cyclic Weathering Resistance | AASHTO R-31 | Blister Size = 10<br>Avg Rust Creep at Scribe ≤0.2 inches, Color retention ΔE≤8, Gloss loss less than 30 units |

Continuation Table 1.1. FDOT Coating Performance Requirements (after FDOT 2013a)

| | | |
|---|---|---|
| Abrasion Resistance | AASHTO R-31 | Wear index ≤2.7mg/cycle |
| Adhesion | AASHTO R-31 | Avg. system tensile strength ≥800 psi |
| Freeze Thaw Stability | AASHTO R-31 | Avg. tensile strength ≥800 psi |
| Coatings Identification | Fourier Transform Infrared Spectroscopy | IR scan (2.5 to 15 um) for each base, catalyst, and mixed coating |
| Impact Resistance | ASTM D2794 | Greater than 25 inch/lbs, ½" impact intrusion |
| Flexibility | AASHTO R-31, ASTM D522, 1 inch cylindrical mandrel | No cracking |
| Outdoor Testing | | |
| Property | Test Method | Requirement |
| Rusting | ASTM D610<br>ASTM D1654 (scribed)<br>ASTM D1654 (unscribed) | ≥9 after 5 years<br>≥9 after 5 years<br>≥9 after 5 years |
| Blistering | ASTM D714 | 10 after 5 years |
| Adhesion | ASTM D4541; annex A4 | ≥ 800 psi (unscribed area) after 5 years |
| Color Retention | ASTM D2244 | ΔE≤8 after 2 years |
| Gloss | ASTM D523 | ≤30 gloss units after 2 years |

Section 975-2 of the 2013 FDOT Standard Specifications for Road and Bridge Construction provides specifications for structural steel coating systems for new structures (including high performance coating systems, inorganic zinc coating systems, and interior box girder coating systems) and for existing structures [Byram, 2005]. The paint system conventionally utilized by FDOT is a 3-coat system with a zinc primer that is repainted every 12 to 20 years [Pouliotte, 2012]. Currently the department is using an inorganic zinc 3-coat system with an expected service life of approximately 30 years. The amount spent for repainting by FDOT is shown in Figure 1.1.

Costs saving initiatives have been presented to incorporate use of weathering steels in suitable environments in Florida with application of inorganic zinc paint systems in aggressive environments or when aesthetics are important.

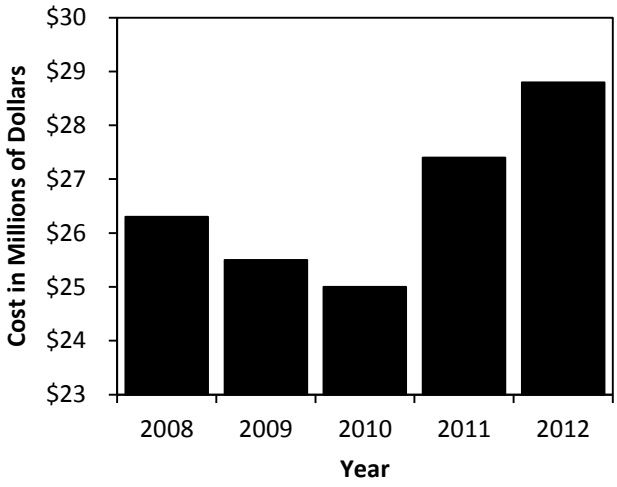


**Figure: 1.1 FDOT Cost Spent for Repainting**. (after Pouliotte, 2012)

## 1.3. CURRENT BRIDGE COATING PRACTICES AND LIMITATIONS

### *1.3.1 Paint Coatings*

#### *1.3.1.1 Three-Coat Systems*

Among accepted paint coatings, the three-coat system has been considered to have good long-term performance and durability, with some case studies showing that these coatings on bridges in non-marine environments were effective for over 40 years [Kline, 2009]. The three-coat system typically consists of either an organic or inorganic zinc-rich primer (although other primers have been formulated) followed by an epoxy midcoat and a topcoat.

The corrosion activity of zinc can provide cathodic protection of the steel substrate [Molnar and Liszi, 2001]. Insoluble corrosion products (such as zinc carbonate) developed by the sacrificial zinc material may fill the pores of the zinc primer layer which may further provide beneficial corrosion mitigation [Calla and Modi, 2000]. Some types of zinc dust used in primers have a plate-like structure which may decrease permeability of the zinc primer layer. In a laboratory study, lamellar zinc particles exhibited the highest anticorrosion efficiency at a concentration around 20 vol% [Kalendova, 2003]. The porosity of zinc powder coatings is less than solvent-based zinc coatings due to their high wetting ability [Marchebois et al., 2002].

Comparison of organic and inorganic zinc is well presented by Chang et al., 1999. A general comparison chart for inorganic and organic zinc-modified coatings, after Chang et al., 1999, is shown in Table 1.2.

Glass flakes have also been used in coating primers. Most glass flakes are produced from either electric glass or ‘C’ type glass. C-glass (chemical glass) contains zinc oxide

which makes the flakes more resistant to chemical degradation. Low alkali content glass known as electrical glass (E-glass) has low electrical conductivity and high temperature resistivity. Flake size and thickness distribution in the resin is an important property for coating durability. The low thickness-to-surface area ratio of glass flakes allows particle overlap providing low permeability and reducing the diffusion rate of moisture and gases. Flakes with a nominal screen dimension of 500 µm are used for spray coating, and flakes with a nominal screen dimension of 1500 µm are used for brush-applied coating [Brigham, 2009]. Higher percentages of glass flake in a coating may increase the rigidity of the coating.

Table 1.2. Comparison of Inorganic and Organic Zinc (after Chang et al., 1999)

| | Inorganic Zinc Primer | Organic Zinc Primer |
|---|---|---|
| Surface Preparation | SSPC-SP10 or SP5†<br>Surface Profile 1-3 mil† | Less subject to critical surface preparation |
| Application | Primer applied in shop (3-5 mils)† | Per manufacturer recommendation typ~3mils. Easier to apply |
| Overall Protection | Better protection | |
| Aging | Not subject to age-related deterioration | Organic coating may be subject to aging |
| Adhesion | ASTM D3359 3A Rating†[1] | Susceptible to coating disbondment |
| Recoatability | | Better recoatability |
| Compatibility | | More compatible with oleoresinous topcoats |
| Underfilm Corrosion | Inorganic binder and steel substrate does not allow underfilm corrosion | Susceptible to underfilm corrosion due to coating disbondment |
| Gassing/ Pinholes | Susceptible to pinholes | Less susceptible due to less porous organic primer |

† AASHTO/NSBA S8.1-2002 Guide Specification for Coating Systems with Inorganic Zinc-Rich Primer. 1. Jagged removal along incisions up to 1/16th inch on either side

The midcoat (typically epoxy binder) is used to provide additional separation of the steel substrate/primer from the environment, to provide a layer to cover defects in the primer, and to reduce moisture and chemical ingress to the steel surface. Three types of epoxy intermediate coats are available including epoxy ester, epoxy lacquer, and a two-component epoxy [Chang and Chung, 1999]. Epoxy ester is a vegetable oil-modified

epoxy resin with superior alkali resistance. Epoxy lacquer is a high molecular weight epoxy with a short curing time. Two-component epoxies are epoxy polyamides with superior flexibility, durability and pot ability. Generally, high-build epoxy is used as an intermediate coat which offers excellent resistance to water and alkali. The disadvantages of epoxies are poor resistance against chalking, poor rating for gloss retention, and they are not recommended for cold temperature because of their expansion and shrinkage rate [Chang and Chung, 1999].

Finishes and topcoats are used to retain coating aesthetics and provide wear and UV resistance. Urethane and polyurethane binders are typically employed as oil-modified urethane, moisture-cured urethane, and two-component urethane [Chang et al., 1999]. Oil-modified pigmented urethanes are not used for exposed structural steel due to their lack of durability. Moisture-cured urethane uses air moisture for curing and produces a hard and tough coating. Pigmentation is difficult, so they are used for clear finishes. Two-component urethanes use polyols, polyethers, polyesters or acrylics. For three-coat systems, hydroxylated acrylic or hydroxylated polyester bonded urethanes are most commonly used as they have the better UV resistance and dry faster.

Inorganic zinc with a waterborne acrylic coating system was used by the Illinois Department of Transportation (IDOT) around the year 2000. The expected life time was 15 to 20 years without major maintenance [Chang and Chung, 1999]. The resins in the waterborne acrylic system give high gloss, and very fast drying with rapid development of film properties. Acrylic is less expensive than urethane and provides good color and gloss retention properties.

Several US transportation departments have reported savings due to the reduced number of repainting cycles for three-coat systems as compared to older coating systems. Maintenance typically would consist of retouching defects in the topcoat incurred by adhesion degradation as well as degradation incurred by weather and vandalism. Of the lifetime costs of the coating system, the larger portion of the costs derives from the initial application [Kline, 2009], and coating systems with fewer layers are being evaluated to reduce those costs [Yao et al., 2011]. The corrosion protection of the three-coat system with inorganic zinc primers was reported to be better than with organic zinc primers for new construction; however, the sensitivity of inorganic zinc primers to surface conditions limits its application to controlled settings in a shop environment.

#### *1.3.1.2 Other Paint Coatings*

Two-coat systems have been described that eliminate the requirement of an intermediate coating [Chong and Yao, 2006]. The zinc-rich primer is topcoated with a polymer coating such as polyurea, polyurethane, polysiloxane, and polyaspartics. Polyurea is a rapid-cure polymer for corrosion and abrasion mitigation. Polyurethane is a high performance topcoat formed by reacting polyisocyanate with polyol or base resin.

Polysiloxane is an inorganic polymer that offers resistance to water, chemicals, and oxidation; and has good color and gloss retention. Polyaspartics are a fast-drying coatings that build on conventional polyurethanes with high thickness. The inorganic zinc and vinyl system is a two-coat system. Interaction of the polyvinyl butyral (PVB) resins with zinc chromate pigments and phosphoric acid provides good adhesion. However, the coating has been reported to perform poorly in terms of gloss and UV prevention [Chang et al, 1999]. Indiana DOT estimated effective life times of about 15 years [Chang and Chung, 1999].

The moisture-cure urethane coating system is a single pack paint used in Wisconsin, Alaska, Maine, Vermont, New Hampshire, New York, Kentucky, and Minnesota with an expected life time of 20 to 30 years. The moisture-cure urethane is less sensitive to surface preparation and atmospheric moisture content. The reaction of the urethane with atmospheric water involves a two-stage process, with the water and the isocyanate group first producing the unstable carbamic acid, which immediately dissociates to form an amine and carbon dioxide. The carbon dioxide leaves the film by evaporation, and the amine reacts with a second group giving a urea [Chang and Chung, 1999].

Calcium sulfonate alkyd (CSA) is a one-coat package system that can be applied with minimum surface preparation using hand tool cleaning and solvent cleaning, ideal to overcoat deteriorated paint. Use has been reported in Missouri [Myers. et al, 2010]. The limitations are a long curing time and according to FHWA, the soft material picks up dirt easily [Myers. et al, 2010]. One-coat systems including polyaspartic, epoxy mastic, high-ratio calcium sulfonate alkyd, glass flake-reinforced polyester, high-build waterborne acrylic, waterborne epoxy, polysiloxane, and urethane mastic were evaluated by the Federal Highway Administration in 2011 [Yao et al., 2011]. General descriptions of the tested one-coat systems after Yao et al., 2011 follow. The polyaspartic coating is produced by reaction of ester compounds providing fast drying time and weatherability. Epoxy mastic is an aluminum-pigmented high-solid epoxy coating. The high-ratio calcium sulfonate alkyd is an alkaline coating that forms ionic bonding with the underlying metal and may promote steel passivity. Glass flake-reinforced polyester coatings have good mechanical properties and chemical resistance. High-build waterborne acrylic and waterborne epoxy coatings have low flammability, odor and VOC. Polysiloxane coatings are organic-inorganic siloxane binders. Urethane mastics are high-build acrylic urethane systems.

#### *1.3.1.3 Performance Evaluations*

Several studies on paint coatings by the Federal Highway Administration were published from 2006 to 2011. The following section contains a synopsis of those studies.

The Federal Highway Administration (FHWA) initiated a research program in August 2009 to identify coating systems that can provide long-term durability with minimal

maintenance. Eight promising coating systems are listed in Table 1.3 [Kodumuri and Lee, 2012]. Evaluation of these systems consisted of accelerated laboratory testing (consisting of cyclic environmental exposure to temperature, UV, and moisture, and salt), and outdoor marine and simulated salt exposure environments. The study concluded that the three-coat systems with zinc-rich epoxy and polyurethane topcoats performed well, but none of the coating systems were expected to meet the 100-year maintenance-free coating specification. The thermally sprayed zinc and zinc two-coat systems had poor performance in the study.

Table 1.3. Coating Systems Tested by FHWA (after Kodumuri and Lee, 2012)

| System ID | Coat | | |
|---|---|---|---|
| | Primer | Intermediate | Top |
| Three Coat | Inorganic zinc-rich epoxy | Epoxy | Aliphatic polyurethane |
| | Zinc-rich epoxy | Epoxy | Aliphatic polyurethane |
| | Moisture-cured urethane-zinc | Epoxy | Fluorourethane |
| Two Coat | Zinc-rich epoxy | | Aliphatic polyurethane |
| | Inorganic zinc | | Polysiloxane |
| | Thermally sprayed zinc | | Linear Epoxy |
| | Zinc | | Linear Epoxy |
| One Coat | High-ratio calcium sulfonate alkyd | | |

FHWA conducted a study in 2006 on two-coat systems to eliminate the intermediate epoxy layer for rapid paint application and economy [Chong and Yao, 2006]. The researchers investigated eight two-coat systems with comparison of three traditional three-coat systems as shown in Table 1.4. Testing consisted of cyclic environmental exposure to temperature, UV, moisture, and salt in accelerated laboratory testing and outdoor exposure. The study concluded that the two-coat systems performed comparably to the three-coat systems. The conventional three-coat systems with aliphatic polyurethane performed better in terms of gloss retention. Two-coat systems with manufacturer design configurations (Systems 1-2, 10-11) performed well but Systems 6-9 with polyaspartic topcoats (not specified by manufacturers of organic-rich

epoxy and inorganic zinc-rich alkyl silicate) had reduced performance including development of topcoat wrinkling and cracking.

Table 1.4. Coating Systems Tested by FHWA (after Chong and Yao, 2006)

| | | |
|---|---|---|
| Three-Coat | Zinc-rich moisture cure urethane/Moisture cure urethane/Aliphatic polyurethane | System 3 |
| | Organic zinc rich epoxy/Epoxy/Aliphatic Polyurethane | System 4 |
| | Inorganic zinc rich alkyl silicate/Epoxy/Aliphatic polyurethane | System 5 |
| Two-Coat | Zinc-rich moisture cure urethane/Polyaspartics | System 1 and 2 |
| | Organic zinc-rich epoxy/Polyaspartics | System 6 and 7 |
| | Inorganic zinc-rich alkyl silicate/ Polyaspartics | System 8 and 9 |
| | Organic zinc-rich epoxy/Aliphatic polyurethane | System 10 |
| | Organic zinc-rich epoxy/Polysiloxane | System 11 |

The Federal Highway Administration conducted a study in 2011 of eight one-coat paint systems including polyaspartic, epoxy mastic, high-ratio calcium sulfonate alkyd, glass flake reinforced polyester, high-build waterborne acrylic, waterborne epoxy, polysiloxane, and urethane mastic [Yao et al., 2011]. The evaluation included accelerated laboratory testing for 6840 hours and three outdoor exposure conditions including marine exposure for 24 months, mild natural weathering for 18 months and a mild natural weathering plus salt solution spray test for 18 months. The evaluation procedure was based on VOC, pigment content, FTIR analysis, sag resistance, drying time, gloss, color, pencil scratch hardness, adhesion, detection of coating defects, blistering, and rust creepage. The study provided performance ranking of the eight one-coat systems as well as a three-coat (zinc-rich epoxy, epoxy, and polyurethane topcoat) and a two-coat system (zinc-rich moisture-cure urethane and polyaspartic topcoat). It was concluded that the one-coat systems did not perform as well as the three-coat system in accelerated laboratory and outdoor test conditions. The two-coat system

(which showed promising results in the study by Chong and Yao in 2006) also showed development of coating defects, rust creepage and significant reduction in gloss.

### *1.3.2 Metallic Coatings*

#### *1.3.2.1 Metallizing*

Metallizing refers to the application of zinc, aluminum, or zinc-aluminum alloy to steel surfaces by thermal spray for corrosion control [Chang et al., 1999; Kogler et al., 1998; Bernecki et al., 1997]. The steel surface is prepared by grit blasting or chemical etching for proper mechanical bonding. Aluminum requires more surface roughness than zinc [Chang and Georgy, 1999]. Surface preparation specifications include SSPC-SP 5 White metal blast cleaning, NACE No 1 White metal blast cleaned surface finish (comparable to SSPC-SP 5), SSPC-SP 10 Near white metal blast cleaning, NACE No 2 White metal blast cleaned surface finish (comparable to SSPC-SP 10) [Chang and Georgy, 1999]. Flame spraying and arc spraying, among spraying techniques, were developed. The coating porosity made by flame spraying may be around 20 percent due to the relatively low application velocity [Chang and Georgy, 1999]. Arc spraying can be more expensive but can create layers with better adhesion, better cohesion, and lower porosity due to the higher application velocity. The molten zinc, aluminum, or zinc-aluminum alloy in both processes is accelerated and the resultant droplets form as splats on the steel substrate. An example of a thermal spray coating of zinc-aluminum alloy on steel and the metallizing material is shown in Figures 1.2 and 1.3. The desired thickness is made by additional passes over the steel. The American Welding Society (AWS) issued a guide, ANSI/AWS C2.18-93 and a joint standard SSPC-CS23.00/AWS C2.23M/NACE No. 12 for thermal spray coatings on steel. Research by the US Navy showed better corrosion mitigation performance with thermally sprayed aluminum than zinc in marine environments [Chang and Georgy, 1999]. Alloys comprised of 85 percent zinc/15 percent aluminum have also been used for thermal spray coatings. Cleanliness is of importance since moisture and contaminants can reduce the strength of the bond between the coating and steel [Chang et al., 1999]. The expected life of metallization is 40 to 60 years if sealers are used [Chang et al, 1999].

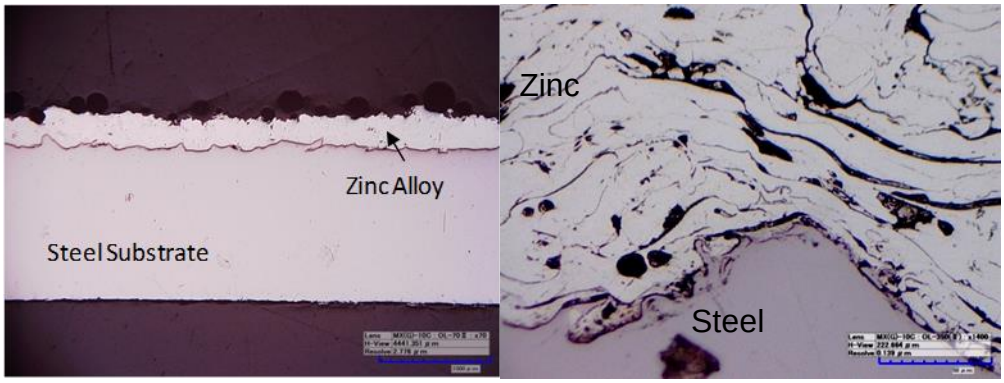


**Figure: 1.2 Thermal Spray Coating. Zinc on Steel**.
(Figure by Lau and courtesy of FDOT.)

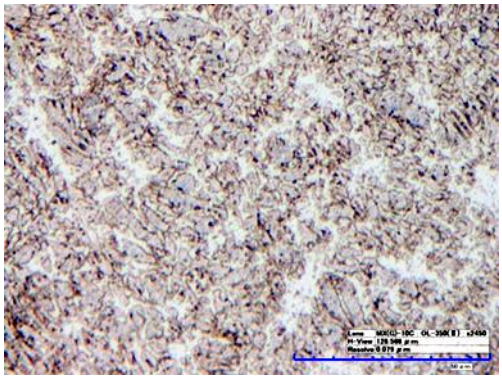

**Figure: 1.3 Hypereutectic Microstructure of ZnAl15.**
(Figure by Lau and courtesy of FDOT.)

Sealers such as acrylic urethanes, polyester urethanes, vinyls, phenolics, epoxy or thermal-sprayed polymer can be used to enhance service life by sealing the pores in the coating. Seal coats are applied on the dry surface before visible oxidation and some protocols to remove moisture by heating (i.e. 120°C) have been suggested [Chang and Georgy, 1999]. Seal coats are typically applied soon after metallizing (i.e. within 8 hours for zinc and zinc alloys and within 24 hours for aluminum application [Chang and Georgy, 1999]).

Many transportation departments have adopted metallization due to its performance, but its high cost has been an important factor. Some transportation departments also include sealers and topcoats for thermal spray coatings for better protection. Thermal spray coatings also require greater control, including surface preparation [Chang and Georgy, 1999] which may limit their efficacy for field application. Of note, localized corrosion was observed in early use of a metallized coating on a bridge in Connecticut due to improper surface preparation [Chang et al., 1999; Kogler et al., 1998].

#### *1.3.2.2 Galvanizing*

Batch hot-dip galvanizing has been the most commonly used method of protecting steel products from corrosion for over 200 years [Zhmurkin 2009]. In this process an adherent, protective coating of zinc or zinc alloy is developed on the surfaces of iron and steel products by immersing them in a bath of molten zinc [Dallin 2012]. The galvanized steel develops a thick zinc-iron alloy coating with layers of different alloy composition. The properties of these layers are given in Table 5 [Dallin 2012].

Table 1.5. Galvanizing Coating Layers (After Dallin, 2012)

| Layer | Alloy | Iron % | Crystal Structure | Alloy Characteristics |
|---|---|---|---|---|
| Eta | Zinc | 0.03 | Hexagonal | Soft, ductile |
| Zeta | $FeZn_{13}$ | 5.7-6.3 | Monoclinic | Hard, brittle |
| Delta | $FeZn_{7}$ | 7-11 | Hexagonal | Ductile |
| Gamma | $FeZn_{10}$ | 20-27 | Cubic | Hard, brittle |
| Steel Base | Iron | 99+ | Cubic | |

The continuous process consists of feeding cold-rolled steel through a cleaner, an annealing furnace, and then into a molten zinc bath at speeds up to 600 fpm (200 mpm). As the steel exits the molten zinc bath, excess coating from the steel sheet is removed to the specified requirement. The galvanized steel can be used as-is, or it can be thermally treated to convert the coating to galvanneal, which is a zinc-iron alloy [Dallin, 2012)]. Many automakers prefer galvanneal to galvanize because of its extremely good paintability, appearance, and corrosion resistance under automotive type paints [Dallin, 2012)].

#### *1.3.2.3 Thermal Diffusion Galvanizing*

Thermal diffusion galvanizing (TDG) was introduced in 1902. Due to a long processing time and difficulty in controlling thickness, use of TDG was diminished by 1950. Interest was renewed by 1993 for coating steel fasteners and hardware. Specification of zinc alloy thermo-diffusion coatings for hardware is made in ASTM A1059.

The process involves vapor diffusion of zinc into steel. The process creates a zinc-iron alloy by penetrating the surface of the steel. The steel components and zinc powder are rotated within a closed cylinder inside of an oven and heated to a temperature of 710° - 1092° F (320° to 500° C) [ASTM A 1059-08]. Zinc sublimation occurs at 500° F and by penetrating the steel, produces Zn/Fe alloy. This process results in the formation of iron-

zinc gamma (solid Zn ions inside Fe substrate), delta ($Fe_{11}Zn_{40}$), and zeta ($FeZn_7$) layers, excluding the external eta layer of pure free zinc [ASTM A 1059-08]. The coating metallurgy of zinc in thermal diffusion galvanizing (TDG) is analogous to hot dip galvanizing, but the longer heat cycle associated with TDG allows much deeper penetration of zinc into the steel substrate. The thickness of the eta (pure zinc) in hot dip galvanizing is significantly thicker than in TDG coating. The eta layer has much less corrosion resistance than the zinc/iron phases. The zinc/iron phases (zeta, delta, and gamma layers) can be thicker in TDG than hot dip galvanizing. A non-scaled comparison is shown in Figure 1.4.

Some properties of TDG from industry literature are described here. TDG produces a material that is hard, weldable, spark-free, anti-galling, non-magnetic, and has a low coefficient of friction. The hardness can exceed 35 Rockwell C depending on coating parameters. The coated parts can be operated at continuous temperature up to 1200° F (650° C). The zinc layers have good adhesion to the steel substrate as the zinc penetrates the base metal about 1/3 of the coating thickness and, as shown in Figure 1.4, the coating consists mainly of the iron-zinc delta phase containing 4 to 10 % of iron. Adhesion of paint and topcoats to the zinc has been reported to be good due to the morphology of the TDG layer. It also has been reported that TDG does not promote hydrogen embrittlement of the steel [ASTM A 1059-08].

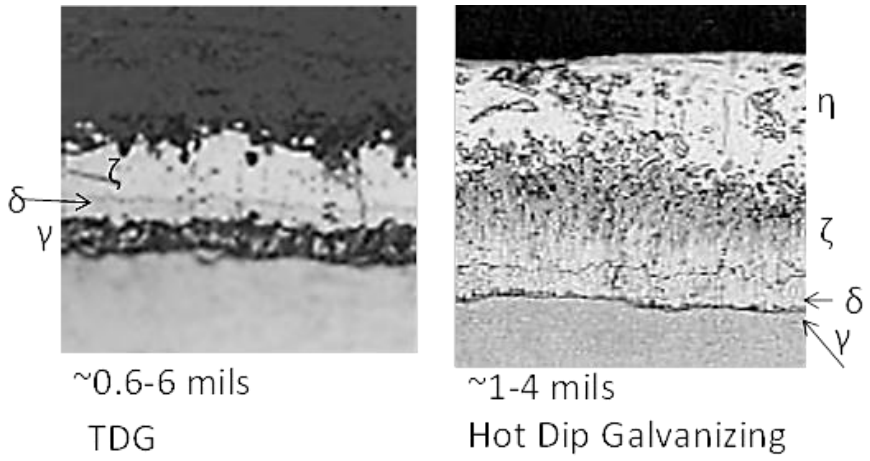


**Figure: 1.4 Microstructure of TDG and Hot Dip Galvanizing.** (after Dallin, 2012)

Thermal diffusion galvanizing was tested on lashing by the U.S. Navy and showed excellent corrosion protection [ArmorGalv 2013]. The Florida Department of Transportation did a cursory evaluation of TDG in 2013 [FDOT 2013b]. The evaluation compared the corrosion development on steel reinforcement coated by TDG and hot-dipped galvanizing after exposure to either a partial immersion condition in 3.5% salt water or in 5% salt fog at 95° F. TDG performed better than the hot-dipped galvanizing.

After 3000 hours in salt-fog condition, no corrosion was observed on the samples coated with TDG, whereas significant corrosion formed on the hot-dipped galvanized samples.

#### *1.3.2.4 Zinc/Aluminum-Rich Paint*

According to the American Galvanizing Association (AGA), cold galvanizing is a marketing term for zinc-rich paint. According to the manufacturers, the coating provides corrosion protection and can be applied as paint. Unlike galvanized coatings, the application of the paint does not create an alloy with the steel. The ability of the zinc (or aluminum in some products) to provide corrosion mitigation may be analogous to mechanisms associated with some metallic coatings; information on these materials are presented here.

The paint can be a barrier coating in the form of an epoxy or alkyd and the zinc dust provides corrosion mitigation characteristics. Although characteristics differ by product, it is typically a single-component zinc coating. The coating adheres to the steel surface by forming electrolytic bonds. The material degrades in a manner analogous to hot dip galvanizing by forming white-grey powder containing zinc salts and zinc carbonates. The expected life time for a cold galvanizing coating (promoted by a manufacturer) is 25 to 30 years for coatings with 80 µm thickness [Rust-anode, 2013]. Additional surface preparation may not be required for application of a topcoat.

### *1.3.3 Other Coatings*

#### *1.3.3.1 Chemical Conversion Phosphate Coating*

Phosphate coating is a chemical conversion coating where metals such as steel are exposed to phosphoric acid and iron, zinc, or manganese phosphate to form a coated layer on the metal substrate [Bogi and Macmillan, 1977]. Phosphate coatings have been used for corrosion protection of steel since the early twentieth century [Bogi and Macmillan, 1977]. In the automotive industry, phosphate coatings have been used as a pretreatment for painting to not only provide corrosion resistance, but also to provide improved bonding of paint [Jalili et al., 2009].

The formation of the phosphate coating involves a series of electrochemical and chemical reactions. The metal, upon immersion in phosphoric acid, is corroded, leading to formation of metal phosphates in various forms depending on changes in the electrolyte chemistry [Bogi and Macmillan, 1977]. Insoluble phosphate forms can deposit, but the mechanism differs depending on the use of zinc phosphate or manganese phosphate. For zinc phosphate, crystallization initiates at the anodic site that later becomes uniform across the metal substrate, predominantly in the form of Hopeite. In the case of manganese, crystallization occurs at cathodic sites and forms as Hureaulite [Bogi and Macmillan, 1977]. Chemical treatment requires high operating

temperatures up to 98°C [Jegannathan et al., 2006]. Phosphate coatings techniques at low temperatures have been presented by Narayanan et al., 2006 and Jegannathan et al., 2006 by cathodic and anodic electrochemical pretreatments, respectively, but mixed results on electrochemical pretreatments were reported. Also, mixed results on the durability of the coating in alkaline environments were reported, which may indicate limited application for reinforced steel in concrete [Sommer and Leidheiser, 1987].

#### *1.3.3.2 Chemically Bonded Phosphate Ceramics*

Chemically bonded phosphate ceramics (CBPC) are a class of broadly defined geopolymers that have amorphous binding phases analogous to cement [Wagh, 2005]. CBPC is made by acid-base reactions between phosphoric acid (or acid phosphates) and inorganic oxides. Aquasols from the dissolved metal oxides react with phosphate ions and condense to form a gel that proceeds to crystallize into a monolithic ceramic [Wagh, 2003]. One example of CBPC developed with magnesium oxide at Argonne National Laboratory is represented by Equation 1.

$$MgO + KH_2PO_4 + 5H_2O = MgKPO_4 \cdot 6H_2O \quad (1)$$

The CBPC coating consists of a two-component acid phosphate and a water-based slurry that contains base minerals and metal oxides (e.g. MgO). These two components are mixed together and sprayed on the metal surface with a dual component spray gun. The acid phosphate and oxides in the slurry interact with the metal substrate to form an insoluble passivation layer of stable oxides (~20-µm thick) that contains ~60% iron with phosphate, potassium, magnesium, silicon, hydrogen, and oxygen [Material Performance , 2011]. A ceramic outer layer forms on top of the oxide layer and its thickness can be increased by applying more material. The exothermic reactions create a temperature rise of 7 to 40° F in the material.

The passivation layer does not support oxidation of the steel substrate and the top dense ceramic outer layer protects the passivation layer and provides abrasion resistance. NACE 3 (commercial blast) or 5 (water-jetting) surface conditions allow for sufficient bonding of the coating with steel structures if all of the old paint materials are removed [Materials Performance, 2011]. The CBPC coating is reported to be compatible with aluminum, portland cement, gypsum, and steel; but cannot be chemically bonded to polymers. The CBPC can be used in environments with temperatures from 35° to 200°F and relative humidity from 0% to 99%. The coating cannot resist strong acids such as hydrochloric acid (HCl) and sulfuric acid ($H_2SO_4$). Testing indicated that the CBPC coating can flex up to 19% before fracture. Applications were found for radioactive waste containment [Cantrell and Westsik, 2011; Wagh, 1999] structural materials, and dentistry [Wagh, 2005].

NASA evaluated CBPC coated steel plates that were exposed to cycles of seawater spray and simulated sunlight. No corrosion was reported up to 170 days [Material Performance, 2011].

### 1.4. COATINGS FOR FURTHER TESTING

The research goal was to examine the corrosion behavior of coating systems not widely associated with highway bridges and identify its possible application for highway bridges. Two coatings of interest include the chemically bonded phosphate ceramics (CBPC) and the thermal diffusion galvanizing. These coating systems have been selected for further testing due to growing interest in corrosion mitigation systems, the scarcity of information detailing application and performance of these coatings on highway bridges, and their current commercial availability. The CBPC was tested in the as-received condition for new application. The thermal diffusion galvanizing has been advocated to include a topcoat because superficial staining due to high iron content can occur. The testing incorporated samples with and without a topcoat in order to elucidate the corrosion behavior of the zinc coating. Conventional three-coat systems and thermal spray coatings were also incorporated into the test matrix for comparison of material behavior with systems already utilized by FDOT.

# CHAPTER TWO: MATERIAL CHARACTERIZATION, SAMPLE PREPARATION, AND TEST ASSEMBLY

## 2.1. INTRODUCTION

Chemically bonded phosphate ceramic (CBPC) coating and the thermal diffusion galvanizing (TDG) coating systems were identified for study. CBPC coatings were of interest due to their beneficial material properties described by the manufacturer as well as the limited information in the technical literature. The properties of interest included the covalent bonding of the coatings, good metal substrate corrosion resistance, and ease of application and repair. Limited testing conducted by the State Materials Office (SMO) indicated the TDG coatings had good corrosion resistance, relative to conventional hot-dipped galvanized steel, in salt-fog and partial salt water immersion environments. After the preliminary testing by SMO, recommendations were made for use of TDG for small hardware if cost can be justified by its performance, but further testing was recommended for other applications.

Additionally, conventional three-coat painting and thermal spray metallizing were selected as control systems as these coating systems were already used as structural steel coatings on bridges in the state.

In addition to addressing application of CBPC and TDG coatings for structural steel, testing methods were designed to determine the performance of these coatings in alkaline environments representative of those encountered for reinforced concrete structures. It is noted here that some of the coating materials tested were not recommended for reinforced concrete applications.

## 2.2. MATERIALS

### *2.2.1 General*

The four coating systems selected for testing were CBPC, TDG, three-coat paint, and thermal-sprayed metallizing. Images of test samples in the as-received condition are shown in Figure 2.1. Initial characterization of the samples in the as-received condition included measurement of coating thickness, coating adhesion, and identification of coating features by optical microscopy. The coating thickness was measured using a DeFelsko Positector 6000 magnetic coating thickness gage. Nine readings were made on the surface of each test coupon. The coating adhesion was measured using a DeFelsko Positest pulloff adhesion tester and following ASTM D4541-02. Metallographic preparation was conducted using a series of 74, 20, and 10μm grit abrasive grinding papers followed by polishing with 3μm diamond suspension and 0.05μm silica suspension.

The base steel coupons for all of the coating systems were from the same material provider. The coupons were cut from a 1/8$^{th}$ inch thick plain carbon steel plate into 3x5 inch coupons. The coupons were sent to the respective coating applicators without any surface preparation. Surface blasting was conducted by the coating applicators according to their best practices prior to application of the coatings. Details of the test coating materials are shown in Table 2.1.

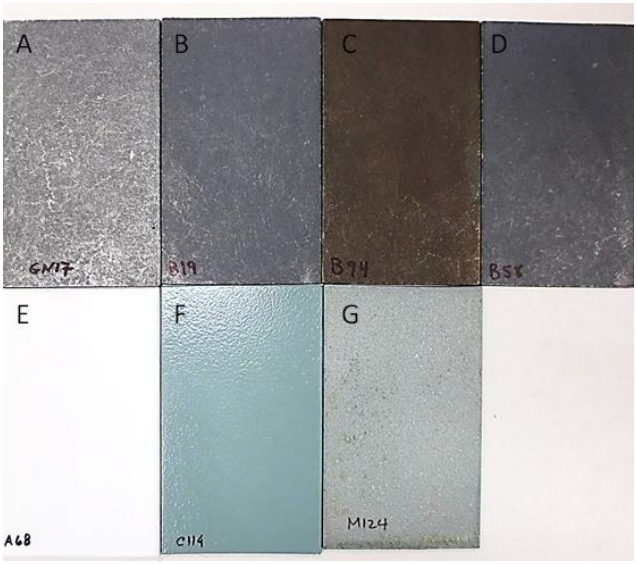


**Figure: 2.1 Coating Systems.**

A) TDG (plain), B) TDG (Topcoat A), C) TDG (Topcoat B), D) TDG (Topcoat A+B), E) CBPC, F) Three-Coat Paint,G) Metallizing

Table 2.1. Coating System

| | No. of Samples | Description |
|---|---|---|
| CBPC | 50 | One-sided |
| | 75 | Two-sided |
| TDG | 25 | Plain |
| | 25 | Topcoat A (trivalent passivate) |
| | 25 | Topcoat B (silicate based sealer) |
| | 60 | Topcoat A+B |
| 3-Coat | 115 | (Inorganic Zinc IOZ),+ (Cycloaliphatic Amine Epoxy)+ (Aliphatic Acrylic-Polyester Polyurethane) |
| Metallizing | 125 | 85/15 Zinc-Aluminum+Urethane |

### *2.2.2 CBPC*

The initial set of CBPC samples received only contained coating on one side of the metal coupon. The manufacturer was directed to coat all sides of the coupon in subsequent coupons. The desired coating thickness was to be based on the coating manufacturers best practice guidelines. However, a large variability in coating thickness was apparent in the received samples, indicating that the manufacturer's coating process was not properly controlled. The micrographs in Figure 2.2 show the typical appearance of the CPBC coating. As seen in Figure 2.3, the coating thickness ranged from ~10-50 mils. Product literature suggests that the coating thickness of the CPBC layer is dependent on the number of passes the sample receives during the spray application process. Samples also had local coating thickness variability with standard deviations ranging from 0.6 to ~6 mils. For testing, samples were sorted by similar coating thickness to avoid possible testing artifacts that may be associated with coating application. Presence of a protective phosphate rich layer on the steel substrate described in product literature as 2-20 µm thick was not readily visible by optical microscopy. At the highest magnification shown in Figure 2.2, there was visual indication of material of varying textures with a layer between the ceramic and steel substrate that was in the order of 50 µm. That intermediate layer did not appear to be continuous throughout the steel-to-ceramic coating interface. As will be described later, imaging with SEM also did not consistently reveal a continuous intermediate layer on the steel substrate.

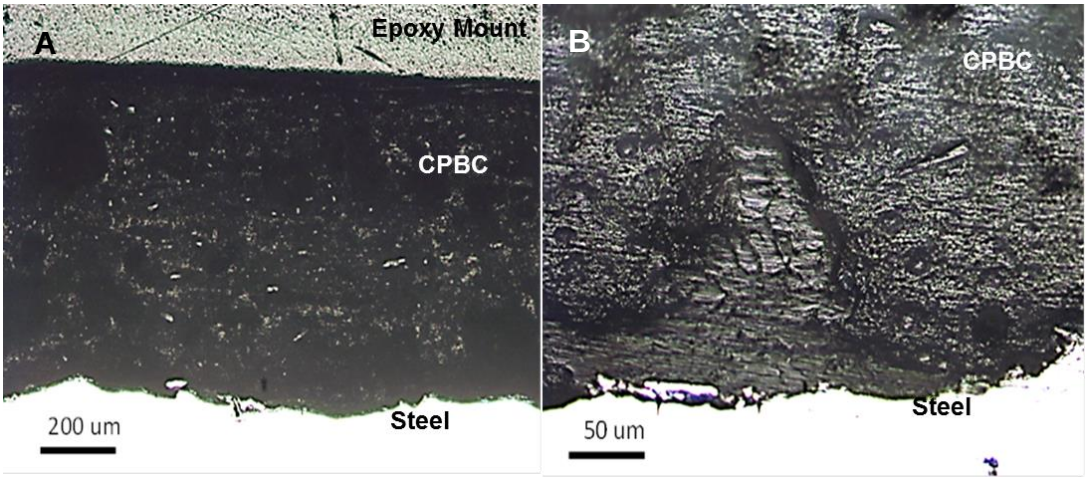


**Figure: 2.2 CBPC Coating on Steel Cross-Section Micrographs**
A) 5X Magnification. B) 20X Magnification.

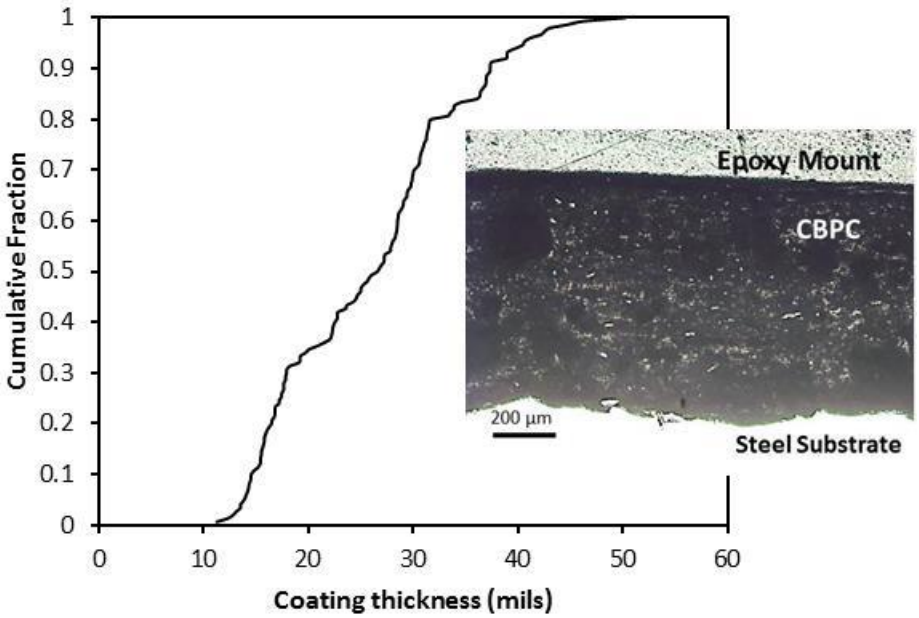


**Figure: 2.3 CBPC Sample Coating Thickness.**

Although variability in the thickness of the CBPC coating was observed, the as-received pull-off strengths were not greatly affected by coating thickness. All pull-off testing of coatings in the as-received condition had removal of the CBPC coating and had strengths less than 200 psi as shown in Figure 2.4. The coating was typically separated at the coating/steel substrate but some residue of the CBPC typically remained on the steel substrate. It is noted that the pull-off strength may not directly indicate efficacy in corrosion mitigation. However, this parameter is expected to give insight on material performance after exposure in aggressive environments such as coating degradation or disbondment that may possibly be important in corrosion development.

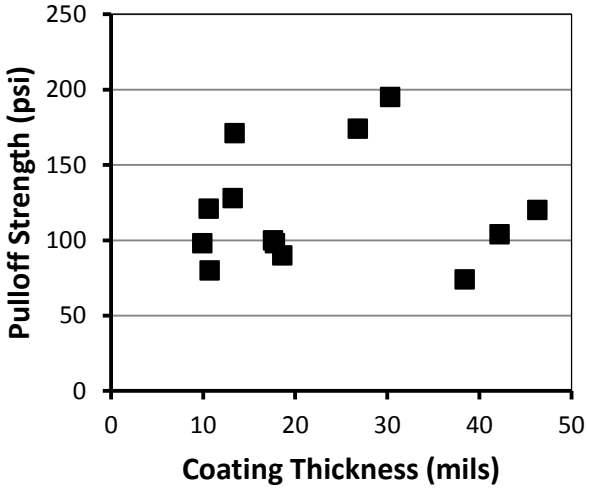


**Figure: 2.4 CBPC Coating Pull-off Strength.**

### *2.2.3 TDG*

Thermal diffusion galvanizing coated steel coupons were provided by the manufacturer with four variations in topcoat application. The TDG layer was to be 40-50 µm (~1.6-2 mils). The first set of samples was Plain TDG with no topcoat. The second set had a single topcoat and was labeled as Topcoat A and the third set had a single coat of a second topcoat and was labeled as Topcoat B. The final set of samples had a single coat each of the two topcoats and was labeled Topcoat A+B. Topcoat A was described in product literature as a trivalent passivate and Topcoat B was described as a silicate-based sealer. Figure 2.5 shows the typical appearance of the TDG coating system with and without topcoat.

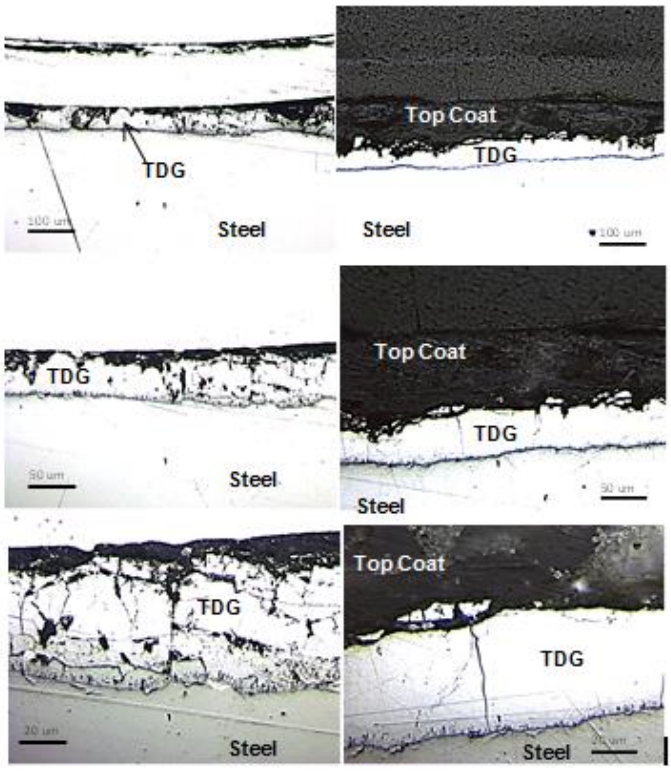


**Figure: 2.5 TDG Coating on Steel Cross-Section Micrographs**.
**Left-Plain. Right-Topcoat A+B.**

The cumulative fraction of coating thickness is shown in Figure 2.6. Coating thickness data were from measurements on both sides of the coupon samples. The coating thickness reported is the total coating thickness including the topcoat application. The thickness of TDG samples observed by optical microscopy was on the order of the median value measured with the magnetic coating thickness gauge. The thickness of the topcoat (on samples with both topcoats, Topcoat A+B) was on the order of 100 µm (~4 mils). Most of the coating thicknesses ranged from about 1.5 mils to about 2.5 mils. About 40% of the plain TDG coupon samples were greater than 2.5 mils (maximum

value was about 7 mils), indicating that the manufacturer's coating process was not properly controlled.

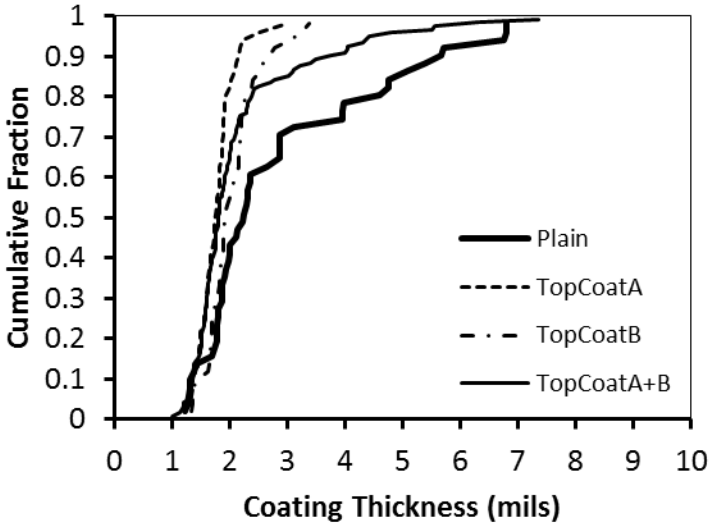


**Figure: 2.6. TDG Sample Coating Thickness.**

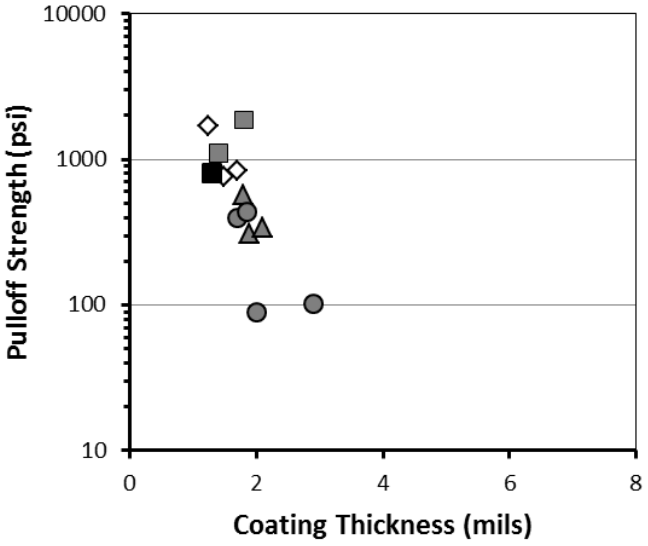


**Figure: 2.7 TDG Coating Pull-Off Strength**.
Diamond - Plain. Square - Topcoat A. Triangle - Topcoat B. Circle -Topcoat A+B. White - Glue Failure. Grey - Topcoat Failure. Black - Coating Failure.

In the test coupons selected for examination by optical microscopy, some of the intermetallic layers were distinguishable. The intermediate layer adjacent to the steel substrate was on the order of 10 µm. The TDG layer had varying levels of defects that were visible as cracks in the zinc material. The cracks in the plain TDG sample

appeared more severe than the cracks observed in the TDG sample with Topcoat A+B. The cracks there did not appear to continue into the topcoat. It is noted that the sample preparation methodology included grinding and coarse polishing with water, which may have caused some degradation of the TDG. Fine polishing used a silica-alumina-based abrasive slurry with alcohol for lubrication.

Variability in pull-off strength was apparent in testing of TDG samples with the various topcoat applications (Figure 2.7). Most of the testing resulted in apparent removal of the topcoat when present, and pull-off strengths less than 1,000 psi. The pull-off strength of samples with Topcoat A appeared to be greater than the strength of samples with Topcoat B, or with both, Topcoat A+B. Pull-off strength of samples with Topcoat A exceeded 1,000 psi except for one that had a pull-off strength of ~800 psi, where some of the metallic coated was removed. Samples without topcoat exhibited adhesive failure, and had pull-off strengths exceeding 800 psi.

### *2.2.4 Three-Coat Paint*

The 3-coat paint system used by the manufacturer consisted of coupons with a solvent based inorganic zinc coat, followed by a Cycloaliphatic Amine Epoxy coat and an Aliphatic Acrylic-Polyester Polyurethane. Typical cross-section appearance is shown in Figure 2.8. The cumulative fraction of coating thickness is shown in Figure 2.9. Coating thickness data was obtained from both sides of the coupon samples. The coating thickness reported is the total coating thickness, comprised of the inorganic zinc (IOZ) layer, epoxy layer, and topcoat.

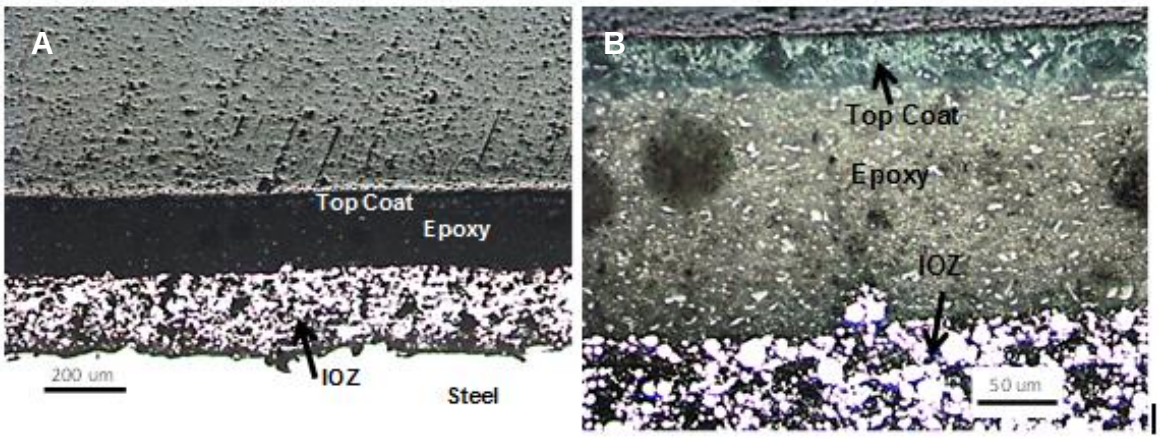


**Figure: 2.8 Three-Coat Paint Coating on Steel Cross-Section Micrographs**.
A) 5X Magnification. B) 20X Magnification.

Pull-off strength testing of the three-coat paint system resulted in failure of the adhesive (Figure 2.10). Poor adhesion of the test dolley to the topcoat resulted in inconclusive

results. Different adhesive epoxies will be used for pull-off strength measurements for this coating system.

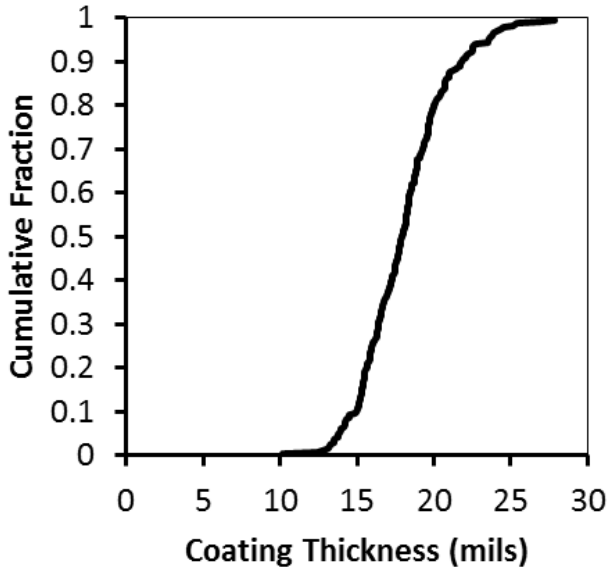


**Figure: 2.9 Three-Coat Paint Sample Coating Thickness**.

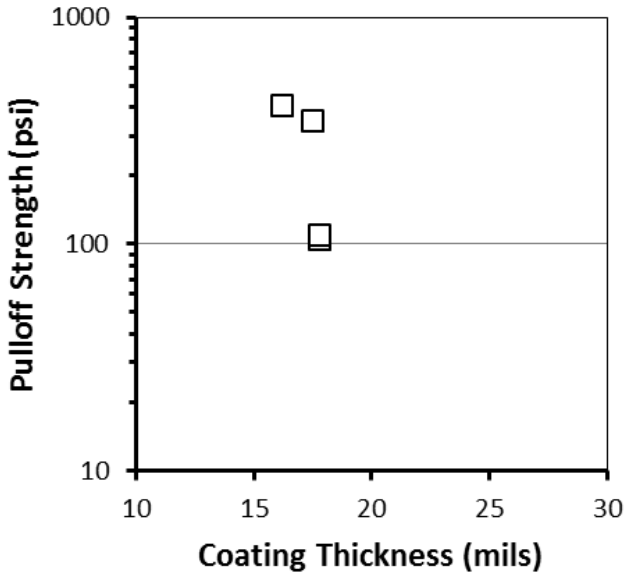


**Figure: 2.10 Three-Coat Coating Pull-Off Strength**.
All testing resulted in failure of the adhesive.

### *2.2.5 Metallizing*

Samples of coupons with 85/15 zinc/aluminum arc-sprayed coating were prepared by a metallizing applicator. The metallizing layer was to be ~200-300 µm (8-12 mils). The

coupon samples were originally intended to be coated with a topcoat and some samples had some visual indication of a surface applied coating material on top of the metallizing. However, limited assessment by optical microscopy did not show the presence of a topcoat. Micrographs of the cross-section are shown in Figure 2.11. The cumulative fraction of coating thickness is shown in Figure 2.12. Coating thickness was measured from both sides of the coupon samples. The coating thickness reported is the total coating thickness.

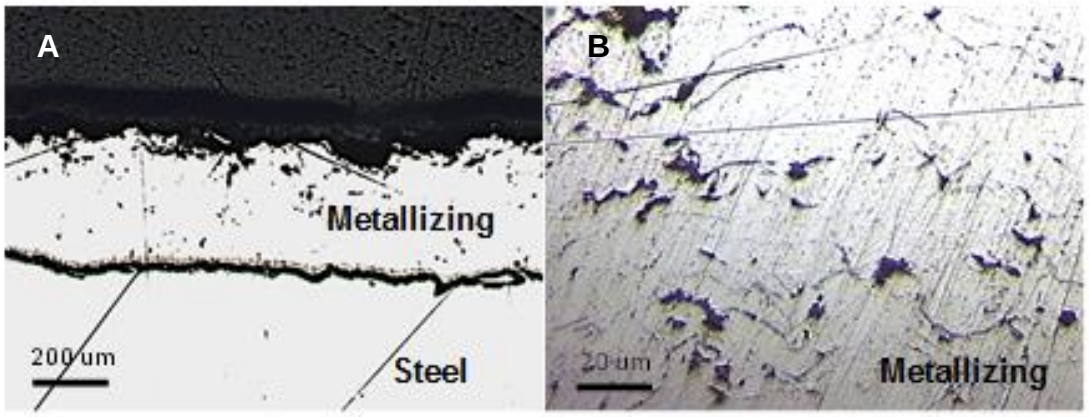


**Figure: 2.11 Metallized Steel Cross-Section Micrographs**.
A) 5X Magnification. B) 50X Magnification.

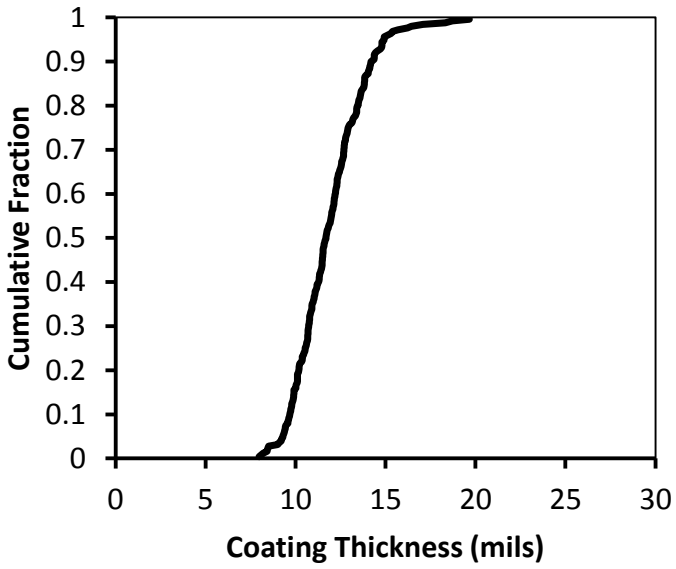


**Figure: 2.12 Metallizing Sample Coating Thickness**.

All coating pull-off strength tests resulted in separation of the zinc coating from the metal substrate and the pull-off strength varied from ~100 to ~1000 psi. The pull-off

strength did not appear to be dependent on the thickness of the coating. The cause for some of the low pull-off strengths was not determined.

### 2.3. DEFECT CONDITIONS

Initial defects were made on select samples by scribing a 1 inch, centered, straight scratch deep enough to penetrate the coating to the underlying metal interface with an Elcometer 1538 DIN scratch tool with 0.5 mm cutter. The scratch was made to help identify corrosion mitigation of the metal substrate by the coating system. Characteristics of interest included identifying the extent of rust accumulation at the scratch, corrosion development under the coating near and away from the scratch, coating disbondment and adhesion/cohesion loss, and coating integrity. Samples were placed in outdoor exposure for extended-term testing, salt-fog chamber for exposure in aggressive salt conditions, and immersed in solutions with various solution chemistries associated with bridge exposure conditions. Figure 2.13 shows results from initial testing of CBPC samples with introduced scratch defects that were immersed in various aggressive chemical solutions. Coating conditions of samples placed in outdoor exposure and salt-fog exposure prior to exposure are shown in Appendix B for documentation.

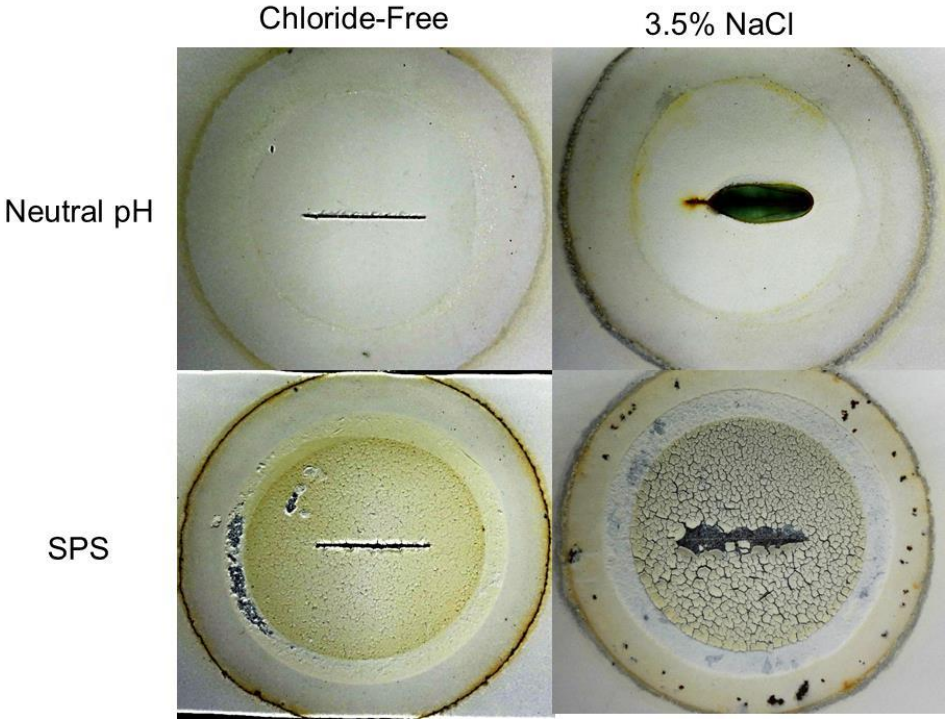


**Figure: 2.13 Preliminary Results of CBPC Coating Performance in Aggressive Chemical Solutions**.

Possible coating defects due to fabrication and bending are not likely to be representative for coating applications on structural steel elements, thus outdoor

exposures of samples with that type of defect were not considered. Coating defects due to fabrication and bending are important factors in the corrosion durability of coated steel reinforcement for reinforced concrete applications. Electrochemical tests were made to identify corrosion behavior. It is noted that severe mechanical deformations were not recommended for these coating systems, but were made to identify possible application for reinforced steel bar that may require fabrication. The mechanical deformations may also provide information on coating application quality and its role in possible corrosion mitigation or corrosion development.

## 2.4. TEST ASSEMBLY

### *2.4.1 Outdoor Exposure*

Two outdoor exposure test sites and exposure racks generally conforming to ASTM G7-11 were prepared in South Florida for testing. The locations of the test sites are shown in Figure 2.14. Aluminum test racks approximately 10 feet in length and 5 feet in height were made available at both sites. One test rack was utilized in the outdoor exposure site referred to as Beach Test Site and two racks were utilized at the Inland Test Site. The test racks have a southern exposure with an angle of 45° with the horizon. The pre-exposure condition of samples placed in outdoor exposure is shown in Appendix B.


**Figure: 2.14 Location of Outdoor Exposure Sites**.

#### *2.4.1.1 Beach Test Site*

The Beach Test Site at Tea Table Key in Islamorada, FL is maintained by FDOT and is situated immediately adjacent to the ocean with a strong presence of warm humid salt air. The test setup is shown in Figure 2.15. The ground cover is typically limestone rock. Video monitoring and weather data is available with the support of existing FDOT weather stations at the site and reports are available online: (http://bridgemonitoring.com/bridges/TT/tt.htm). It is noted that there was some shading

on part of the test rack in the late afternoon due to overgrown vegetation adjacent to the test site.

Initial outdoor exposure was started on November 1, 2013. Forty-eight coated samples, 16 each of CBPC, three-coat paint, and metallizing were installed; 8 in the as-received condition and 8 with a scratch defect. Twenty-four TDG samples were installed; 16 samples with Topcoat A+B (8 in the as-received condition and 8 with a scratch defect), and 8 plain samples with no topcoat and with a scratch defect.

**Figure: 2.15 Outdoor Exposure of Coupons at Beach Test Site**.

### *2.4.1.2 Inland Test Site*

The Inland Test Site was located on the Florida International University engineering campus in Miami, FL approximately 10 miles from the coast. The ground cover at the Inland Test Site was short grass. The test setup is shown in Figure 2.16.

Initial outdoor exposure was started on November 1, 2013. Forty-eight coated samples, 16 each of CBPC, three-coat paint, and metallizing were installed; 8 in the as-received condition and 8 with a scratch defect. Forty TDG samples were installed; 16 samples with Topcoat A+B (8 in the as-received condition and 8 with a scratch defect), 8 plain samples with no topcoat and with a scratch defect, 8 samples with Topcoat A and with a scratch defect, and 8 samples with Topcoat B and with a scratch defect.

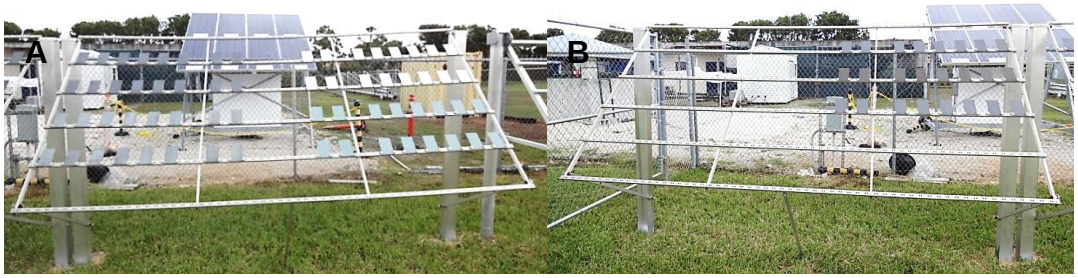


**Figure: 2.16 Outdoor Exposure of Coupons at Inland Test Site**.
A) CBPC, Three-coat and Metalized samples. B) TDG samples.

### *2.4.2 Salt-Fog Exposure*

A salt-fog chamber conforming to ASTM B117-03 was set up at Florida International University (Figure 2.17). Salt solution was prepared by mixing 5 parts by mass of analytical grade sodium chloride, NaCl, with 95 parts by mass of distilled water. The coated metal coupons were held upright, typically at a 40 degree angle. The pre-exposure condition of samples placed in the salt-fog chamber is shown in Appendix B.

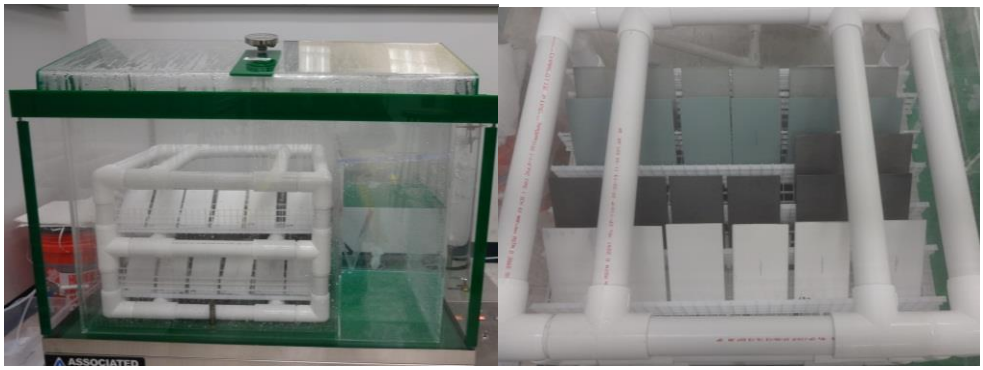

**Figure: 2.17 Test setup for Salt-Fog testing**.

### *2.4.3 Laboratory Electrochemical Testing*

Laboratory testing of the samples included electrochemical testing of the coated steel coupons. Acrylic test assemblies, as shown in Figure 2.18, were fabricated to allow exposure of part of the test coupons to aggressive chemical solutions. Electrochemical testing included use of a Gamry Reference 600 potentiostat and impedance analyzer as well as an ECM8 Multiplexer.

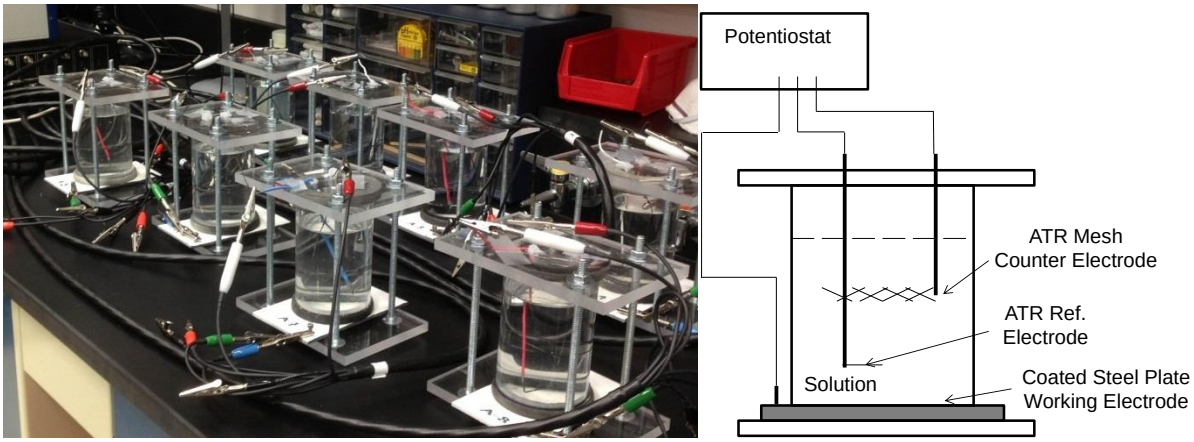


**Figure: 2.18 Test Setup for Electrochemical Testing**.

Test cells were made to accommodate reference and auxiliary electrodes required for corrosion and electrochemical impedance spectroscopy (EIS) testing. Activated titanium was used as temporary reference and counter electrodes [Castro et al., 1992]. The activated titanium reference electrode was calibrated with a saturated calomel reference

electrode (SCE). The neutral pH solution simulating runoff and pooled drainage water was made from distilled water with and without 3.5% sodium chloride. High pH solution (pH ~13) with and without 3.5% sodium chloride was made to simulate pore water solution in aggressive marine conditions [Lau and Sagüés, 2009]. Corrosion testing involved open-circuit potential (OCP) measurements, linear polarization resistance (LPR) measurements, and electrochemical impedance spectroscopy (EIS). LPR testing was done from the initial OCP to -25mV vs. OCP at a scan rate of 0.05mV/s.

The corrosion currents, $I_{corr}$, measured by a linear polarization method, were calculated by Faradic Conversion [Fontana and Greene, 1986] using Equation 2,

$$I_{corr} = \frac{B}{Rp} \tag{2.}$$

where the Stern-Geary coefficient, B, was assumed to be 26 mV for active corrosion conditions and Rp, polarization resistance, is defined as the ratio of change in potential to amount of required current [Vetter, 1967]

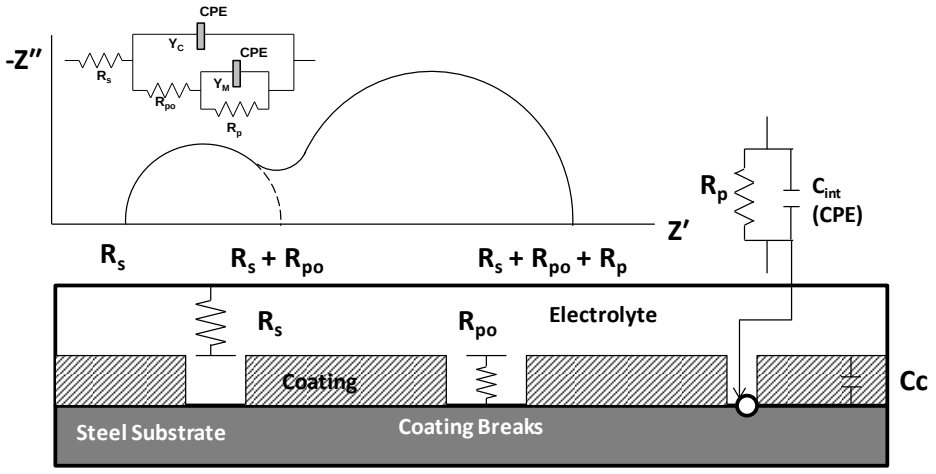


**Figure 2.19 Idealized Impedance Diagram of Coated Metal System with Coating Breaks and Equivalent Circuit Analog.**

EIS testing was done at the OCP condition with 10mV AC perturbation voltage [Murray, 1997; El-Mahdy et al., 2000; Mahdavian et al., 2006] with frequencies between 1 mHz and 100 kHz. The impedance behavior was considered to be characteristic of a coated metal with coating breaks, as shown in the Figure 2.19, and with total impedance expressed as shown in Equation 3.

$$Z = Rs + \cfrac{1}{Y_{oc}(j\omega)^{n_c} + \cfrac{1}{Rpo + \cfrac{1}{Y_{om}(j\omega)^{n_m} + \cfrac{1}{Rp}}}} \tag{3}$$

The solution resistance, $R_s$, is the resistance between the working and reference electrodes, the pore resistance, $R_{po}$, is the resistance associated with pores and defects in the coating, the polarization resistance, and $R_p$, is a function of the corrosion rate. The impedance of the electrical double layer and the coating capacitance are expressed in the form of constant phase elements $Z_{CPE} = 1/(Y_o(j\omega)^n$ [Orazem and Tribollet, 2008] where $Y_o$ is the pre-exponential term, ω is the angular frequency, and n is a real number $0<n<1$. The subscripts c and m refer to the impedance of the coating and double layer, respectively.

Scratches exposing the underlying steel, 25.4 mm in length and 0.5 mm wide, were made in selected samples exposed in aqueous immersion environments. Further details are provided in Chapter 3.

## CHAPTER THREE: IMMERSION EXPOSURE AND ELECTROCHEMICAL TESTING

A summary of the findings discussed below is provided in Appendix A.

### 3.1 CBPC WITH SCRIBE COATING DEFECTS

Initial electrochemical testing of coating corrosion mitigation performance in solution commenced with exposing CBPC coated metal coupons to neutral pH water or high pH solution with and without chlorides. Immersion in neutral pH water provided an aggressive environment analogous to coatings exposed to wet environments (e.g. pooled runoff water). The simulated pore solution (SPS), pH 13.3, provided an environment simulating conditions in concrete to identify performance of coated steel in reinforced concrete applications. More aggressive conditions were created by adding three point five percentages by weight of sodium chloride. Furthermore, on some samples a 1-inch long scratch was made that exposed the base steel substrate so that this area would be immediately at risk for corrosion.

As described earlier, the as-received pull-off strengths of the CBPC-coated samples were less than 200 psi, with all tests resulting in partial separation of the ceramic material from the steel substrate. Testing of samples after immersion in neutral pH resulted in similar strengths (Figure 3.1). Optical microscopy of sample cross-sections indicated some coating degradation in regions where the coatings were submerged (Figure 3.2). Significant coating degradation was observed for samples immersed in chloride and chloride-free SPS (Figure 3.3).

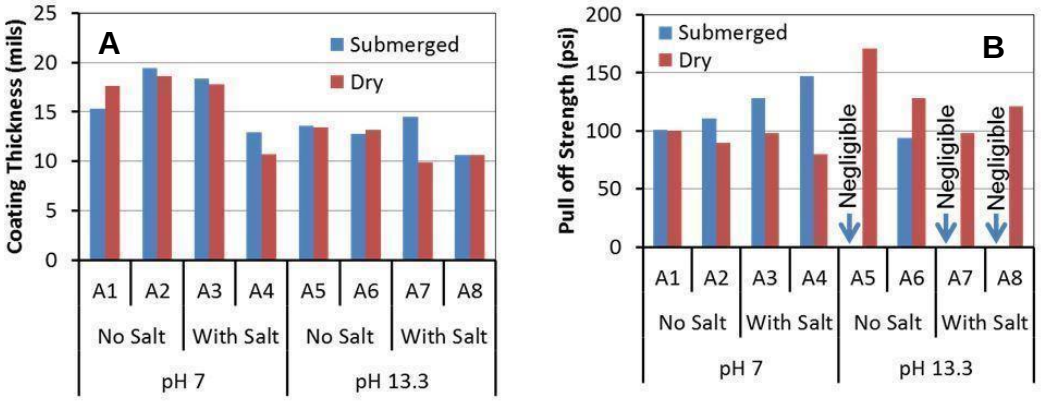


**Figure: 3.1 CBPC Coating Thickness and Pull-off Strength.**
A) Coating thickness. B) Coating pull-off strength.

As expected, corrosion developed in samples immersed in chloride solutions. Electrochemical potentials of the samples in chloride solutions were typically more negative than -500 $mV_{SCE}$ (Figure 3.4). Interestingly, the corrosion current declined during testing of samples immersed in chloride SPS even though coating degradation

and increases in exposed steel surface area occurred. Expectation would be that the corrosion current would increase for active steel with increased exposed steel area. Furthermore, corrosion of the exposed steel submerged in the salt solution was minimal. However, localized corrosion did occur in crevice regions of the test samples where a gasket was placed. In these regions, there was visual evidence of coating degradation due to the alkaline solution, and localized corrosion developed. In the chloride neutral pH solution, the corrosion current remained high and there was significant rust accumulation in the vicinity of the scratch defect.

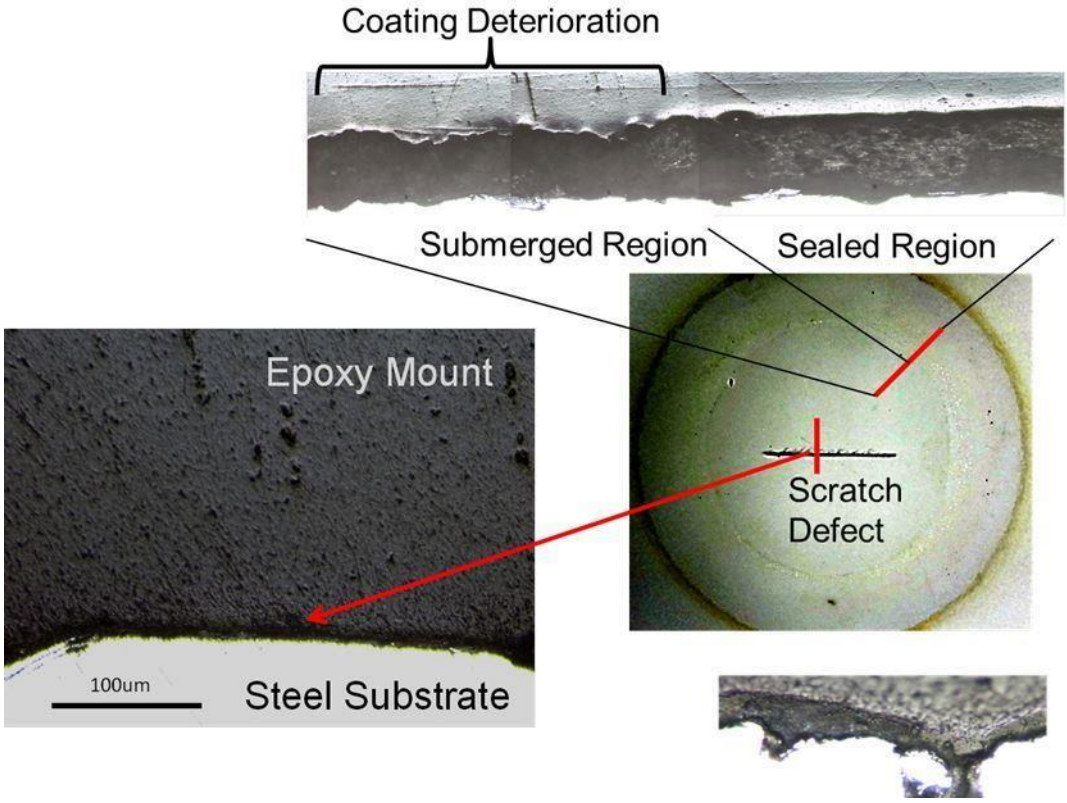


**Figure: 3.2 Coating Degradation in Submerged Condition.**

Results of electrochemical impedance spectroscopy are shown in Figure 3.5. The results did not reveal significant differentiation in the solution or coating characteristics even though significant coating degradation occurred. It was likely that the impedance behavior was dominated by the steel-solution interface at the scratch defects. The measurements were sensitive to identify salt presence in the solution. Both the solution resistance and pore resistance resolved from impedance spectroscopy for samples immersed in solution with no salt additions were greater than those in chloride solutions (Figure 3.6). The coating pore resistance increased for the scribed coated samples placed in the neutral pH chloride solution, which indicated accumulation of corrosion product in the vicinity of the scratch defect.

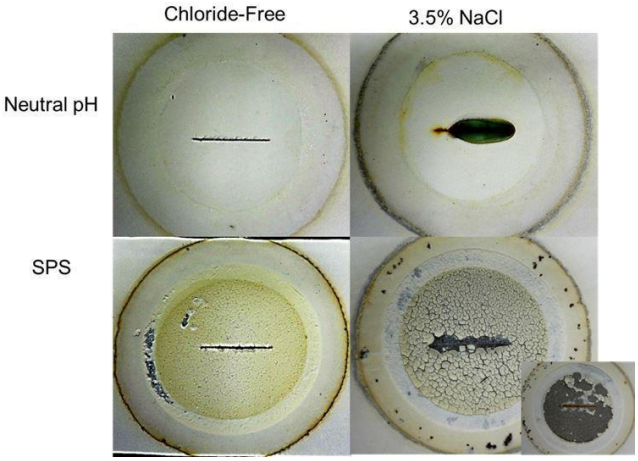


**Figure: 3.3 Coating Degradation after Electrochemical Test.**

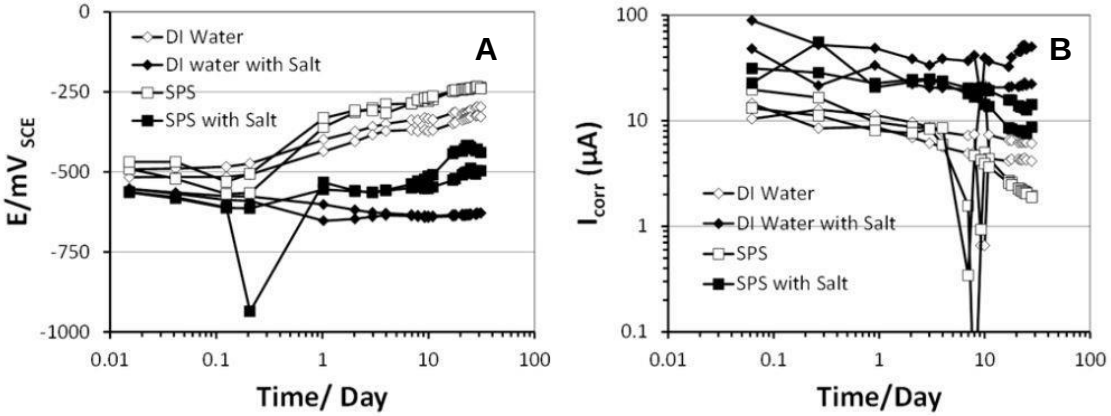


**Figure: 3.4 OCP and Corrosion Current during Exposure of CBPC.**
A) Open circuit potential. B) Corrosion current.

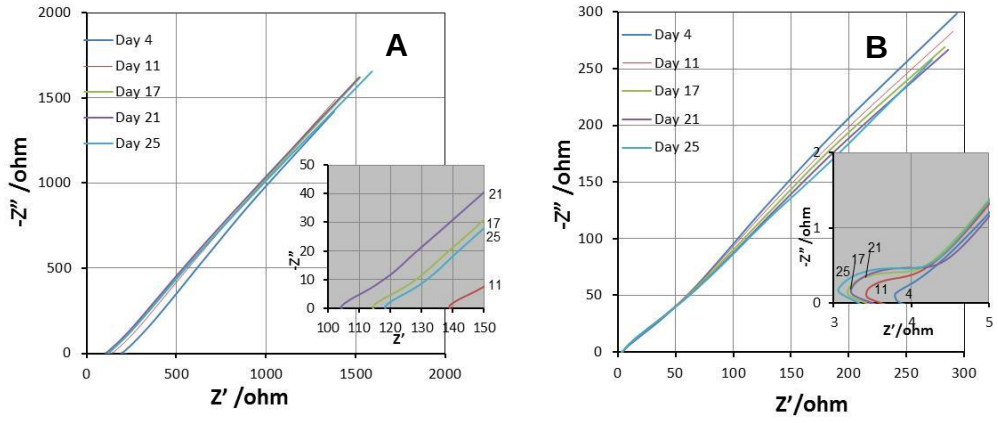


**Figure: 3.5 Nyquist Plot of CBPC Samples in Neutral pH.**
A) Without chloride. B) With chloride.

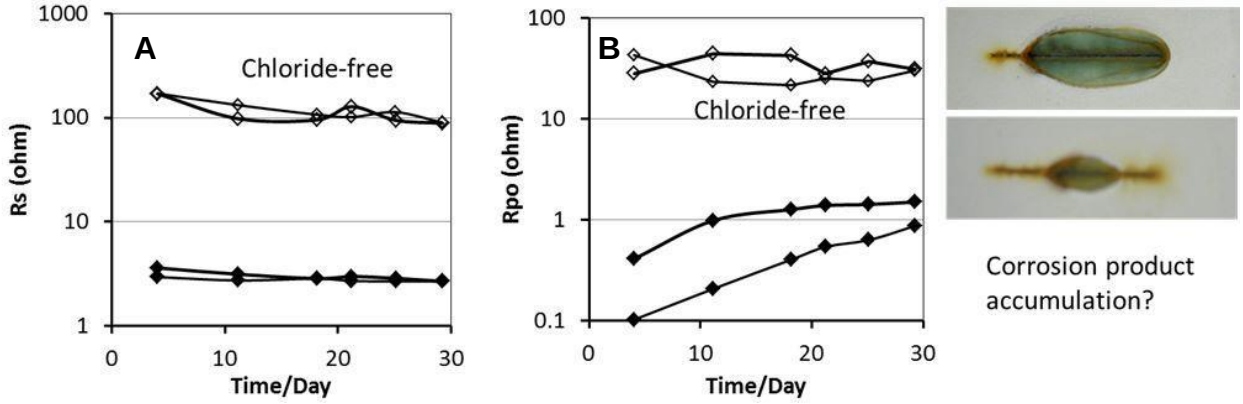


**Figure: 3.6 Electrochemical Parameters for CBPC Sample in Neutral pH.**
A) Solution resistance. B) Pore resistance.

### 3.2 CBPC IN NON-SCRIBED CONDITION

Degradation of the phosphate ceramic coating was observed during initial testing in solution, especially in alkaline solutions. Additional testing was conducted to better understand its performance in those environments. In this case however, no defects emanated from the surface so that the coating degradation and corrosion mitigation performance could be evaluated in the coating as-received condition.

As seen in Figures 3.7-3.8 and in comparison with Figure 3.4, the electrochemical behavior of the coated systems with and without defects exposing steel was identical in all tested solutions (including neutral and pH13 solution, with and without chloride ion). This was not necessarily expected, as the coating without defects exposing steel was thought to maintain characteristics of a barrier coating. Upon moisture penetration through the coating pores, the metal substrate developed electrical potentials generally indicative of passive corrosion conditions in the salt-free solutions and active corrosion in the chloride solutions. The corrosion currents determined by linear polarization resistance measurements furthermore supported the level of corrosion activity of the steel beneath the ceramic coating.

Significant coating degradation was observed when exposed to SPS solution, Figure 3.9. Similar to earlier testing with exposed steel at scratch defects, there was not excessive accumulation of corrosion product even though significant surface area was exposed to the chloride solution after severe degradation of the coating. Crevice corrosion also developed where a rubber gasket was placed in the test cell.

Severe coating degradation was also observed for one of the duplicate samples immersed in chloride neutral pH solution. In that sample, small corrosion spots developed throughout the exposed surface. In the second sample, visual observation indicated that the coating remained generally intact while immersed in solution (cracks

formed during drying). In the earlier testing of samples with introduced scratch defects, corrosion occurred at the exposed steel. As such, it was expected that the coating in the as-received condition would mitigate corrosion formation, but as shown in Figures 3.7 and 3.8, high corrosion activity was measured for the duplicate samples in the neutral pH chloride solution. However, upon examination after exposure in solution (Figure 3.10), significant corrosion developed under the region of the coating that was immersed in solution. The rust accumulation there was not attributed to pre-existing surface rust because the degree of corrosion was much less in the regions of the samples not immersed in solution. This finding indicates that localized undercoating corrosion occurred.

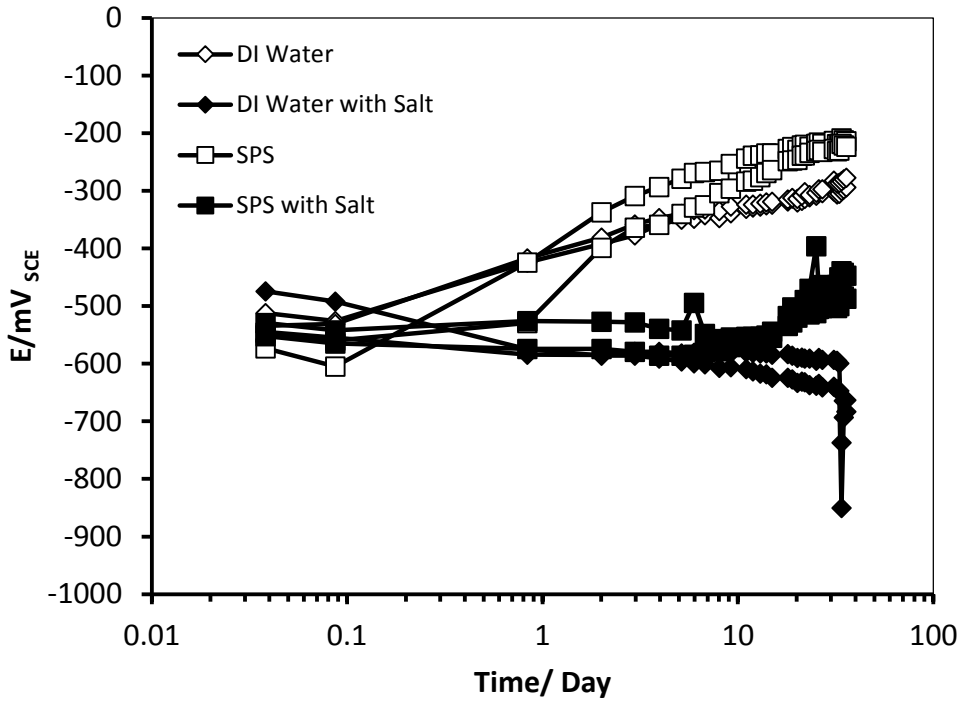


**Figure: 3.7 Open Circuit Potential of CBPC Coated Steel.**

The coating thickness was initially measured at a fixed position in the center of the test sample prior to immersion in solution. After immersion in solution for ~30 days, the coating thickness at the same location was measured again. It was evident that most samples exposed in the pH 13 solution showed a decrease in the coating thickness and, in an extreme case, the coating was completely removed showing 100% loss, Figure 3.11. Unexpectedly, some coating thickness measurements made after immersion showed greater values than for the as-received condition prior to immersion. Since the measurements were made at the same location on the test sample, it was difficult to reconcile this difference, barring operator error. However, it was noted that corrosion product accumulation was present in the cases where this aberration was most prominent, particularly in solution with salt. It was thought that the coating

thickness measurements may have accounted for undercoating corrosion development such as that shown in Figure 3.10.

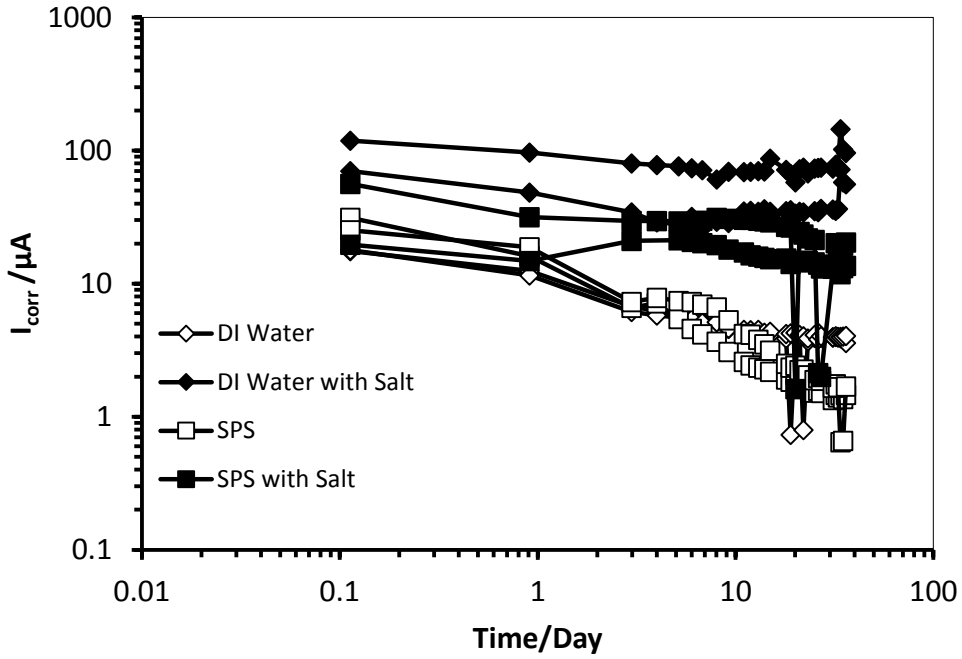


**Figure: 3.8 Corrosion Current for CBPC Coated Steel.**

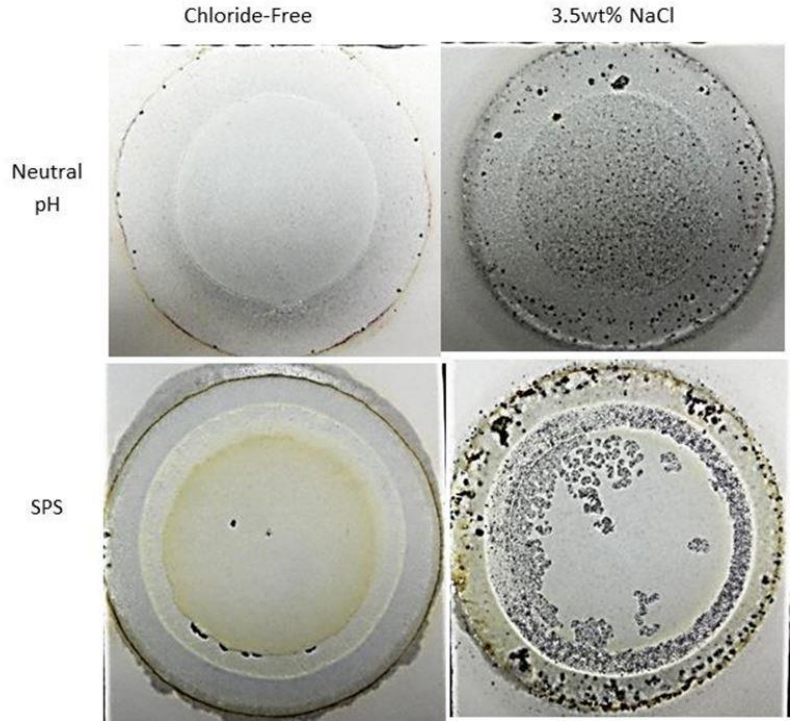


**Figure: 3.9 CBPC Coating After Immersion in Solution.**

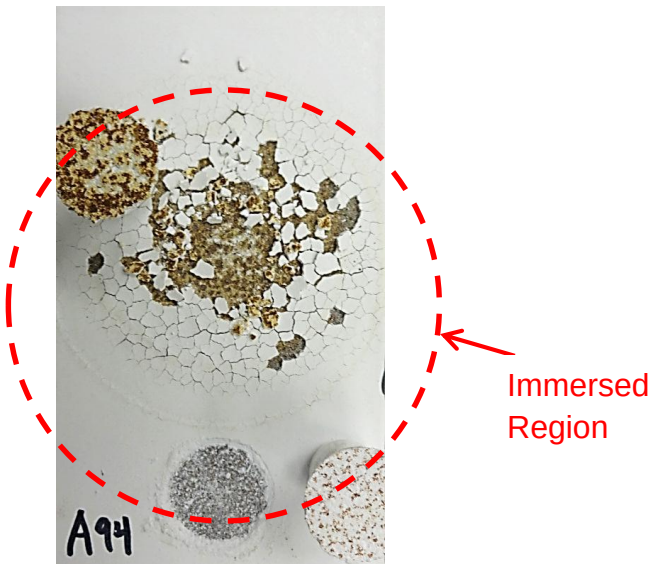


**Figure: 3.10 Under Coating Corrosion Development** (Neutral pH, 3.5wt% NaCl).

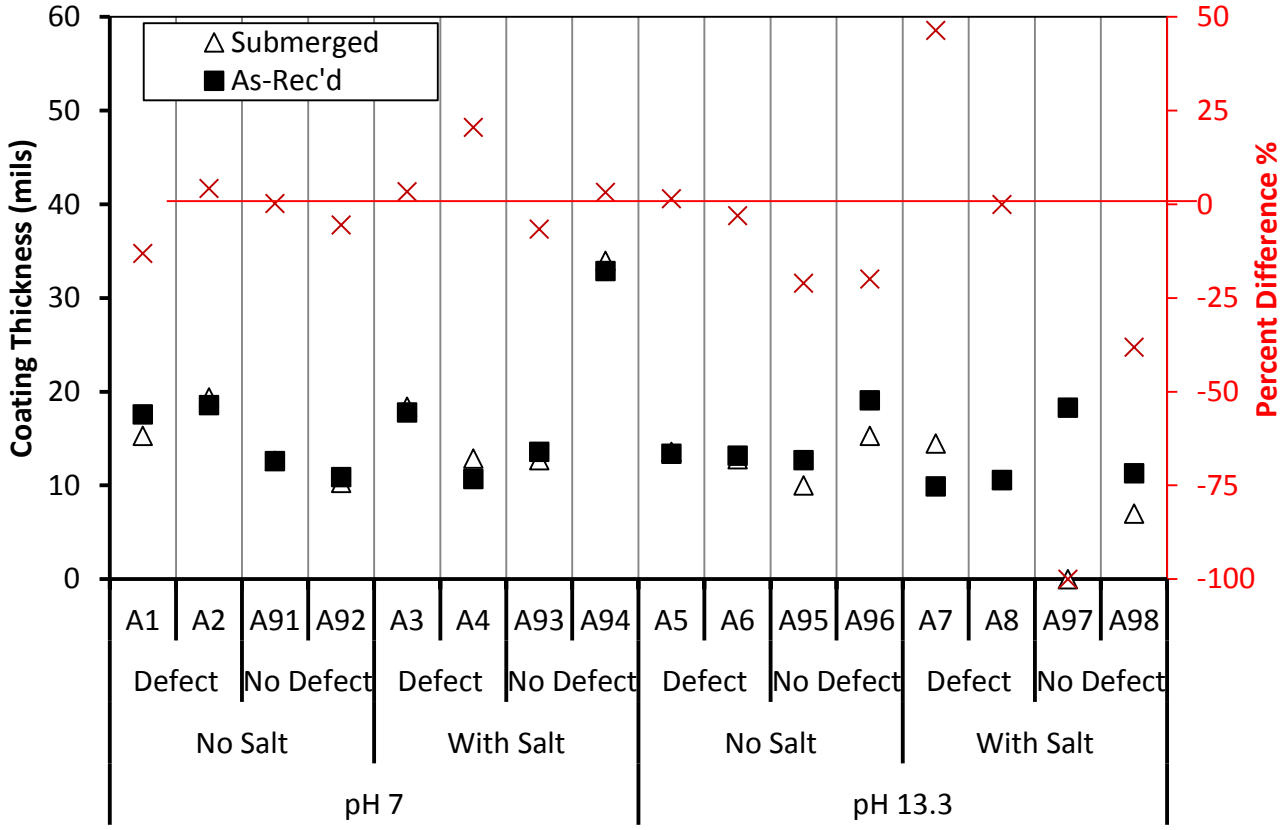


**Figure: 3.11 Coating Thickness.**

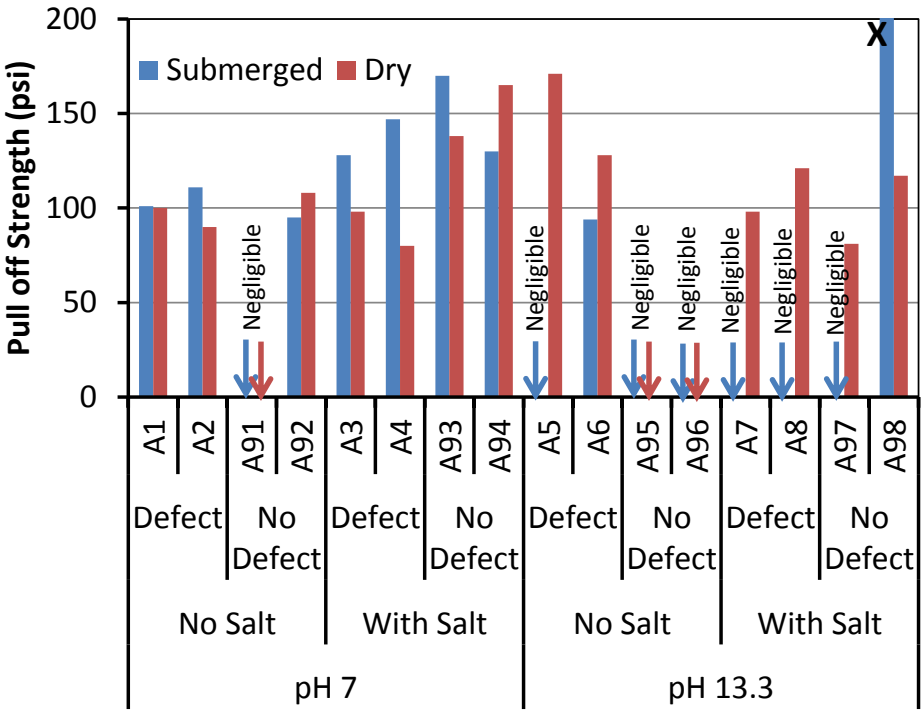


**Figure: 3.12 Adhesion Pull-Off Strength.**
X: Glue failure of test dolley set on exposed steel surface.

The coating adhesion pull-off strength (Figure 3.12) was measured on the samples after immersion testing. The center portion of the sample that was immersed, as well as a location on the perifery of the test sample not subjected to immersion, were tested (as demonstrated in Figure 3.10). Similar to earlier findings, the coating adhesion pull-off strength was typically less than 200 psi. Also similar to earlier finding, the high pH solution had a severe impact on the durability of the coatings as evidenced by the low/negligible pull-off strengths of the coatings after immersion in those environments. In one case, a pull-off strength greater than 700 psi was measured, but that was due to the fact that the coating had been completely separated from the metal substrate and the test dolley was set on the metal surface. One sample placed in pH 7 solution also had low pull-off strengths.

### 3.3 TDG

TDG steel coupons with Topcoat A and Topcoat B were immersed in neutral and alkaline solutions for ~40 days. Electrochemical impedance spectroscopy testing of TDG with Topcoat A and Topcoat B provided a non-destructive method to assess the electrochemical properties of the corrosion system and a method to assess physical coating conditions by comparing the impedance response to the corresponding electrical analog [Barsoukov and MacDonald, 2005]. The conventional interpretation of

the impedance response of a coated metal interface was assumed as a first approach to evaluate possible degradation. An equivalent circuit analog described in Chapter 2 was used to fit the impedance data to the physico-electrochemical parameters associated with that system. As part of preliminary analysis, high frequency impedance values found in the range of 10 kHz to100 kHz that deviated from behavior described by the chosen circuit analog were truncated and not used in the analysis. Furthermore, the low frequency impedance values found in the range of 1 mHz to 10 mHz were also truncated. Sensitivity of fitting of high frequency impedance response with those low frequency impedance data was not evaluated. The exact impedance behavior of the topcoats will require better modeling that takes into account the physico-electrochemical interactions of the topcoat materials with the TDG, the electrolyte, as well as possible heterogeneities related to crevice development. Non-ideal capacitive behavior and other factors due to heterogeneities, including non-uniform current distribution in the coating and metal-electrolyte interface, were represented in part by constant phase elements. Typical results of impedance testing of the TDG samples are presented in Figure 3.13. For brevity, impedance diagrams from other testing are not shown. Instead, only a general description and trend in resolved pore resistance are described next. The solution resistance is shown as the high frequency real impedance limit. As expected, the solution resistance was characteristic of the mixed solution. SPS and salt solutions had low $R_s$ values on the order of 1 ohm throughout the duration of the test. The chloride-free, neutral pH solution had initially very high values, on the order of several thousand ohms, and decreased to below 1000 ohm. Initial and final solution conductivity measurements verified those trends.

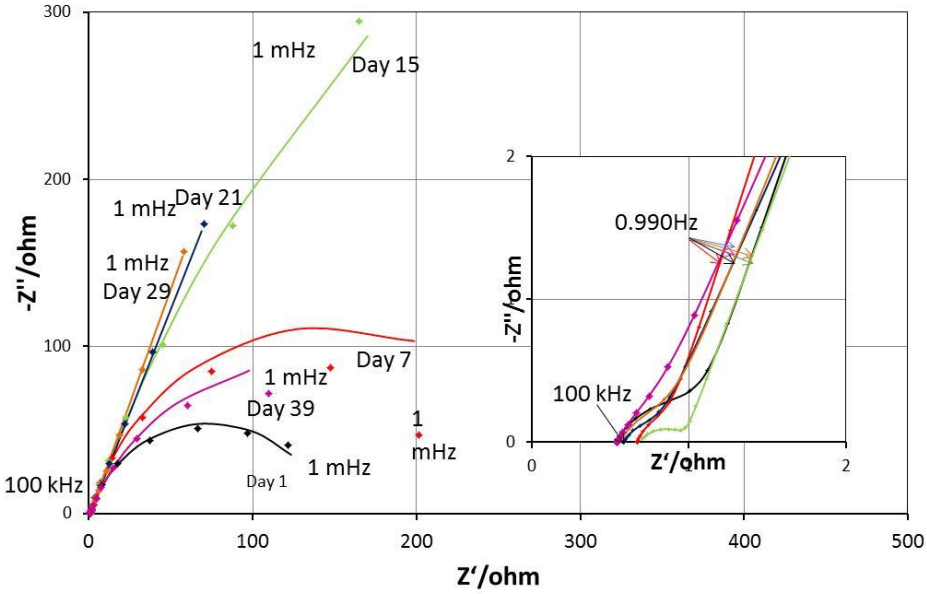


**Figure: 3.13 Nyquist diagram for TDG** (Topcoat B) sample in High pH with Salt.

Assuming that the coating defects can be idealized as a distribution of cylindrical pores [Grundmeier et al., 2000] of radius r, the pore resistance, $R_{po}$, may be evaluated as $R_{po}=\rho d/(n\pi r^2)$ where ρ is the electrolyte resistivity within the pore, d is the thickness, r is the pore radius, and n is the number of pores. Even though the as-received coating thickness for TDG samples with Topcoats A and B were about the same, ranging from 32 to 40 µm and the same solution mixes (with identical electrolyte conductivity per solution type) were used, the resolved initial $R_{po}$ from curve fitting was generally higher for TDG with Topcoat A in each tested solution. Variability in the steel area exposed by the scribe line would likely have influence, especially due to the different physical properties of the topcoat. However, a cursory view of the findings with the general relationship described above indicates that fewer, smaller, or less permeable defects were present for the samples with Topcoat A than Topcoat B. The $R_{po}$ trends (Figure 3.14) with time indicated a general decrease in pore resistance for TDG with Topcoat B in SPS solution after approximately one week which may be indicative of disturbances to the coating. This trend also corroborates with the visual and physical indication of coating damage in alkaline solution described earlier. $R_{po}$ trends for TDG with Topcoat A in alkaline solution indicate the resistance was mostly stable. $R_{po}$ trends with time for Topcoats A and B in neutral pH solution increased, which may be indicative of pore blocking by passivating zinc. A larger increase in $R_{po}$ with time for Topcoat B compared to Topcoat A may indicate greater effect from this phenomenon.

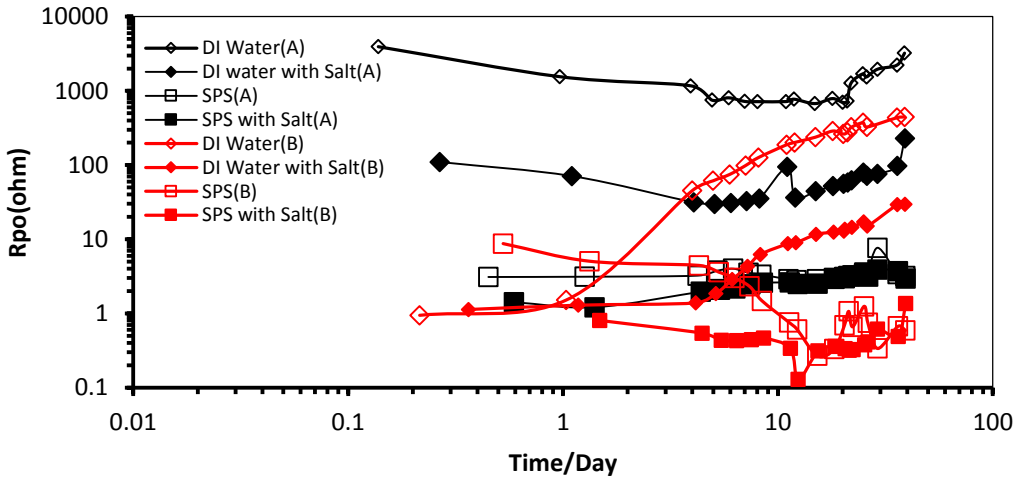


**Figure: 3.14 Coating pore resistance for TDG with Topcoat A and Topcoat B.**

The durability of the topcoat would inevitably affect the long-term performance of the TDG layer. It was thought that moisture presence would be of importance to determine the efficacy of the TDG either as a barrier coating or providing beneficial cathodic interaction with the steel substrate. For structural steel components, prolonged exposure to moisture from runoff may lead to aggressive environmental exposure, especially in marine environments where airborne salts may accumulate. TDG samples

with Topcoats A and B were tested in immersion cells to elucidate individual topcoat material performance. The same topcoat materials were tested in alkaline solution as well, although these conditions are not necessarily appropriate for reinforced concrete applications. The immersion tests were also intended to provide indication of the corrosion behavior of the coating systems in relevant aqueous environments and coating conditions. The coating surfaces of all test samples for the immersion tests were scribed to expose the underlying steel substrate as described in the methodology section. As expected, the developed open circuit potential, OCP, was generally indicative of active zinc conditions (Figure 3.15). In the alkaline solutions, potentials more negative than -1000 $mV_{SCE}$ were measured throughout the length of the ~40 day exposure. In chloride-free neutral pH solution, the OCP was relatively stable at ~-500 $mV_{SCE}$ after about 4 days, which may indicate some form of passivation occurring. Much more active potentials were measured in the chloride solution (~-900 $mV_{SCE}$).

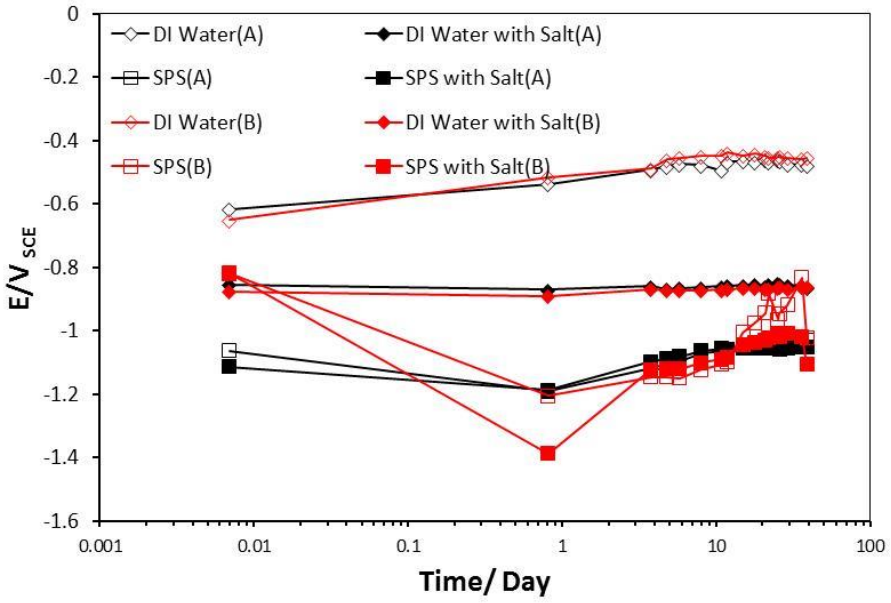


**Figure: 3.15 OCP for TDG with Topcoat A and Topcoat B.**

As expected, large corrosion currents (Figure 3.16) were measured for TDG immersed in alkaline solution where active zinc had OCP < -1000 $mV_{SCE}$. Lower corrosion rates were observed in the neutral pH solutions where OCP was between ~-500 and ~-900 $mV_{SCE}$ in chloride and chloride-free solutions, respectively. All TDG samples immersed in chloride solution, as expected, showed greater reaction rates than chloride-free solutions. TDG samples with scribed Topcoat A and scribed Topcoat B in all test solutions showed an initial trending decay in corrosion rate with time after day 1 (Figure 3.16). The overall decay in corrosion current for TDG in neutral pH solution was viewed as due to slower anodic dissolution of the exposed TDG layers along the perimeter of the scribe. The decrease in current is consistent with an increase in pore resistance

(Figure 3.14) for TDG in neutral pH solution, which may indicate TDG tendency to more passive-like behavior at the scribe periphery and thus less dissolution of metal at the scribe edge. Electrolytic contact with the TDG layer would be initially confined to the periphery of the defect and corrosion product accumulation in the scribed crevice may reduce the overall current related to zinc activity. Similar tendencies, but with less efficacy, may be in place for TDG with Topcoat A in alkaline solution. Other conditions that may lead to reduced current such as oxygen availability, zinc passivation, and interaction with topcoat material may be relevant as well. Figure 3.17 shows the surfaces of the immersion test samples where the annular regions subjected to immersion in solution show differentiation in coating color and texture, especially for Topcoat B.

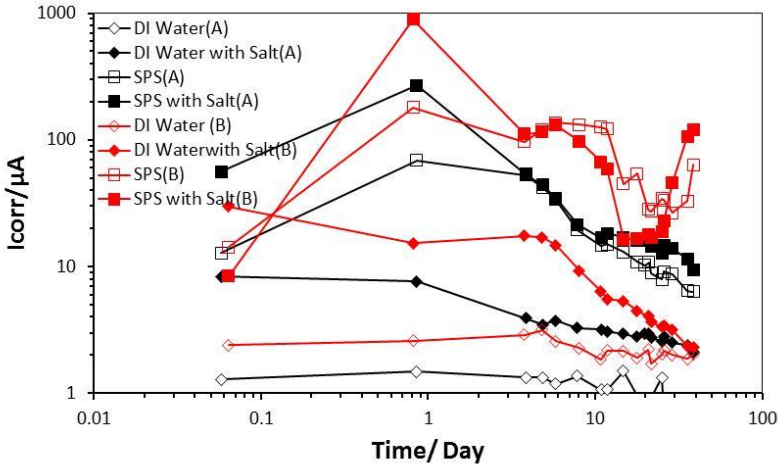


**Figure: 3.16 Corrosion current for Topcoat A and Topcoat B.**

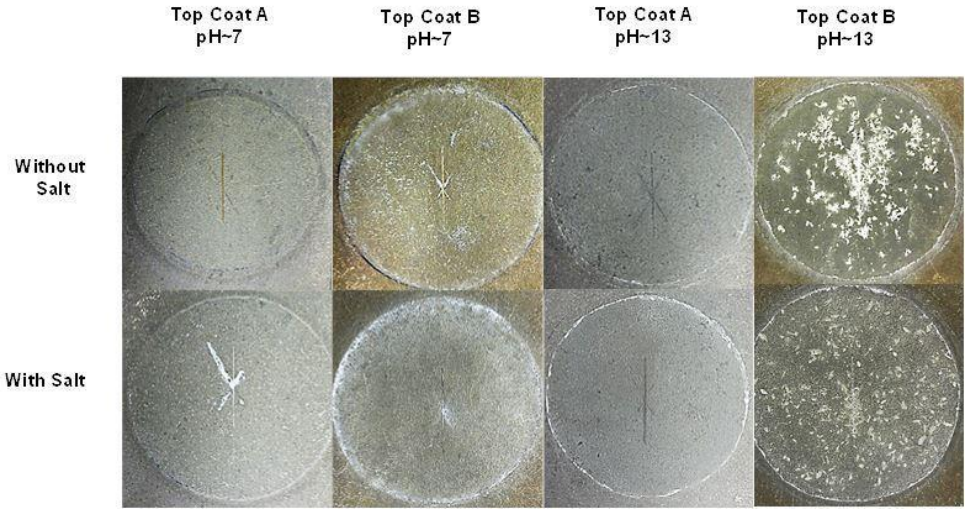


**Figure: 3.17 Visual appearance of TDG (Topcoat A and Topcoat B) after Electro-Chemical testing.**

The corrosion rate calculations indicated greater anodic activity on samples with Topcoat B than Topcoat A in all test solution conditions. The coating trends in atmospheric exposure described earlier indicated poorer topcoat qualities (including adhesive strength and color retention) than Topcoat A and susceptibility to early degradation. There was an initial decrease and then increase in corrosion current for TDG with Topcoat B (Figure 3.16) that followed a similar trend in pore resistance (Figure 3.14). This is contrasted to TDG with Topcoat A in alkaline exposure where (as described above) a steady decrease in corrosion current and relatively stable $R_{po}$ occurred throughout the test period (Figures 3.16 and 3.14). With Topcoat B, high initial corrosion rates during the first week of exposure, coincident with a corresponding decrease in pore resistance, may indicate degradation of the topcoat and of the underlying exposed zinc layers. A drop in corrosion current after the first week could indicate tendency towards passive-like conditions. Similar trends towards passive-like conditions with TDG with Topcoat A in alkaline solution were apparent. The increase in corrosion current after about day 25 for Topcoat B in simulated pore solutions corresponded to increase in $R_{po}$, and was thought to indicate further moisture availability to exposed active portions of the TDG coating. Further analysis is needed to elucidate the coating and corrosion behavior.

It was noted that there was no indication of significant corrosion development of the steel substrate at the defect site or anywhere else in the Topcoat B samples immersed in SPS and SPS plus salt (Figure 3.18)

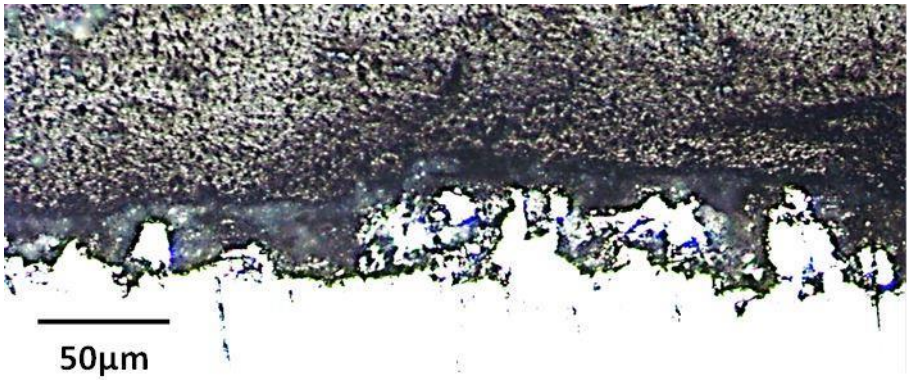


**Figure: 3.18 Optical micrograph for TDG (Topcoat B) samples in simulated pore solution with 3.5% NaCl.**

## CHAPTER FOUR: COATING DETERIORATION AFTER SHORT-TERM OUTDOOR AND SALT-FOG EXPOSURE

A summary of the findings discussed below is provided in Appendix A.

### 4.1. INTRODUCTION

Chemically bonded phosphate ceramic (CBPC), thermal diffusion galvanizing (TDG), thermal-spray metallizing, and conventional three-coat test coupons were prepared and placed for short-term exposure in outdoor weathering conditions (Figure 4.1) for 4 months and accelerated salt-fog exposures for 2200 hours.

**Figure: 4.1 Outdoor Exposure Site. Top- Beach Site. Bottom- Inland Site**.

The short-term outdoor testing at the Tea Table Key beach test site as well as at the FIU inland test site was proposed to identify early indicators of coating degradation and corrosion development and also to identify coating parameters that may be significant to later coating deterioration and corrosion development.

Coated steel coupons were initially installed on November 1, 2013 and were removed on February 28, 2014. Due to the late initial installation of the samples in the fall season, the samples were exposed for an additional month from the originally planned 3 month exposure for a total of 120 days (~17 weeks). Even in the late fall and winter months, temperature highs in south Florida reached above 85°F and relative humidity

typically exceeded 80%. A record of environmental parameters at the test sites is shown in Figure 4.2 Weather conditions at the two outdoor test sites were comparable. The total amount of precipitation at the Tea Table Key and FIU outdoor test sites was at least 18.7 and 13.5 inches, respectively.

Samples were exposed to salt-fog conditions with 5% NaCl solution for at least 2200 hours to approximate coating and corrosion conditions in aggressive environmental conditions. Salt-fog chamber temperature was ~32$^{o}$C. The samples were placed at a ~40$^{o}$ inclination with support along the bottom edge of the coupon and along an edge at the upper third of the sample.

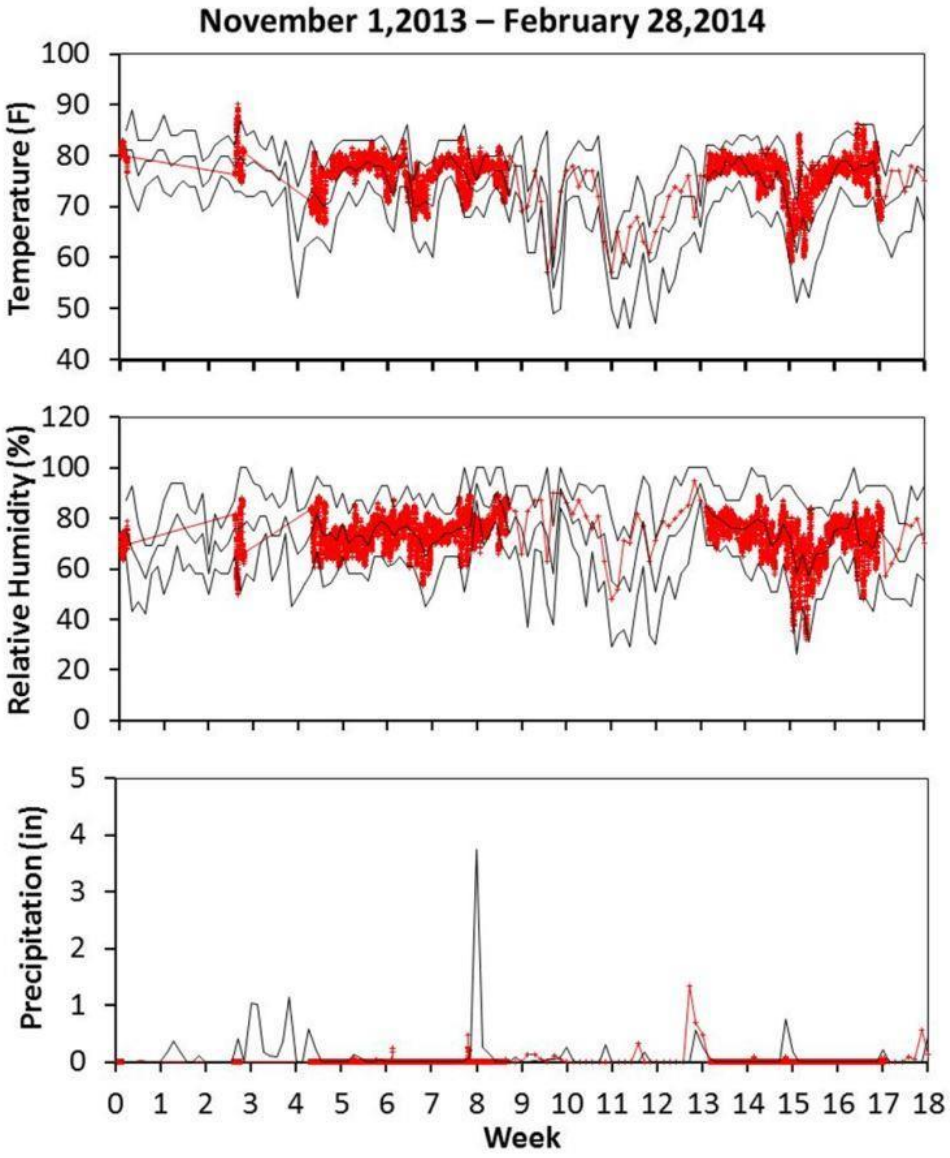


**Figure: 4.2 Environmental Conditions at Outdoor Test Sites**.
Black (FIU). Red (Tea Table).

Table 4.1. Matrix of Samples Removed from Testing after 3-4 Months

| Coating | | Exposure | | Condition | Removed after 3-4 months | Total Tested |
|---|---|---|---|---|---|---|
| CBPC | | Outdoor | Inland | As Rec'd | 1 | 8 |
| | | | | Scribed | 1 | 8 |
| | | | Beach | As Rec'd | 1 | 8 |
| | | | | Scribed | 1 | 8 |
| | | Salt-Fog | | As Rec'd | 2 | 9 |
| | | | | Scribed | 2 | 9 |
| TDG | Plain | Outdoor | Inland | Scribed | 1 | 8 |
| | | | Beach | Scribed | 1 | 8 |
| | | Salt-Fog | | Scribed | 2 | 8 |
| | A | Outdoor | Inland | Scribed | 1 | 8 |
| | B | Outdoor | Inland | Scribed | 1 | 8 |
| | A+B | Outdoor | Inland | As Rec'd | 1 | 8 |
| | | | | Scribed | 1 | 8 |
| | | | Beach | As Rec'd | 1 | 8 |
| | | | | Scribed | 1 | 8 |
| | | Salt-Fog | | As Rec'd | 2 | 6 |
| | | | | Scribed | 2 | 6 |
| Metallizing | | Outdoor | Inland | As Rec'd | 1 | 8 |
| | | | | Scribed | 1 | 8 |
| | | | Beach | As Rec'd | 1 | 8 |
| | | | | Scribed | 1 | 8 |
| | | Salt-Fog | | As Rec'd | 2 | 6 |
| | | | | Scribed | 2 | 6 |
| Three-Coat | | Outdoor | Inland | As Rec'd | 1 | 8 |
| | | | | Scribed | 1 | 8 |
| | | | Beach | As Rec'd | 1 | 8 |
| | | | | Scribed | 1 | 8 |
| | | Salt-Fog | | As Rec'd | 2 | 6 |
| | | | | Scribed | 2 | 6 |
| Total | | | | | 38 | 222 |

The coated steel coupons installed for outdoor and salt-fog exposures are listed in Table 4.1. Fifty CBPC, 84 TDG, 44 metallized, and 44 three-coat test coupons were

initially installed. Of those, 38 were removed for destructive testing after the first 3-4 months of exposure. For the CBPC, Metallized, and Three-Coat coating systems, two scribed coupons and two coupons in as-received condition that were exposed in outdoor environments, and likewise for samples in the salt-fog environments, were removed. Furthermore, in similar fashion, TDG samples with Topcoat A+B were removed. An additional 6 TDG samples were removed for destructive testing. Those included two scribed plain TDG samples and two scribed TDG samples with single topcoat (Topcoat A or B) exposed to outdoor environment as well as two scribed plain TDG samples exposed to salt-fog environment.

After short-term exposure to outdoor weathering and salt-fog, non-destructive qualitative visual comparisons were made between the exposed sample conditions and the as-received sample conditions. Evaluation included the initial coating condition (coating defects and thickness) and the final coating condition (coating degradation, the presence and degree of corrosion, and the coating thickness). Destructive testing of samples included coating adhesive strength, coating degradation based on changes in coating thickness, and grinding and polishing of sawed sample cross-sections for assessment of corrosion development by optical microscopy.

Chapter 4.2 discusses photographic comparisons of the coatings before and after exposure to outdoor or salt-fog environments. Chapters 4.3 and 4.4 compares coating thicknesses and coating pull-off strengths after outdoor and salt-fog exposures. Typical measurement locations are shown schematically in Figure 4.3.

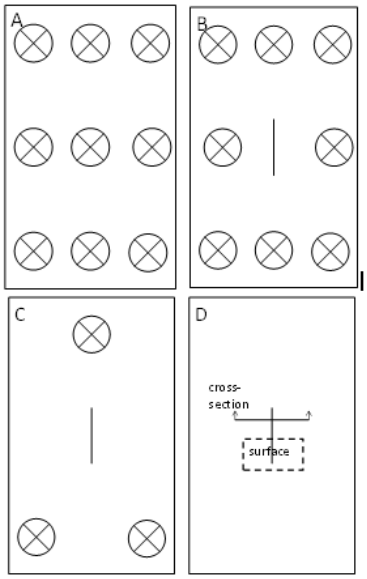


**Figure: 4.3 Sample Testing Surface Locations**.
A) Approximate coating thickness locations for as-rec'd coupon.
B) Approximate coating thickness locations for scribed coupon. C) Approximate coating pull-off locations. D) Approximate locations for metallographic sampling.

The coating thickness or change of coating thickness from pre-exposure conditions was calculated from the average of multiple readings on the surface of the coated samples. For non-scribed samples, the coating thickness was measured at 9 locations on the coupon front face. For scribed samples, the coating thickness was measured at 8 locations on the coupon front face. The coating thickness was measured using a DeFelsko Positector 6000 magnetic coating thickness gage.

The reported coating pull-off strengths are from at least three locations on the sample surface for both scribed and non-scribed samples. Metal dollies were glued to the surface of the coated coupon using a two-part epoxy and allowed to set for 24 hours. The perimeter around the fastened dolly was then scored down to the steel substrate prior to testing with a DeFelsko Positest pulloff adhesion tester.

The coating thicknesses and pull-off strength were meant to evaluate changes due to exposure conditions and not necessarily the effect of the scribe defect. Local coating degradation due to the presence of the scribe was to be evaluated by optical and microscopy. Typical sampling locations are shown in Figure 4.3.

## 4.2. VISUAL INSPECTION

### *4.2.1 Chemically Bonded Phosphate Coating*

#### *4.2.1.1 Outdoor Exposure*

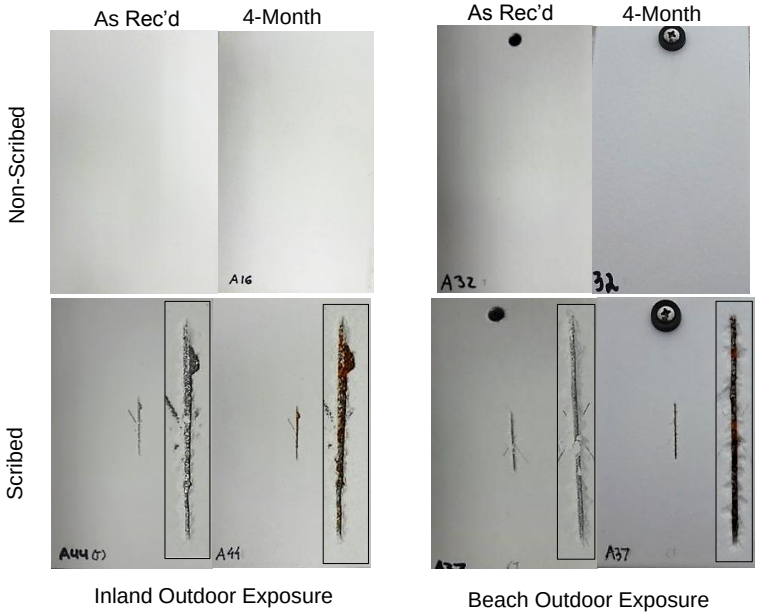


**Figure: 4.4 CBPC Outdoor Exposure**.

Photographs of representative scribed and non-scribed CBPC samples before and after 4-month outdoor exposure are shown in Figure 4.4. One scribed and one non-scribed sample were removed from the Inland and Beach outdoor exposure test racks. Samples from the Inland and Beach sites in each condition were considered to be replicate for analysis.

No major outward appearance of coating deterioration was observed on the 16 scribed or 16 non-scribed samples from either outdoor testing location after 4 month exposure (Under coating corrosion observations are described later). Rust was observed within the scribe location of 11 the 16 scribed samples. Typical rust appearance within the scribe is shown in Figure 4.4.

#### *4.2.1.2 Salt-Fog Exposure*

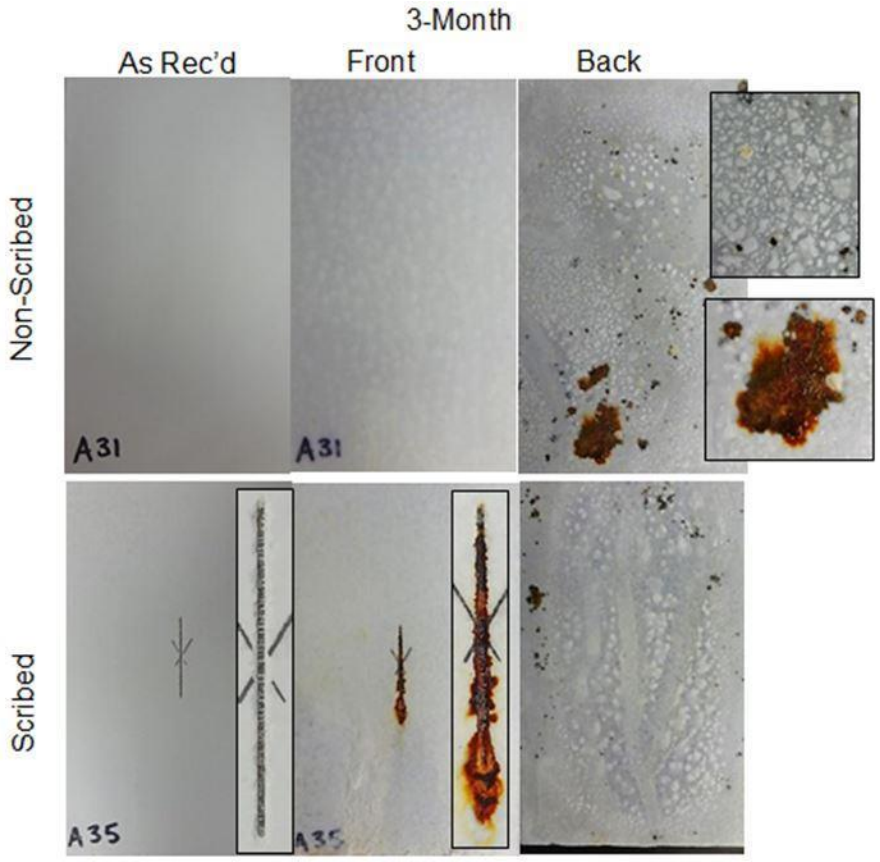


**Figure: 4.5 CBPC Salt-Fog Exposure**.

Photographs of representative scribed and non-scribed CBPC samples before and after 2200 hours salt-fog exposure are shown in Figure 4.5. Two scribed and two non-scribed samples were removed from the salt-fog chamber after ~2200 hours.

Varying levels of coating deterioration were observed on the 9 scribed and 9 non-scribed samples exposed to salt-fog for 2200 hours. Some runoff and salt deposition was apparent on some of the samples. Nevertheless, the coating degradation appeared as scouring and re-deposition (roughening) of the ceramic coating material and development of rust at defect or pore sites on the coating that sometimes led to larger rust accumulation. This type of coating deficiency developed more severely on the backside of the coated coupon. Severe localized steel corrosion was observed on 5 of the 9 non-scribed samples. Severe localized steel corrosion was observed at sites away from scribes on 3 of the 9 scribed samples. Steel corrosion was observed at scribe locations on 3 of the 9 scribed samples. Typical appearance of steel corrosion within the scribe is shown in Figure 4.5.

### *4.2.2 Thermal Diffusion Galvanizing*

#### *4.2.2.1 Outdoor Exposure*

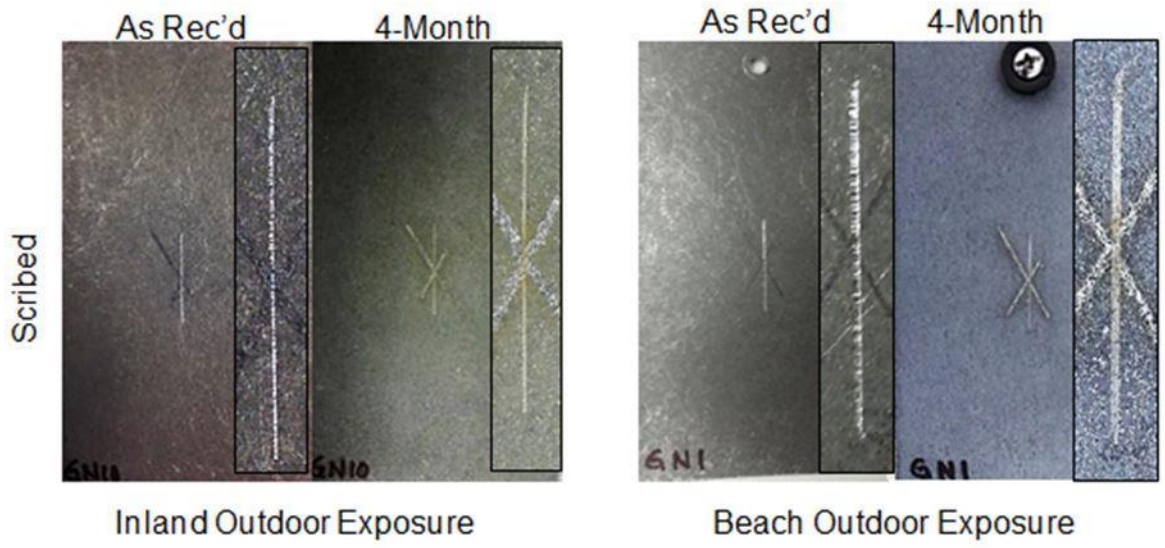


**Figure: 4.6 TDG Without Topcoat Outdoor Exposure**.

Photographs of representative scribed plain TDG steel samples before and after 4-month outdoor exposure are shown in Figure 4.6. One of the scribed samples was removed from each of the Inland and Beach outdoor exposure test racks. Samples from the Inland and Beach sites were considered to be replicate. Photographs of representative scribed TDG steel samples with either Topcoat A or Topcoat B, before and after 4-month outdoor exposure, are shown in Figure 4.7. One of the scribed samples with Topcoat A and one of the scribed samples with Topcoat B were removed from the Inland outdoor exposure test rack for further lab testing. The two samples were considered to be replicate. No major surface degradation or significant oxide accumulation on the outer zinc alloy layer of the 16 plain samples and 16 TDG samples

was apparent by visual observation. No significant steel corrosion was observed in any of those samples, but tarnishing of portions of scribed exposed steel substrate was observed in some cases.

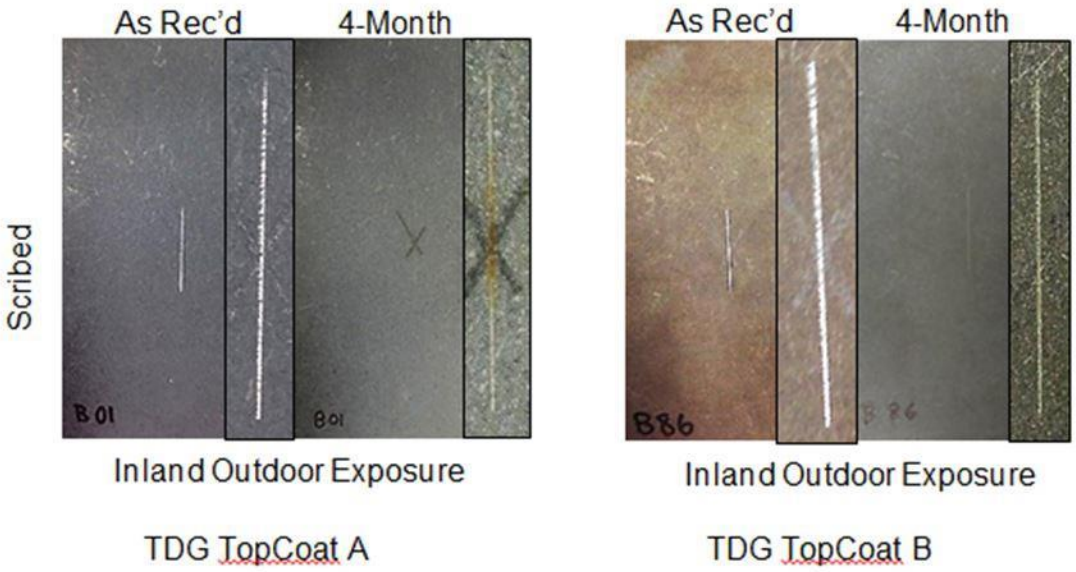


**Figure: 4.7 TDG With Single Topcoat Outdoor Exposure**.

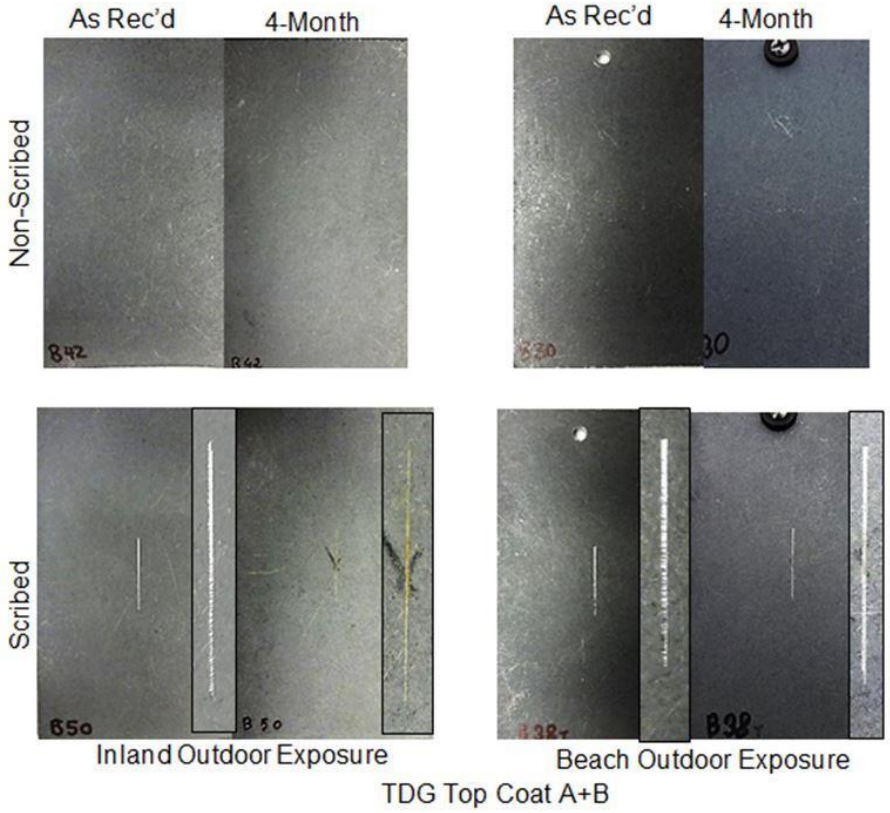


**Figure: 4.8 TDG Double Topcoat Outdoor Exposure**.

Photographs of representative scribed and non-scribed TDG samples with topcoat (Topcoat A+B) before and after 4-month outdoor exposure are shown in Figure 4.8. One scribed and one non-scribed sample were removed from the Inland and Beach outdoor exposure test rack. Samples from the Inland and Beach sites in each condition were considered to be replicate for analysis.

No major coating deterioration or indication of significant zinc corrosion product was observed on the 16 scribed or 16 non-scribed samples from either outdoor testing location after 4-month exposure. No steel corrosion was observed on the 16 non-scribed samples after 4-month exposure. Tarnishing was observed within the scribe location on 9 of the 16 scribed samples. Typical appearance within the scribe is shown in Figure 4.8.

#### *4.2.2.2 Salt-Fog Exposure*

Photographs of representative scribed and non-scribed TDG steel samples before and after 2200 hours salt-fog exposure are shown in Figure 4.9. Only plain TDG and TDG with Topcoat A+B were exposed to salt-fog. Two scribed plain TDG samples were removed from the salt-fog chamber after ~2200 hours. Two scribed and two non-scribed TDG samples with Topcoat A+B were removed from the salt-fog chamber after ~2200 hours.

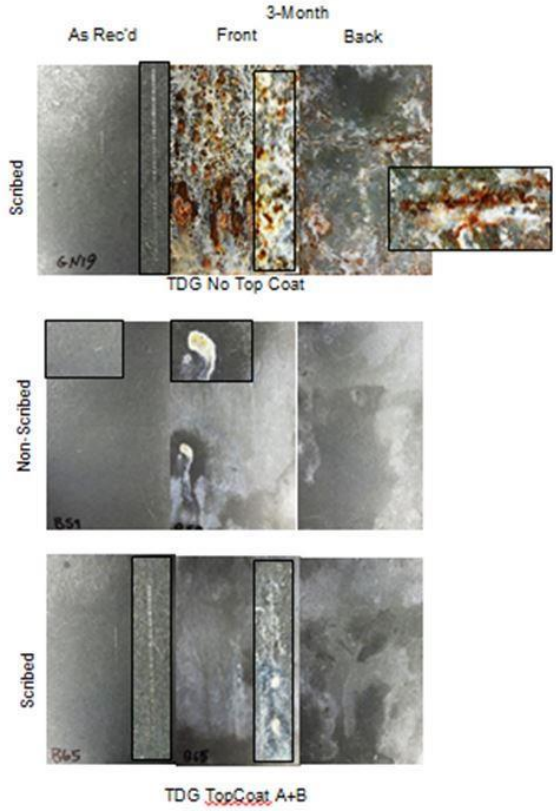


**Figure: 4.9 TDG Salt-Fog Exposure**.

Significant corrosion activity was apparent on all 8 plain TDG samples exposed to salt-fog for 2200 hours. Manufacturers of the coating present this behavior as corrosion of iron contaminants within the TDG coating and recommend the use of a topcoat with TDG. The corrosion appeared throughout the surface of the coupons and appeared more severe on the top face of the coupon. The extent of corrosion did not appear more severe at scribe locations; and upon closer examination, the location of the original scribe could not be easily retraced. The corrosion behavior of the steel substrate is discussed later.

The coupons with Topcoat A+B placed in salt-fog had significantly less iron corrosion product. Those samples (6 scribed and 6 non-scribed) appeared to have zinc activity based on the white oxide product deposited on parts of the coupon surface. The role of the topcoat is discussed later. On 2 samples, significant runoff of the deposited product was seen at local coating defect sites (Figure 4.9). Runoff was also seen at some of the scribed locations. No corrosion of the steel substrate exposed by scribing was observed.

### *4.2.3 Metallizing*

#### *4.2.3.1 Outdoor Exposure*

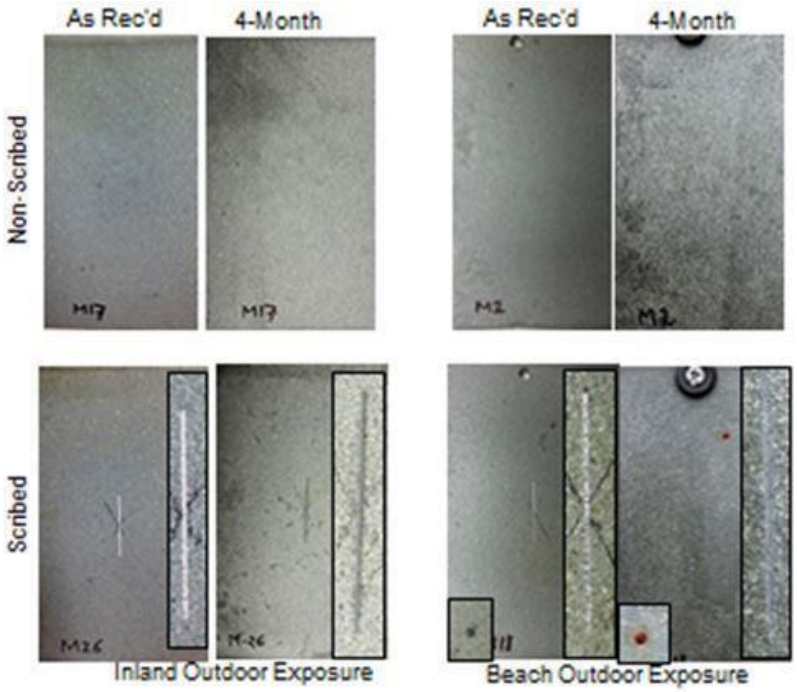


**Figure: 4.10 Metallizing Outdoor Exposure**.

Photographs of representative scribed and non-scribed metallized steel samples before and after 4-month outdoor exposure are shown in Figure 4.10. One scribed and one non-scribed sample were removed from the Inland and Beach outdoor exposure test rack. Samples from the Inland and Beach for each condition were considered to be replicate.

Some activity of the zinc metallizing layer was observed on the 16 scribed and 16 non-scribed samples from both outdoor testing locations. The samples, more so for the 8 samples from the Beach outdoor exposure location, had a mottled white surface appearance consistent with oxidation of the zinc layer. No steel corrosion was observed for non-scribed samples in either outdoor exposure locations. No steel corrosion was observed within the scribed region of any of the scribed samples in either outdoor exposure. A small region of steel corrosion was observed outside of the scribed region on one of the scribed samples placed in the Beach outdoor test rack. As seen in Figure 4.10, that corrosion occurred at a local coating deficiency.

#### *4.2.3.2 Salt-Fog Exposure*

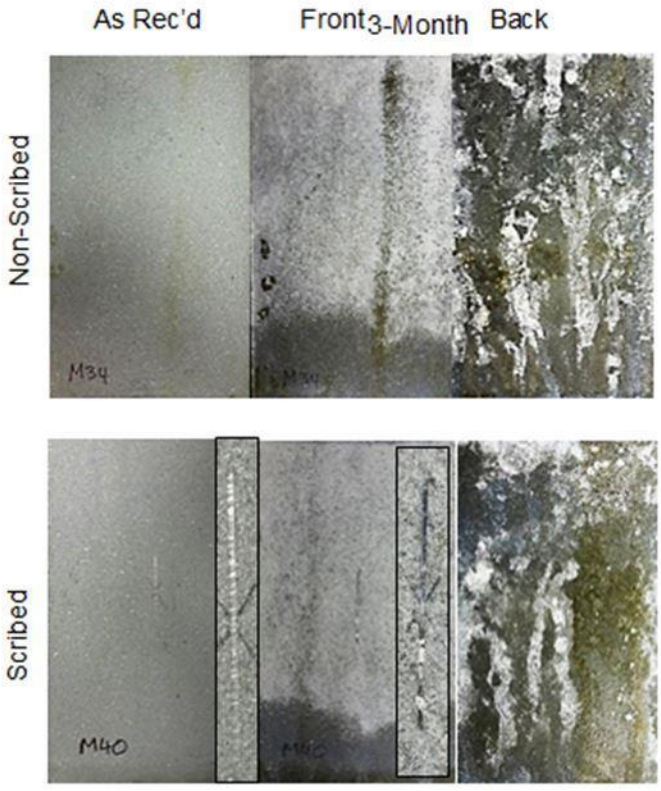


**Figure: 4.11 Metallizing Salt-Fog Exposure**.

Photographs of representative scribed and non-scribed metallized steel samples before and after 2200 hours salt-fog exposure are shown in Figure 4.11. Two scribed and two non-scribed samples were removed from the salt-fog chamber after ~2200 hours.

Coating degradation appeared as zinc activity throughout the front surface of the coupon. The appearance of zinc oxide was more prominent on the front surface of the coupon. It was suspected that non-uniform application of a topcoat and runoff of salt fog condensate resulted in the disparate appearance of the coupon surface. No steel corrosion was observed on any of the 6 scribed or 6 non-scribed coupons after 2200 hours.

### *4.2.4 Three-Coat*

#### *4.2.4.1 Outdoor Exposure*

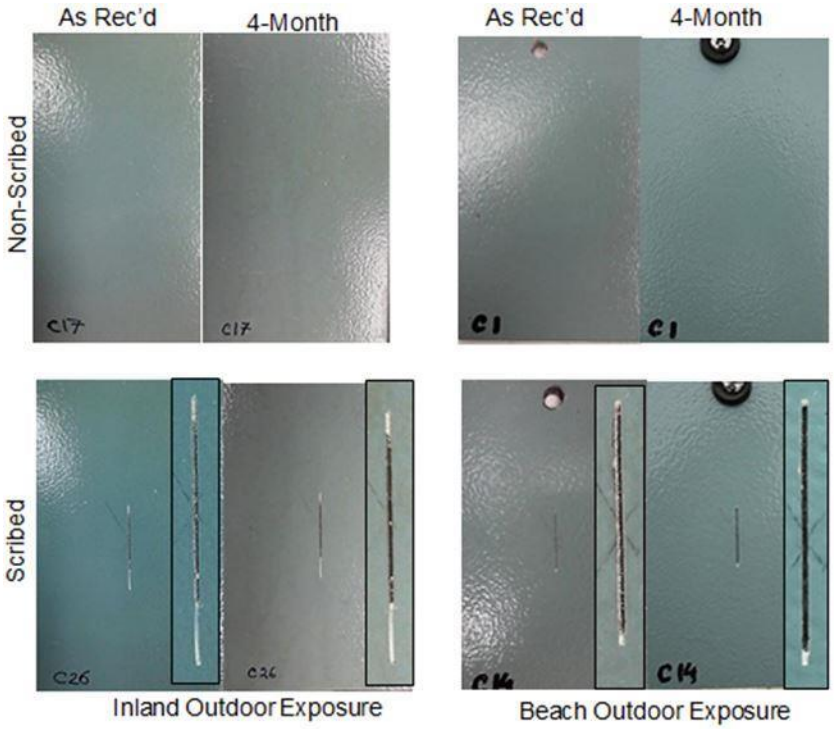


**Figure: 4.12 Three-Coat Outdoor Exposure**.

Photographs of representative scribed and non-scribed Three-Coat steel coupons before and after 4-month outdoor exposure are shown in Figure 4.12. One scribed and one non-scribed sample were removed from the Inland and Beach outdoor exposure test rack. Samples from the Inland and Beach in each condition were considered to be replicate.

No major coating deterioration was observed visually on the 16 scribed or 16 non-scribed samples from either outdoor testing location. No corrosion was observed on the 16 non-scribed samples.

#### *4.2.4.2 Salt-Fog Exposure*

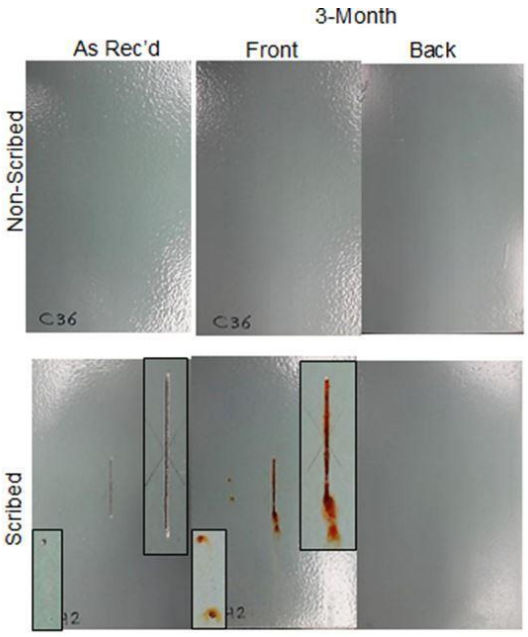


**Figure: 4.13 Three-Coat Salt-Fog Exposure.**

Photographs of representative scribed and non-scribed three-coat steel samples before and after 2200 hours salt-fog exposure are shown in Figure 4.13. Two scribed and two non-scribed samples were removed from the salt-fog chamber after ~2200 hours.

No coating degradation was apparent for any of the 6 scribed or 6 non-scribed samples after 2200 hours of salt-fog exposure. Corrosion was observed within the scribe in 5 of the 6 scribed coupons. Typical corrosion appearance is shown in Figure 4.13. In one of the scribed samples, corrosion developed at two spots away from the scribe. That corrosion developed at localized coating defects.

## 4.3. COATING THICKNESS

### *4.3.1 Chemically Bonded Phosphate Coating*

The average coating thickness as measured with the magnetic thickness gage before and after exposure to outdoor or salt-fog weathering is shown in Figure 4.14a. Direct comparison of the average coating thickness of a sample before and after exposure are shown in Figures 4.14b and 4.14c. Figure 4.14b shows the calculated difference in measured coating thickness and Figure 4.14c shows the percent difference in the average coating thickness relative to the average as-received thickness. There is a caveat in the interpretation of the data because the reported thickness was the calculated average of multiple spot measurements throughout the coupon surface and there was apparent local thickness variability. Positive values in Figures 4.14b and 4.14c indicate a decrease in coating thickness after exposure.

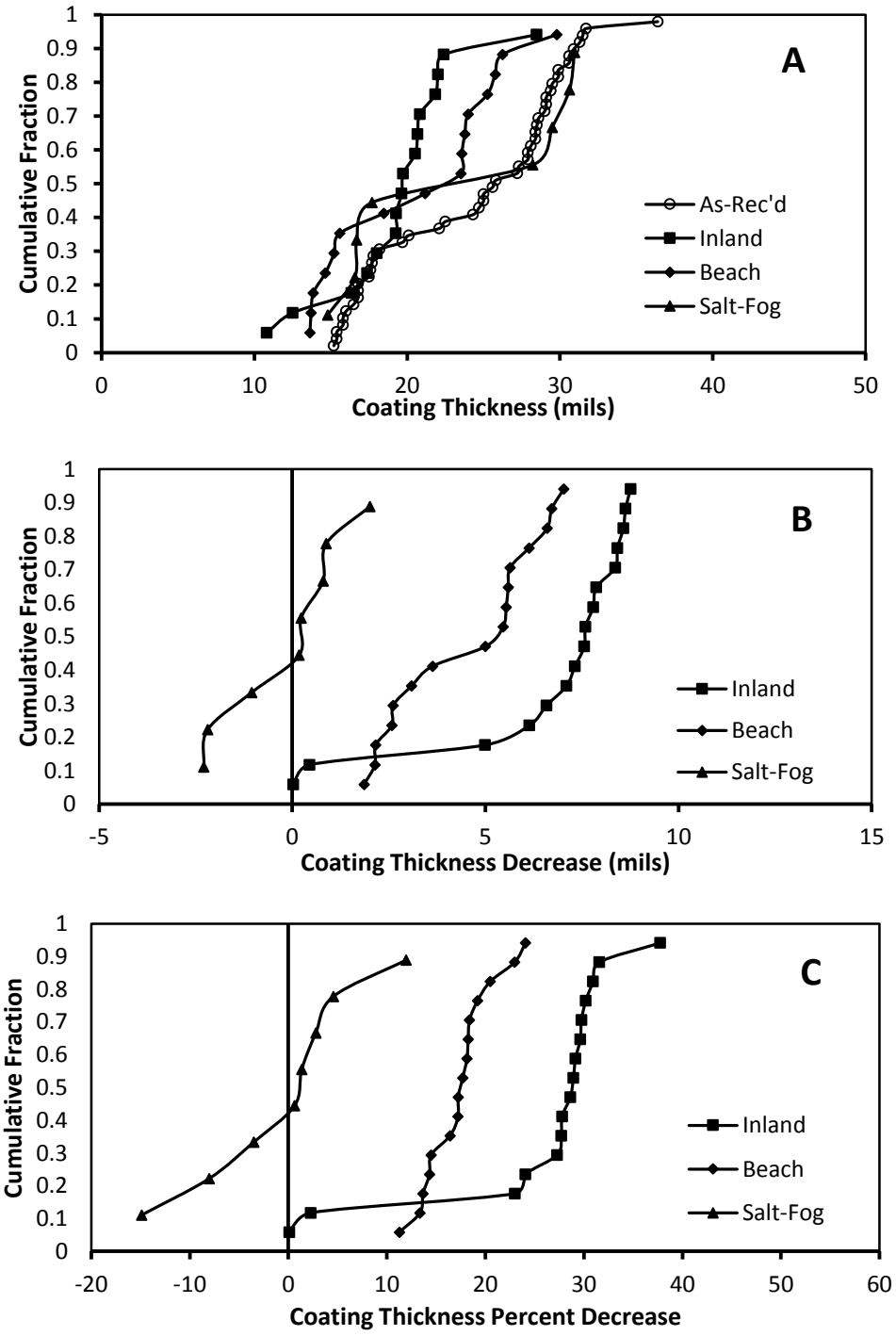


**Figure: 4.14 CBPC Coating Thickness Decrease**.
A) Actual coating thickness. B) Change of coating thickness. C) Percent change of coating thickness.

Reduction in coating thickness ranging from ~2-8 mils was measured for CBPC coated steel samples exposed in outdoor conditions. Decrease in coating thickness at the inland outdoor exposure site was similar if not more adverse than the beach outdoor

exposure site. As there was variability in original coating thickness, the percent decrease in coating thickness for the test population likewise varied. Also, error was likely incurred, due to variability in thickness measurements and degradation rates at each measurement location on the exposed samples, which can be manifested in the presented coating-thickness-percent-decrease values. There was indication of correlation between the average original thickness and loss of coating thickness. As shown in Figure 4.15, samples with thicker CBPC coatings tended to have greater reduction in coating thickness after outdoor exposure. Samples exposed in salt-fog environments did not show similar trends of material loss as the samples exposed in outdoor conditions. In some cases, samples exposed in salt-fog environment had an increase in thickness. The increase in thickness was thought to be due to surface roughening of the coating as described earlier and undercoat corrosion development described in the next chapter. Further discussion is provided later.

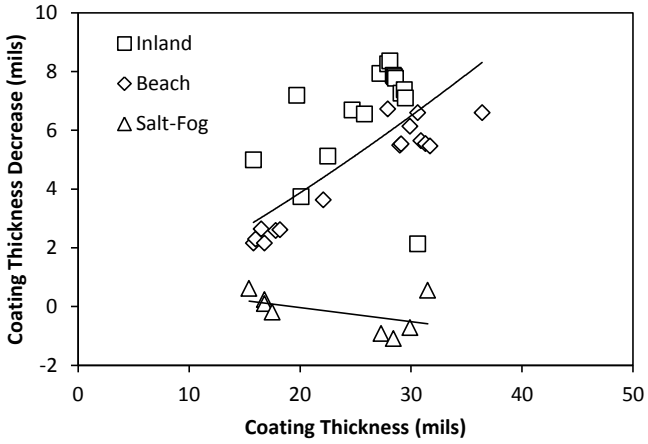


**Figure: 4.15 CBPC Coating Thickness Decrease vs. As-Received Coating Thickness**.

### *4.3.2 Thermal Diffusion Galvanizing*

The average coating thickness for TDG with Topcoat A+B and without topcoat as measured with the magnetic thickness gage before and after exposure to outdoor or salt-fog weathering is shown in Figure 4.16a and 4.16d, respectively. Direct comparison of the average coating thickness of samples before and after exposure are shown in Figures 4.16b-4.16c. and Figure 4.16e-4.16f. There is a caveat in the interpretation of the data because the reported thickness was the calculated average of multiple spot measurements throughout the coupon surface, and there was apparent local thickness variability. Positive values indicate a decrease in coating thickness after exposure. Figure 4.16b and Figure 4.16e show the difference in the average measured coating thickness for TDG with and without topcoat and Figures 4.16c and 4.16f show the

percent difference in coating thickness of TDG samples with and without topcoat relative to the as-received thickness.

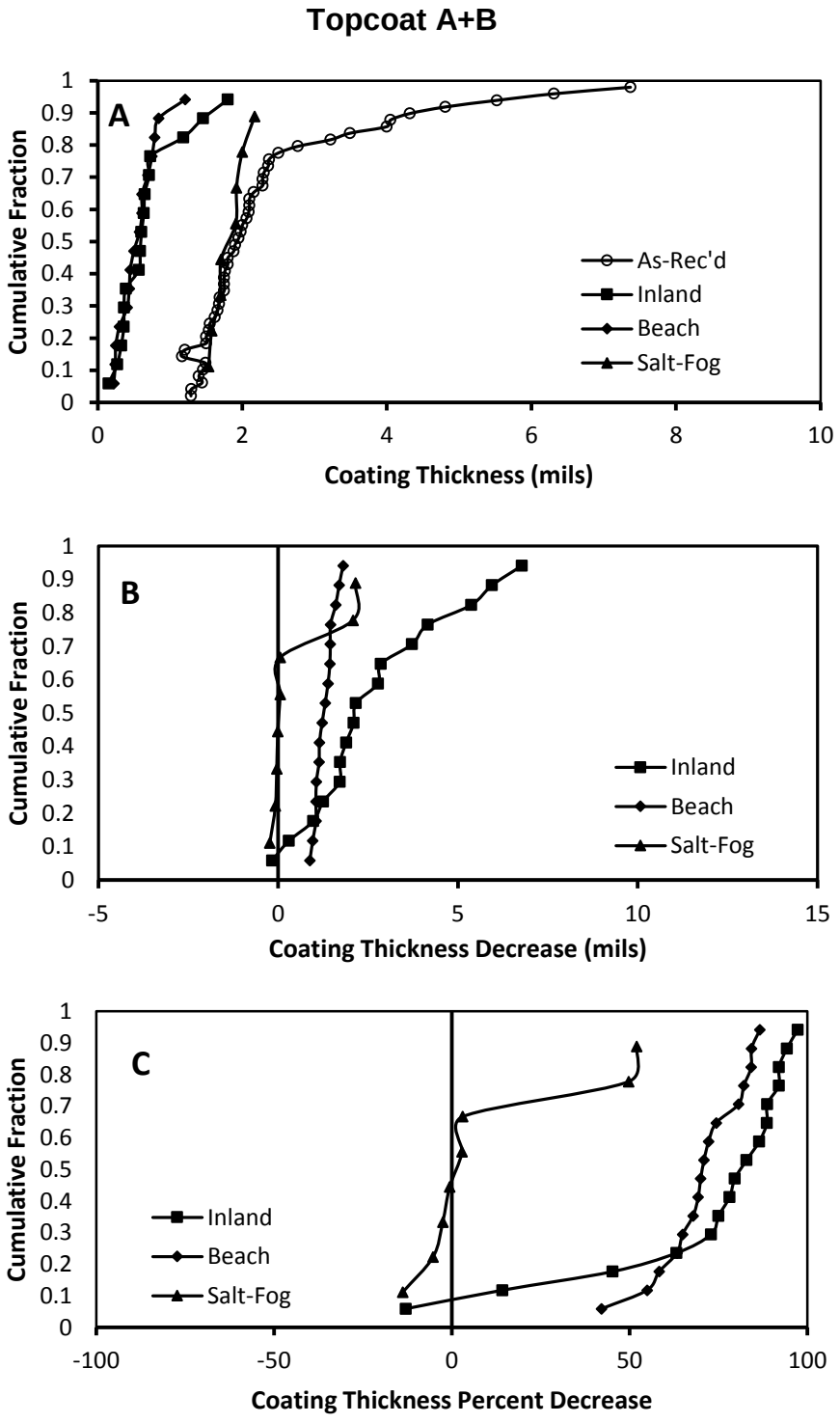


**Figure: 4.16 TDG Coating Thickness Decrease (cont.)**.
A) Actual coating thickness. B) Change of coating thickness. C) Percent change of coating thickness.

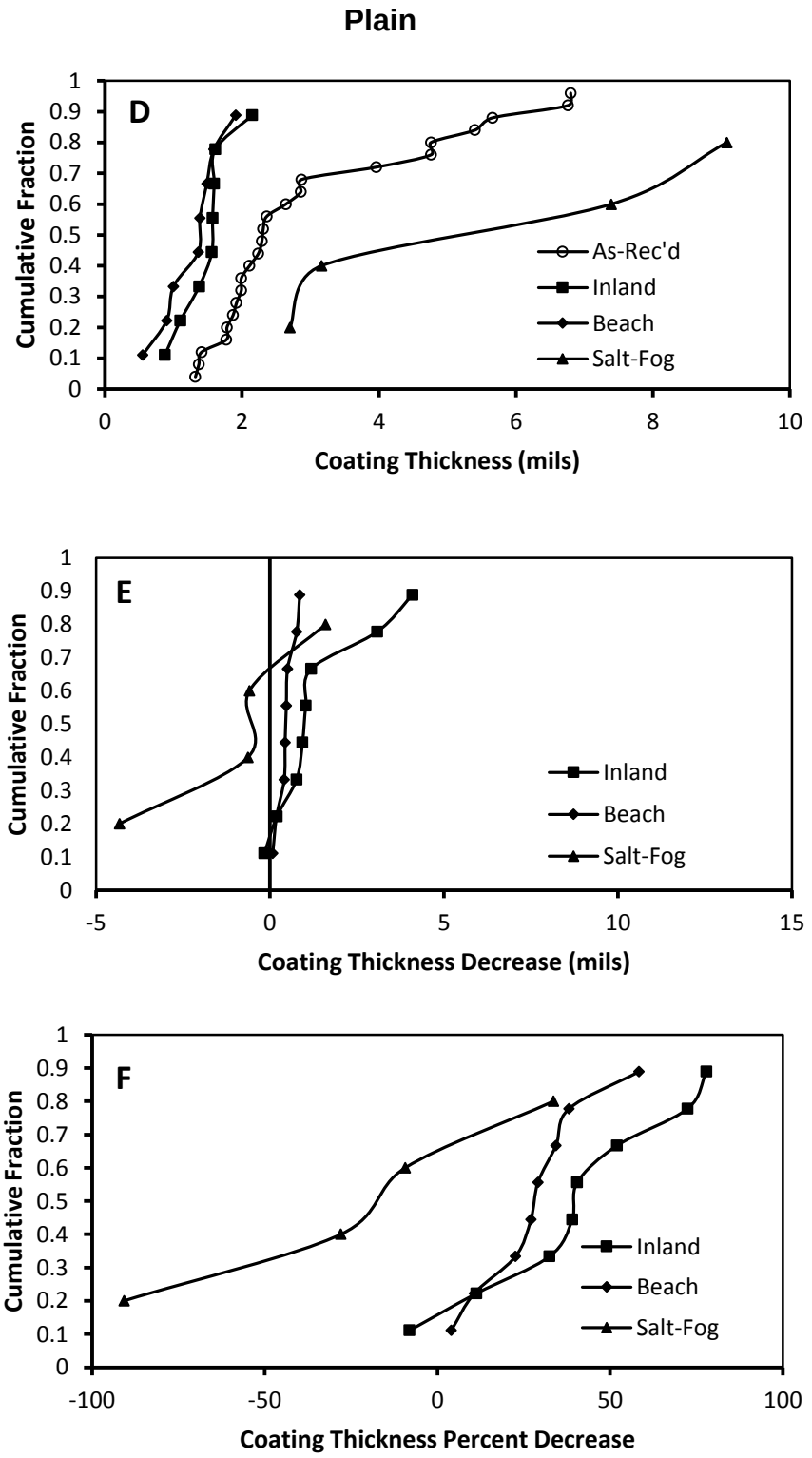


**Continuation of Figure: 4.16 TDG Coating Thickness Decrease**.
D) Actual coating thickness. E) Change of coating thickness. F) Percent change of coating thickness.

Approximately 70% of the sample population of TDG coated steel coupons without topcoat had an original average thickness between about 1 and 2.5 mils. Most of the coupons without topcoat placed in outdoor exposure conditions were comprised of those samples. Outdoor exposure reduced the average coating thickness by about 0.2 to 2 mils. The coupons without topcoat placed in salt-fog exposure were comprised of samples with average thicknesses ranging from about 2.5 to 6.5 mils. After 2200 hour exposure to salt-fog, the average thickness of those samples remained greater than 2.5 mils, although the increased average thickness (up to 9 mils) on some samples was attributed to the oxidation of the zinc layer and buildup of zinc oxide on the coupon surface.

Similar to the uncoated TDG samples, approximately 70% of the sample population of TDG coated steel coupons with Topcoat A+B had original average thicknesses ranging from about 1 to 2.5 mils and ~30% had average thicknesses greater than 2.5 mils. The majority of samples with original average thicknesses greater than 2.5 mils were placed at the inland outdoor exposure site. After outdoor exposure, the range of average coating thicknesses (including those thicker coating samples) was about 0.2 to 2 mils. This is indicative of loss of coating material during outdoor exposure. Similar to the plain TDG samples, the coated samples exposed to salt-fog increased in thickness; however, the coated TDG performed better than the plain samples. The coating thickness increase, due to oxide buildup at deficient surface locations on the coated TDG, was over an order of magnitude smaller than in the case of the plain TDG where there was widespread oxide buildup.

It was stated above that more severe coating loss was apparent at the inland outdoor exposure test site. At that test site, TDG without topcoat and with topcoat variations were compared. Interestingly, TDG with only a single application of Topcoat A or Topcoat B performed better (in terms in change in thickness) than coupons with application of both topcoats (Figure 4.17).

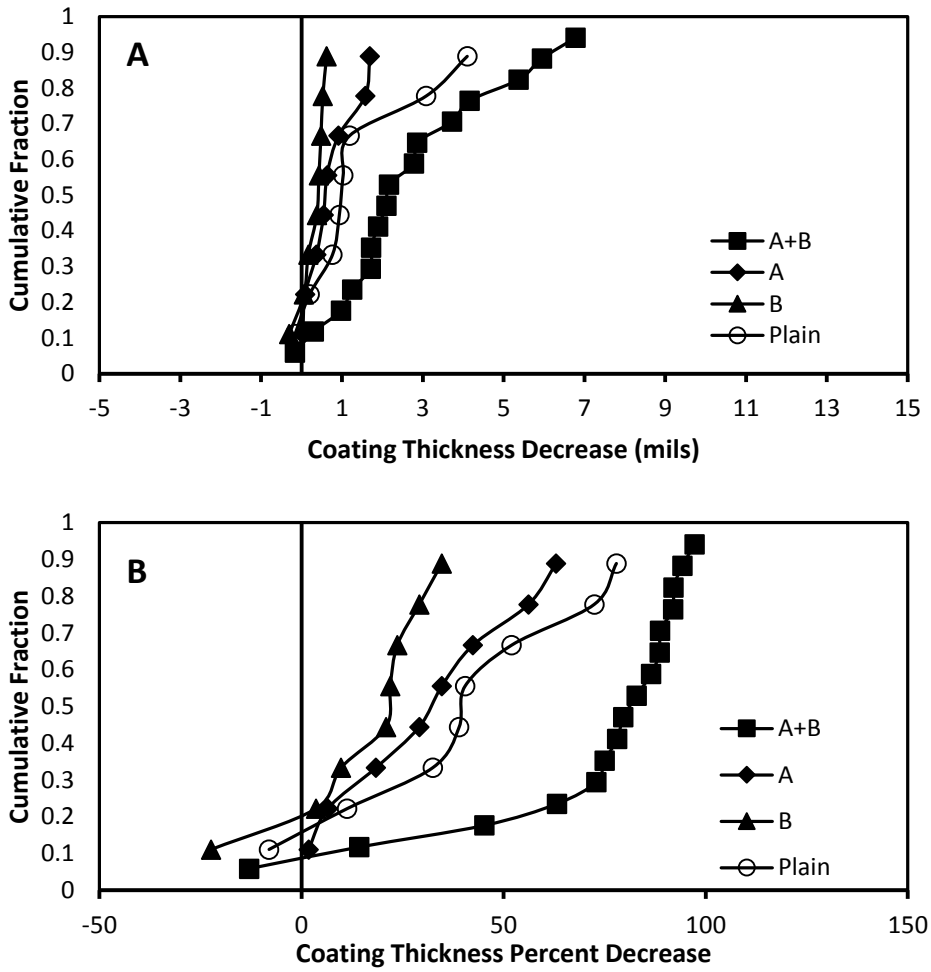


**Figure: 4.17 TDG Topcoat Coating Thickness (Inland Outdoor Exposure)**.
A) Change of coating thickness. B) Percent change of coating thickness.

As shown in Figure 4.18, there is an apparent trend between coating thickness loss after outdoor exposure and initial coating thickness. This trend (especially for TDG Topcoat A+B in inland outdoor exposure) indicates coating thickness loss near the initial coating thickness. Per earlier caveat, the calculated thickness decrease is subject to error incurred by averaging coating thickness from local point measurements.

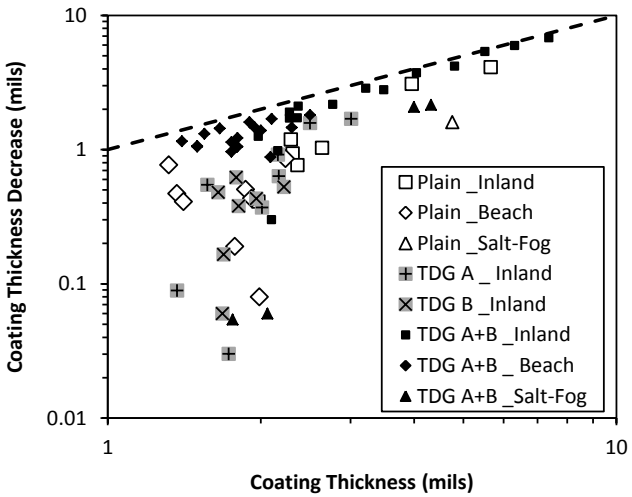


**Figure: 4.18 TDG Coating Thickness Decrease vs. As-Received Coating Thickness**.

### *4.3.3 Metallizing*

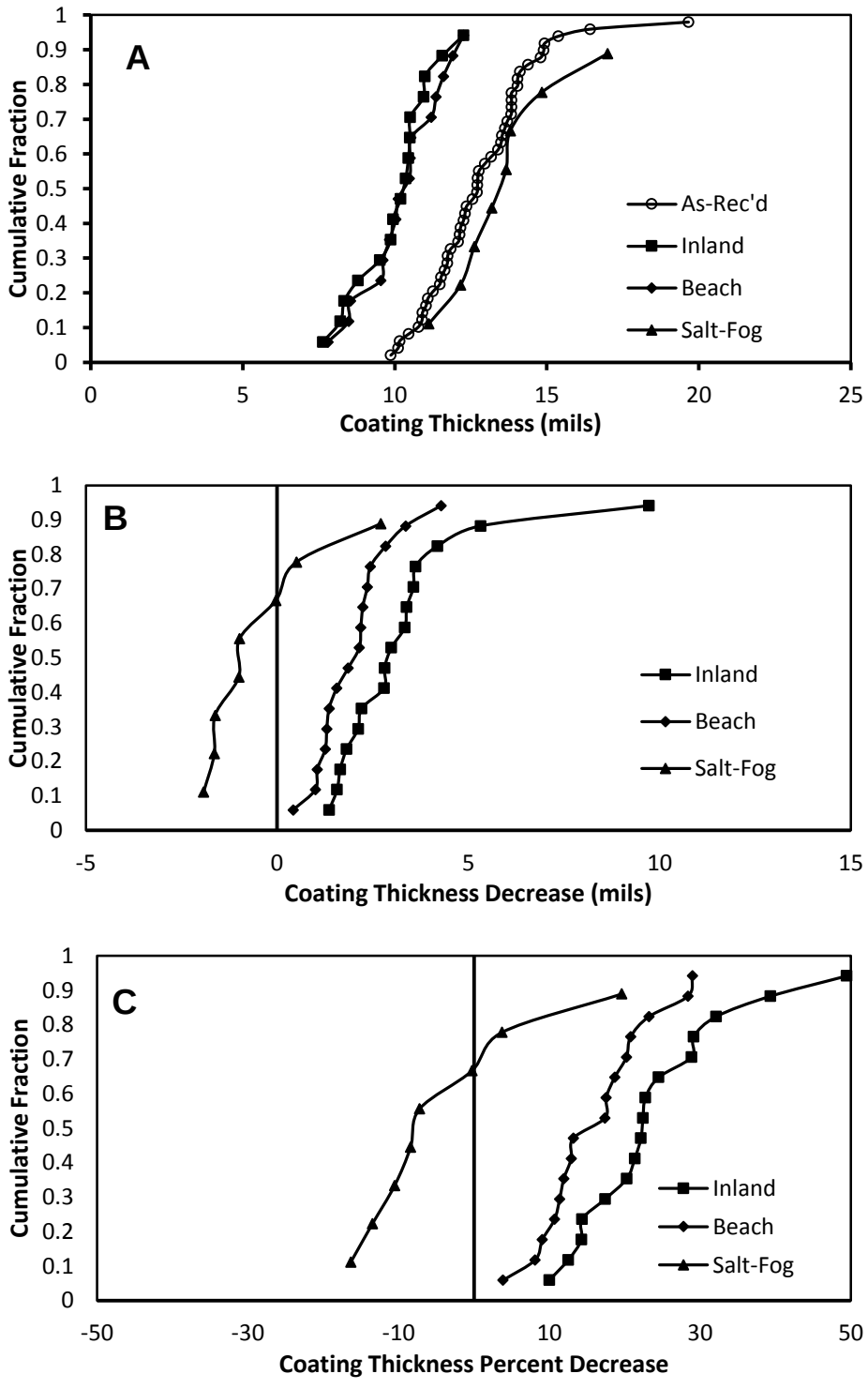


**Figure: 4.19 Metallizing Coating Thickness Decrease**.
A) Actual coating thickness. B) Change of coating thickness. C) Percent change of coating thickness.

The average coating thickness, as measured with the magnetic thickness gage before and after exposure to outdoor or salt-fog weathering, is shown in Figure 4.19a. Direct comparisons of the average coating thicknesses of samples before and after exposure are shown in Figures 4.19b and 4.19c. Figure 4.19b shows the calculated difference in average coating thickness and Figure 4.19c shows the percent difference in the average coating thickness relative to the average as-received thickness. There is a caveat in the interpretation of the data because the reported thickness was the calculated average of multiple spot measurements throughout the coupon surface and there was apparent local thickness variability. Positive values in Figures 4.19b and 4.19c indicate a decrease in coating thickness after exposure.

Reduction in average coating thickness ranging from about 0.5 to 10 mils was measured for metallized coated steel samples exposed in outdoor conditions. Decrease in coating thickness at the inland outdoor exposure site was similar or significantly greater than the beach outdoor exposure site. Six of the eight samples exposed to salt-fog environments showed an increase in average coating thickness. This increase was attributed to the accumulation of zinc oxide products on the coupon samples that had non-uniform application of a topcoat as described earlier. Manifested in the variability of the percentage decreases in coating thicknesses are the variability in the calculations of the average coating thicknesses before and after exposure, in the coating application, and in the rates and modalities of coating degradation. For the metallized coating samples, there was no indication of correlation between the original thickness and loss of coating thickness for any of the environmental exposure conditions (Figure 4.20).

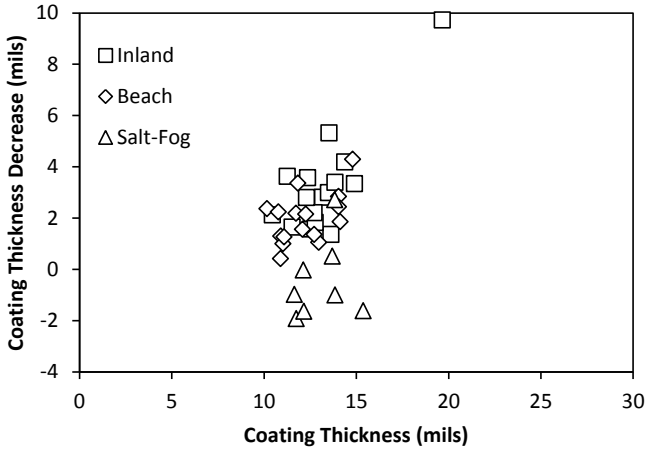


**Figure: 4.20 Metallizing Coating Thickness Decrease vs. As-Received Coating Thickness.**

### *4.3.4 Three-Coat*

The average coating thickness as measured with the magnetic thickness gage before and after exposure to outdoor or salt-fog weathering is shown in Figure 4.21a. Direct

comparison of the average coating thickness of a sample before and after exposure are shown in Figures 4.21b and 4.21c. Figure 4.21b shows the calculated difference in average coating thickness and Figure 4.21c shows the percent difference in the average coating thickness relative to the average as-received thickness. There is a caveat in the interpretation of the data because the reported thickness was the calculated average of multiple spot measurements throughout the coupon surface and there was apparent local thickness variability. Positive values in Figures 4.21b and 4.21c indicate a decrease in coating thickness after exposure.

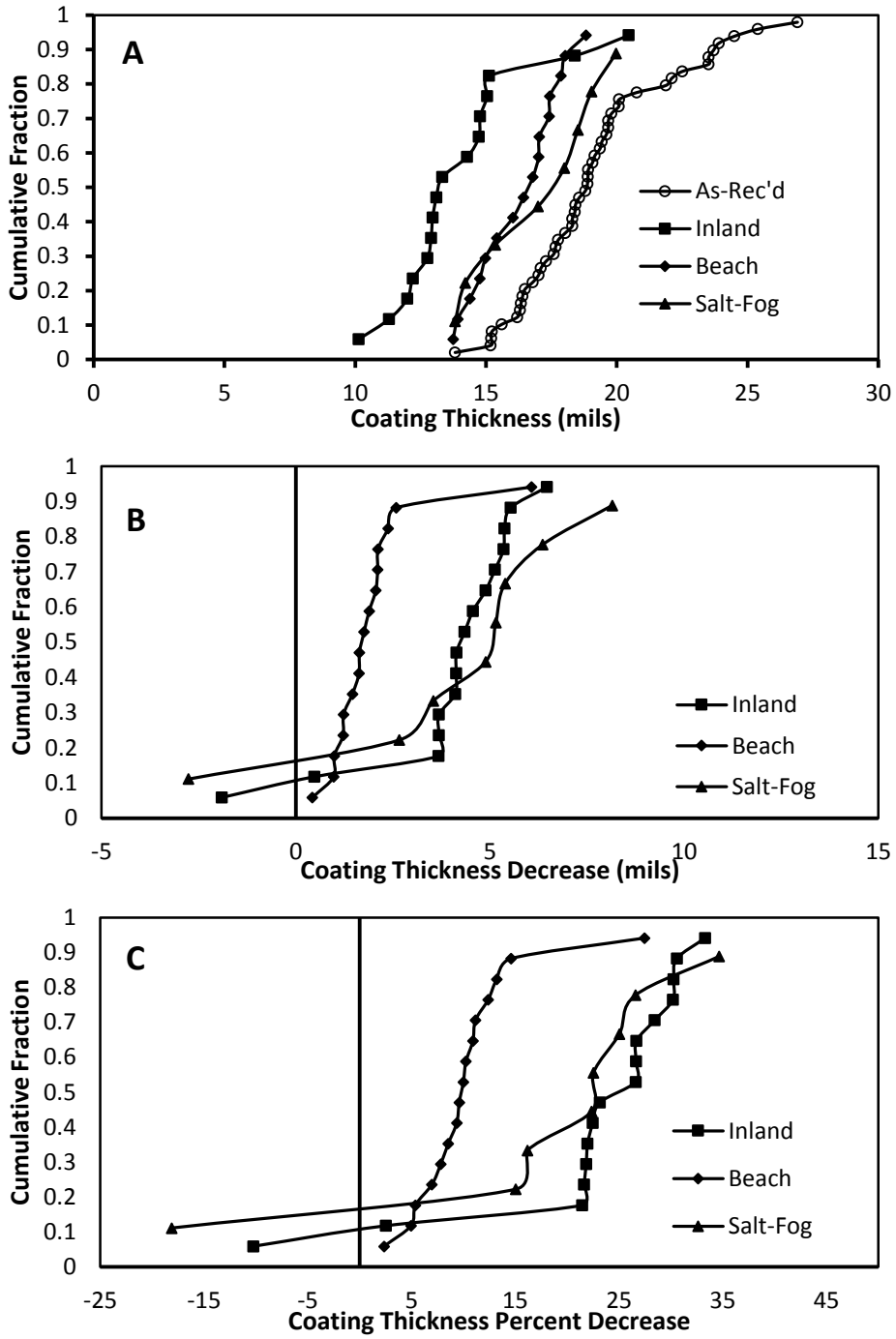


**Figure: 4.21 Three-Coat Coating Thickness Decrease**.

A) Actual coating thickness. B) Change of coating thickness. C) Percent change of coating thickness.

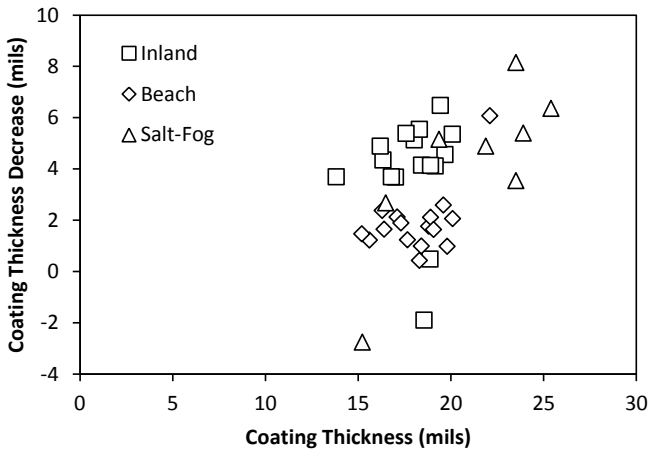


**Figure: 4.22 Three-Coat Coating Thickness Decrease vs. As-Received Coating Thickness**.

Reduction in average coating thickness up to ~6 mils was measured for 3-coat coated steel samples exposed in outdoor conditions. Decrease in coating thickness at the inland outdoor exposure site was similar or significantly greater than the beach outdoor exposure site. Similar decrease in coating thickness was calculated for coupons exposed to salt-fog environment. Manifested in the variability of the percent decrease in coating thickness is the variability in the calculations of the average coating thickness before and after exposure, in the coating application process, and in the rates and modalities of degradation. There was not a strong correlation between the original thickness and loss of coating thickness for any of the environmental exposure conditions (Figure 4.22).

## 4.4. COATING PULL-OFF STRENGTH

### *4.4.1 Chemically Bonded Phosphate Coating*

Photographs of the coated steel coupons after adhesion pull-off strength testing are shown in Figure 4.23 for as-received samples and Figure 4.24 for outdoor and salt-fog exposures. For the as-received samples, failure occurred at the metal-coating interface. The exposed metal surface was relatively clean with only minor surface rust.

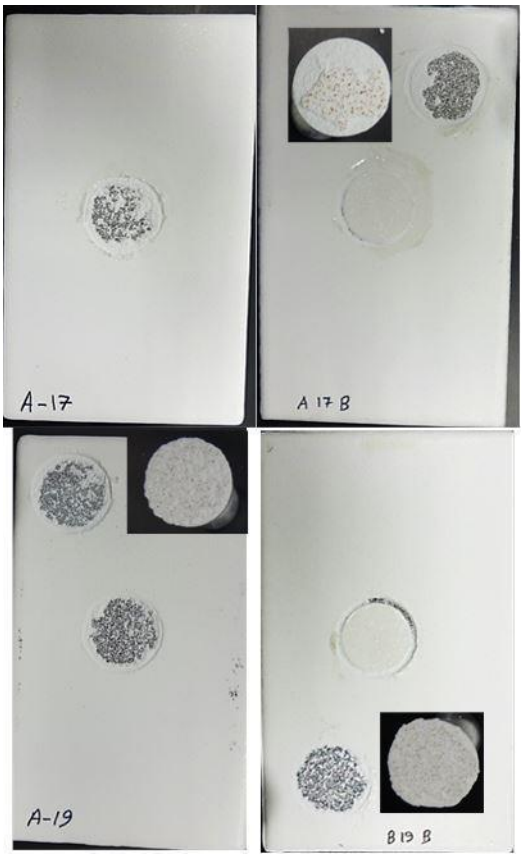


**Figure: 4.23 CBPC Coating Pull-Off in As-Received Condition**.


**Figure: 4.24 CBPC Coating Pull-Off after Outdoor (Top) and Salt-Fog Exposure (Bottom)**.

The surface appearance of coupons exposed to outdoor and salt-fog conditions after pull-off strength testing is shown in Figure 4.24. Pull-off adhesion testing was performed for the top surfaces of samples as well as the bottom surfaces. The ceramic coating showed indications of material degradation in all samples exposed to outdoor and salt-fog conditions. This was exemplified by partial coating failure, indicated by incomplete separation of the ceramic coating from the metal substrate, at strengths typically less than 200 psi, Figure 4.25. Two of four samples placed in salt-fog exposure had partial coating failure with negligible applied force. Furthermore, many test locations on each sample had shown significant rust development under the ceramic coating even though no outward indication, prior to the removal of the coating, was observed. In those cases, the coating could be fully separated from the metal substrate. It was thought that exposure led to deterioration of the porous ceramic coating which provided availability of moisture to penetrate the coating to the metal surface.

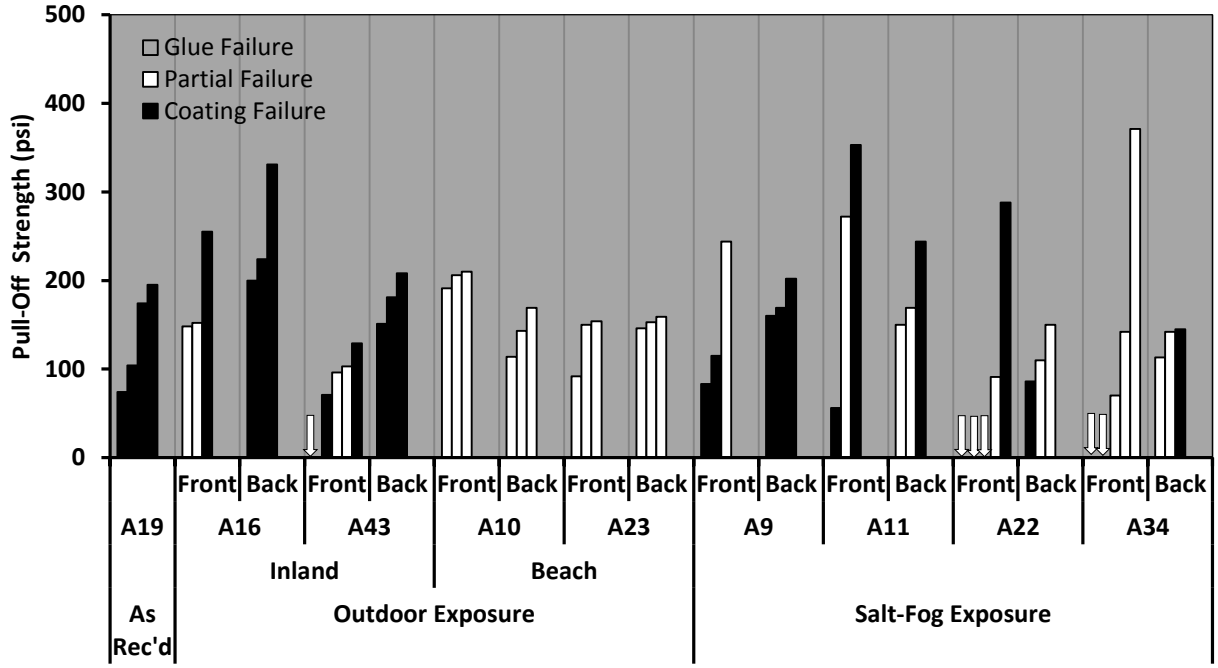


**Figure: 4.25. CBPC Coating Pull-Off Strength**.

The extent of undercoating rusting was apparently more severe in the backside of the test samples. This observation cannot be fully explained by the physical evidence. It was thought that there could be prolonged presence of moisture on the back face of the coupon due to condensation buildup, moisture runoff, and less evaporative heating by the sun for the outdoor samples. In the salt-fog chamber, moisture run-off due to condensation of the salt-fog and sample placement at an incline may create greater contact time with moisture.

As shown in Figure 4.25, the adhesive strength of the CBPC coating was typically less than 200 psi. With the exception of the samples in the salt-fog chamber with partial coating failure at negligible stresses, no differentiation in the coating strength after exposure could be readily identified due to the inherent relative low pull-off strength of the coating. All pull-off measurements were less than 400 psi and all measurements in the as-received condition were less than 200 psi. The somewhat greater strengths sometimes measured for samples after exposure was thought to be in part due to glue penetration in the degraded coating (i.e. surfacing roughening and thickness reduction) and general variability in the supplied test materials.

### *4.4.2 Thermal Diffusion Galvanizing*

Photographs of the coated steel coupons after adhesion pull-off strength testing are shown in Figures 4.26-4.29. In the as-received condition, part of the coating system could be removed from the coupon surface. The underlying coating surface after pull-off testing typically showed a speckled appearance where the topcoat (when present) and part of the zinc coating were pulled off. The underlying coating did not show any steel surface rust. As shown in Figures 4.30-4.32, the coating pull-off strength of the plain TDG and TDG with Topcoat A in the as-received condition was ~750-2,000 psi. The high values in these coating configurations were thought to be due to the strength of the zinc alloy layers. The coating pull-off strength of TDG with Topcoat B and Topcoat A+B was less than 600 psi. Sample variability cannot be completely ruled out, but the low values were thought to be related to the adhesion of the topcoat. Adhesion of Topcoat B appears to be weaker than that of Topcoat A.

The surface appearance of coupons exposed to outdoor and salt-fog conditions after pull-off strength testing is shown in Figures 4.27 and 4.29. Pull-off adhesion testing was made for the top surface of the coupon as well as the surface on the backside of the test samples.


**Figure: 4.26. TDG Coating Pull-Off in As-Received Condition**.

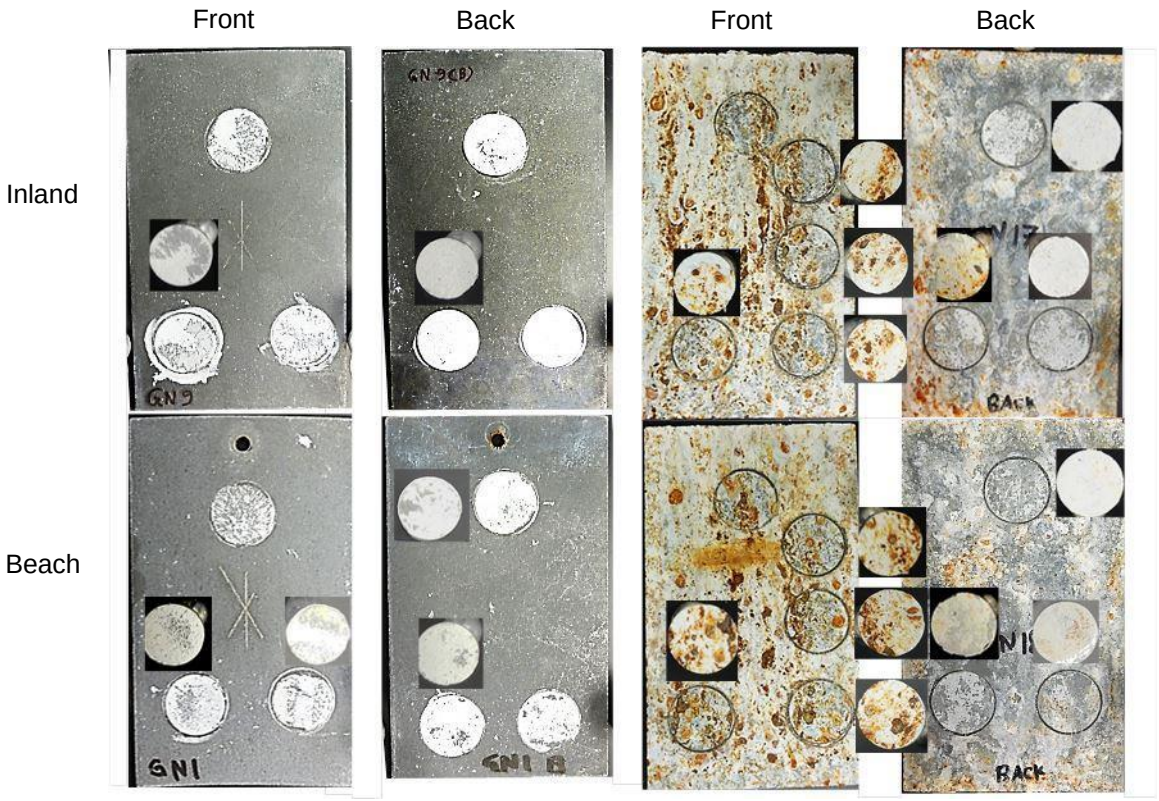


**Figure: 4.27 TDG Without Topcoat Coating Pull-Off After Outdoor/Salt-Fog Exposure.**

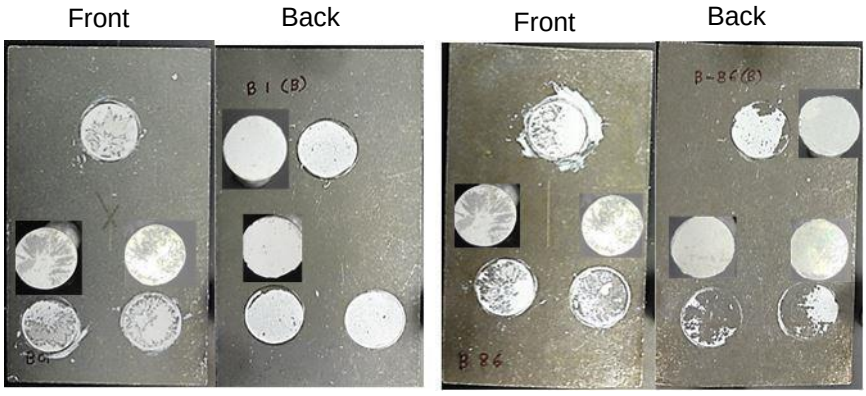


**Figure: 4.28 TDG with Single Topcoat Coating Pull-Off After Inland Outdoor Exposure.**

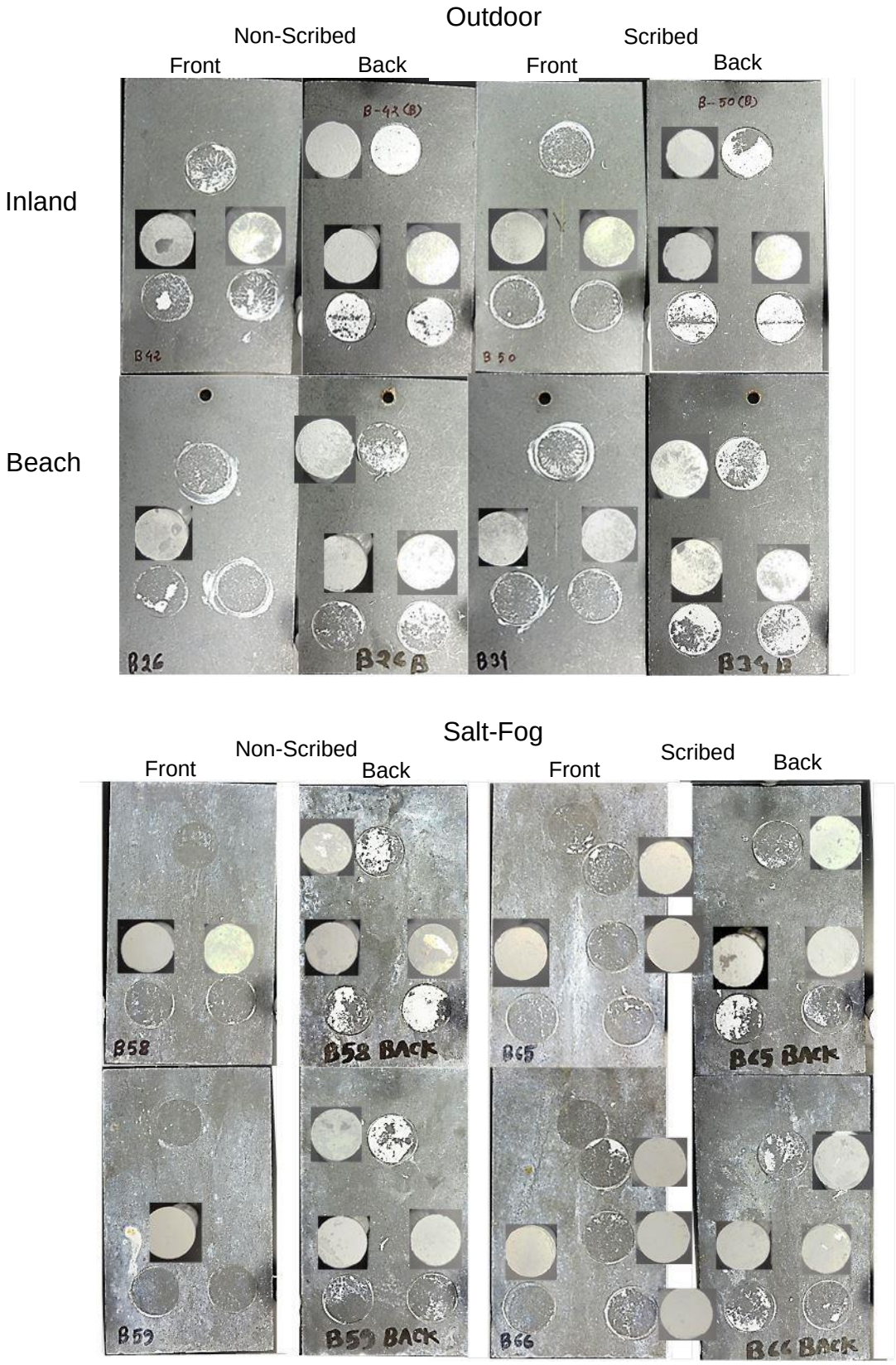


**Figure: 4.29 TDG with Topcoat A+B Coating Pull-Off After Outdoor/Salt-Fog Exposure.**

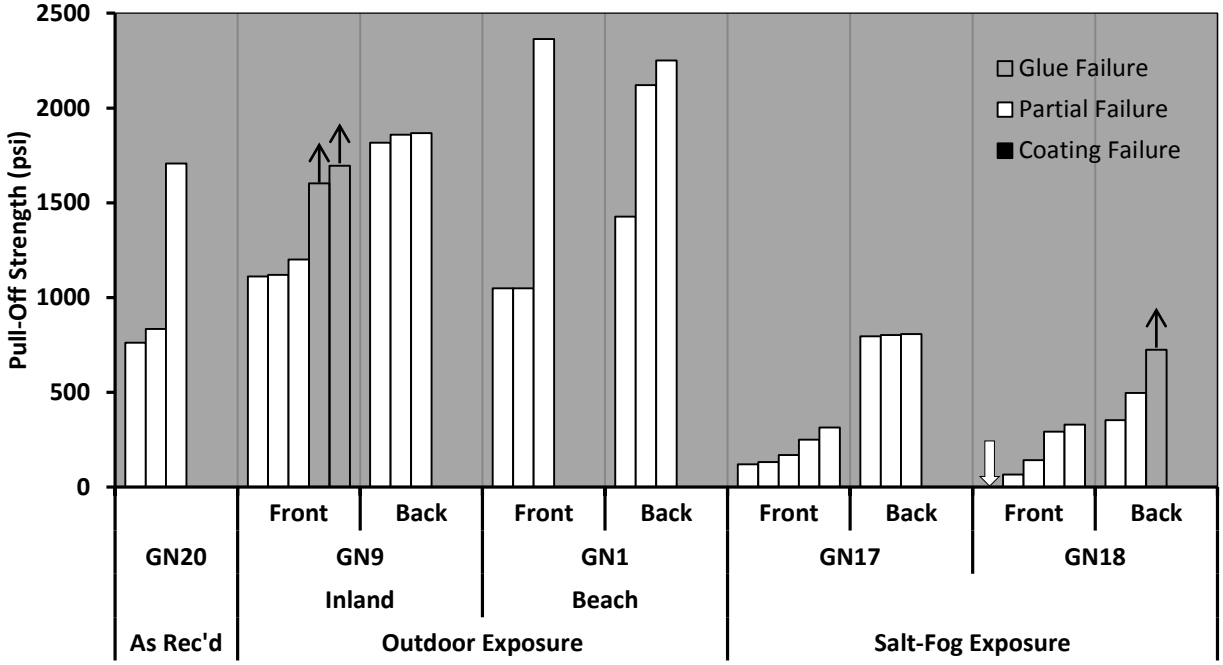


**Figure: 4.30 Plain TDG Coating Pull-Off Strength**.

Consistent with the visual observation of minimal zinc oxide accumulation on the plain TDG samples during outdoor exposure testing, there was no major differentiation in pull-off strength from the as-received condition (Figure 4.30). Post outdoor-exposure pull-off strengths were typically greater than 1,000 psi.

Results of pull-off testing of coated samples exposed to 4-month outdoor exposure typically resulted in partial coating failure where zinc layers could be separated from the surface. No indication of steel corrosion was observed at the pull-off locations. Consistent with pull-off measurements in the as-received condition, the pull-off strength for TDG with Topcoat A was greater than pull-off strength of TDG with Topcoat B; however, the pull-off strengths for both coatings were generally greater than the as-received condition (Figure 4.31). Similar trends were observed for TDG with Topcoat A+B (Figure 4.32). It was thought that degradation of the topcoat could lead to better penetration of the glue resulting in enhanced strengths of the pull-off dolly to the sample surface.

Only plain TDG and TDG with Topcoat A+B were evaluated in salt-fog exposure. As shown earlier, significant iron corrosion products formed on the surface of the plain TDG samples in salt-fog exposure. The coating manufacturer attributed the appearance to iron in the coating and recommended use with topcoat. In the heavy presence of iron oxide product, the pull-off strength is significantly reduced in comparison to the as-

received condition (Figure 4.30) and separation of the material occurred due to cohesive strength failure of the corrosion product.

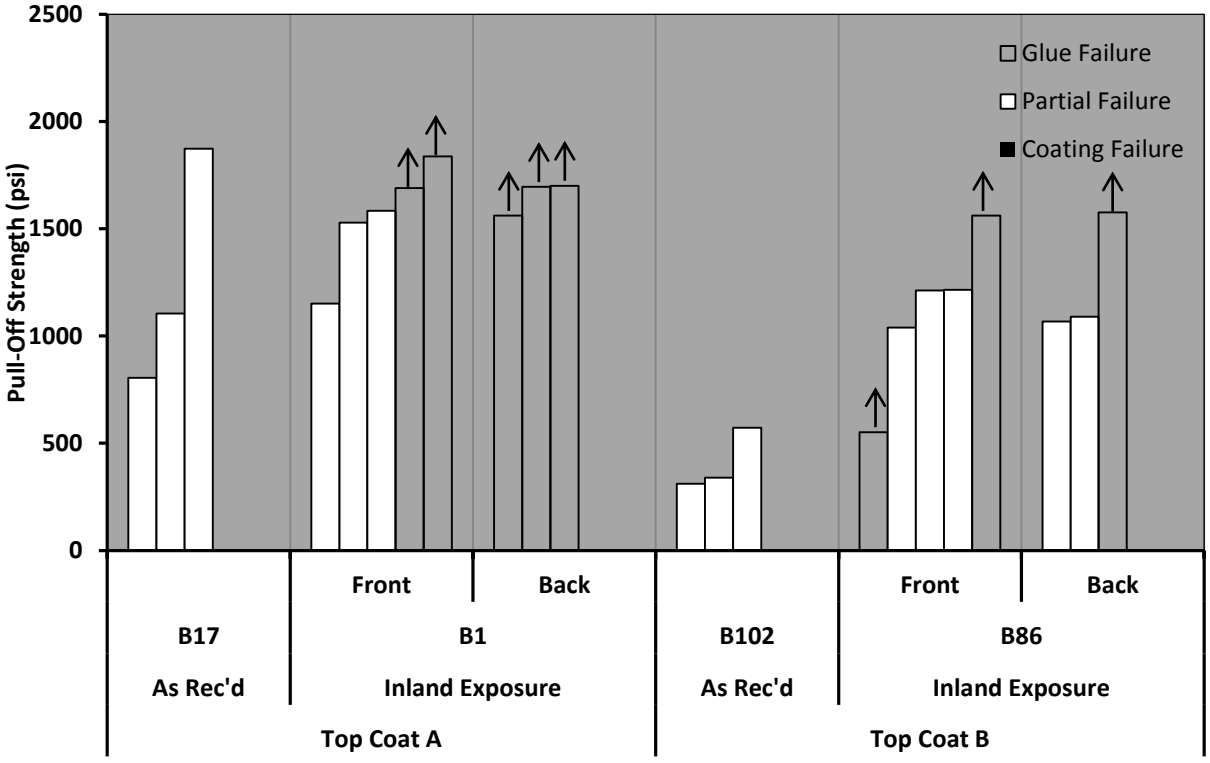


**Figure: 4.31 TDG with Single Topcoat Coating Pull-Off Strength**.

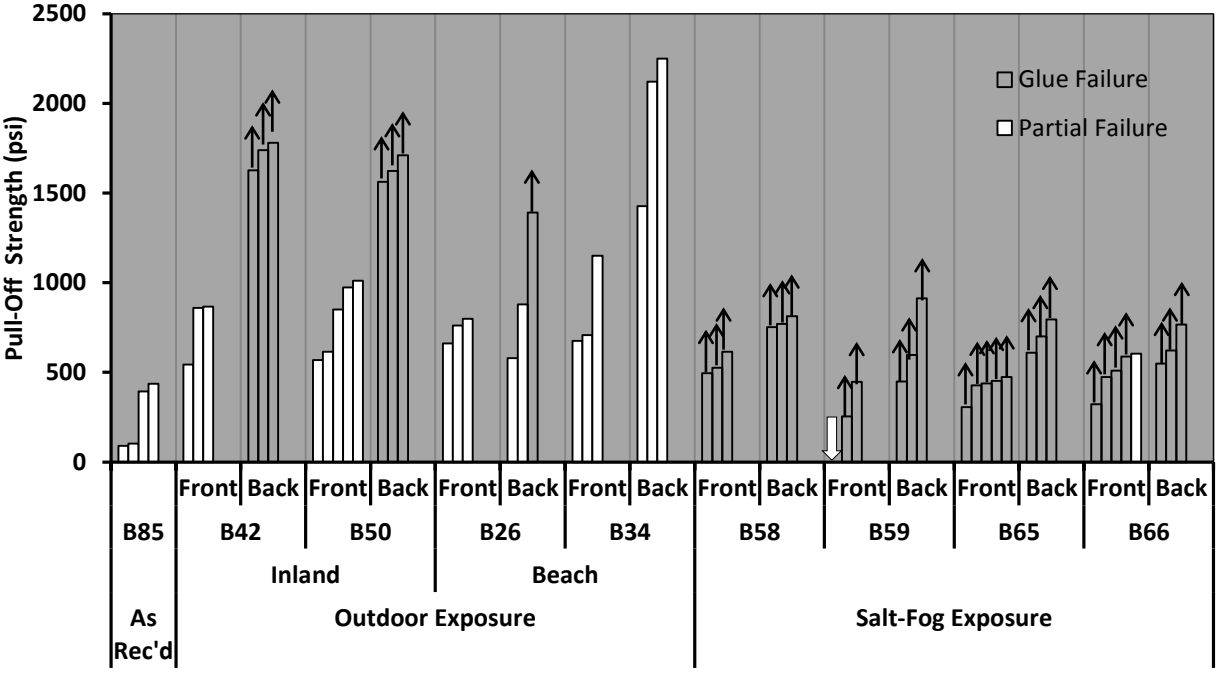


**Figure: 4.32 TDG with Topcoat A+B Coating Pull-Off Strength**.

The appearances of the coupons with Topcoat A+B exposed in salt-fog after pull-off testing are shown in Figure 4.29. Most of the pull-off testing after salt-fog exposure resulted in adhesion failure of the glue (some indication of partial coating separation was apparent but typically negligible); however, those minimum values were still greater than the pull-off strength of the coating in the as-received condition. As suggested earlier, the low pull-off strength of TDG with Topcoat A+B in the as-received condition was thought to be due to poor adhesion of the topcoat. Due to the apparent formation of zinc oxide products on the surface of the coupon after salt-fog exposure, a further reduction in pull-off strengths was expected. However, the apparent increase in pull-off strength could be due in part to degradation of the topcoat, zinc oxide development and subsequent infiltration of the glue to the zinc/iron substrate resulting in strengths relatable to the non-coated condition.

Interestingly, for all coating configurations and exposure environments, the coupon back face showed indication of greater pull-off strength. Except for the note that less iron rust developed on the back face of plain TDG in salt-fog environment, there was no major differentiation in appearance for the other coating configurations and exposure conditions. Coating thickness of the back face was not measured. The differences in pull-off strength may be indicative the influence of moisture and drying.

### *4.4.3 Metallizing*


**Figure: 4.33 Metallized Coating Pull-Off in As-Received Condition.**

Photographs of the coated steel coupons after adhesion pull-off strength testing are shown in Figures 4.33 and 4.34. In the as-received condition, Figure 4.33), the metallized coating could be fully extracted from the metal surface. The underlying metal typically had clean surface conditions with no surface rust. As shown in Figure 4.35, the adhesive strength of the as-received metallized coating was typically less than 1,000 psi.

The surface appearance of coupons exposed to outdoor and salt-fog conditions after pull-off strength testing is shown in Figure 4.34. Pull-off adhesion testing was done for

the top surface of the coupon as well as the surface on the backside of the test samples.

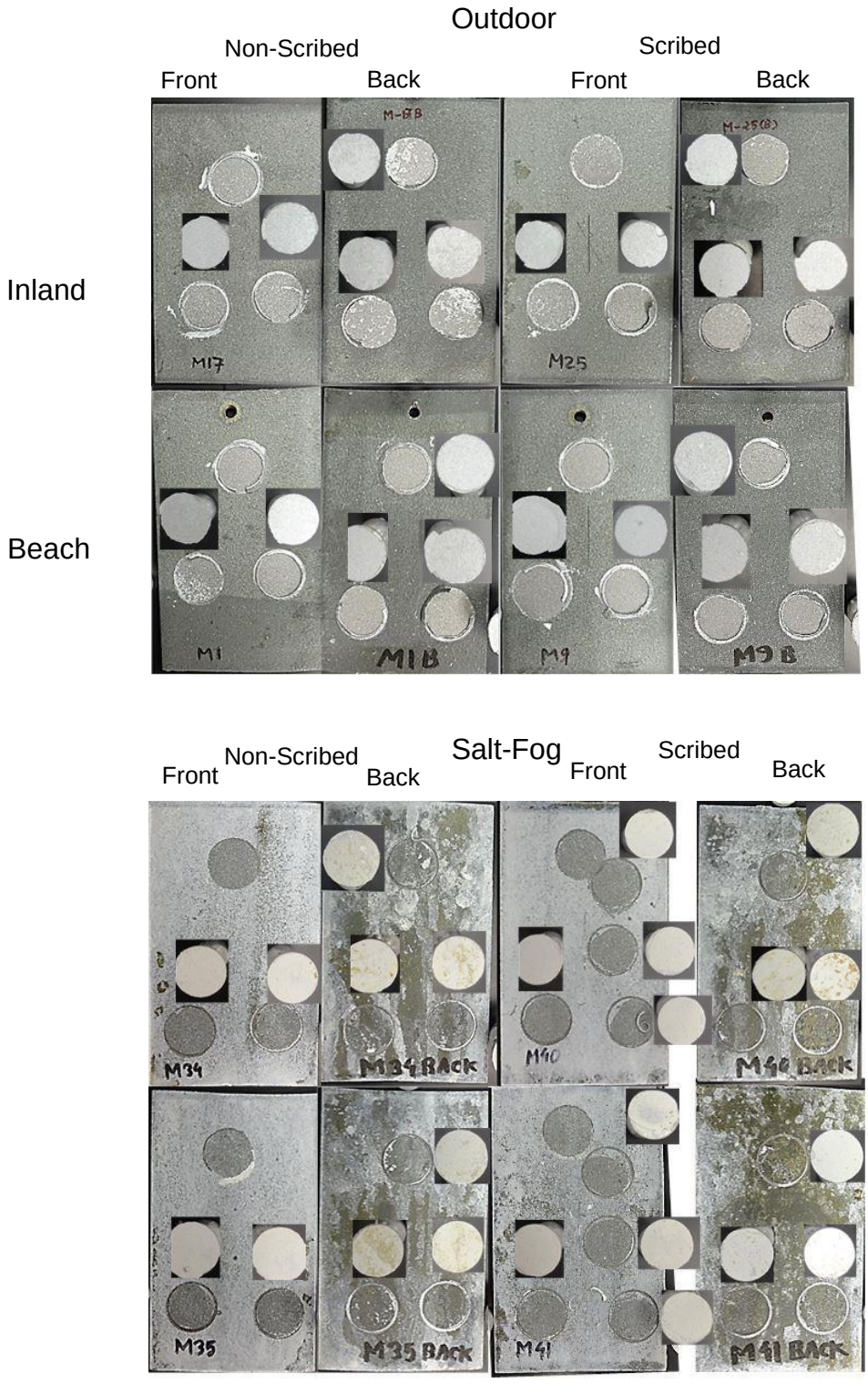


**Figure: 4.34 Metallized Coating Pull-Off after Outdoor/Salt-Fog Exposure**.

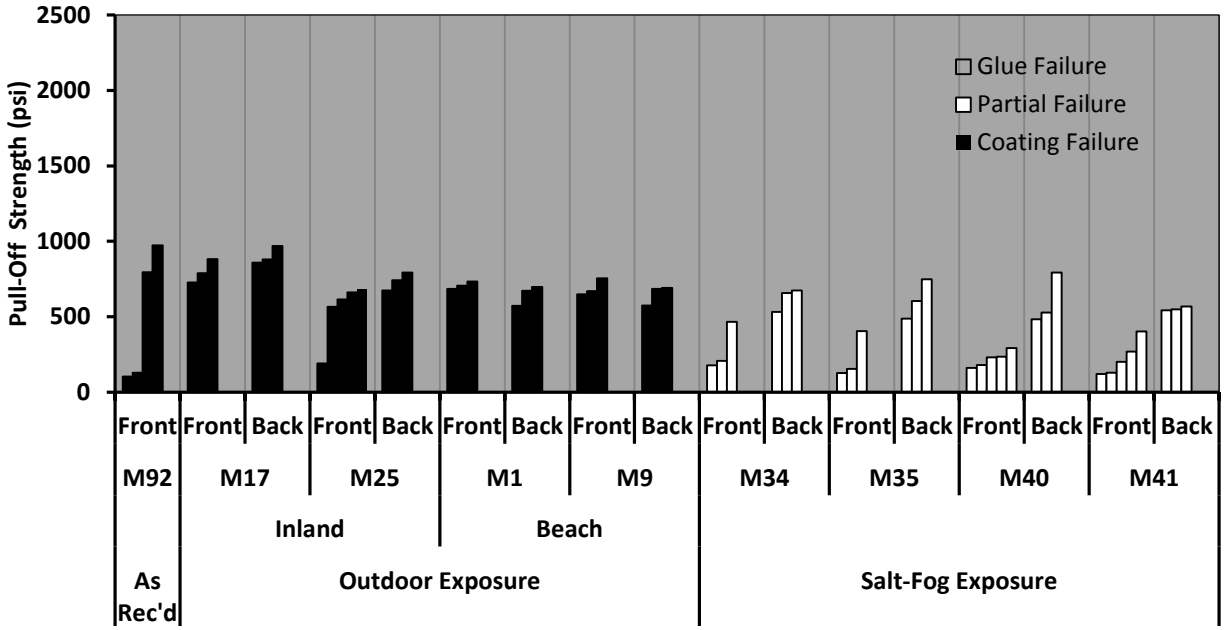


**Figure: 4.35 Metallized Coating Pull-Off Strength**.

Portions of the coating were removed in all tested samples exposed to outdoor and salt-fog conditions. In outdoor exposure (similar to the as-received condition) the arc-sprayed zinc coating could be completely separated from the substrate. No major differentiation in pull-off strength was observed between samples in the as-received condition and those placed in 4-month outdoor exposure. Samples placed in 2200 hours salt-fog exposure showed zinc activity as exemplified by the accumulation of white zinc corrosion product on the surface. This accumulation developed more uniformly on the top surface than the sample back surface. Quality of topcoat application may be related to this observation but could not be substantiated. Because of the oxide accumulation on the sample surfaces, the pull-off tests resulted in removal of the zinc oxide product and generally lower strengths than compared to the outdoor exposure condition. As a result of better topcoat integrity and less zinc oxide production on the back surface, the pull-off strength was generally higher there than for the coating on the front face.

### *4.4.4 Three-Coat*

**Figure: 4.36 Three-Coat Coating Pull-Off in As-Received Condition**.

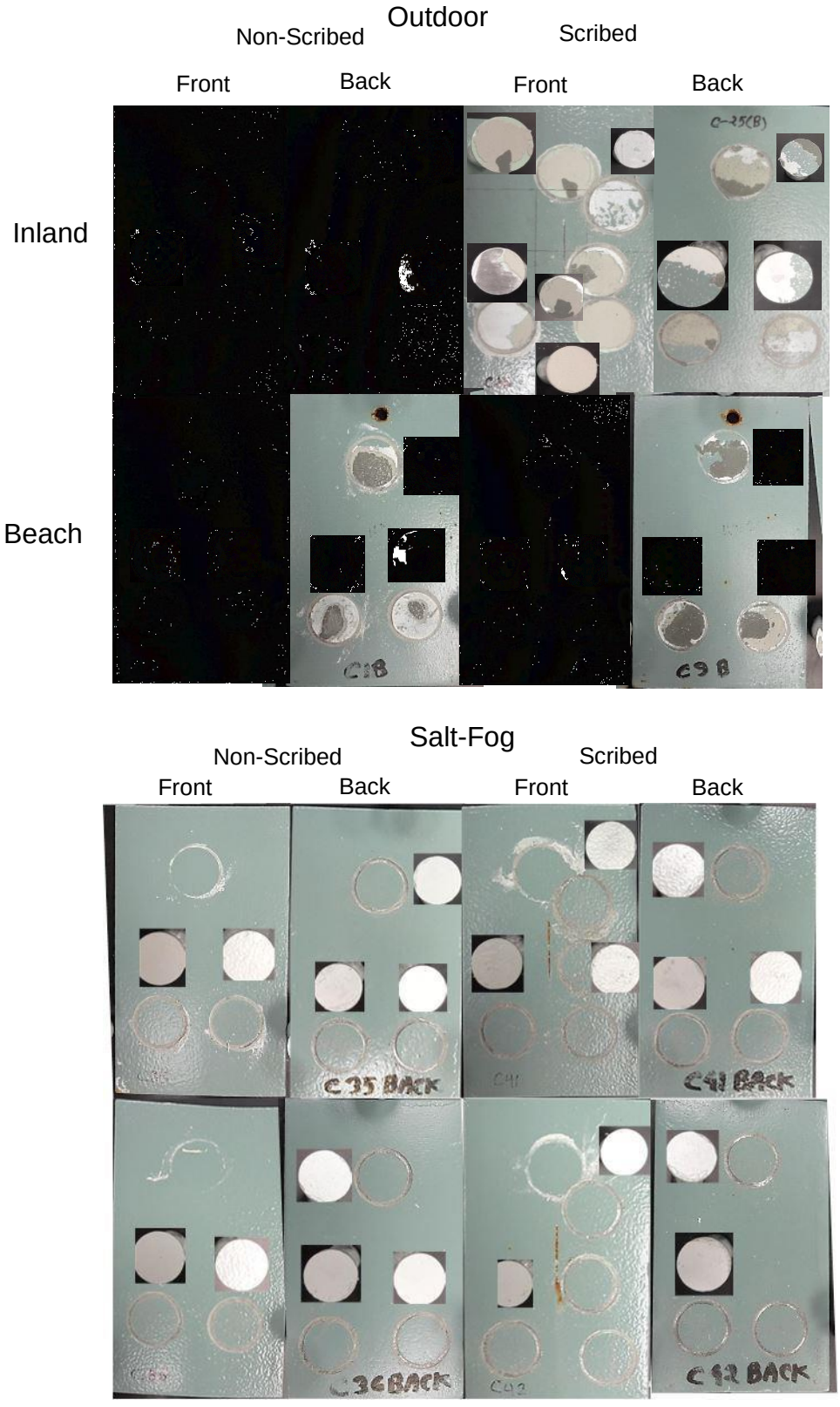


**Figure: 4.37 Three-Coat Coating Pull-Off after Outdoor/Salt-Fog Exposure**.

Photographs of the coated steel coupons after adhesion pull-off strength testing is shown in Figures 4.36 and 4.37. In the as-received condition, Figure 4.36, the pull-off testing resulted in failure of the epoxy used to mount the pull-off dolly to the coupon surface. Testing in as-received condition was inconclusive and is pending additional testing.

The surface appearance of coupons exposed to outdoor and salt-fog conditions after pull-off strength testing is shown in Figure 4.37. Pull-off adhesion testing was done for the top surface of the coupon as well as the surface on the backside of the test samples.

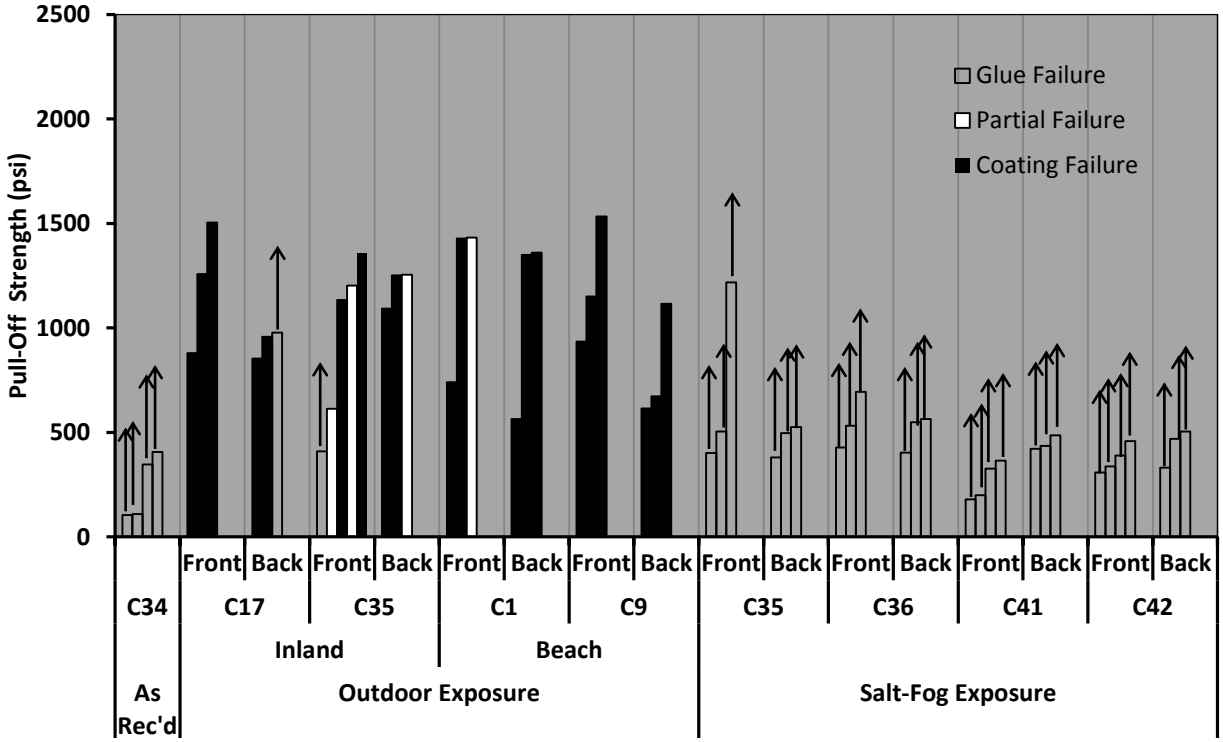


**Figure: 4.38 Three-Coat Coating Pull-Off Strength**.

Portions of the coating were removed in all tested samples exposed to outdoor conditions. After 4-month outdoor exposure, pull-off testing completely separated the coating from the substrate. The pull-off strength ranged from ~500 to ~1500 psi (Figure 4.38). No under-coating steel corrosion was observed. Samples placed in 2200 hours salt-fog exposure showed steel corrosion only at local coating defects. All pull-off testing of samples placed in salt-fog exposure resulted in adhesion failure of the epoxy (typically less than 700 psi) used to mount the pull-off dolly to the coating surface and results were inconclusive. Surface preparation procedures for pull-off testing will be reviewed for testing after 8-month exposure.

## 4.5. DISCUSSION

### *4.5.1 Chemically Bonded Phosphate Coating*

Testing of physical coating parameters and observation of corrosion development for CBPC-coated steel coupons subjected to outdoor exposure for 4 months and salt-fog exposure for 2200 hours were intended to provided earlier performance indicators on general durability of the coating in atmospheric conditions.

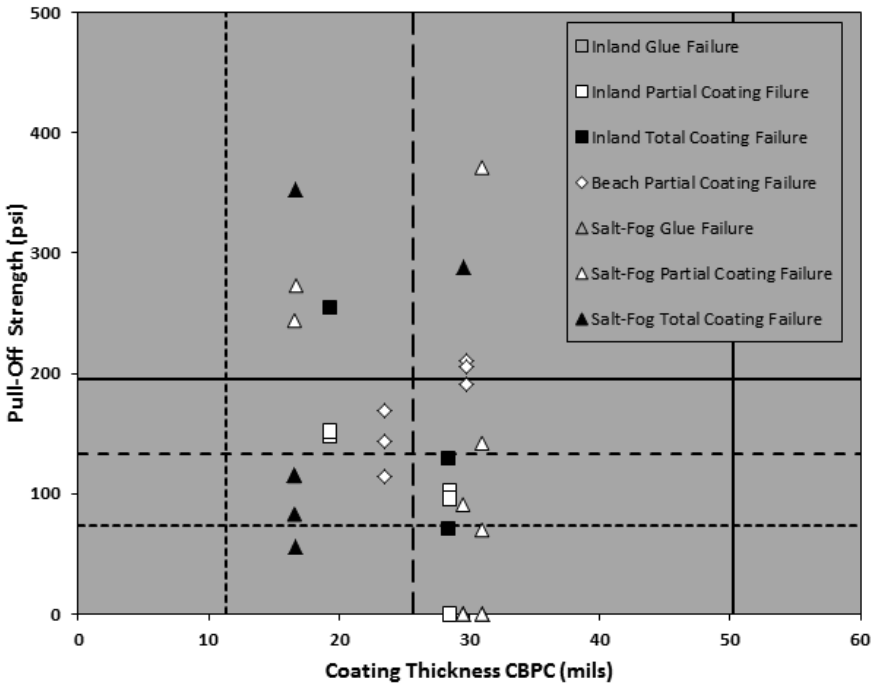


**Figure: 4.39 CBPC Coating Degradation** (The three horizontal and vertical lines represent minimum, median and maximum value).

Figure 4.39 shows a compilation of post-exposure coating thickness and pull-off strength measurements for the samples removed from the test site for destructive testing. Even though those samples were randomly selected, they did not fully represent the coating parameter variability observed for the entire test population. Nevertheless, the figure correlates the tested coating parameters after 4-month outdoor exposure and 2200 hours salt-fog exposure, and compares them to coating parameters of the total population of samples in the as-received condition. The values in the as-received condition are shown as minimum, mean, and maximum values.

Per earlier caveat, there was sample variability in those coating parameters, so the pull-off strength measurements are correlated to a general descriptor of coating thickness throughout the coupon surface and not necessarily the thickness at the location of the pull-off test. The post-exposure coating thickness measurements were the average of multiple spot readings throughout the coupon front face and the same thickness value

was reported for the multiple pull-off strength measurements. As an example, a sample exposed at the outdoor beach site had an average as-received coating thickness of ~36 mils, and the average after-exposure coating thickness was ~30 mils indicating small loss in coating material. However, as shown in the composite micrograph in Figure 4.40 for an approximate 0.5 cm cross section length, the CBPC coating thickness after 4-month exposure in the outdoor beach exposure was ~965 µm (~38 mils). In consideration of the compiled data, no definite correlation could be made between the pull-off strength and the average post-exposure coating thickness. Portions of the test population had coating thickness loss and portions of the test population saw a change in pull-off strength. Also no distinct trend in modality of pull-off failure to coating thickness and strength could be determined.


**Figure: 4.40 CBPC Coating Micrograph after 4-Month Outdoor Beach Exposure**.

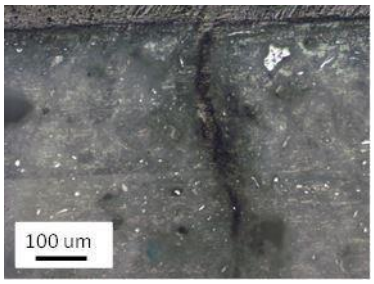


**Figure: 4.41 Crack in CBPC Coating Micrograph**.

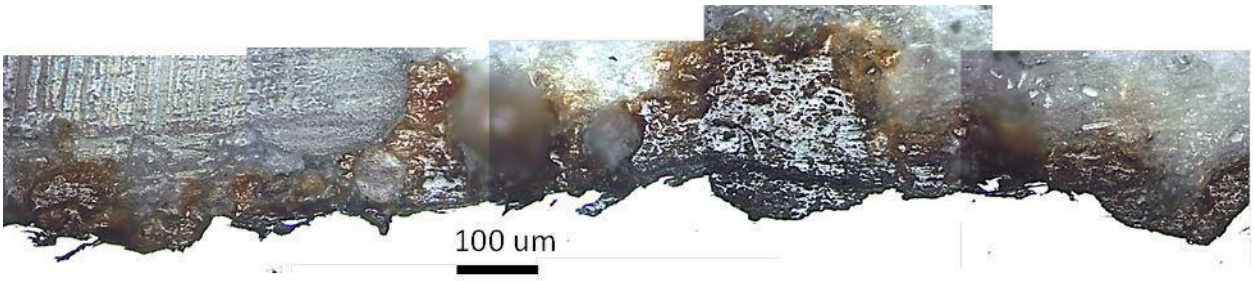


**Figure: 4.42 CBPC Undercoating Rust Development Micrograph**.

Generally speaking from testing observations in outdoor and salt-fog exposure, the CBPC coating in the condition provided for testing showed some susceptibility to degradation of the ceramic barrier coating. As seen in Figures 4.40-4.42, defects in the ceramic coating were observed. These defects and general material porosity may lead to enhanced moisture presence within the coating and at the metal interface. The integrity of the ceramic coating was shown to be compromised and lost cohesive strength when exposed in high moisture conditions. In outdoor exposure, although little coating degradation was outwardly observed, pull-off testing showed either coating strength loss (which can be indicative of coating deterioration) or undercoating corrosion development as seen in Figure 4.42. In aggressive salt-fog exposure, coating material degradation, subsequent surface roughening, moisture penetration, and undercoating steel corrosion were apparent. Scribing resulted in no differentiation (beneficial or aggravating) in coating durability due to the presence of exposed steel in atmospheric exposure testing.

Based on the initial results, compromise in coating durability results from degradation of the ceramic coating in the presence of high moisture content and a subsequent increase in moisture at the steel substrate interface where coating defects and large coating pore provided direct access to the steel. Greater moisture penetration with aggressive chemical constituents such as chloride ions would accelerate corrosion development. Interestingly, observed undercoating corrosion was in between the ceramic coating and another layer at the steel substrate and does not appear to penetrate into the steel substrate.

### *4.5.2 Thermal Diffusion Galvanizing*

Figure 4.43 shows compilation of post-exposure coating thickness and pull-off strength measurements for the plain TDG and TDG with double topcoat (Topcoat A+B) samples removed from the test sites for destructive testing. The figure correlates the tested coating thickness with pull-off strength after 4-month outdoor exposure and 2200 hours salt-fog exposure and compares them to coating thickness and pull-off strength of samples in the as-received condition from the total population. Per earlier caveat, there was sample variability in those coating parameters. The values in the as-received condition were shown as minimum, mean, and maximum values. The post-exposure coating thickness measurements were the average of multiple spot readings throughout the coupon front face and the same value was reported for the multiple pull-off strength measurements.

TDG coated steel coupons subjected to outdoor exposure for 4 months generally showed positive results. No indication of steel rust development was observed, although a change in coating thickness was observed. Figures 4.44 and 4.45 show micrograph cross-sections of TDG coated samples, with and without topcoat, after 4-month outdoor beach exposure. Figure 4.44 shows micrographs of two samples with Topcoat A+B. The

micrograph on the left shows the TDG coating largely intact with thickness ~1.6 mils (but with indication of TDG coating defects). The micrograph on the right shows significant loss of the TDG coating with the thickness of the fragmented TDG layer <1 mil. Both samples showed degradation of the topcoat. Micrographs of a plain TDG sample after exposure (Figure 4.45) show significant degradation of the TDG coating.

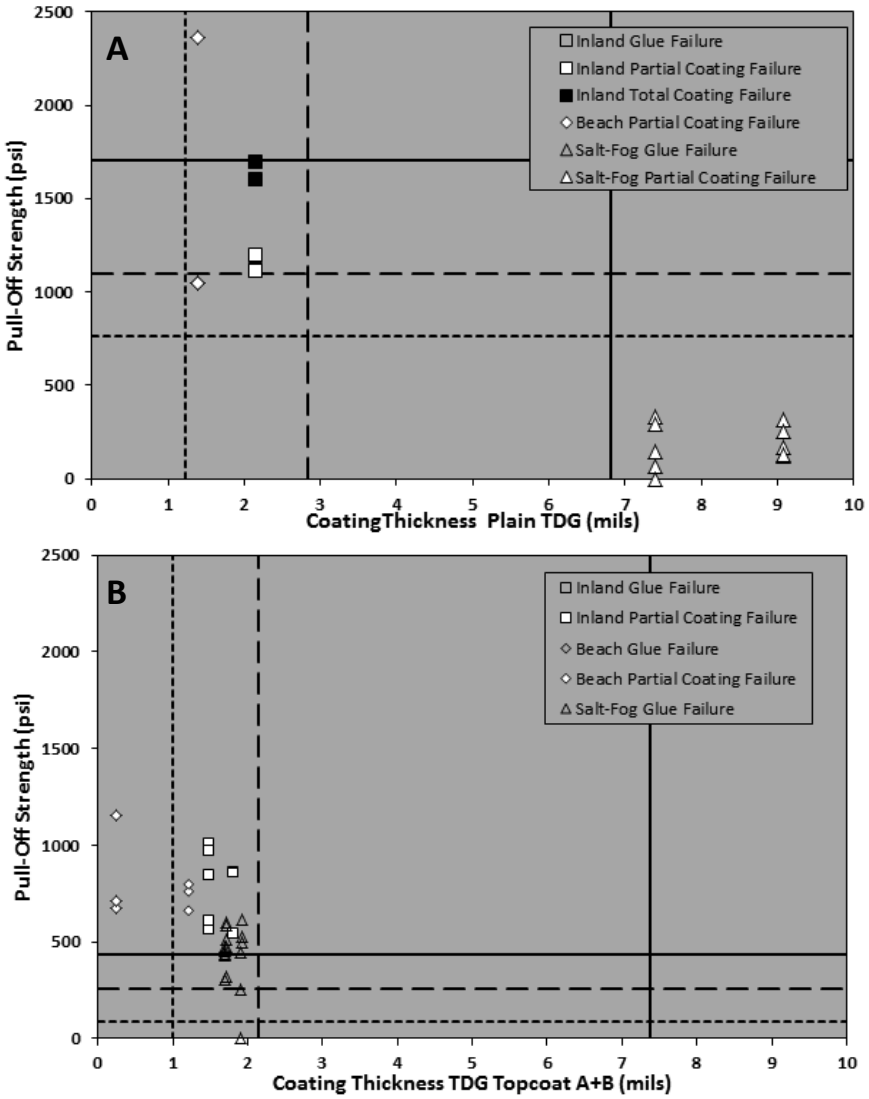


**Figure: 4.43 TDG Coating Degradation** (The three horizontal and vertical lines represent minimum, median and maximum value).
A) Plain TDG. B) TDG with topcoat A+B

In the short term outdoor exposure, there was indication of varying performance of the TDG coating. As described earlier, variations in topcoat applications result in varying coating performance. As seen in Figure 4.43, there was indication of increase in pull-off strength for coated samples whose post-exposure coating thickness tended to be below the mean as-received coating thickness. These results were thought to indicate, in part,

degradation of the topcoat and subsequent degradation of the TDG, where coating degradation due to exposure would lead to better adhesion of the mechanical pull-off dolly to the metal alloy layers during pull-off testing.

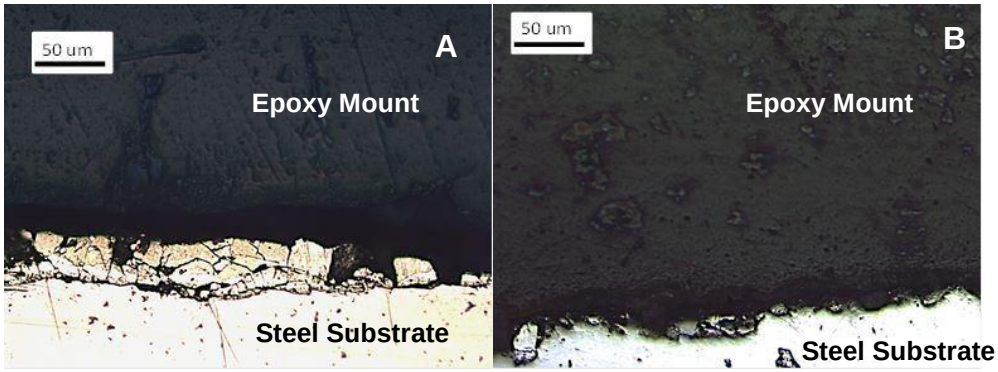


**Figure: 4.44 TDG Coating with Topcoat A+B after 4-Month Outdoor Beach Exposure Micrograph.**

A) 20X Magnification B) 20X Magnification

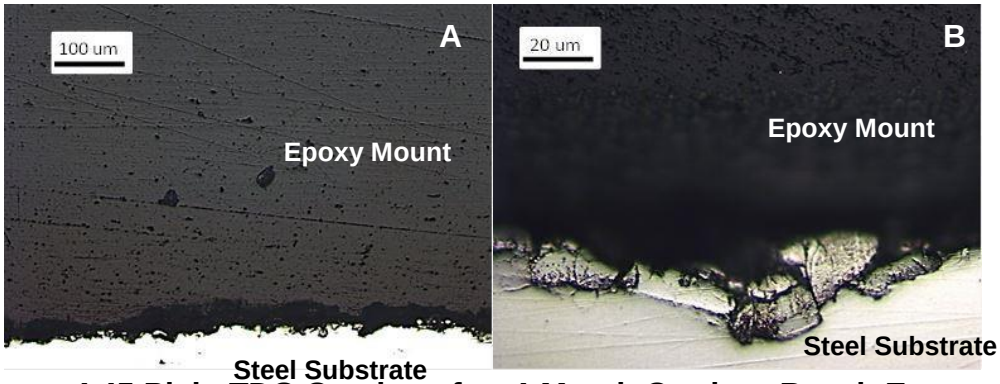


**Figure: 4.45 Plain TDG Coating after 4-Month Outdoor Beach Exposure Micrograph.**

A) 10X Magnification B) 50X Magnification.

2200 hour salt-fog testing did show major iron corrosion product accumulation on plain TDG samples. As shown in Figure 4.43, the accumulated rust resulted in greater coating thickness and reduced pull-off strength. This rust had been suggested by the manufacturer to be caused by iron within the TDG coating and topcoats were suggested to mitigate the aesthetics concerns. However, there remains concern about coating durability in the presence of local defects where localized iron corrosion products may impact the whole coating system. Indeed pull-off testing of plain TDG samples with rust accumulation indicated poor adhesion of the surface rusts. On a promising note, in the 2200 hours salt-fog testing of coated TDG, no iron corrosion products developed even in the presence of local scribed defects exposing the metal substrate. There, activity of the zinc alloy layers was apparent. The durability of the topcoat is important for the overall durability of the coated system for bridge application.

### *4.5.3 Metallizing*

Figure 4.46 shows a compilation of post-exposure coating thickness and pull-off strength measurements for the metallized steel samples removed from the test site for destructive testing. The figure correlates the aforementioned coating parameters after 4-month outdoor exposure and 2200 hour salt-fog exposure and compares them to samples in the as-received condition from the total population. Per earlier caveat, there was sample variability in those coating parameters. The values in the as-received condition were shown as minimum, mean, and maximum values. The post-exposure coating thickness measurements were the average of multiple spot readings throughout the coupon front face and the same value was reported for the multiple pull-off strength measurements.

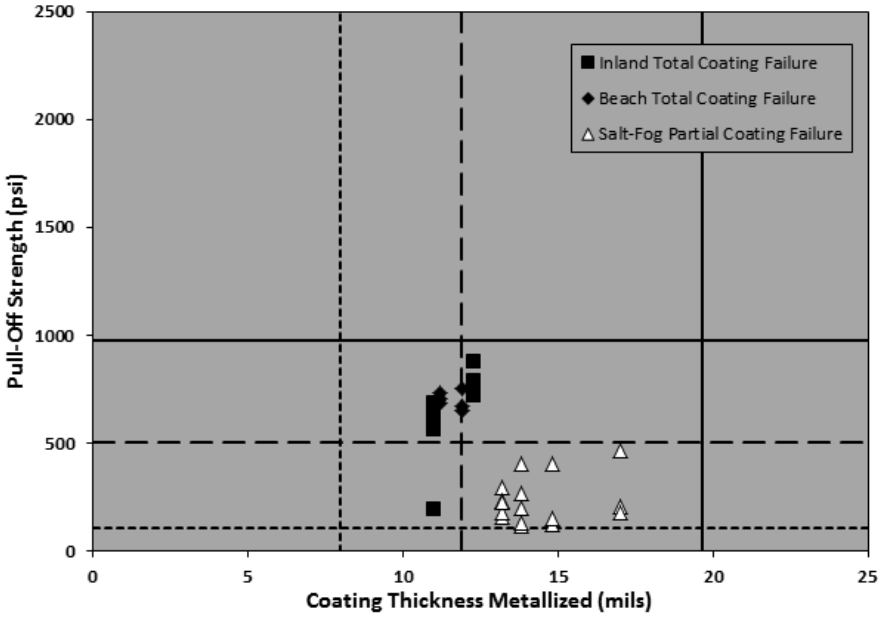


**Figure: 4.46 Metallized Coating Degradation** (The three horizontal and vertical lines represent minimum, median and maximum value).

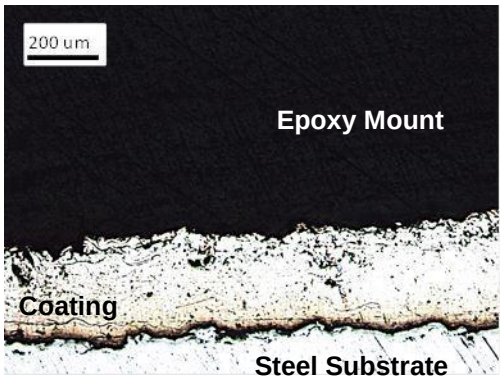


**Figure: 4.47 Metallized Coating after 4-Month Outdoor Beach Exposure**.

Testing of physical coating parameters for metallized coated steel coupons subjected to outdoor exposure for 4 months and in salt-fog for 2200 hours generally showed positive results. Although some change in coating thickness was observed, no major degradation of the metallized coating was observed. As seen in Figure 4.47, the metallized layer remained intact after 4-month outdoor beach exposure. Testing did not show major steel corrosion product accumulation. However, accumulated zinc oxide in salt-fog testing resulted in greater coating thickness and reduced pull-off strength (Figure 4.41). No steel corrosion product developed in the presence of local scribed defects exposing the metal substrate in any of the testing. As shown earlier, some steel rust did form at local coating defect spots. Activity of the zinc layer was apparent in all test environments. The durability of the topcoat is important for the overall durability of the coated system for bridge application. Initial testing in salt-fog environment did show varying topcoat performance.

### *4.5.4 Three-Coat*

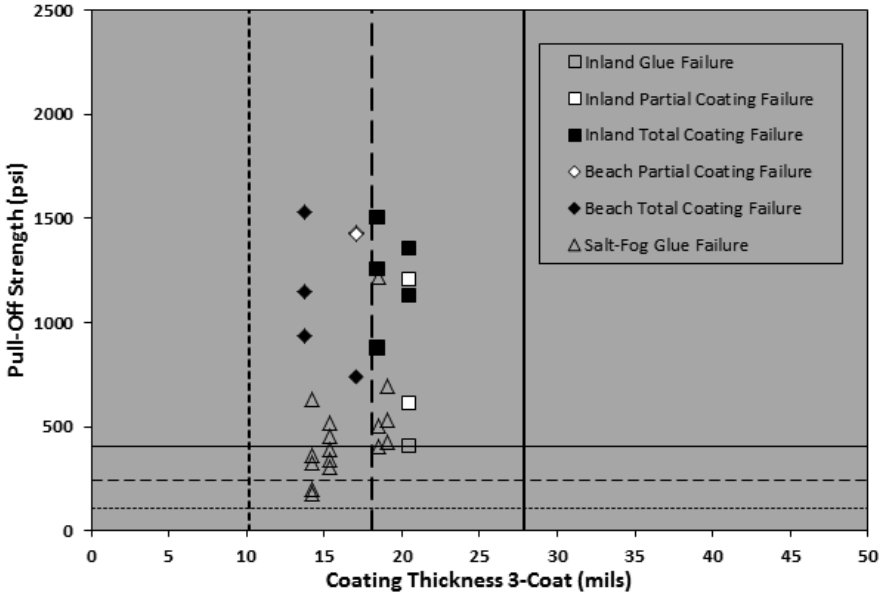


**Figure: 4.48 Three-Coat Coating Degradation** (The three horizontal and vertical lines represent minimum, median and maximum value).

Figure 4.48 shows compilation of post-exposure coating thickness and pull-off strength measurements for the 3-coat steel samples removed from the test site for destructive testing. The figure correlates the aforementioned tested coating parameters after 4-month outdoor exposure and 2200 hours salt-fog exposure and compares them to samples in the as-received condition from the total population. Per earlier caveat, there was sample variability in the coating parameters. The values in the as-received condition were shown as minimum, mean, and maximum values. The post-exposure

coating thickness measurements were the average of multiple spot readings throughout the coupon front face and the same value was reported for the multiple pull-off strength measurements. Strengths measured were low due to adhesive failure between the sample and pull-off dolly. Thus the minimum, mean, and maximum as-received pull-off strengths represented failure of the adhesive and not of coating adhesion failure.

Testing of coated steel coupons in outdoor exposure for 4 months and in salt-fog for 2200 hours generally showed positive results. Testing did not show major steel corrosion product accumulation. Steel corrosion products did form at scribed locations of coatings exposed in salt-fog environment. Loss of coating adhesion due to processes such as coating disbondment could not be evaluated at this time due to inconclusive pull-off strength results. Figure 4.49 shows micrographs of a sample after 4-month outdoor beach exposure. The topcoat, epoxy, and zinc-rich primer remained intact, even at points adjacent to a scribe exposing the steel substrate.

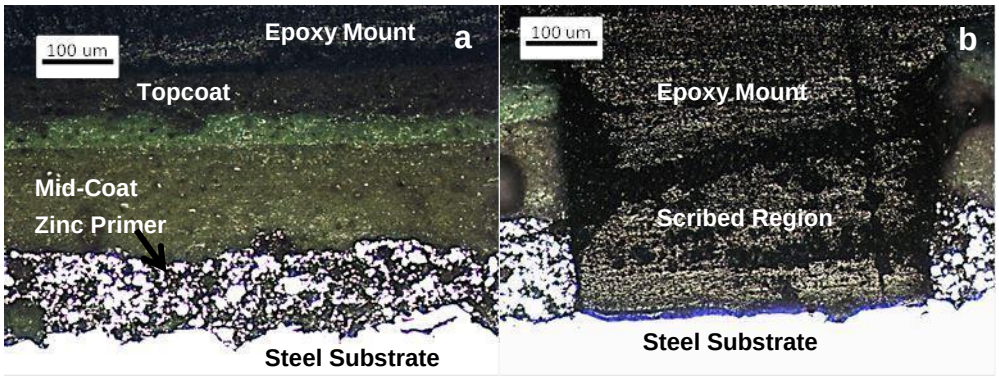


**Figure: 4.49 Three-Coat Coating after 4-Month Outdoor Beach Exposure**.
a) Micrograph for non-scribed location. b) Micrograph for scribed location.

## CHAPTER FIVE: COATING DETERIORATION AFTER EXTENDED EXPOSURE

A summary of the findings discussed below is provided in Appendix A.

### 5.1. INTRODUCTION

Chapter 5 discusses results for extended exposure, and is divided into 4 sections. The first, Section 5.1 is the introduction, and Section 5.2 shows photographic comparisons of coatings before and after exposure to outdoor or salt-fog environments. Sections 5.3 and 5.4 show comparisons of coating thicknesses and coating pull-off strengths after outdoor and salt-fog exposures. The environmental conditions for outdoor exposures are shown in Figure 5.1 and typical measurement locations are shown schematically in Figure 5.2 and Figure 5.3.

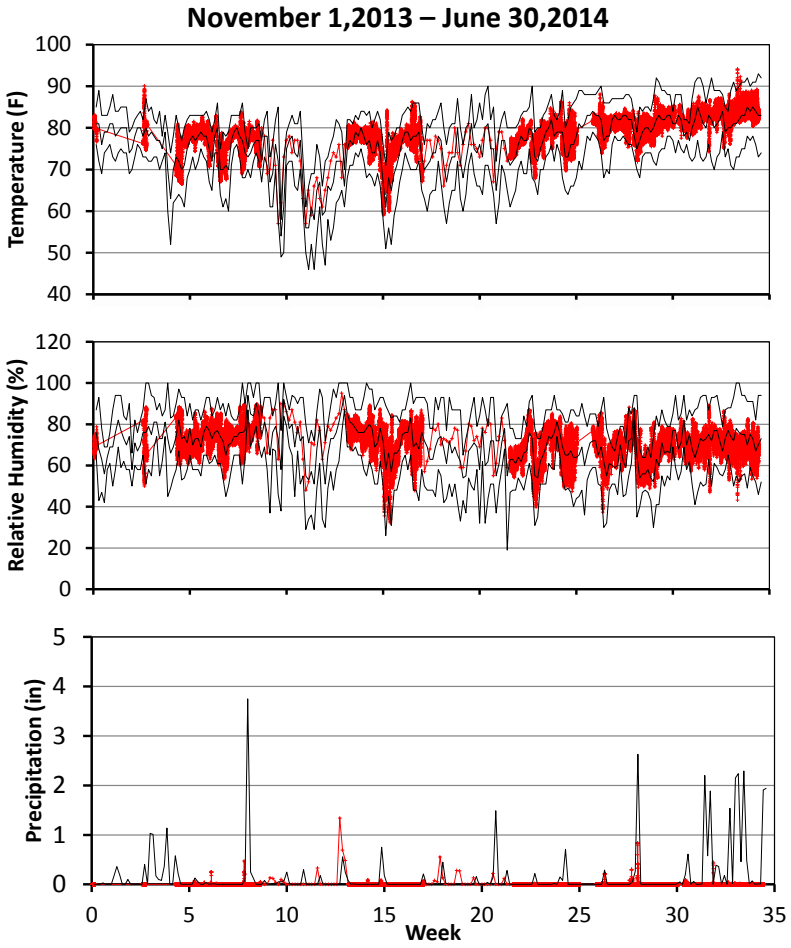


**Figure: 5.1 Environmental Conditions at Outdoor Test Sites**.
Black (FIU). Red (Tea Table).

Chemically bonded phosphate ceramic (CBPC), thermal diffusion galvanizing (TDG), thermal-spray metallizing, and conventional three-coat test coupons were prepared and placed for exposure in outdoor weathering conditions for 8 months and accelerated salt-fog exposures for 5800 hours. In this chapter, the evaluation results of 8-month outdoor and 5800 hours of salt-fog exposed samples will be presented.

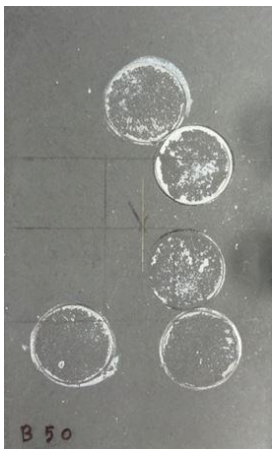


**Figure: 5.2 Typical Measurement Locations.**

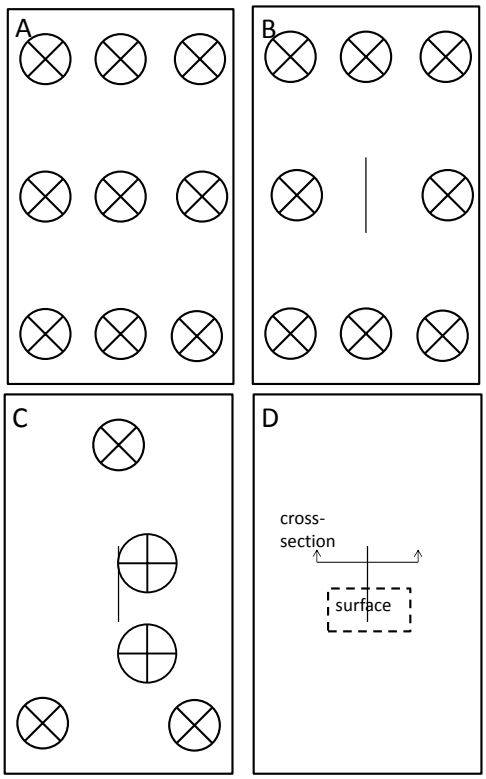


**Figure: 5.3 Sample Testing Surface Locations**. A) Approximate coating thickness locations for as-rec'd coupon. B). Approximate coating thickness locations for scribed coupon. C) Approximate coating pull-off locations. D) Approximate locations for metallographic sampling.

The extended-term outdoor testing at the Tea Table Key beach test site as well as at the FIU inland test site was intended to provide supporting evidence of coating durability or degradation in realistic ambient conditions and to contrast findings in accelerated salt-fog and immersion testing.

Sample installation and results after 4-month outdoor testing was described in Chapter 4. The final set of samples was removed on July 01, 2014. The final set of collected samples was exposed for a total of 242 days (~34 weeks). The recorded high temperatures in south Florida reached the low 90's in degree Fahrenheit in the summer months and the daily high temperature was typically above 80$^{o}$F. The relative humidity highs typically exceed 80% throughout the exposure. Record of environmental parameters of the test sites is shown in Figure 5.1. Weather conditions at the two outdoor test sites were comparable. The total amount of precipitation at the Tea Table Key and FIU outdoor test site was at least 40.01 and 40.17 inches, respectively.

Samples were exposed to salt-fog conditions with 5% NaCl solution for at least 5800 hours to identify coating and corrosion conditions in aggressive environmental conditions. Test conditions were identical to that used for the short term exposure. Salt-fog chamber temperature was ~32$^{o}$C. The samples were placed at a ~40$^{o}$ inclination with support along the bottom edge of the coupon and along an edge at the upper third of the sample.

Table 5.1. Matrix of Samples Removed from Testing

| Coating | | Exposure | | Condition | Removed after 3-4 months | Removed after 7-8 months | Total Tested |
|---|---|---|---|---|---|---|---|
| CBPC | | Outdoor | Inland | As Rec'd | 1 | 1 | 8 |
| | | | | Scribed | 1 | 1 | 8 |
| | | | Beach | As Rec'd | 1 | 1 | 8 |
| | | | | Scribed | 1 | 1 | 8 |
| | | Salt-Fog | | As Rec'd | 2 | 2 | 9 |
| | | | | Scribed | 2 | 2 | 9 |
| TDG | Plain | Outdoor | Inland | Scribed | 1 | 1 | 8 |
| | | | Beach | Scribed | 1 | 1 | 8 |
| | | Salt-Fog | | Scribed | 2 | 2 | 8 |
| | A | Outdoor | Inland | Scribed | 1 | 1 | 8 |
| | B | Outdoor | Inland | Scribed | 1 | 1 | 8 |
| | A+B | Outdoor | Inland | As Rec'd | 1 | 1 | 8 |
| | | | | Scribed | 1 | 1 | 8 |
| | | | Beach | As Rec'd | 1 | 1 | 8 |
| | | | | Scribed | 1 | 1 | 8 |
| | | Salt-Fog | | As Rec'd | 2 | 2 | 6 |
| | | | | Scribed | 2 | 2 | 6 |
| Metallizing | | Outdoor | Inland | As Rec'd | 1 | 1 | 8 |
| | | | | Scribed | 1 | 1 | 8 |
| | | | Beach | As Rec'd | 1 | 1 | 8 |
| | | | | Scribed | 1 | 1 | 8 |
| | | Salt-Fog | | As Rec'd | 2 | 2 | 6 |
| | | | | Scribed | 2 | 2 | 6 |
| Three-Coat | | Outdoor | Inland | As Rec'd | 1 | 1 | 8 |
| | | | | Scribed | 1 | 1 | 8 |
| | | | Beach | As Rec'd | 1 | 1 | 8 |
| | | | | Scribed | 1 | 1 | 8 |
| | | Salt-Fog | | As Rec'd | 2 | 2 | 6 |
| | | | | Scribed | 2 | 2 | 6 |
| Total | | | | | 38 | 38 | 222 |

The coated steel coupons installed for outdoor and salt-fog exposures are listed in Table 5.1. 50 CBPC, 84 TDG, 44 metallized, and 44 three-coat test coupons were initially installed. Of those, 38 were removed for destructive testing after the first 3-4 months of exposure and another 38 samples were removed after 8 months of exposure. For each of the CBPC, metallized, and three-coat coated samples, exposed in outdoor and salt-fog environments, two scribed coupons and two as-received coupons were removed for testing. Furthermore, in similar fashion, TDG samples with double topcoats (Topcoat A+B) were removed. An additional 6 TDG samples were removed for destructive testing. Those included two scribed plain TDG samples and two scribed TDG samples with single topcoat (Topcoat A or Topcoat B) exposed to outdoor environment as well as two scribed plain TDG samples exposed to salt-fog environment.

After exposure to outdoor weathering and salt-fog, non-destructive evaluations of sample degradation from their as-received conditions included: a) qualitative visual assessments of coating degradation, b) degree of corrosion development at the scribed sites, on the surfaces, and at defect sites, and c) changes in coating thickness. Destructive testing of removed coupon samples included assessment of coating adhesive strength, coating degradation and corrosion development by optical microscopy of coating cross-sections.

Test measurements were identical to methodology used for the short term exposure. The reported metric for coating thickness or change of coating thickness from pre-exposure conditions was calculated from the average of multiple readings on the surface of the coated samples. For non-scribed samples, the coating thickness was measured at 9 locations on the coupon front face. For scribed samples, the coating thickness was measured at 8 locations on the coupon front face. The coating thickness was measured using a DeFelsko Positector 6000 magnetic coating thickness gage.

The reported coating pull-off strengths are from at least three locations on the sample surface for both scribed and non-scribed samples. Metal dollies were glued to the surface of the coated coupon using a two-part epoxy and allowed to set for 24 hours. The perimeter around the fastened dolly was then scored down to the steel substrate prior to testing with a DeFelsko Positest pulloff adhesion tester.

The coating thicknesses and pull-off strengths were meant to evaluate changes due to exposure conditions and not necessarily the effect of the scribe defect. However, two additional pull-off adhesion tests adjacent to the scribe defect were made for the samples tested after 8 months outdoor exposure and 5800 hour salt-fog exposure. Typical sampling locations are shown in Figure 5.3.

## 5.2. VISUAL INSPECTION

### *5.2.1 Chemically Bonded Phosphate Ceramic Coating*

#### *5.2.1.1 Outdoor Exposure*

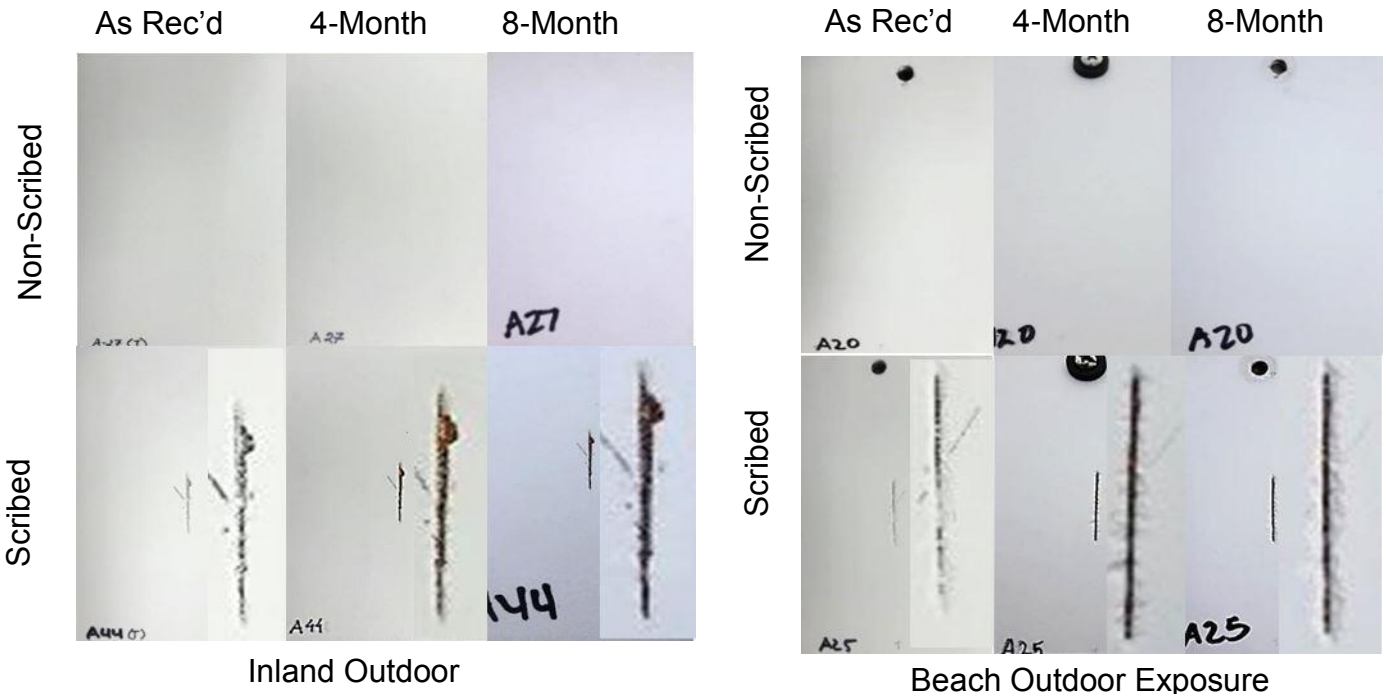


**Figure: 5.4 CBPC Outdoor Exposure.**

Photographs of representative scribed and non-scribed CBPC samples before and after outdoor exposure are shown in Figure 5.4. One scribed and one non-scribed sample were removed from the Inland and Beach outdoor exposure test racks. Samples from the Inland and Beach sites in each condition were considered to be replicate for analysis.

No major coating damage causing any outward indication of steel corrosion was observed on the 14 scribed or 14 non-scribed samples from either outdoor testing location after 8 month exposure but significant coating degradation in the form of surface roughening and weathering into loose powder occurred on all samples. Rust was observed within the scribe location on all 14 of the scribed samples. Typical rust appearance within the scribe is shown in Figure 5.4.

### *5.2.1.2 Salt-Fog Exposure*

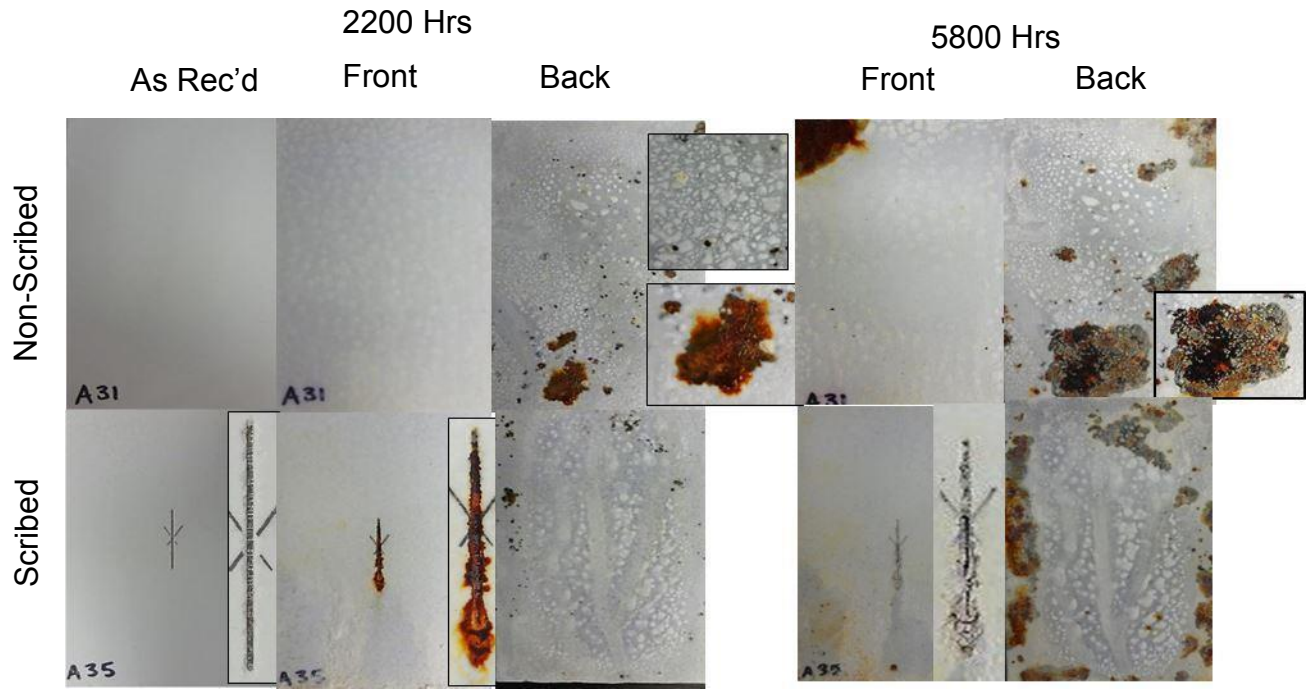


**Figure: 5.5 CBPC Salt-Fog Exposure**.

Photographs of representative scribed and non-scribed CBPC samples before and after salt-fog exposure are shown in Figure 5.5. Two scribed and two non-scribed samples were removed from the salt-fog chamber after ~5800 hours.

Varying levels of coating deterioration were observed on the 7 scribed and 7 non-scribed samples exposed to salt-fog for 5800 hours. Some runoff and salt deposition were apparent on some of the samples. Nevertheless, the coating degradation appeared as scouring and re-deposition (roughening) of the ceramic coating material and development of rust at defect or pore sites on the coating that sometimes led to larger and more severe degradation (particularly on the sample backside). This coating damage and corrosion development on all 7 of the non-scribed samples and at sites away from scribe defects on 3 of the 7 scribed samples worsened in the time interval from 4 to 8 months. Steel corrosion was observed at the scribe locations on 4 of the 7 scribed samples but in contrast to the corrosion at other surface locations, the rust within the scribe did not appear to worsen from the condition observed after 4-months. The typical appearance of steel corrosion after 4 and 8 months is shown in Figure 5.5.

### *5.2.2 Thermal Diffusion Galvanizing*

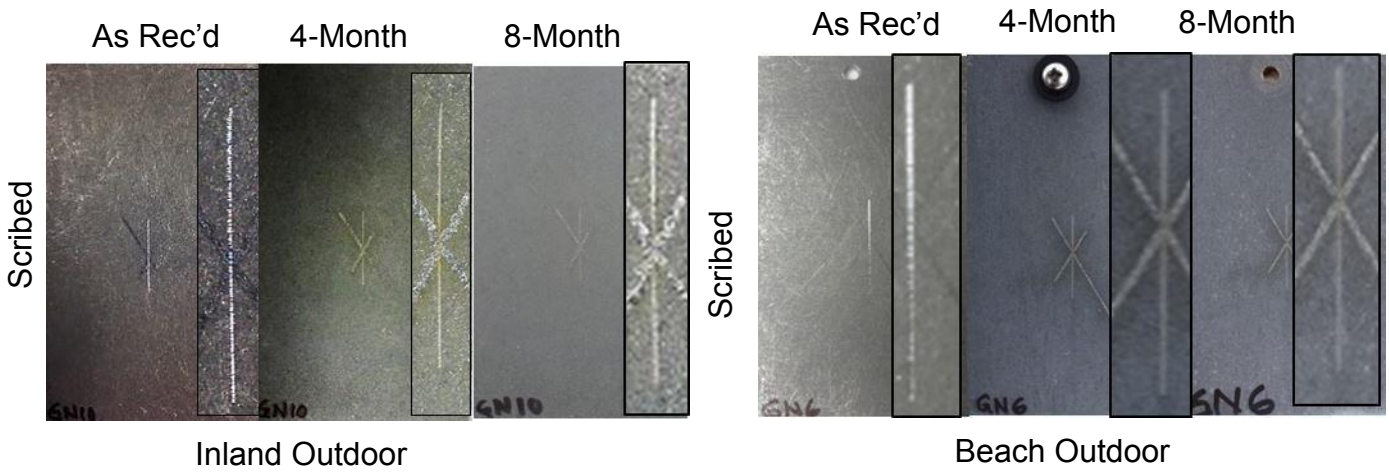


**Figure: 5.6 TDG without Topcoat Outdoor Exposure**.

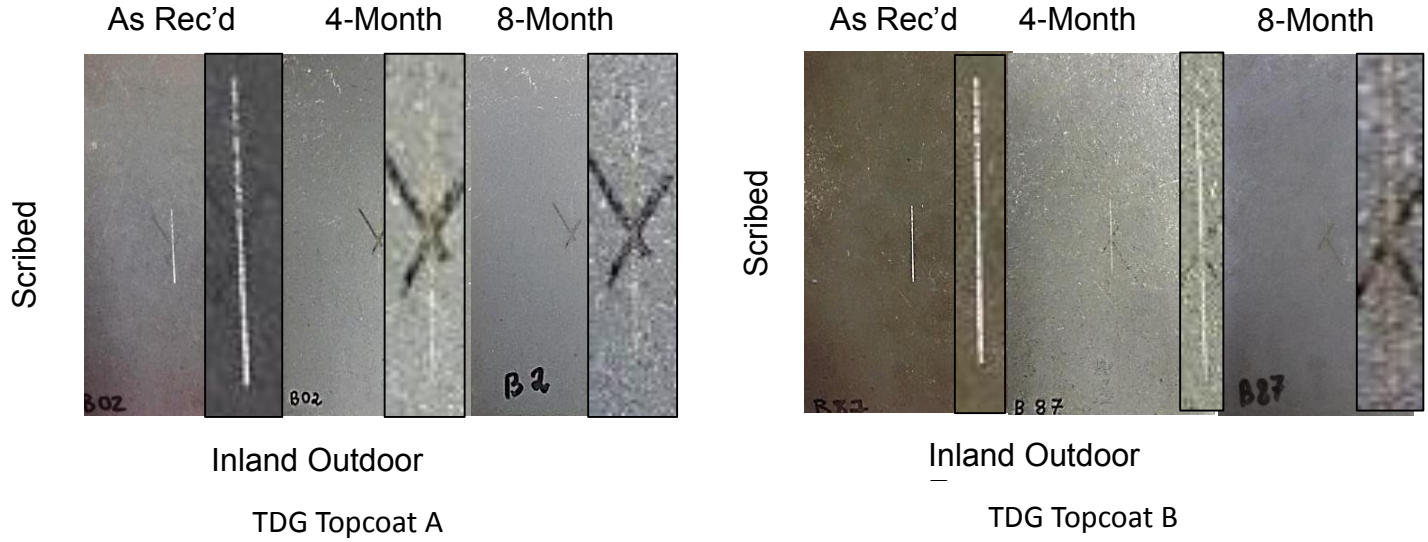


**Figure: 5.7 TDG with Single Topcoat Outdoor Exposure**.

Photographs of representative scribed plain TDG steel samples before and after outdoor exposure are shown in Figure 5.6. One of the scribed samples was removed from each of the Inland and Beach outdoor exposure test racks. Samples from the Inland and Beach sites were considered to be replicate. Photographs of representative scribed TDG steel samples with either Topcoat A or Topcoat B before and after outdoor exposure are shown in Figure 5.7. One of the scribed samples with Topcoat A and one of the scribed samples with Topcoat B were removed from the Inland outdoor exposure test rack for further lab testing. No major surface degradation or significant

accumulation of oxides from the outer zinc alloy layer was apparent by visual observation after 8 months of outdoor exposure of the 14 plain TDG and 14 scribed TDG samples with a single layer of Topcoat A or Topcoat B. Tarnishing of portions of scribed, exposed steel substrates was observed in some cases. Activity of the zinc alloy was evident on the plain TDG by the appearance of white oxides, surface discoloration, and tarnishing. Surface discoloration was also evident on TDG with Topcoat A and Topcoat B, which may indicate topcoat degradation, especially in samples with Topcoat B.

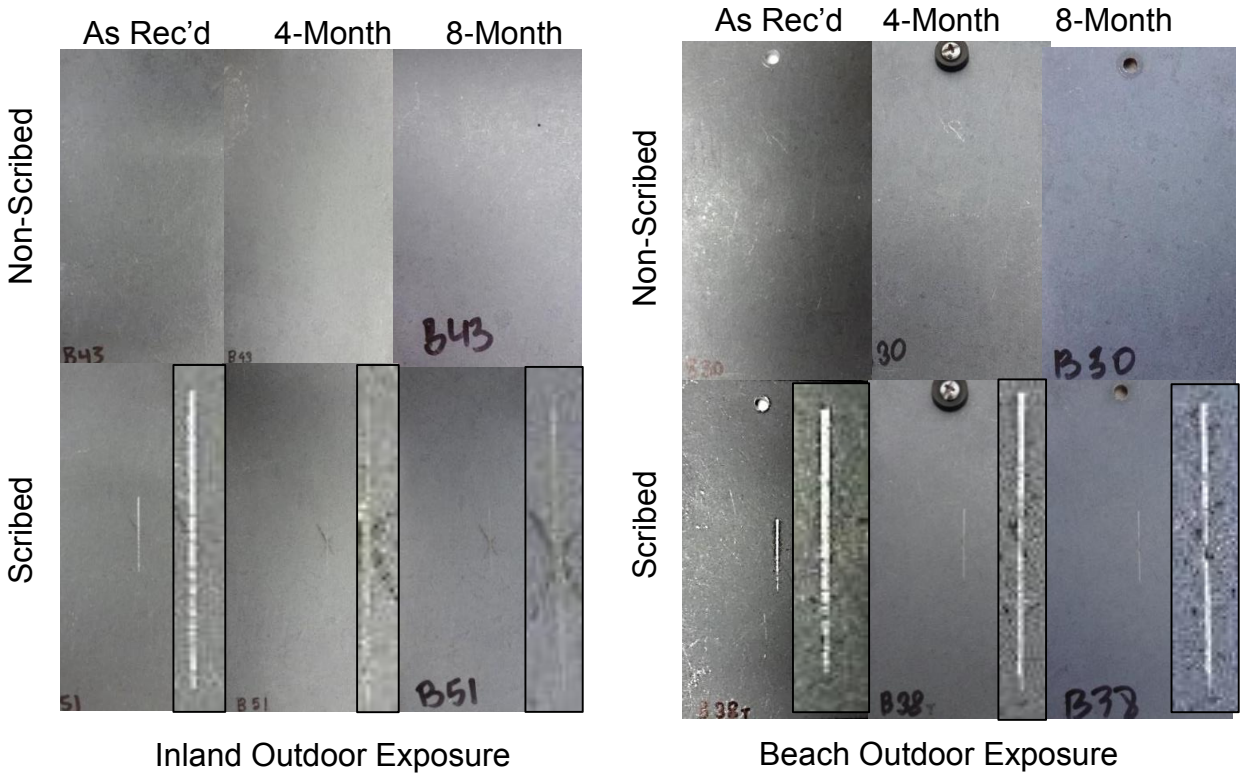


**Figure: 5.8 TDG Double Topcoat Outdoor Exposure.**

Photographs of representative scribed and non-scribed TDG samples with Topcoat A+B before and after outdoor exposure are shown in Figure 5.8. One scribed and one non-scribed sample were removed from the Inland and Beach outdoor exposure test rack. Samples from the Inland and Beach sites in each condition were considered to be replicate for analysis.

No major coating deterioration or indication of significant zinc corrosion product was observed on any of the 14 scribed and 14 non-scribed samples from either outdoor testing location after 8-month exposure. Some minor trace of zinc corrosion product was observed on 7 of the 28 samples. No steel corrosion was observed on the 14 non-

scribed samples after 8-month exposure. Tarnishing was observed within the scribe location on all 7 of the scribed samples in inland test exposure. Typical appearance within the scribe is shown in Figure 5.8.

### *5.2.2.2 Salt-Fog Exposure*

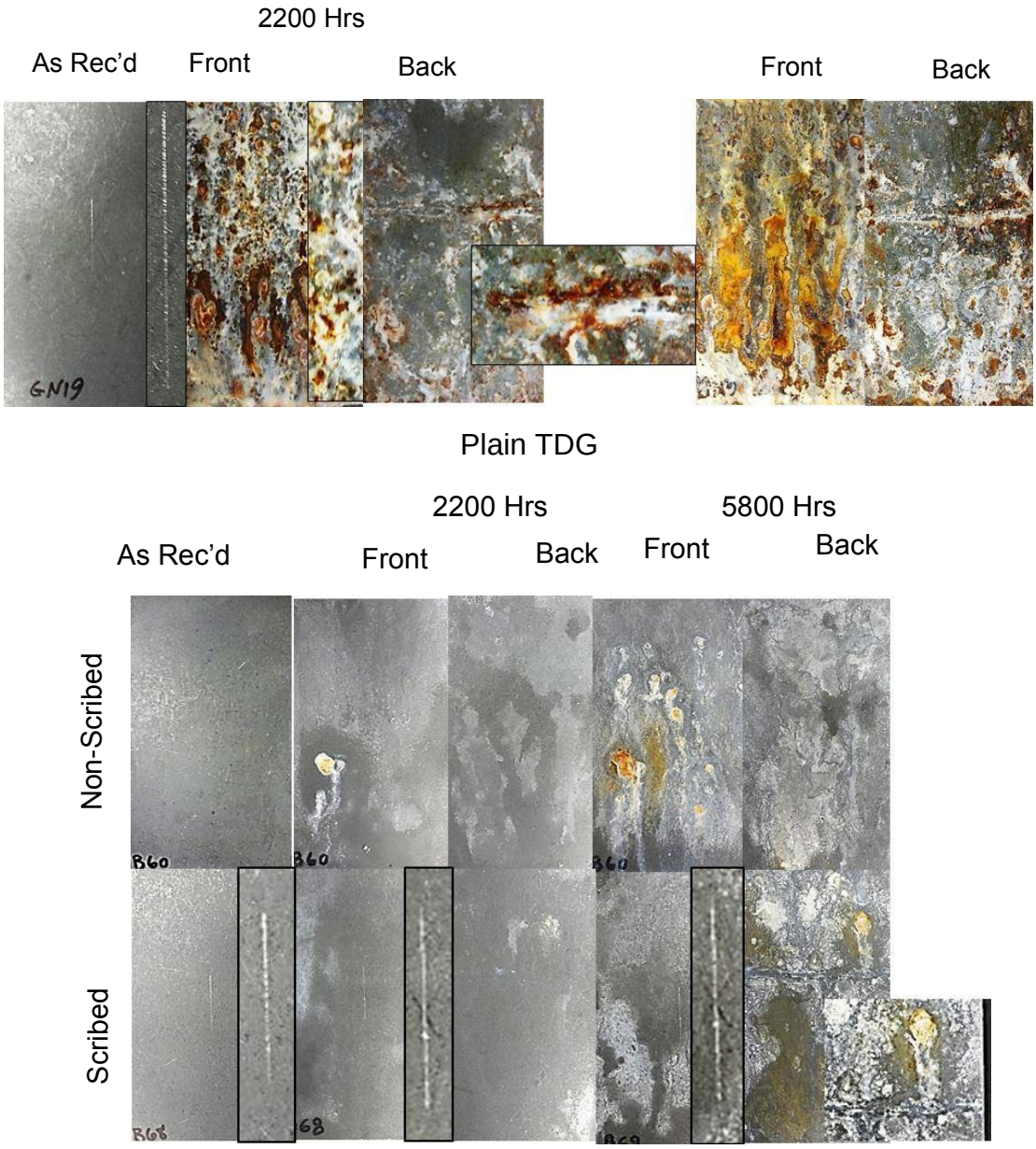


**Figure: 5.9 TDG Salt-Fog Exposure.**

Photographs of representative scribed and non-scribed TDG steel samples before and after salt-fog exposure are shown in Figure 5.9. Only plain TDG and TDG with Topcoat A+B were exposed to salt-fog. Two scribed plain TDG samples as well as two scribed

and two non-scribed TDG samples with Topcoat A+B were removed from the salt-fog chamber after ~5800 hours.

Significant corrosion activity was apparent on all 6 plain TDG samples exposed to salt-fog for 5800 hours, and the level of surface deterioration was more severe than after the 2200 hours. Manufacturers of the coating present this behavior as corrosion of iron contaminants within the TDG coating and suggest use of TDG with topcoat. The corrosion appeared throughout the surface of the coupons but appeared more severe on the top face. The extent of rust accumulation did not appear more severe at scribe locations, and upon closer examination, the location of the original scribe could not be easily seen.

The extent of iron corrosion product accumulation on the coupons with Topcoat A+B placed in salt-fog was, as expected, less than that of Plain TDG, but corrosion sometimes occurred at local coating defects. The number of local corrosion spots increased and the corrosion at existing defects after 2200 hours worsened in the extended exposure period. The localized corrosion was observed on 5 out of 10 samples. Zinc activity was indicated by the presence of a white oxide product on parts of the coating surface. This type of activity is more visible on the bottom face of the coupons. Significant runoff of apparent oxide product was seen at local coating defect sites (Figure 5.9).

### *5.2.3 Metallizing*

#### *5.2.3.1 Outdoor Exposure*

Photographs of representative scribed and non-scribed metallized steel samples before and after outdoor exposure are shown in Figure 5.10. One scribed and one non-scribed sample were removed from the Inland and Beach outdoor exposure test rack. Samples from the Inland and Beach in each condition were considered to be replicate.

Some activity of the zinc metallizing layer was observed on the 14 scribed and 14 non-scribed samples from either outdoor testing location. The discoloration of the coupon surface during the exposure is indicative of degradation of the topcoat. No steel corrosion was observed for non-scribed samples in either outdoor exposure locations. No significant steel corrosion was observed within the scribed region of any of the scribed samples in either outdoor exposure, but tarnishing was observed. A small region of steel corrosion was observed outside of the scribed region at a local coating defect on one of the scribed samples placed in the Beach outdoor test rack, but the extent of corrosion there did not worsen during the extended exposure period.

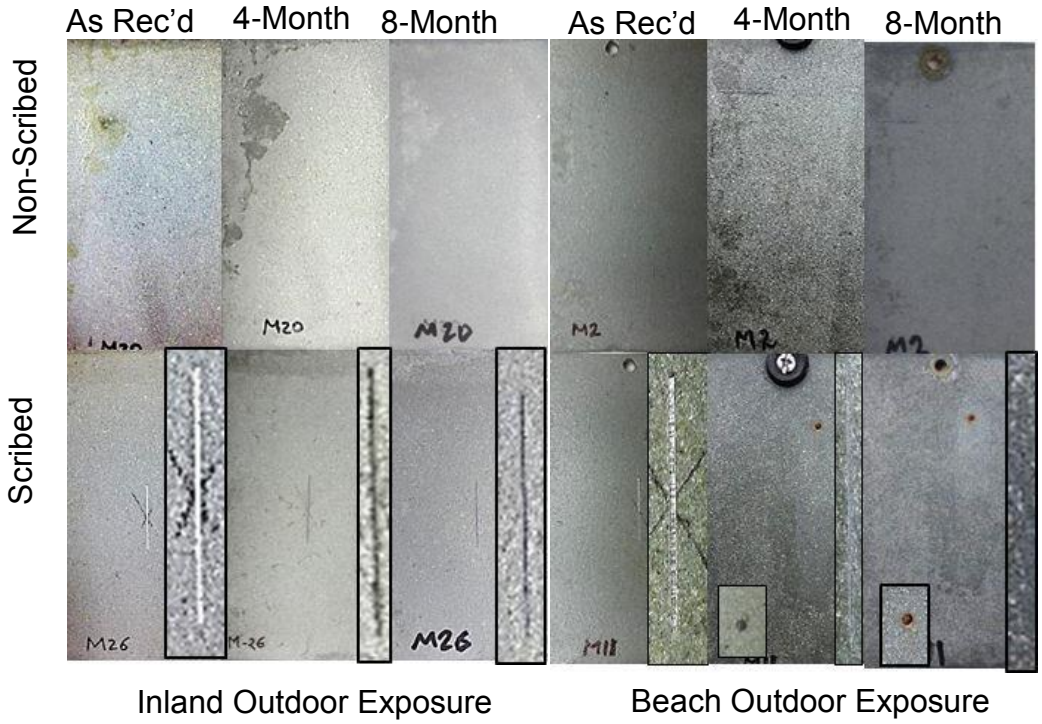


**Figure: 5.10 Metallizing Outdoor Exposure.**

#### *5.2.3.2 Salt-Fog Exposure*

Photographs of representative scribed and non-scribed Metallized steel samples before and after salt-fog exposure are shown in Figure 5.11. Two scribed and two non-scribed samples were removed from the salt-fog chamber after ~5800 hours.

Coating degradation appeared as zinc corrosion activity throughout the front surface of the coupon. The apparent zinc oxide was more prominent on the back surface of the coupon. It was suspected that there was no metallization on the back side and runoff of salt fog condensate at the back side may have aggravated coating degradation conditions. No steel corrosion was observed on any of the 5 scribed or 5 non-scribed coupons after 5800 hours of exposure.

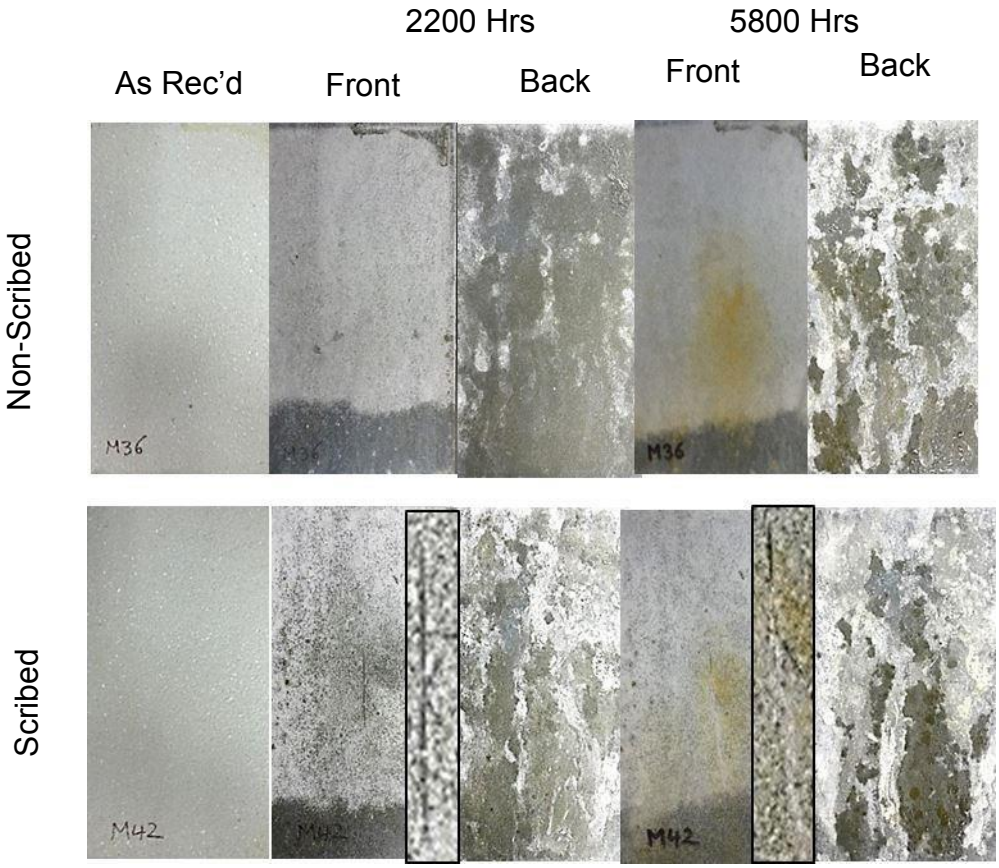


**Figure: 5.11 Metallizing Salt-Fog Exposure**.

### *5.2.4 Three-Coat*

#### *5.2.4.1 Outdoor Exposure*

Photographs of representative scribed and non-scribed three-coat steel coupons before and after outdoor exposure are shown in Figure 5.12. One scribed and one non-scribed sample were removed from the Inland and Beach outdoor exposure test rack. Samples from the Inland and Beach in each condition were considered to be replicate.

No major coating deterioration was observed visually on the 15 scribed or 15 non-scribed samples from either outdoor testing location. Some round rust spots, initiated during the first 4 months of exposure, were observed on 4 of 15 samples; however, no indication of further corrosion development was seen during the extended exposure period. No corrosion was observed on the 30 non-scribed and scribed samples, but significant change of color was observed after 8-month of exposure.

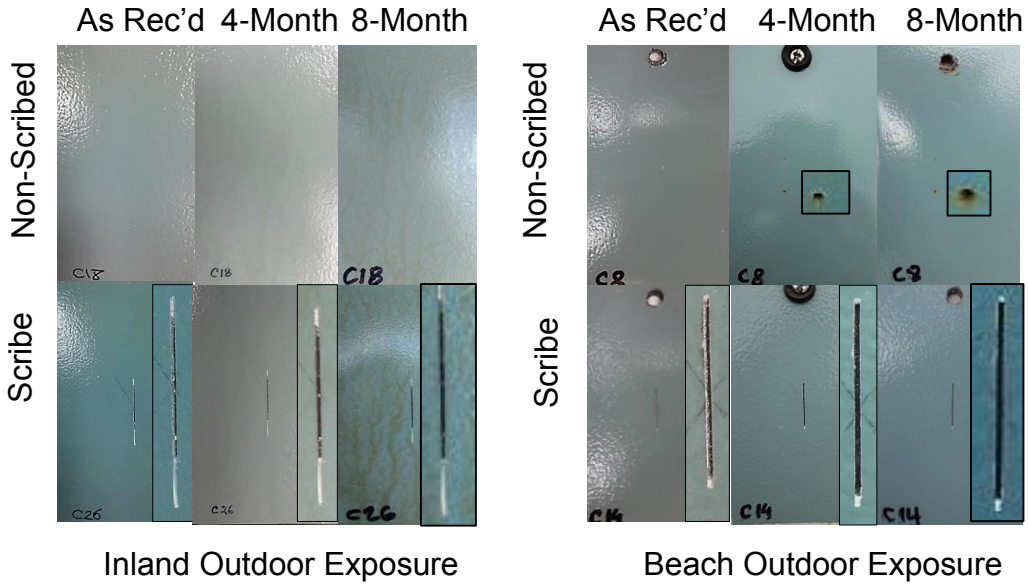


**Figure: 5.12 Three-Coat Outdoor Exposure.**

### *5.2.4.2 Salt-Fog Exposure*

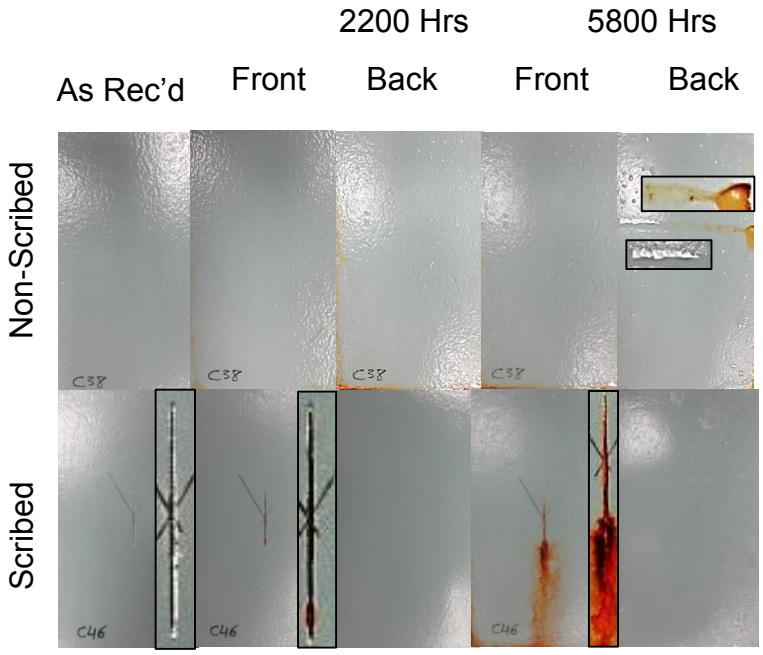


**Figure: 5.13. Three-Coat Salt-Fog Exposure.**

Photographs of representative scribed and non-scribed three-coat steel samples before and after salt-fog exposure are shown in Figure 5.13. Two scribed and two non-scribed samples were removed from the salt-fog chamber after ~5800 hours.

No coating degradation was apparent for any of the 4 scribed or 4 non-scribed samples after salt-fog exposure, but 3 of the 8 samples showed some deficiency such as abrasion on the coating surface due to the prolonged contact with the sample holder. Corrosion was observed within the scribe defect in 4 of the 4 scribed coupons. The extent of corrosion there after 5800 hours was more significant than originally observed after 2200 hours of exposure.

## 5.3. COATING THICKNESS

### *5.3.1 Chemically Bonded Phosphate Coating*

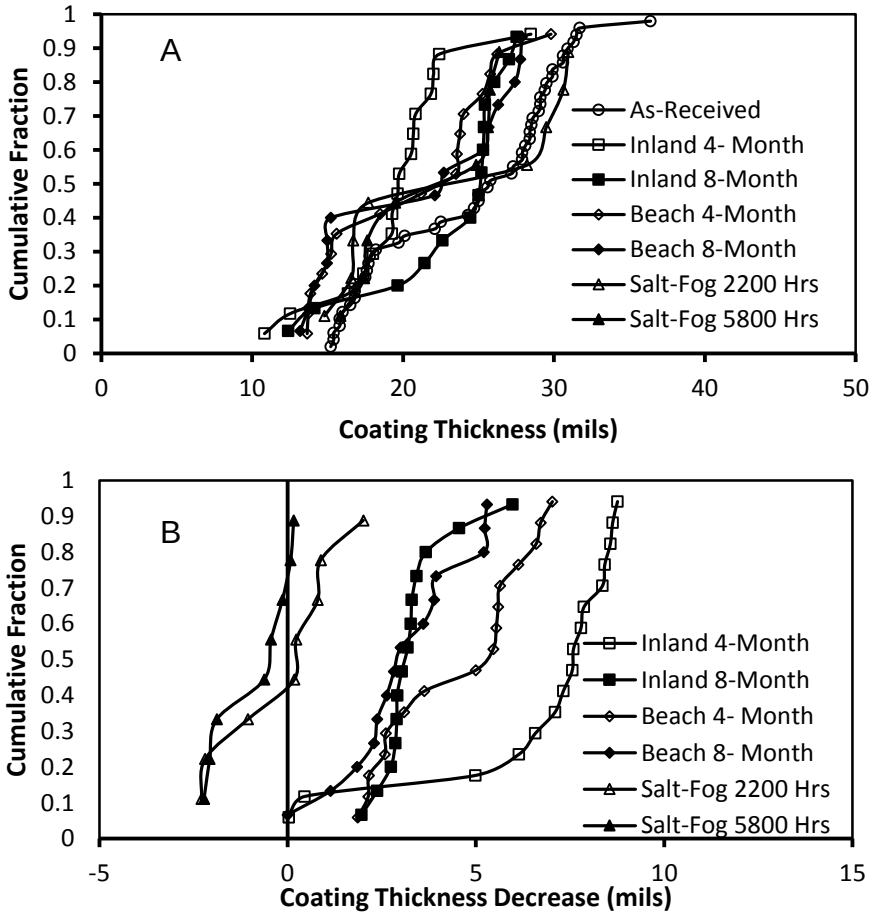


**Figure: 5.14 CBPC Coating Thickness Decrease (cont.).**
A) Actual coating thickness. B) Change of coating thickness.

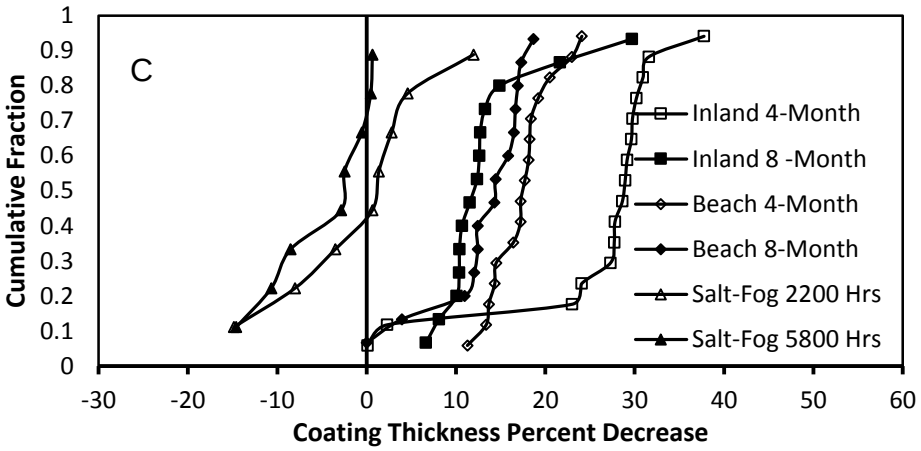


**Continuation of Figure: 5.14 CBPC Coating Thickness Decrease.**
C) Percent change of coating thickness.

The average coating thicknesses of the CBPC samples, as measured with the magnetic thickness gage before and after exposure to outdoor and salt-fog weathering, is shown in Figure 5.14a. Direct comparisons of the average coating thicknesses of samples before and after exposure are shown in Figures 5.14b and 5.14c. Figure 5.14b shows the calculated difference in measured coating thickness and Figure 5.14c shows the percent difference in the average coating thickness relative to the average as-received thickness. There is a caveat in the interpretation of the data because the reported thickness was the calculated average of multiple spot measurements throughout the sample surface and there was significant local thickness variability. Positive values in Figures 5.14b and 5.14c indicate a decrease in coating thickness after exposure.

Coating thickness reduction ranging from ~0 to 8 mils was measured for CBPC-coated steel samples exposed in outdoor inland conditions for 4 months, but the net reduction was ~0 to 6 mils after 8-month exposure, which indicates that the coating thickness may have increased during the extended exposure period. In this case, the mean values after 8 months were ~5 mils greater that for the 4-month outdoor exposure. This coating thickness increment may suggest formation of some reduced product under the coating. This behavior was similar for the outdoor beach site, but was less developed compared to samples placed at the inland outdoor site. As there was variability in original coating thickness, the percent decrease in coating thickness for the test population would likewise vary.

The initial loss of coating material described above was thought to be due to moisture availability and drying conditions. In the outdoor 4-month exposure tests, the CBPC coating was weaker and more friable than in the as-received condition. This deterioration eventually resulted in the calculated thickness reduction. During the subsequent 4-months of exposure, moisture could be more readily available to the steel substrate due to the deterioration of the CBPC. This would promote subsequent

formation of corrosion product underneath the coating, which would increase the measured coating thickness. The apparent increment of the net coating thickness was typically followed by observed undercoating corrosion product accumulation.

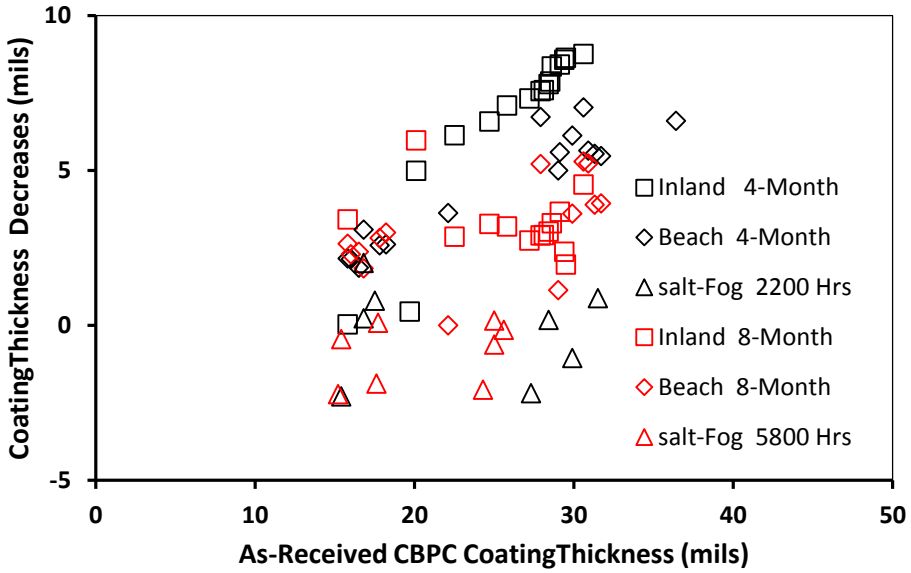


**Figure: 5.15 CBPC Coating Thickness Decrease vs. As-Received Coating Thickness.**

As shown in Figure 5.15, samples with thicker CBPC coatings tended to have greater reduction in coating thickness after the first 4 months of outdoor exposure. However, consistent with the observation of undercoating rust accumulation, trends in the coating thickness decrease after 8 months were less apparent, as the net coating thickness measurements would also incorporate the underlying rust development. The thickness of that underlying rust may be greater than the relative difference in coating thickness because the CBPC layer may be susceptible to continued decay during the last 4 months of exposure. This cannot be easily verified by microscopy due to the fact that the sample population had significant thickness variability. However, for the purpose of discussion a deterioration sequence is proposed.

For illustration, a sample that had an original coating thickness of 30 mils saw a coating decrease of ~8 mils after 4 months of exposure. After an additional 4 months of exposure, the net coating decrease dropped to ~4 mils. If the rate of coating degradation were to continue at a uniform rate, the thickness loss of the CBPC may be as much as ~16 mils. At this rate then, the amount of oxide development would need to be as much as 12 mils. This amount of oxide development is excessive and was not observed in examinations of cross-sections. This would then indicate that the rate of coating material loss would be decelerating with time.

For discussion purposes here only, the corrosion current from the immersion tests of CBPC in neutral pH salt solution can be considered as an extreme condition for corrosion activity. Assuming that the density of the corrosion product is ~5 g/cm$^3$ and that the stoichiometric ratio of ferrous iron ions from the corrosion product is 2 by relevant reaction paths, the amount of rust accumulation in 8 months calculated by Faradaic conversion would not be greater than the difference in coating thickness from the values measured after 4 and 8 months. Therefore, the rate of ceramic coating thickness loss would seem to be significantly retarded after the initial early degradation. The apparent increase in coating thickness shown in Figure 5.15 may then be more representative of rust accumulation. The role of any intermediate oxide from the CBPC could not be elucidated from the testing.

As described earlier, the extent of coating degradation and rust development can be severe on samples exposed to the aggressive salt-fog environment. Consistent with the observation of undercoating rust accumulation, the coating thickness measurements largely showed increases that were greater for samples after 5800 hours than after 2200 hours. Due to the diverging effects of CBPC coating degradation and undercoating rust accumulation, the coating thickness measurements alone do not explicitly describe the magnitude of the coating degradation. The measured decrease in the positive coating thickness values during the extended exposure period was indicative that the amount of rust accumulation tends to exceed the amount of coating material loss. This indicates that the amount of rust accumulation was increased after initial coating deterioration. This is consistent with the high moisture and chloride availability in the aggressive salt fog environment. As will be discussed later, microscopy of sample cross-sections revealed significant loss of coating material and showed undercoating corrosion development.

### *5.3.2 Thermal Diffusion Galvanizing*

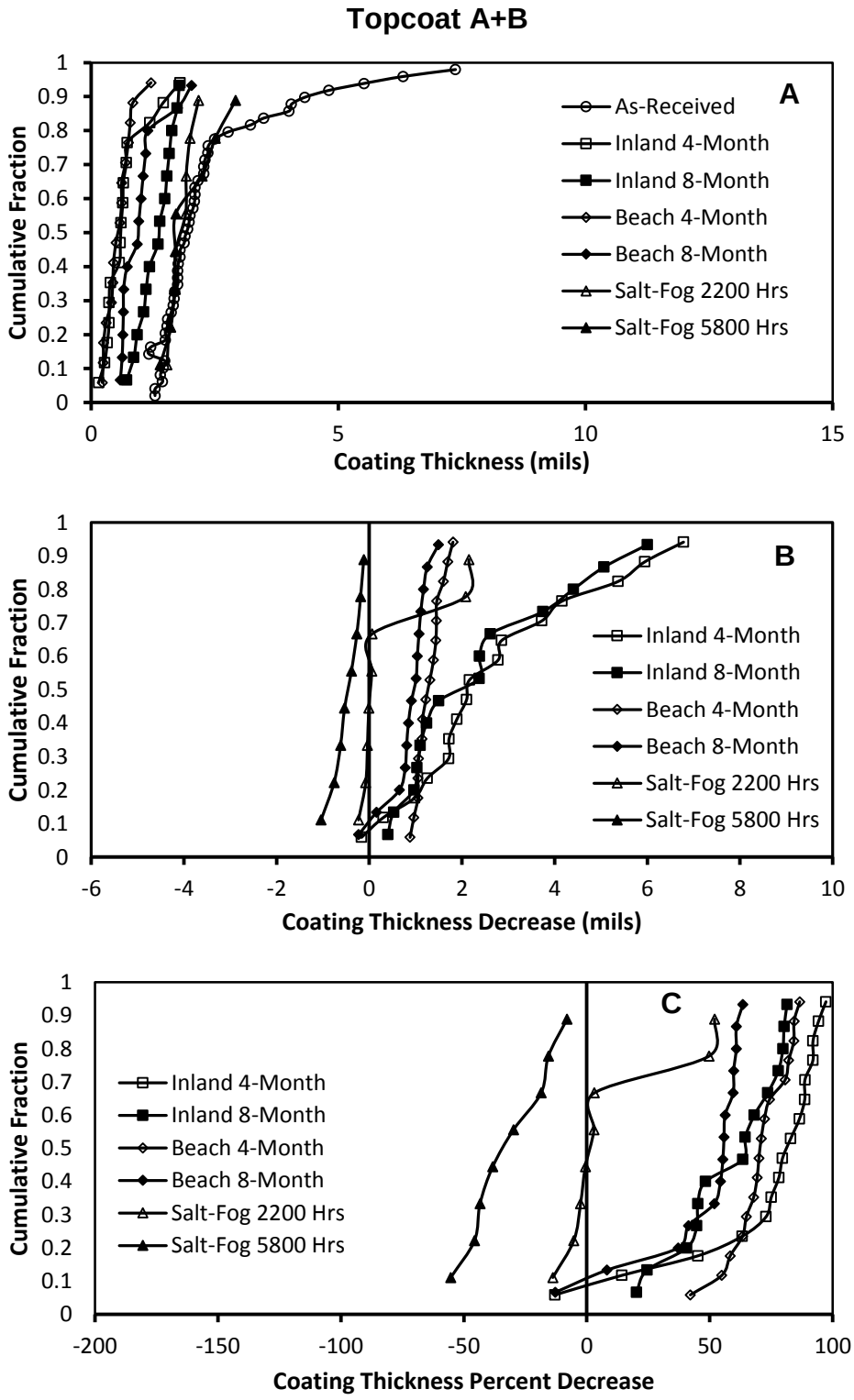


**Figure: 5.16 TDG Coating Thickness Decrease (cont.).**

A) Actual coating thickness. B) Change of coating thickness. C) Percent change of coating thickness.

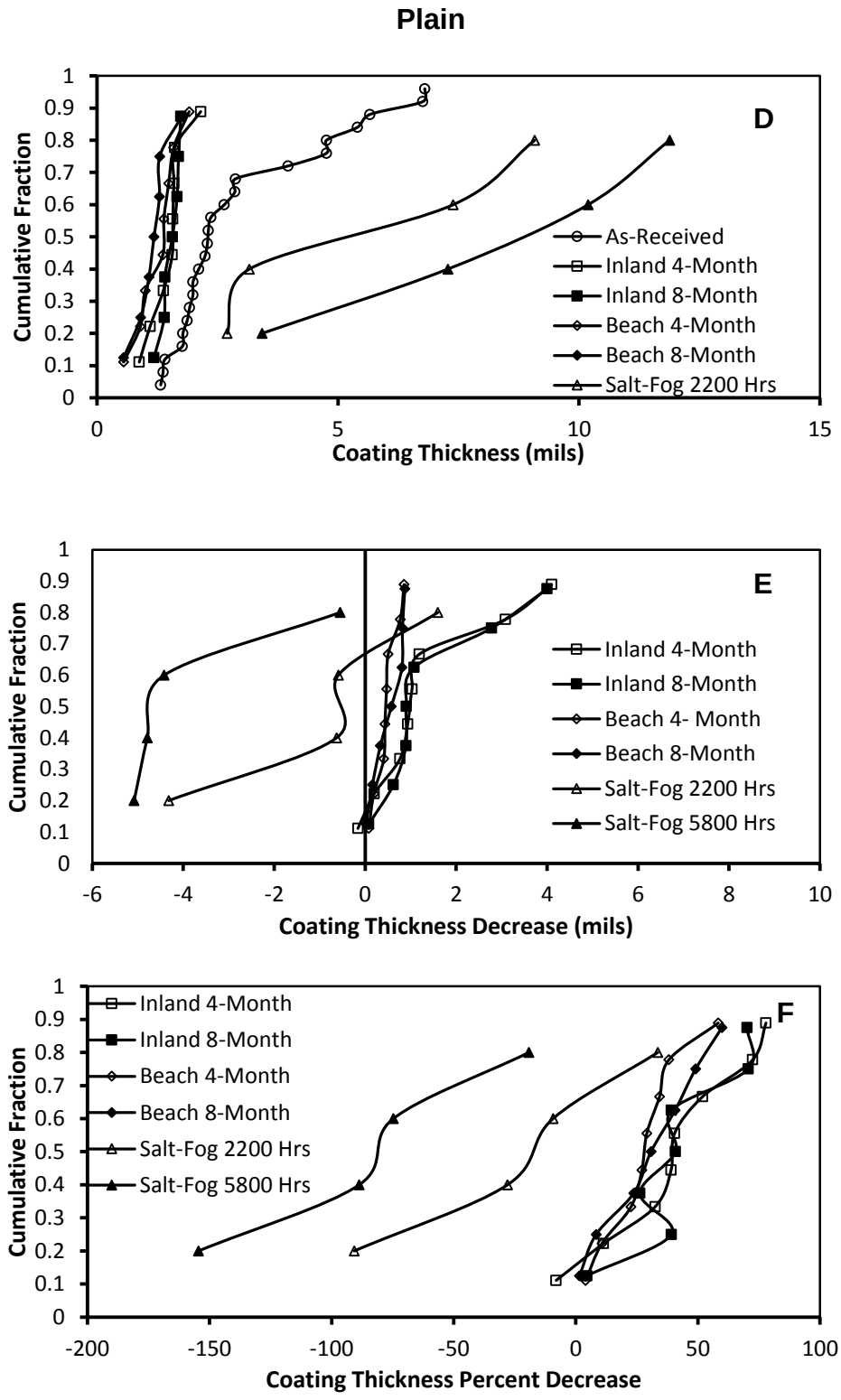


**Continuation of Figure: 5.16 TDG Coating Thickness Decrease.**

D) Actual coating thickness. E) Change of coating thickness. F) Percent change of coating thickness.

The average coating thickness for TDG with Topcoat A+B and Plain TDG, measured with the magnetic thickness gage before and after exposure to outdoor or salt-fog weathering, is shown in Figures 5.16a and 5.16d, respectively. Direct comparisons of the average coating thicknesses of samples before and after exposure are shown in Figures 5.16b-5.16c and Figures 5.16e-5.16f. There is a caveat in the interpretation of the data because the reported thicknesses were the calculated averages of multiple spot measurements throughout the coupon surfaces, and there was local thickness variability. Positive values indicate a decrease in coating thickness after exposure. Figure 5.16b and Figure 5.16e show the difference in the average measured coating thicknesses for TDG with and without topcoat, and Figures 5.16c and 5.16f show the percent differences in coating thicknesses of TDG samples with and without topcoat, relative to the as-received thicknesses.

Approximately 70% of the sample population of Plain TDG steel coupons had original average thicknesses ranging from about 1 to about 2.5 mils. Most of the Plain TDG coupons placed in outdoor exposure conditions were comprised of those samples. Outdoor exposure for 4 months reduced the average coating thicknesses to a range of about 0.2 to about 2 mils, but the coating thicknesses did not further decrease significantly during the four additional months of outdoor exposure. The initial loss of material would indicate susceptibility of the outer portion of the TDG layer to break down after a relatively short exposure period.

The Plain TDG samples placed in salt-fog exposure had as-received average coating thicknesses ranging from about 2.5 to about 6.5 mils. After salt-fog exposure for 2200 and 5800 hours, the plain TDG samples showed an increasing trend towards greater coating thicknesses. The increased coating thickness (up to 9 mils after 2200 hours and 12 mils after 5800 hours) was attributed to the oxidation of the zinc layer and buildup of zinc oxide on the coupon surface.

Similar to the Plain TDG samples, approximately 70% of the sample population of TDG-coated steel coupons with Topcoat A+B had original average thicknesses ranging from about 1 to about 2.5 mils and ~30% were greater than 2.5 mils. The majority of samples with original average thickness greater than 2.5 mils were placed at the outdoor exposure sites. After 4-month outdoor exposure, the range of average coating thickness (including those thicker coating samples) was about 0.2 to about 2 mils. It was observed that significant coating loss occurred (up to ~80% of the coating thickness). This is indicative of loss of topcoat and perhaps some of the zinc layer as well during the short-term outdoor exposure. Contrastingly, the distribution of measured coating thicknesses after the extended outdoor exposure indicated a trend of coating thickness increase after the additional 4 months. This trend follows the observations of zinc oxidation formation for the Plain TDG samples in a salt-fog environment. Despite some surface discoloration due to the zinc oxidation after 8 months, no steel corrosion was observed.

Since most of the TDG samples with Topcoat A+B that were placed in outdoor exposure had average thicknesses greater than 2.5 mils, the majority of the samples placed in salt-fog exposure had average thicknesses less than 2.5 mils. Similar to the Plain TDG samples, the TDG samples with Topcoat A+B that were exposed to salt-fog increased in thickness; however, the coated TDG performed better than the plain samples. After 8 months, the percent increase in mean coating thickness for coated TDG was 29%, whereas plain TDG had percent increases in mean coating thickness as high as 74% due to substantial rust accumulation. The difference between the original coating thickness of plain and coated TDG in salt-fog exposure was not expected to be a major contributing factor on oxide formation and the thickness increase. The coating thickness increase, due to zinc and iron oxide buildup at deficient surface locations on the coated TDG, was over an order of magnitude smaller than in the case of the plain TDG, where there was widespread oxide buildup.

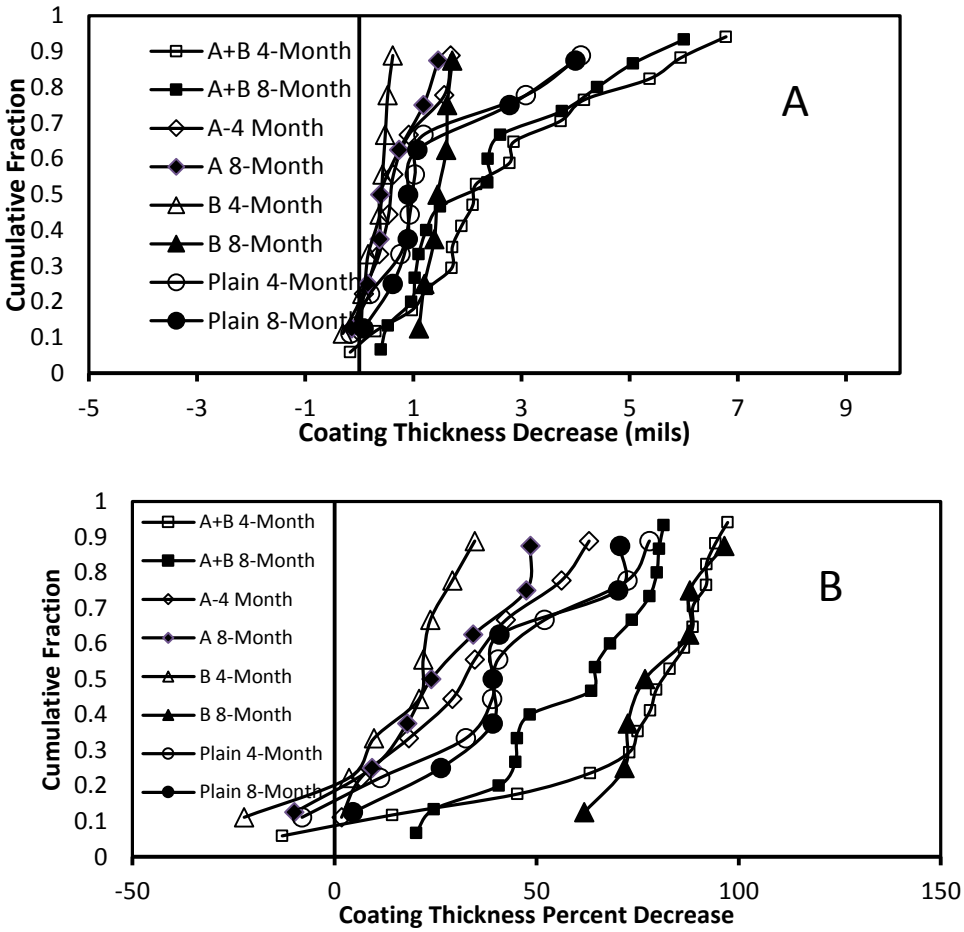


**Figure: 5.17 TDG Topcoat Coating Thickness (Inland Outdoor Exposure)**. A) Coating Thickness Decrease. B)Thickness Percent Decrease. Data for TDG with Topcoat A+B reproduced from Figure 5.16 b, c.

Figure 5.17 shows the coating thickness measurements for TDG with Topcoat A, Topcoat B, and for comparison, Topcoat A+B and plain TDG. In the first four months of outdoor exposure, it was apparent that the extent of coating loss of Topcoat A or Topcoat B was significantly less than for Topcoat A+B. After the subsequent four months of outdoor exposure, TDG with Topcoat B continued to show a decrease in thickness, and thus material loss, whereas the TDG with Topcoat A and Topcoat A+B showed an increase during the extended exposure. The initial decrease in coating thickness in TDG incorporating Topcoat A after the first four months would indicate deterioration of the topcoat. The subsequent exposure of the TDG layer would cause some depletion of the top zinc layers but the resulting accumulation of oxide products would result in an increment in thickness as observed after 8 months. The continued decrease in coating thickness observed for TDG with Topcoat B would implicate progressive degradation of the topcoat and also possibly part of the TDG. Aside from coating thickness loss and surface discoloration, no major steel corrosion was observed in the inland outdoor exposure test conditions. TDG with Topcoat A or Topcoat B were not exposed to salt-fog conditions.

As shown in Figure 5.18, there was an apparent trend between coating thickness loss after outdoor exposure and initial coating thickness. This trend (especially for TDG Topcoat A+B in inland outdoor exposure) would indicate coating thickness loss nearly equal to the initial coating thickness. The trend and magnitude for 4- and 8-month inland outdoor exposure are consistent with the interpretation of topcoat depletion by 4 months and subsequent oxide growth on the TDG surface as described earlier. Per earlier caveat, the calculated thickness decrease is subject to error incurred by averaging coating thicknesses from local point measurements.

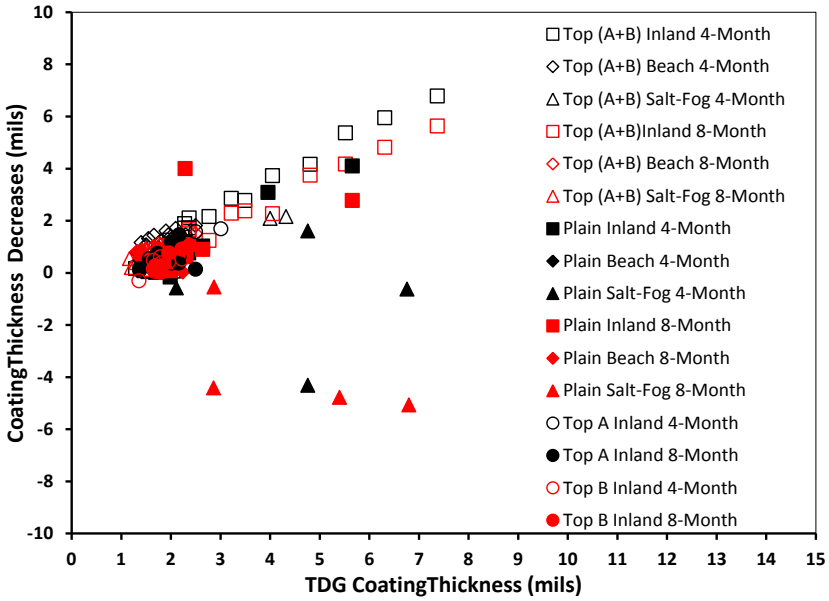


**Figure 5.18 TDG Coating Thickness Decrease vs. As-Received Coating Thickness.**

### *5.3.3 Metallizing*

The averages coating thicknesses measured before and after exposure to outdoor or salt-fog weathering are shown in Figure 5.19a. Direct comparisons of the average coating thicknesses of samples before and after exposure are shown in Figures 5.19b and 5.19c. Figure 5.19b shows the calculated differences in average coating thicknesses and Figure 5.19c shows the percent differences in the average coating thicknesses relative to the average as-received thicknesses. There is a caveat in the interpretation of the data because the reported thicknesses were the calculated averages of multiple spot measurements throughout the coupon surfaces and there were local thickness variations. Positive values in Figures 5.19b and 5.19c indicate decreases in coating thicknesses after exposure.

Reductions in coating thicknesses ranging from about 0.5 to about 10 mils were measured for metallized coated steel samples exposed in outdoor conditions for 4 months. For 8-month exposure, no significant further reduction of coating thickness was measured for samples exposed in the outdoor beach exposure but some thickness gain was measured for samples placed at the inland outdoor test site. Furthermore, progressive increases in coating thicknesses were measured for samples placed in salt-fog exposures for up to 5800 hours. The thickness increases were considered to be due to similar mechanisms as described for TDG.

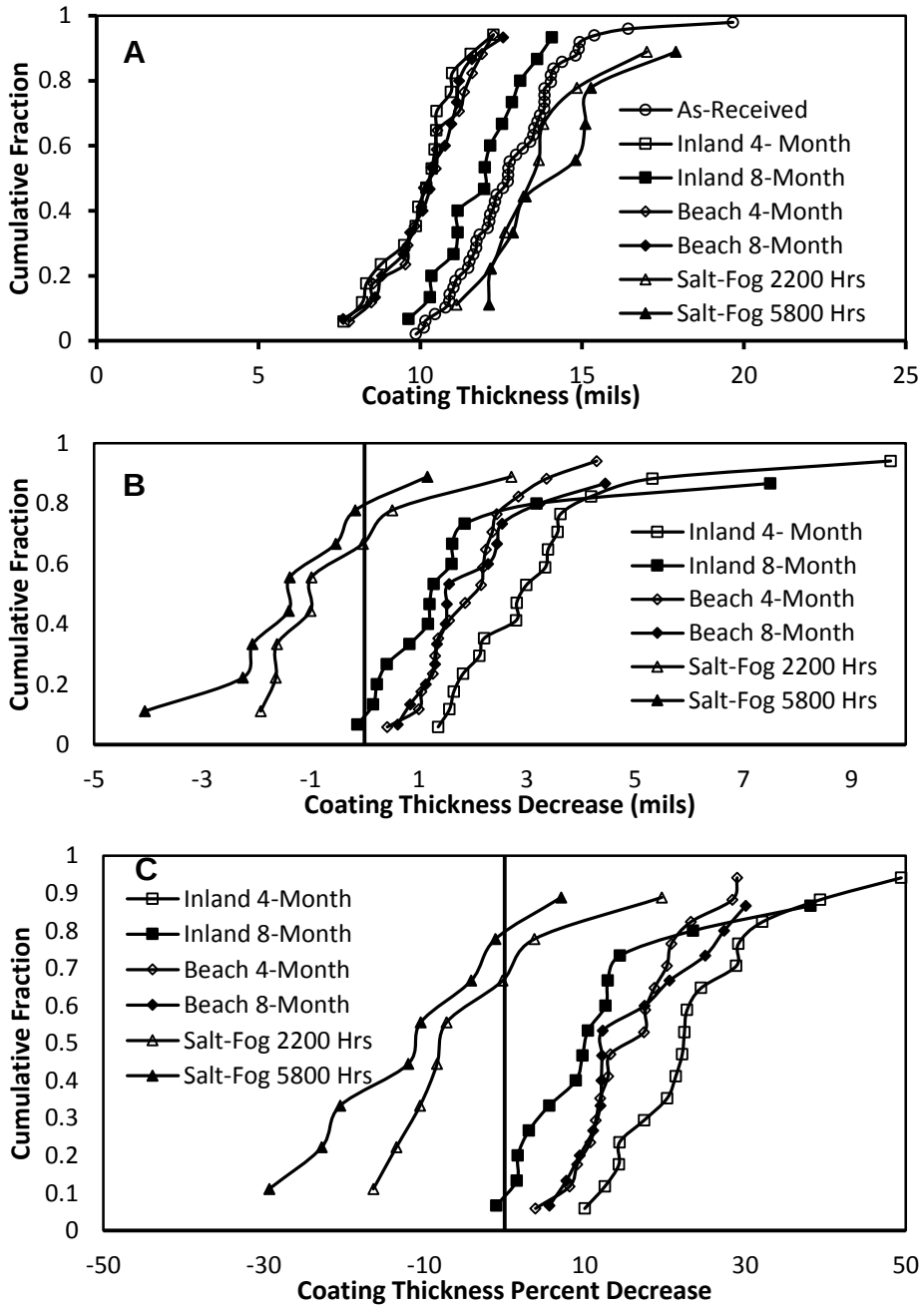


**Figure: 5.19 Metallizing Coating Thickness Decrease.**

A) Actual coating thickness. B) Change of coating thickness. C) Percent change of coating thickness.

As shown in Figure 5.20, there is no major trend between coating thickness loss after exposure and original coating thickness. The correlation of these parameters observed in TDG and CBPC indicated that significant loss of material was due to the early degradation of porous layers such as the topcoat in TDG and the ceramic layer CBPC. The compact splat layers of the metallized samples and the original inconsistent application of topcoat to the coupons precluded similar processes from occurring here.

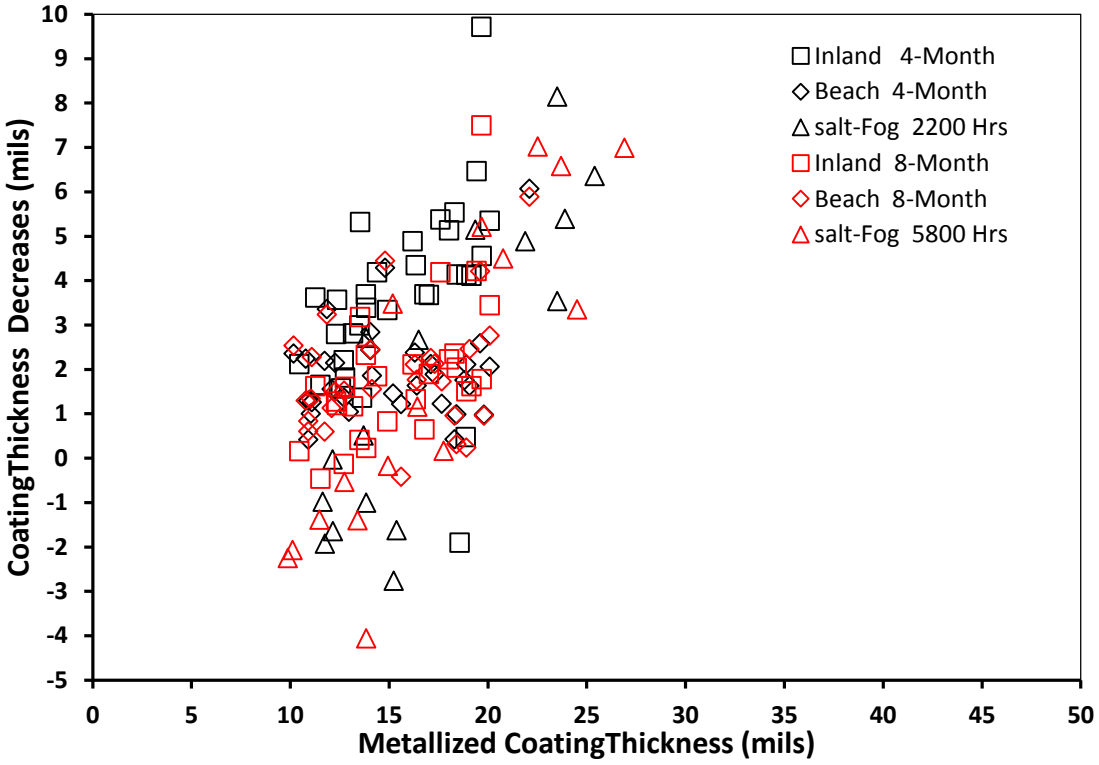


**Figure: 5.20 Metallizing Coating Thickness Decrease vs. As-Received Coating Thickness.**

### *5.3.4 Three-Coat*

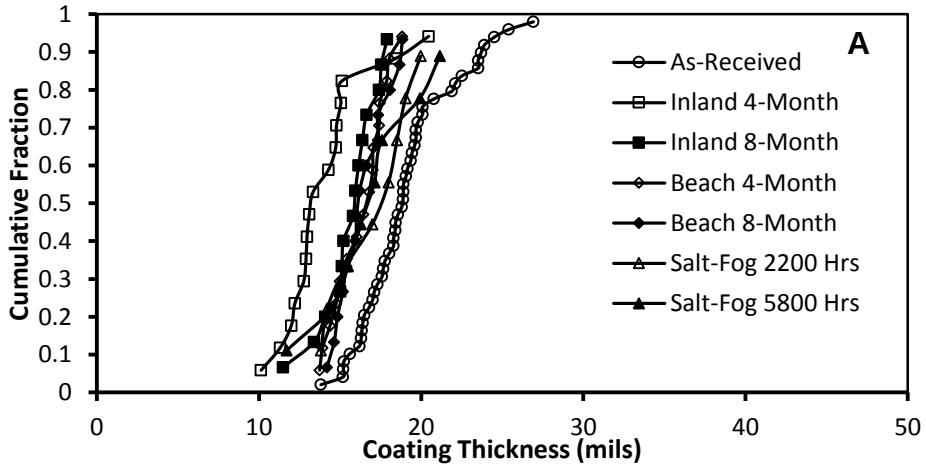


**Figure: 5.21 Three-Coat Coating Thickness Decrease (cont.).**

A) Actual coating thickness.

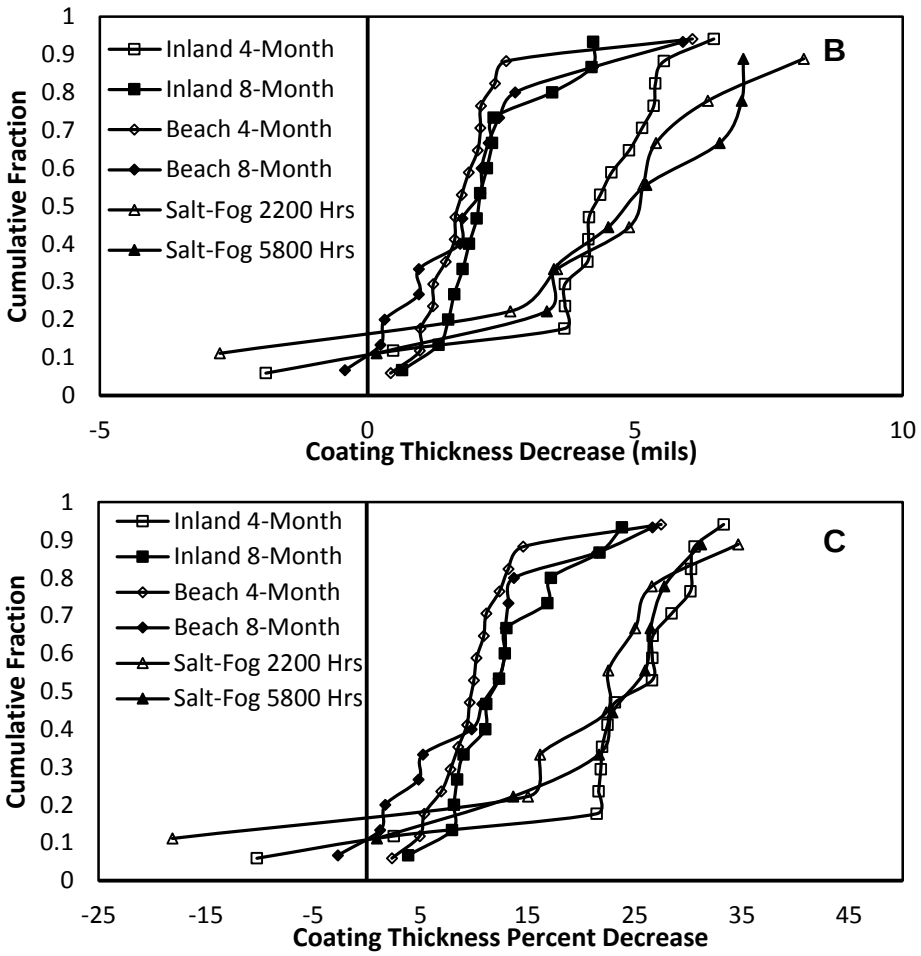


**Continuation of Figure: 5.21 Three-Coat Coating Thickness Decrease.**
B) Change of coating thickness. C) Percent change of coating thickness.

The average coating thickness before and after exposure to outdoor or salt-fog weathering is shown in Figure 5.21a. Direct comparisons of the average coating thicknesses of samples before and after exposure are shown in Figures 5.21b and 5.21c. Figure 5.21b shows the calculated differences in average coating thicknesses and Figure 5.21c shows the percentage differences in the average coating thicknesses relative to the average as-received thicknesses. There is a caveat in the interpretation of the data because the reported thicknesses were the calculated averages of multiple spot measurements throughout the coupon surfaces and there were local thickness variations. Positive values in Figures 5.21b and 5.21c indicate decreases in coating thicknesses after exposure.

Generally, it was observed that coating thicknesses decreased after environmental exposures. It was apparent that the salt-fog environment was particularly harsh (Figure 5.21c). For samples exposed at the inland outdoor exposure site, coating thickness decrease was significant during the initial 4 months, but there was indication of some form of coating thickness increase during the subsequent four months. In the other

exposure conditions, there was no major differentiation between the initial exposure and the extended exposure.

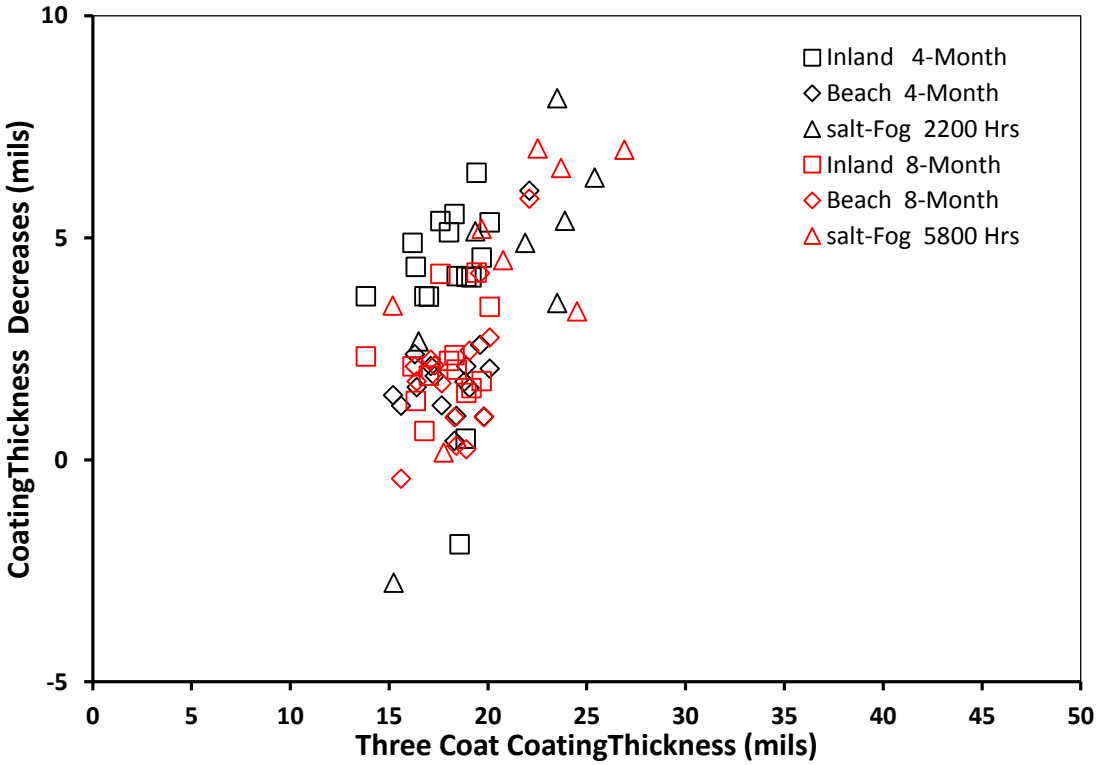


**Figure: 5.22 Three-Coat Coating Thickness Decrease vs. As-Received Coating Thickness.**

Manifested in the variability of the percentage decreases in coating thicknesses are the variability in the calculations of the average coating thicknesses before and after exposure, in the coating application process, and in the rates and modalities of coating degradation. There was not a strong correlation between the original thickness and loss of coating thickness for any of the environmental exposure conditions (Figure 5.22).

## 5.4. COATING PULL-OFF STRENGTH

### *5.4.1 Chemically Bonded Phosphate Coating*

The surfaces of coupons exposed to outdoor and salt-fog conditions after pull-off adhesion testing are shown in Figure 5.23 and Figure 5.24. Pull-off adhesion testing was done on the top and back surfaces of the coupons. Testing up to 8 months in outdoor exposure as well as up to 5800 hours in salt-fog resulted in separation of the ceramic coating from the sample by adhesive and cohesive coating failure.

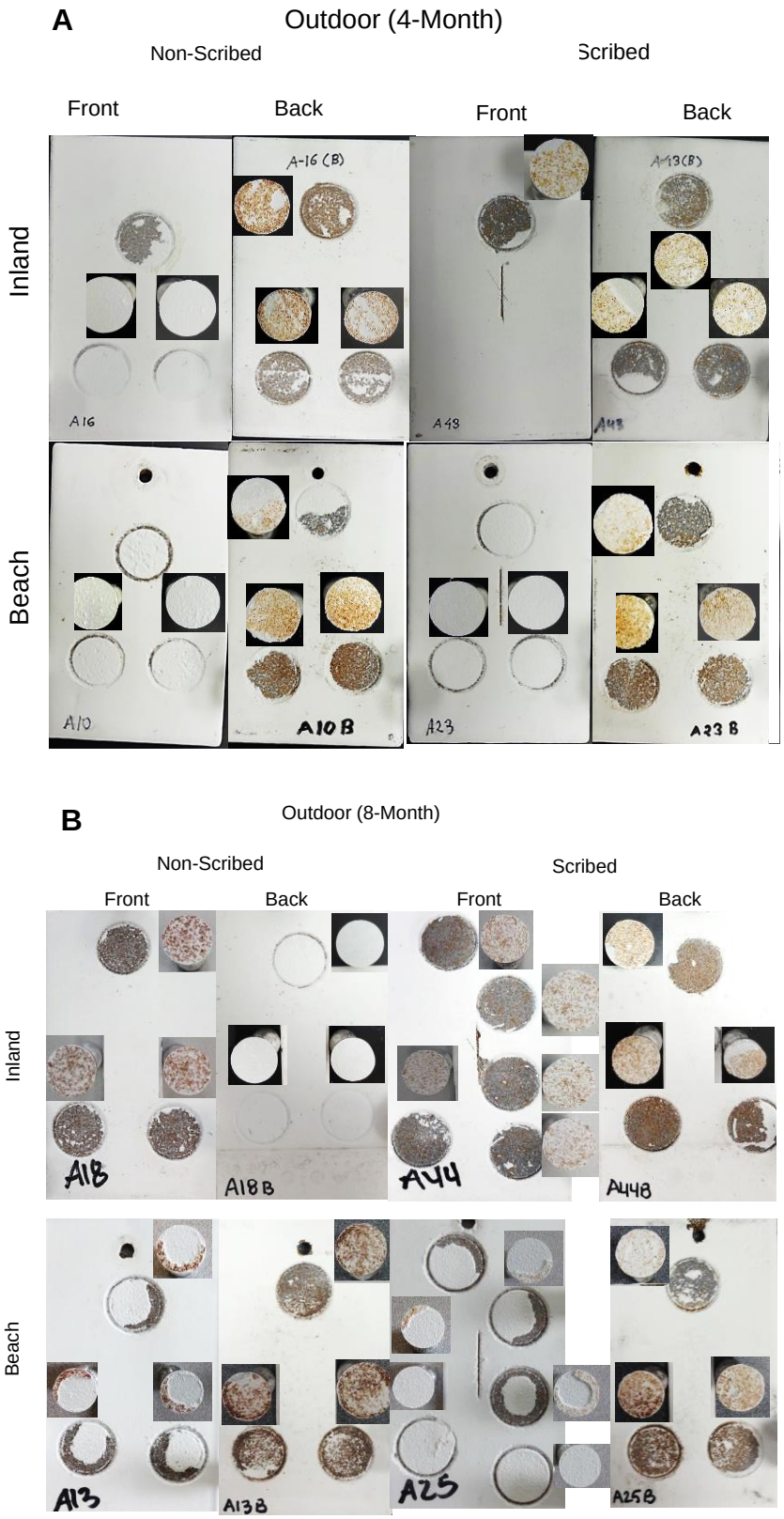


**Figure: 5.23 CBPC Coating Pull-Off after Outdoor Exposure.**
A) 4-month exposure. B) 8-month exposure

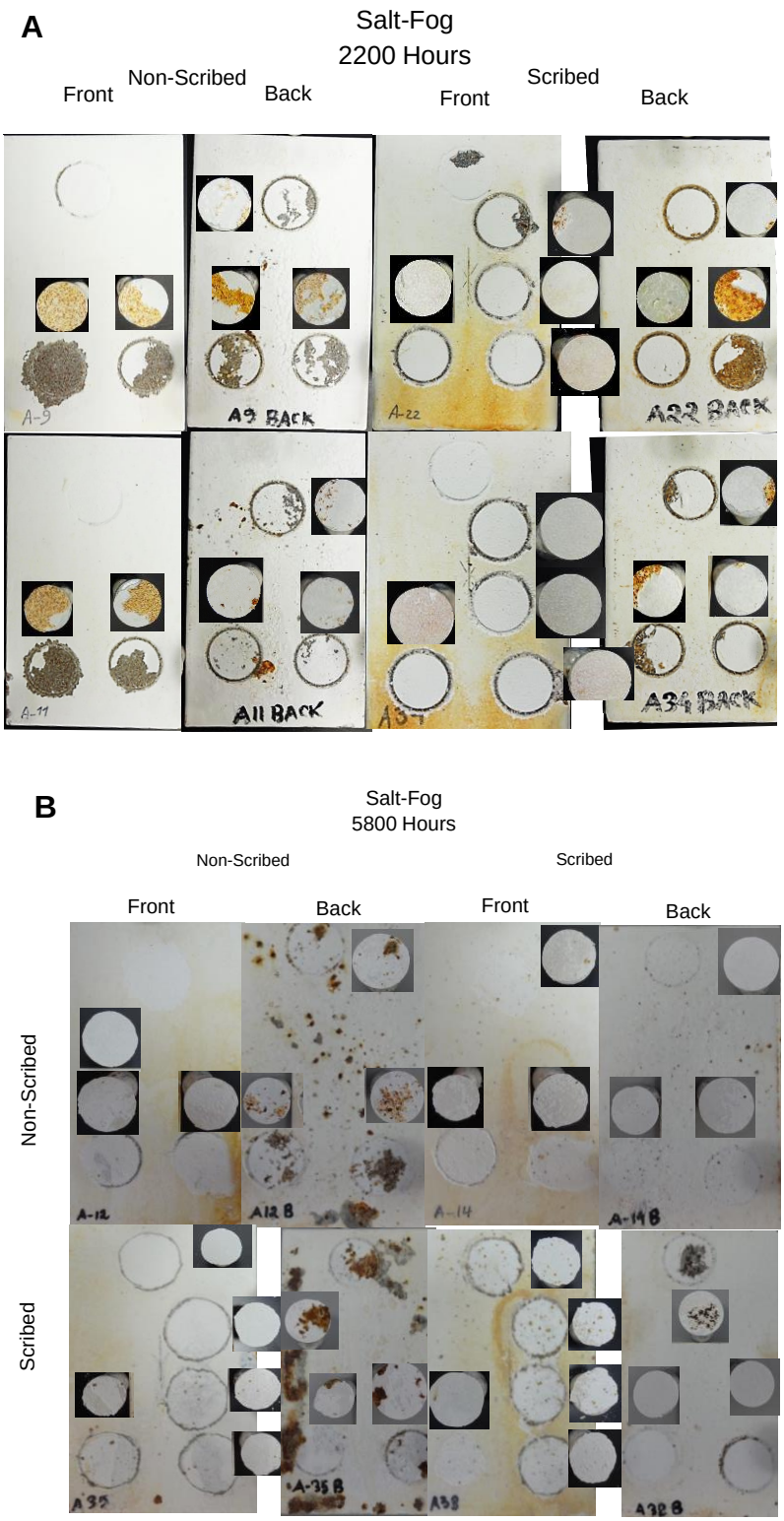


**Figure: 5.24 CBPC Coating Pull-Off after Salt-Fog Exposure.**
A) 2200 hours exposure. B) 5800 hours exposure.

Pull-off strengths in Figure 5.25 on the front faces of the CBPC samples after 4-month outdoor exposure were on the order of ~100-200 psi, with failures occurring within the coatings. Pull-off testing on the back faces resulted in failures at the coating-substrate interfaces, with strengths on the order of ~100-300 psi. These strengths were somewhat greater than for the front faces (coating failure) and similar to the as-received strengths. It was thought that the presence of more moisture on the front faces during exposure resulted in greater integrity loss of the coating compared to the back face. After 8 months of outdoor exposure, pull-off testing resulted mainly in failures at the coating-substrate interfaces on both front and back faces, with strengths on the order of 0-500 psi. From the coating thickness data, it seemed that the rate of ceramic material loss may decrease with time. The loose, powdery ceramic material that was evident during the early coating degradation would likely be partially washed away by rain.

After extended salt-fog exposure, pull-off testing resulted mainly in coating failures due to weakening of the ceramic material. Although some partial and total failures at the coating-substrate interfaces were observed, failure within the coating seemed dominant in this aggressive environment, even though significant oxide accumulation was observed (especially after 5800 hours, where rust upwardly penetrated through the ceramic material). After 2200 hours, the oxide accumulation resulted in failure at the coating-substrate interface, with bond strengths on the order of ~100-350 psi. This behavior seemed to be consistent with the observations of coating separation after extended outdoor exposure. Conversely, after 5800 hours, the characteristic coating failure resulted in very low bond strengths, on the order of ~0-150 psi. The constant high humidity would have resulted in high moisture contents in the porous CBPC coatings, possibly further compromising the coating integrity.

Coating failure during pull-off testing was consistent with weakening of the CBPC coating by high-humidity weathering and subsequent material loss. Early coating failures were observed in outdoor exposures. Furthermore, the enhanced moisture presence in the accelerated salt-fog exposures allowed for significant deterioration of the CBPC coating, causing very low coating strengths. The coating-substrate failure was related to the amount of red/brown oxide buildup on the substrate. The surface revealed by the mechanical pull-off often contained small clumps of the coating material. Some indication of rust at the exposed substrate was apparent, but much of the red/brown coloration appeared incorporated into the ceramic clumps above the substrate. Although the oxide accumulation can affect the bond strengths, as observed by some pull-off tests showing negligible strengths, the overall strengths of CBPC coatings with oxide accumulation did not seem to greatly differ from the as-received condition. Although it was evident that degradation of the ceramic coating (with reduced cohesive strength) was paired with oxide accumulation, the apparent greater bond strength measured for samples with oxide accumulation may likely be due to the

removal of the loose powder ceramic materials by the weather and the subsequent improved ability of the adhesive to penetrate the coating..

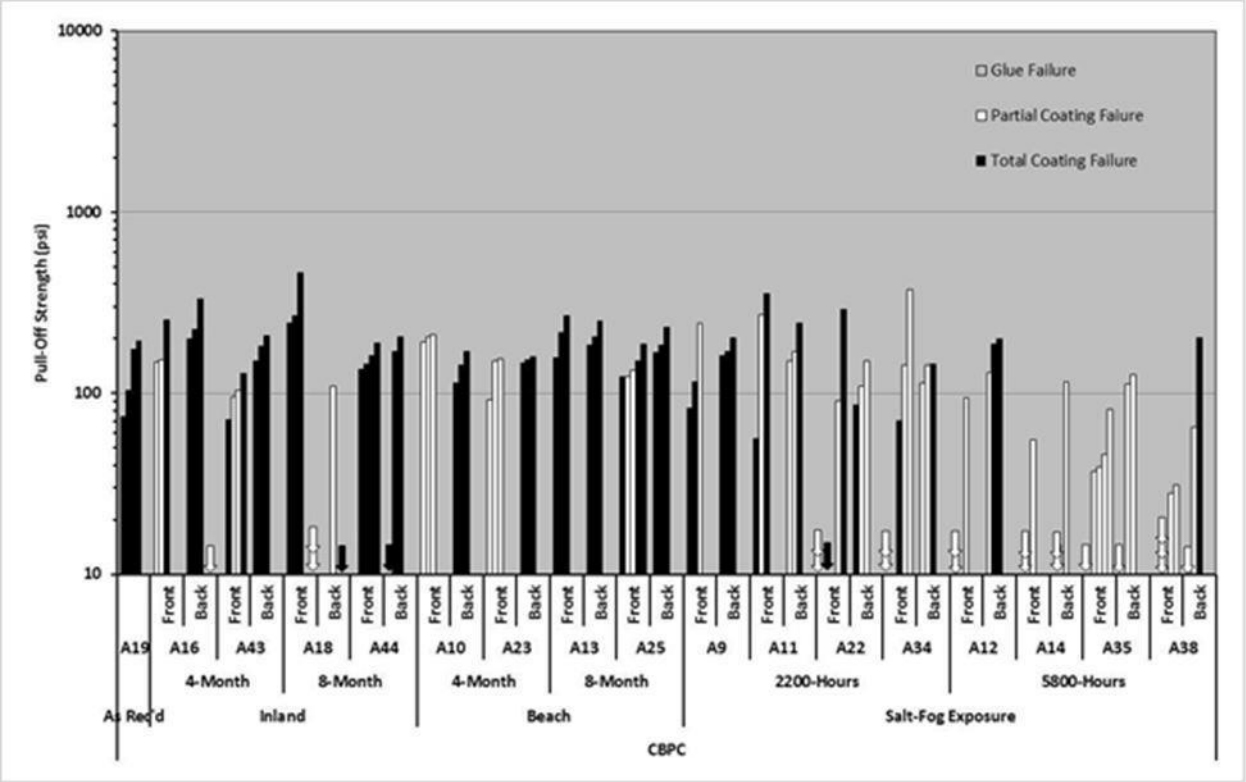


**Figure: 5.25 CBPC Coating Pull-Off Strength**.

### *5.4.2 Thermal Diffusion Galvanizing*

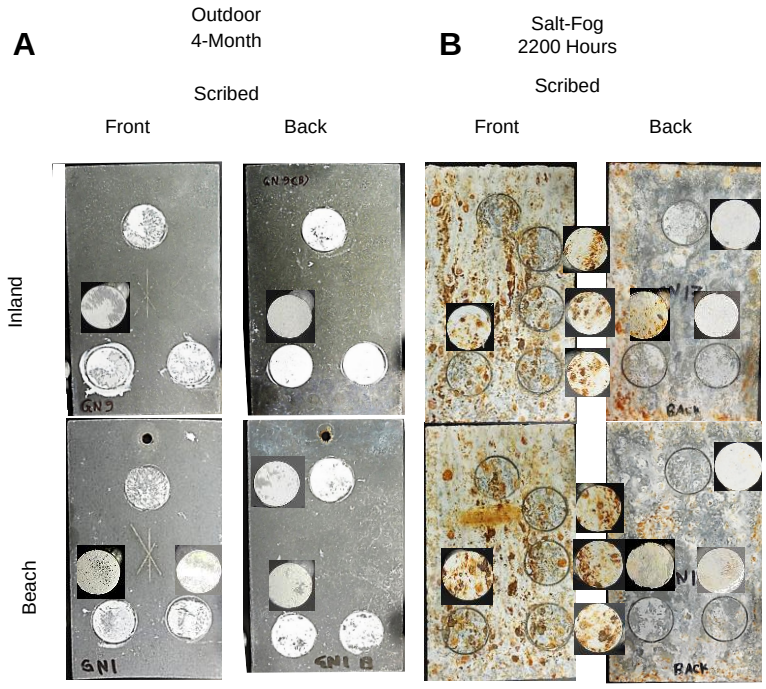


**Figure: 5.26 TDG Without Topcoat Coating.**

A) 4-month outdoor exposure. B) 2200 hours salt-fog exposure

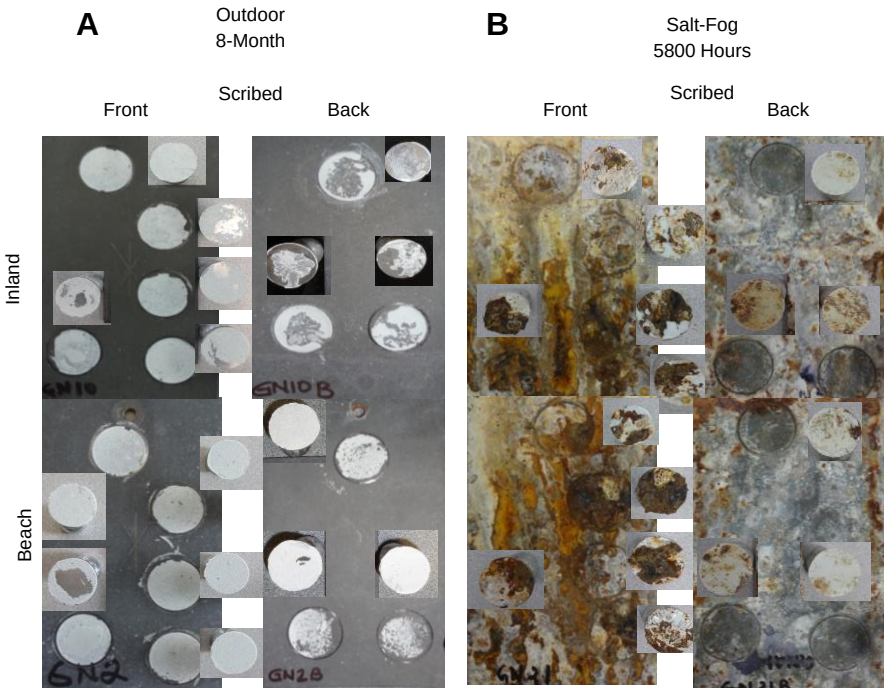


**Figure: 5.27 TDG Without Topcoat Coating.**

A) 8-month outdoor exposure. B) 5800 hours salt-fog exposure

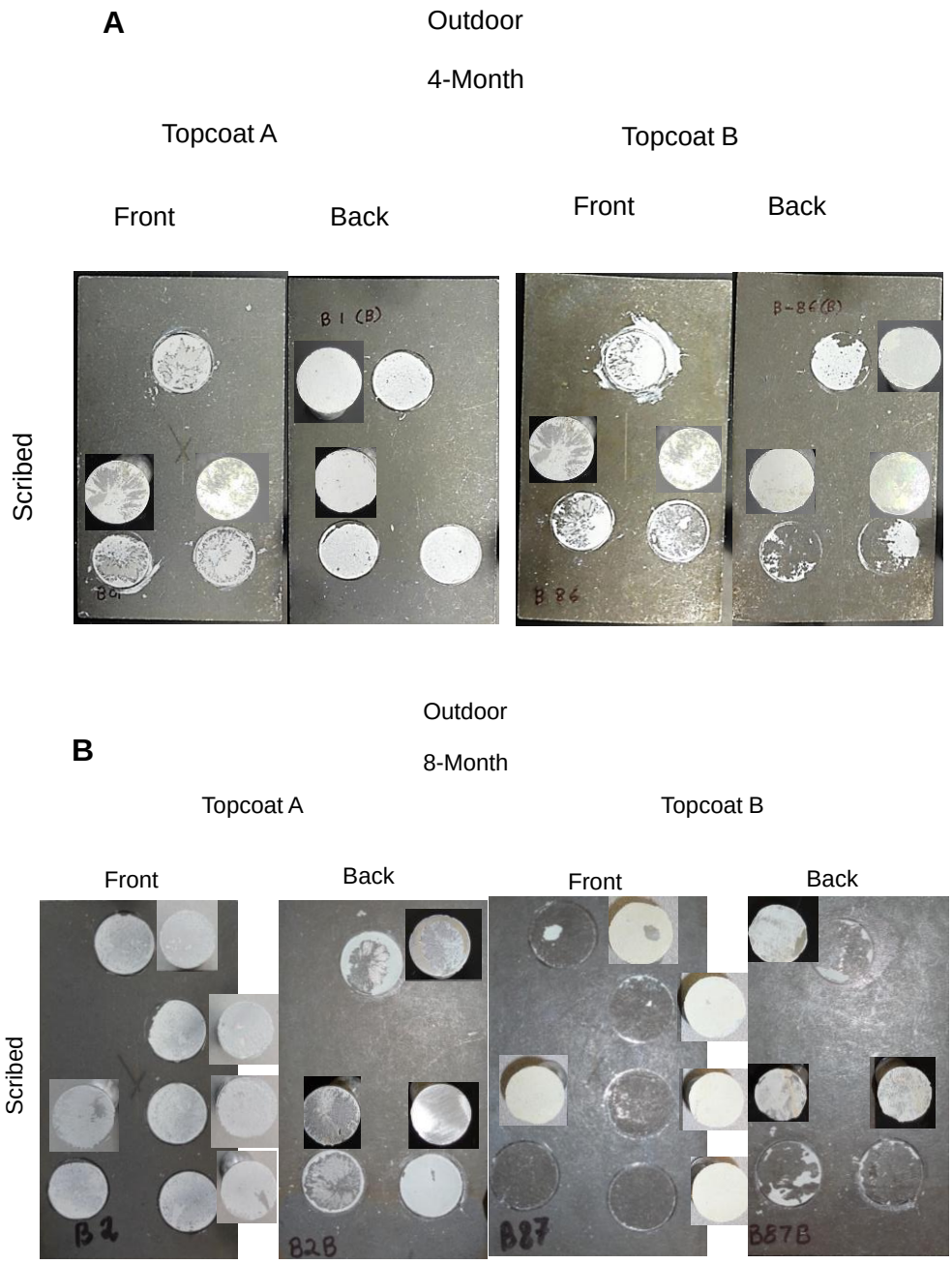


**Figure: 5.28 TDG with Single Topcoat Coating Pull-Off After Inland Outdoor Exposure.**

A) 4-month exposure. B) 8-month exposure.

The surface appearance of TDG coupons with various topcoat applications exposed to outdoor and salt-fog conditions after pull-off strength testing is shown in Figures 5.27-5.30. Pull-off adhesion testing was done for the top surface of the coupon as well as the surface on the backside of the test samples.

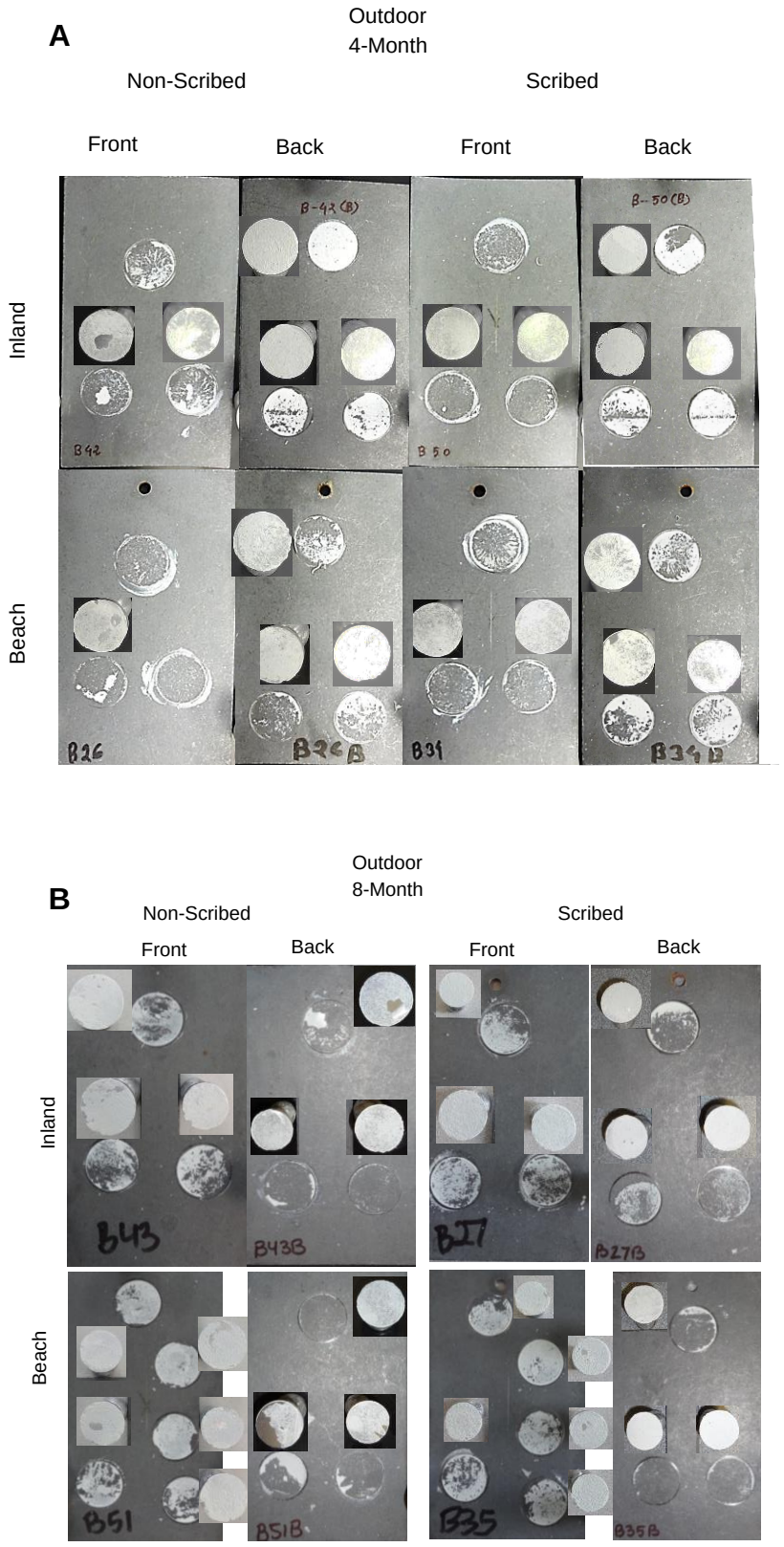


**Figure: 5.29 TDG with Topcoat A+B Coating Pull-Off After Outdoor**
A) 4-month exposure. B) 8-month exposure

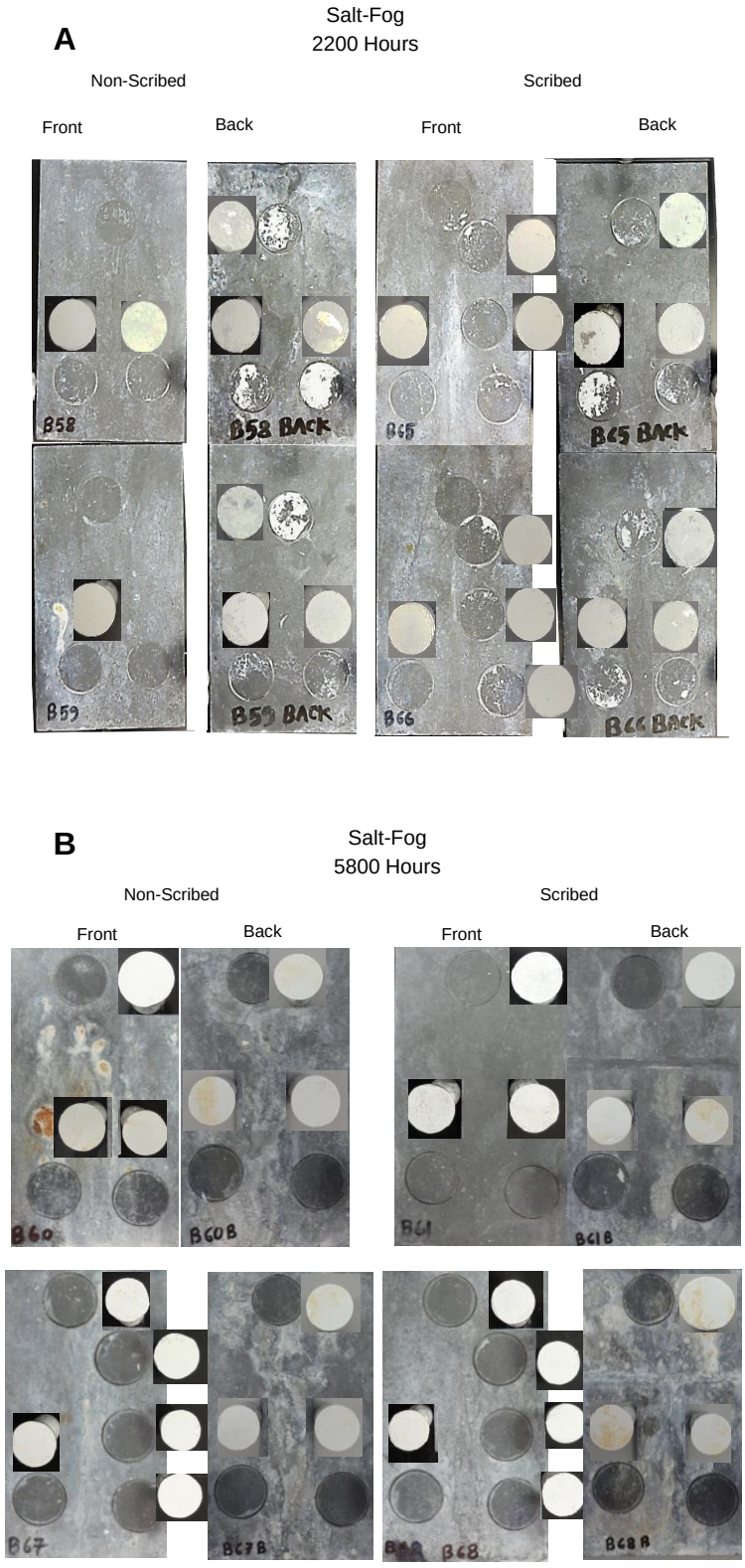


**Figure: 5.30 TDG with Topcoat A+B Coating Pull-Off After Salt-Fog Exposure.**
A) 2200 hours exposure. B) 5800 hours exposure.

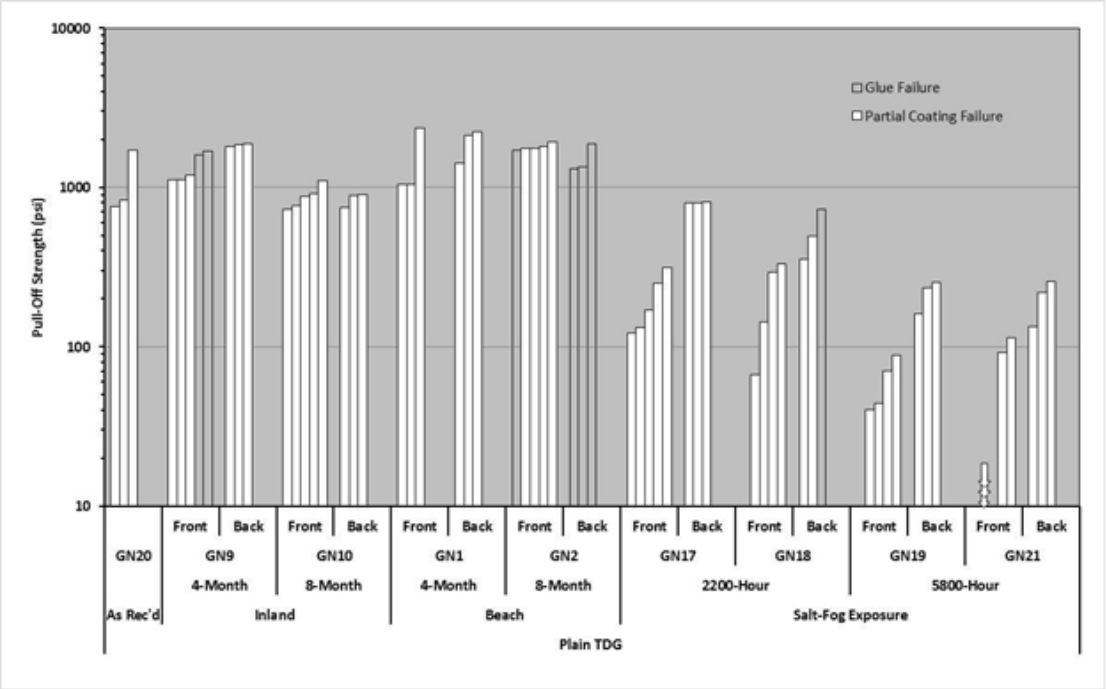


**Figure: 5.31 Plain TDG Coating Pull-Off Strength.**

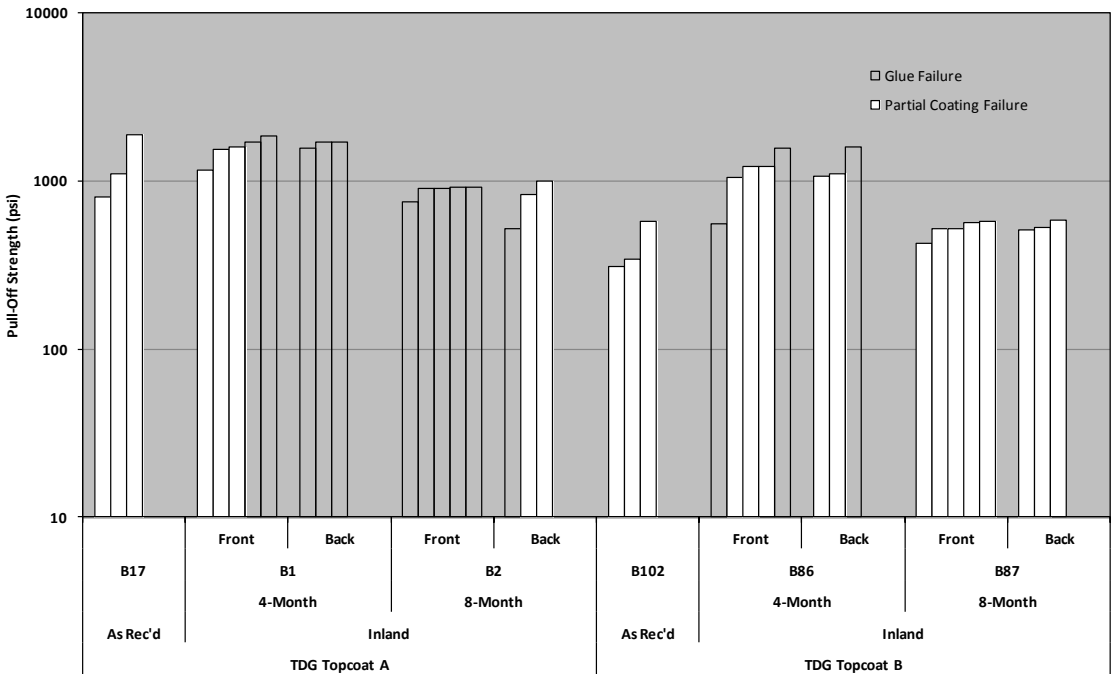


**Figure: 5.32 TDG with Single Topcoat Coating Pull-Off Strength.**

Pull-off testing of samples exposed to outdoor exposure for up to 8 months typically resulted in partial removal of the coating from the substrate. Pull-off strengths for exposed TDG with various applications of topcoat are shown in Figures 31-33. It was noted that surface discoloration and zinc oxidation was apparent on all samples. In

addition to that, TDG with Topcoat B appeared to have a significant color change of the topcoat consistent with the progressive material loss described earlier. The presence of surface oxide formation on all of the samples in outdoor exposure was indicative that the topcoat, when present, had degraded to some degree. Due to the relatively similar coating degradation (topcoat deterioration followed by oxide accumulation), no major differentiation in the pull-off modality was readily apparent for any of the topcoat applications. Metallic particles could be observed on the pull-off dolly after testing.

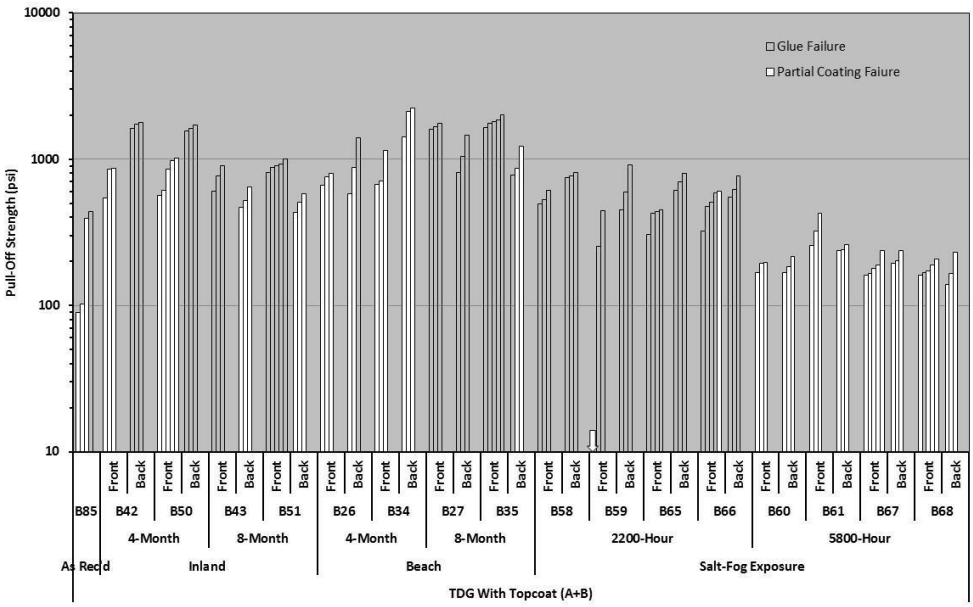


**Figure: 5.33 TDG with Topcoat A+B Coating Pull-Off Strength.**

Plain TDG exposed in aggressive salt-fog exposure for up to 5800 hours showed significant progressive iron rust formation throughout its surface. TDG with Topcoat A+B exposed in salt-fog exposure for up to 5800 hours performed much better, as expected. However, significant zinc oxidation did occur, indicating degradation of the topcoat material. Furthermore, in some samples, iron rust accumulation formed in localized spots indicating complete loss of the topcoat in some locations. Pull-off failures were typically characterized by separation of the poorly cohesive oxide products.

No major trends in pull-off strengths (for Plain TDG- Figure 5.31, TDG with Topcoat A- Figure 5.32, with Topcoat B- Figure 5.32, and Topcoat A+B-Figure 5.33) samples in outdoor exposure were observed with time in spite of indications of topcoat degradation and zinc oxide accumulation. Plain TDG and TDG with Topcoat A had pull-off strengths that exceeded 500 psi. TDG with Topcoat B and Topcoat A+B sometimes had relatively low pull-off strengths below 500 psi. The pull-off strengths for TDG with Topcoat B were generally lower than the other coating systems. The only major trend in pull-off strengths observed was the progressive decrease in pull-off strengths of the Plain TDG

and TDG with Topcoat A+B exposed in salt-fog exposure, where sometimes negligible bond strengths were measured due to the loose formation of iron and zinc oxides.

### *5.4.3 Metallizing*

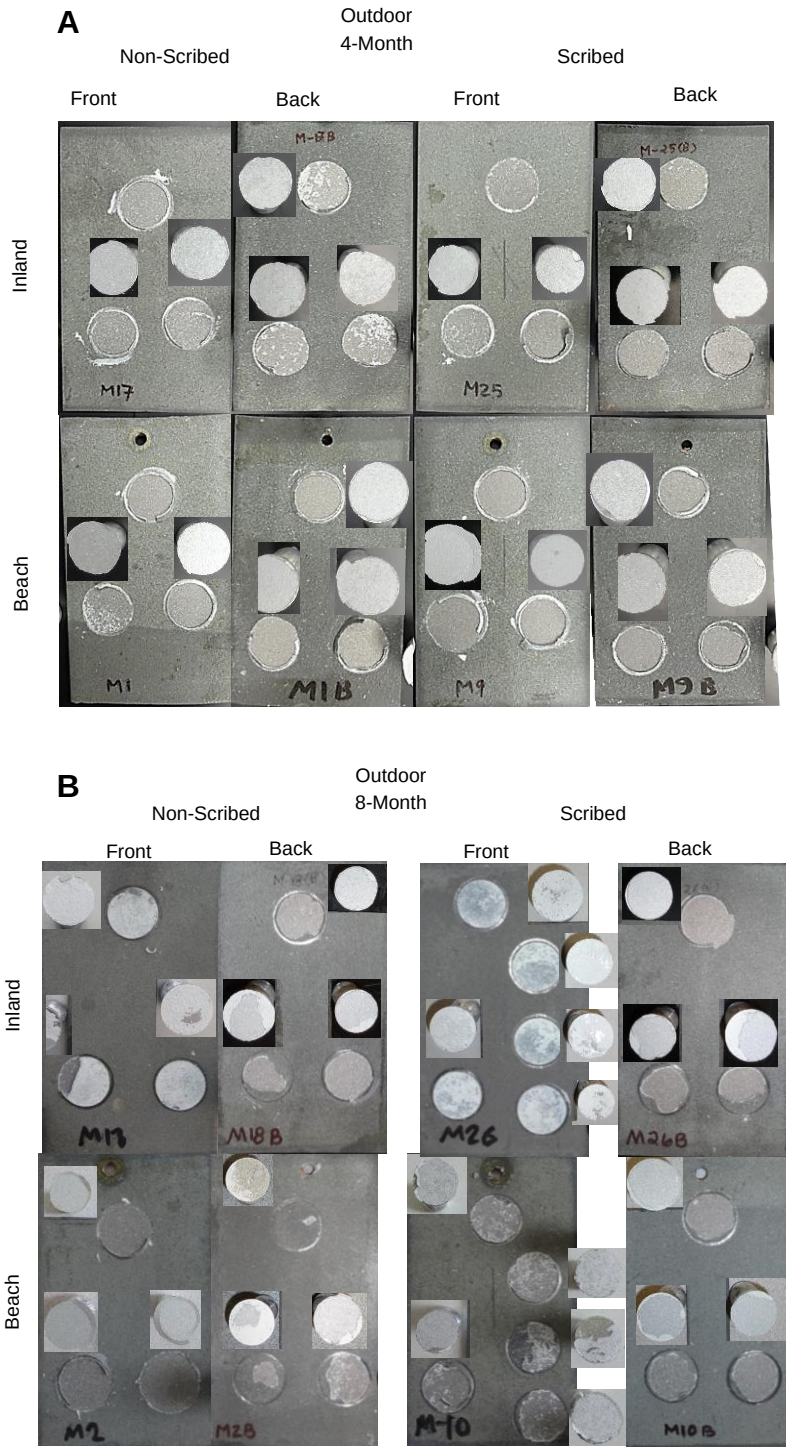


**Figure: 5.34 Metallized Coating Pull-Off after Outdoor.**
A) 4-month exposure. B) 8-month exposure

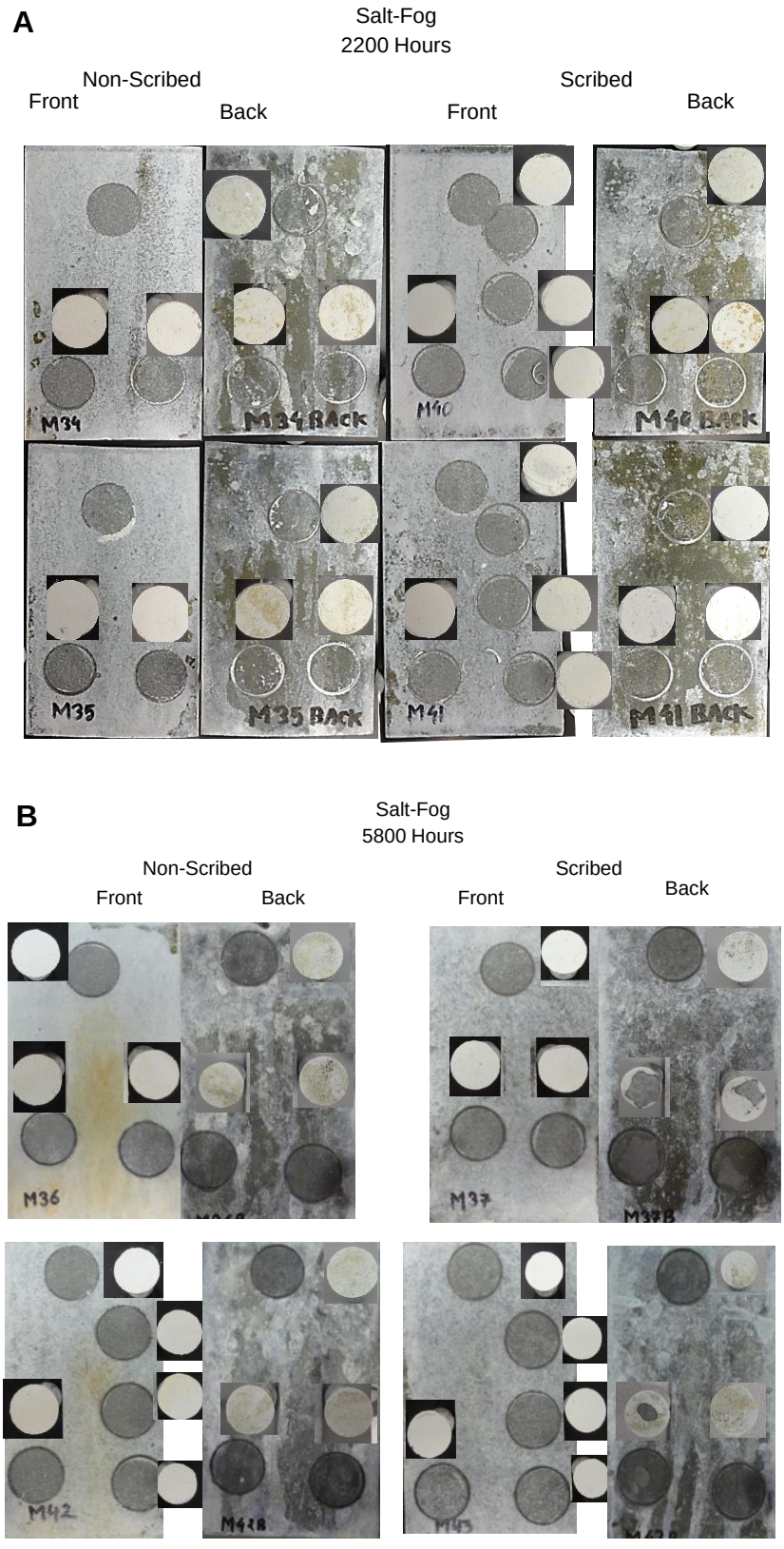


**Figure: 5.35 Metallized Coating Pull-Off after Salt-Fog Exposure.**
A) 2200 hours exposure. B) 5800 hours exposure.

The surface appearance of coupons exposed to outdoor and salt-fog conditions after pull-off strength testing is shown in Figures 5.34 and 5.35, respectively. Pull-off adhesion testing was made for the top surface of the coupon as well as the surface on the backside of the test samples

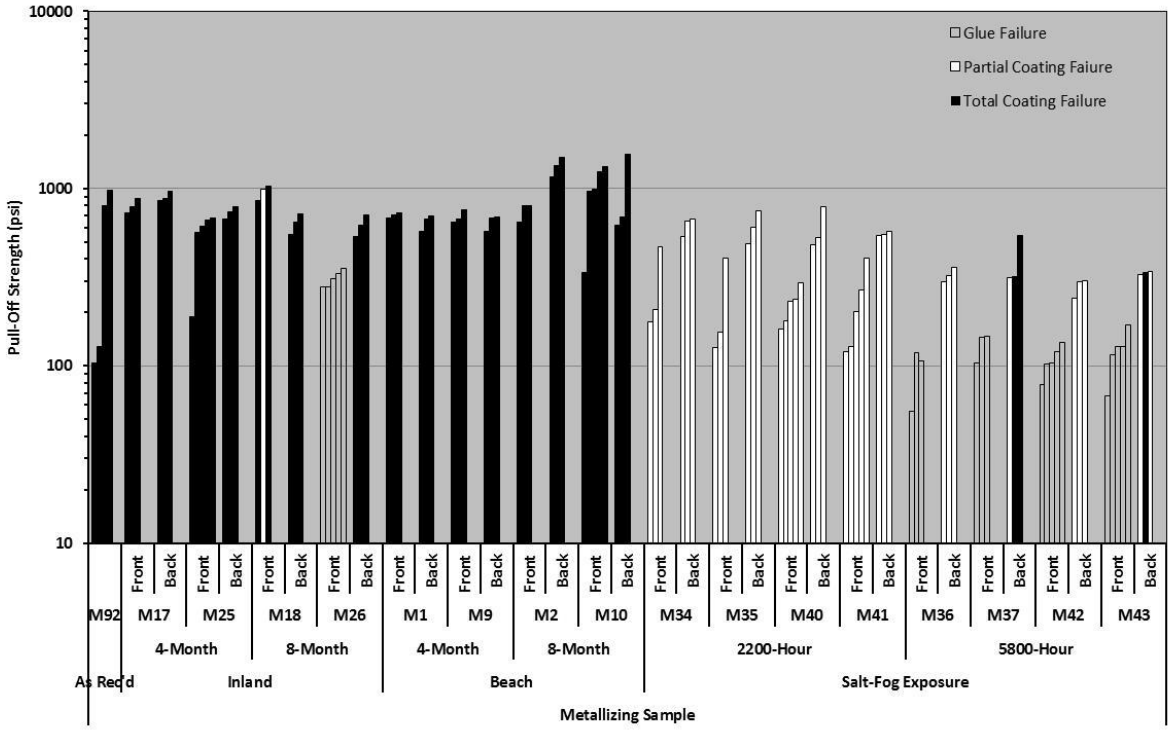


**Figure: 5.36 Metallized Coating Pull-Off Strength.**

For metallized samples in outdoor exposure (similar to the as-received condition), most of the arc-sprayed zinc coating could be completely separated from the substrate with less than ~1500 psi after 8-month exposure (Figure 5.36). No major change in the pull-off strengths was observed with time and in comparison to the as-received metallized samples. For samples in salt-fog exposure for up to 5800 hours, the majority showed partial coating failure at pull-off strengths less than 500 psi due to the accumulation of the oxides on the surface of the samples. Although a major strength reduction in comparison to the as-received samples was apparent, no major change in pull-off strengths was observed with time for the coatings exposed for up to 5800 hours in salt-fog conditions.

### *5.4.4 Three-Coat*

The surface appearance of coupons exposed to outdoor and salt-fog conditions after pull-off strength testing is shown in Figures 5.37 and 5.38. Pull-off adhesion testing was done for the top surfaces of the samples as well as the surface on the backside of the samples (Figure 5.39).

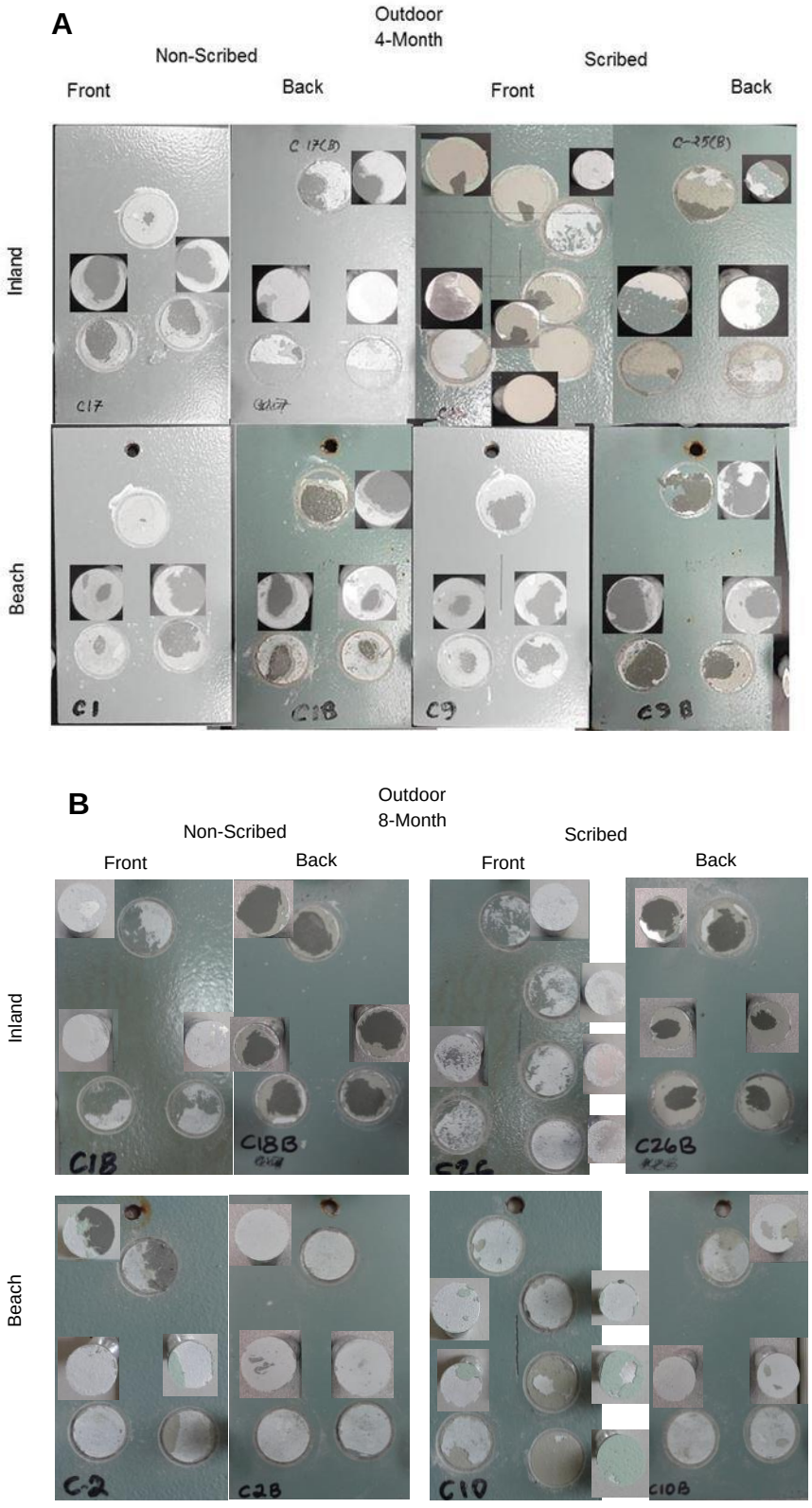


**Figure: 5.37 Three-Coat Coating Pull-Off after Outdoor.**
A) 4-month exposure. B) 8-month exposure

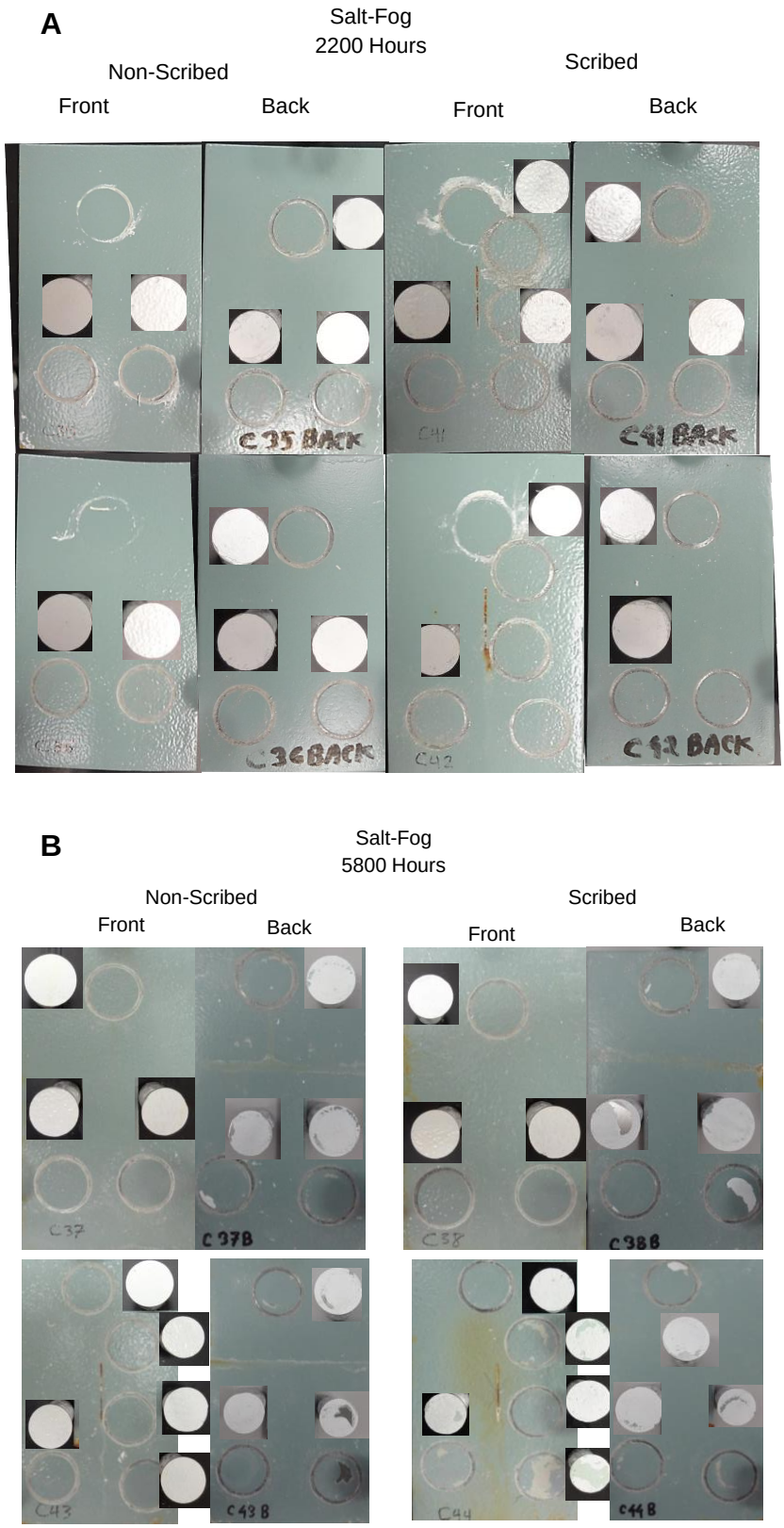


**Figure: 5.38 Three-Coat Coating Pull-Off after Salt-Fog Exposure.**
A) 2200 hours exposure. B) 5800 hours exposure.

Reduced pull-off strengths were obtained for three-coat samples, in the as-received condition, due to failures of the adhesive between the pull-off dolly and sample. The test procedure did not incorporate any type of surface preparation to improve the bond between the adhesive and sample, and the smooth, glossy surface of the as-received topcoat limited the bond of the dolly to the coating. Pull-off testing of as-received three-coat samples produced strengths up to ~400 psi, but did not result in separation of any of the coating materials.

For three-coat samples in outdoor exposure, portions of the coatings were removed in all samples. Exposure to the environment may have caused some deterioration and roughening of the topcoat, exemplified in part by some early coating thickness loss. Partial coating separation of the topcoat or epoxy layers as well as total failure with separation at the zinc paint layers were observed. After up to 4 months of outdoor exposure, the pull-off tests resulted in separation of the coating at the zinc-rich paint layer with strengths ranging from ~500 to 1500 psi. For samples exposed in the inland outdoor exposure site for up to 8 months, pull-off testing produced similar material separation at the zinc-rich paint layer at comparable bond strengths. After up to 8 months outdoor exposure at the beach site, the coating separated by cohesive failure of the intermediate epoxy layer (second coat) with pull-off strengths ranging from ~200 to ~2200 psi (Figure 5.39).

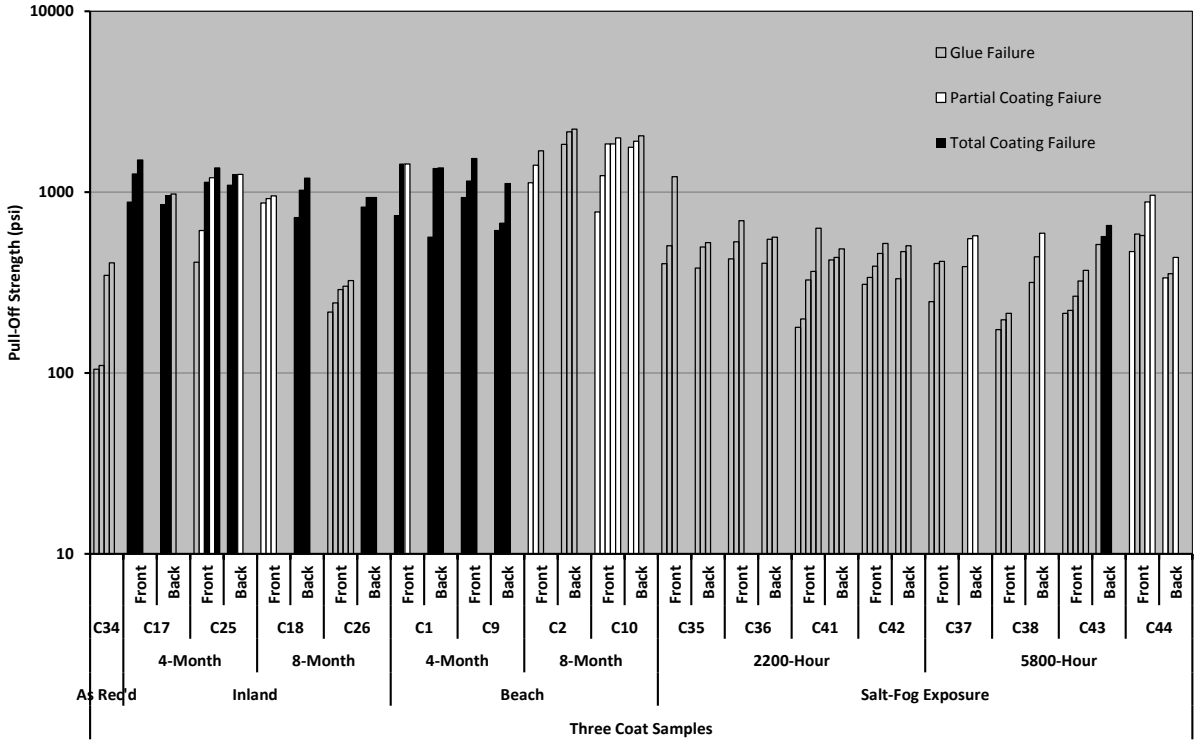


**Figure: 5.39 Three-Coat Coating Pull-Off Strength.**

As described earlier, no major coating deterioration was visually observed for the samples placed in salt-fog exposure for up to 5800 hours, but there was indication of thickness loss due to the harsh exposure there. However, differentiation of coating bond characteristics from the exposure in salt-fog was inconclusive, as most of the testing resulted in adhesive failure of the dolly to the coating surface. Some test results after 5800 hours indicated coating separation at stresses less than 500 psi.

# CHAPTER SIX: GENERAL DISCUSSION, CONCLUSIONS AND RECOMMENDATIONS

## 6.1 GENERAL DISCUSSION

### *6.1.1 Chemically Bonded Phosphate Coating*

Much of the results and discussion presented earlier alluded to the difficulty in analyzing the data due to the inherent large variability of the coating thickness in the as-received condition. Nevertheless, the findings lead to commonalities from the outdoor, accelerated immersion, and salt-fog tests, where a sequence of steps in coating degradation can be proposed.

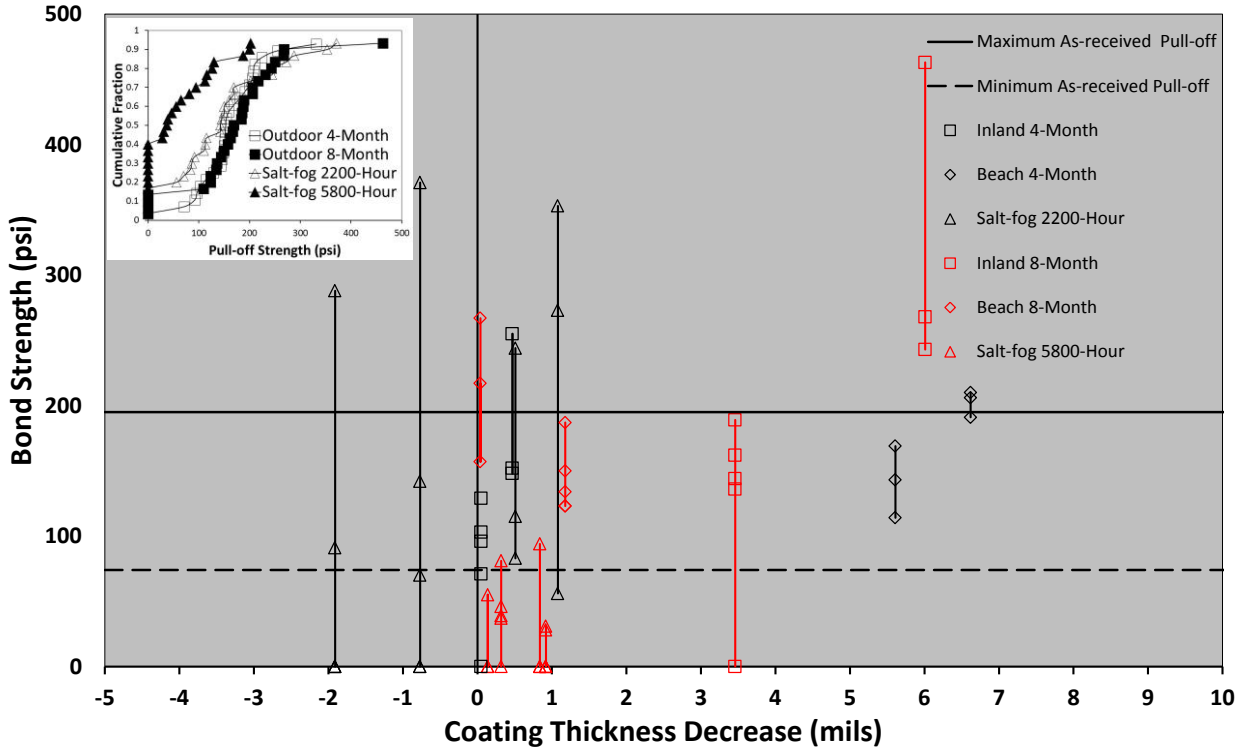


**Figure: 6.1 CBPC Coating Degradation.**

Figure 6.1 shows a graph plotting the coating degradation parameters, pull-off strength, $\sigma_{po}$, and apparent coating thickness decrease, $t'_d$, for samples where both parameters could be measured or calculated for the same test coupon. Per caveat above, the coated samples were randomly selected from sample populations that were not large enough to insure a representative sample, and this sometimes allowed for a skew in the measured values. For this reason, identifiers on the figure (such as pull-off strength and thickness decrease) for the particular test conditions were not considered reliable. However, the graph can show the relative degradation of the coatings in each exposure condition.

On the ordinate, the pull-off strength, $\sigma_{po}$, represents the pull-off strength where either cohesive or adhesive failure of the ceramic occurred. On the abscissa, the apparent coating thickness decrease $t'_d$, was the estimated thickness loss of the CBPC coating, $t'd(t) = t_o-(t_{M,t}-t_{R,t})$ where $t_o$ was the original measured coating thickness, $t_{M,t}$ was the total measured coating thickness at time t, and $t_{R,t}$, was the estimated undercoating rust accumulation at time t for the outdoor or salt-fog exposure. The value $t_d$ described in previous sections was simply $t_d=t_o-t_M$. It was assumed that the corrosion rate determined by LPR measurements in immersion tests could represent worse case corrosion conditons for the coupons placed in outdoor and salt-fog environments. Corrosion rates from LPR measurements in zero-chloride solutions were used to determine corrosion rates in outdoor conditions irrespective of the actual chloride presence. The corrosion rates from LPR measurements in chloride solution were used to determine the corrosion rate of the coated samples in a salt-fog environment. In these calculations, it was assumed that uniform corrosion occurred throughout the entire surface of the coupon with the rust density of ~5 g/cm$^3$ and that the stoichiometric equivalent of ferrous iron ions from the iron oxidation rection was 2. The estimated rust accumulation after 8 months in chloride conditions was ~0.8 mils. As seen in Figure 6.2, the apparent localized rust accumulation was comparable, ~2 mils for 5800-hour salt-fog exposure.

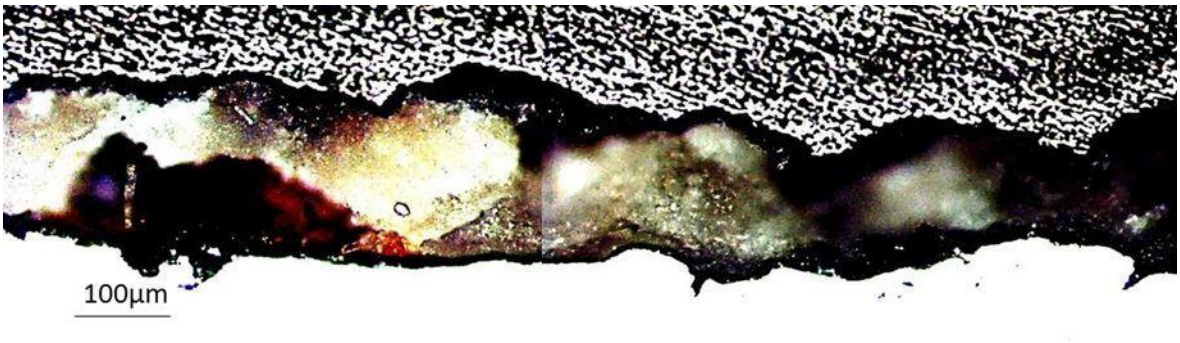


**Figure: 6.2 CBPC Undercoating Rust Development Micrograph** (Image after 5800 hours salt-fog exposure).

It was noted that even after this first approach to normalize the ceramic coating degradation, negative $t'_d$ values were calculated. Even though the corrosion rate was not expected to be higher, greater rust accumulation, as demonstrated in the comparison above, may be possible if more expansive corrosion products developed. Another feature of the compiled test results shows that some pull-off strengths were greater than the range of values from the as-received condition after environmental exposure. These values were still relatively low (less than 500 psi) and were attributed to sample variability. Of note (as described in earlier sections), some pull-off strengths were negligible and were attributed to coating deterioration.

One important trend that can be gleaned from Figure 6.1 is the poor correlation between coating degradation parameters $\sigma_{po}$ and $t'_d$. For environments with constant high humidity and moisture content (such as in the extreme case of the salt-fog environment), it can be seen that major pull-off strength decreases can occur regardless of significant thickness change. This suggests that the ceramic coating degrades by internal deterioration rather than surface weathering in high moisture conditions. The apparent porous nature of the coating, as seen in Figure 6.3, would allow better transport of moisture and and other chemical species. The availability of moisture within the coating would lead to degradation and significant cohesive strength loss. Observations of coating degradation in immersed conditions, where the ceramic became exfoliated from the substrate in flakes, further corroborates this finding. Also, EIS pore resistance measurements from immersion testing of non-scribed samples did not show a major decreasing trend with time, but rather a constant to somewhat increasing trend in $R_{po}$, which would not support the notion that coating weathering would be dominant here.

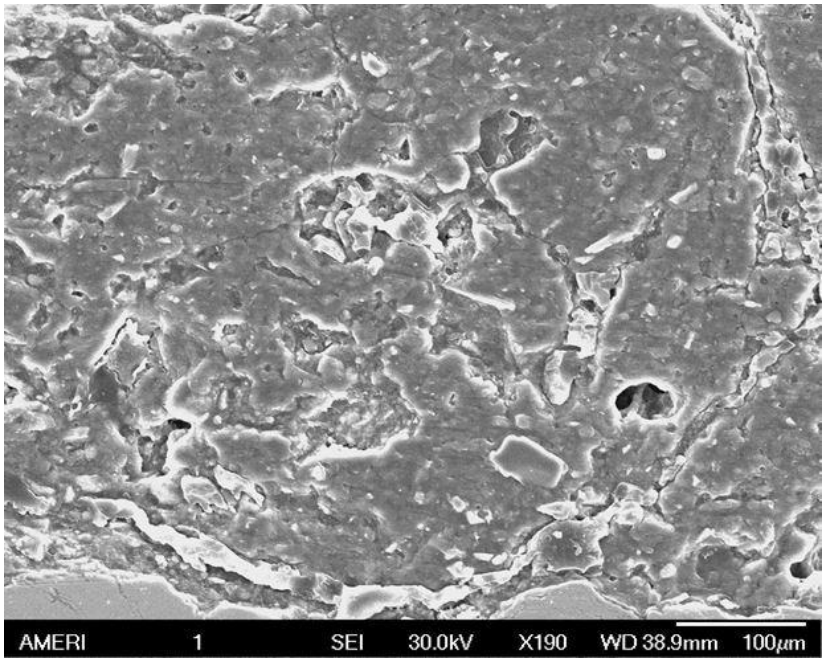


**Figure: 6.3 SEM Image of Porous Characteristics of CBPC** (Sample 4 month Outdoor Exposure).

Conversely, ambient exposure would provide conditions such that the outer portion of the coating would be most susceptible to wetting and drying and thus surface degradation of the coating. The lower pull-off strengths measured for samples in outdoor exposure for 4 months (with sometimes signficant thickness reduction) were the result of testing on the coupon surface where the coating degradation left powder residue. After 8 months outdoor exposure, the extent of coating material loss was not necessarily greater, but pull-off strengths were apparently greater. As described in

earlier sections, the rate of material loss may decrease with time and the extended exposure would likely cause some removal of loose particles from the sample surface. Subsequent pull-off testing would cause failure at the ceramic-substrate, where the bond is weakest due to rust accumulation.

It is noted again that the material used in testing was intended to be prepared and coated in accordance to manufacturer best practices, but indications of significant sample variability were observed. As with any test program with provided test materials, the findings described are solely based on the testing results for the materials received, and may not necessarily reflect material behavior due to any changes by the materials providers. Also, the outdoor exposure periods used here were rather short to fully identify long term behavior, and accelerated tests in salt-fog and solution immersion were aggressive and not necessarily representative of field conditions. However, the findings from this study were meant to be preliminary to provide indicators of major material incompatibility with environments relevant to highway bridges. As such, the scope of the work was broad and did not focus on any particular application or environment. As part of the preliminary work, some advantages and disadvantages in certain broad environments were identified.

From findings discussed in detail in Chapter 3, it was observed that severe degradation of CBPC in alkaline solution can occur. The high pH used in testing (pH 13.3) was intended to simulate conditions in the pore water of a freshly cast concrete. From this observation, corrosion protection that may be afforded by the bulk CBPC in applications such as coated reinforcing bar in concrete could be significantly impaired. Although testing in solution likely provided conditions of enhanced moisture availability and consequent enhanced degradation of the coating compared to a hardened concrete environment, it can be argued that wet concrete conditions with high pH can be present during early life as well as in high quality concrete in marine environments. The pH of 13 was in the upper range of concrete pore water pH, and was thought to be a rather aggressive condition. Other pH conditions representative of mature concretes or concrete pore water in service were not evaluated. The cohesive weakening of the coating was apparent in solution where convection was not restricted. The behavior of the coating when embedded in a matrix (such as concrete) was not evaluated. However, mechanical issues due to the degradation of the bulk coating, such as stress development along the length of the reinforcing steel, would need to be evaluated. Although, significant degradation of the CBPC coating occurred in alkaline solution, severe corrosion of the exposed steel substrate in solution with 3.5% NaCl did not develop, and there was indication that the corrosion rate decreased with time.

Furthermore, when coating defects were present in the CBPC coating, the extent of rust creepage away from the defect was minimal. It was noted that localized undercoating corrosion could develop in regions where a crevice condition was formed on top of the

ceramic coating. The coating manufacturer states that there is formation of a corrosion-resistant intermediate alloy layer up to 20 μm thick. Optical and electron microscopy (exemplified in Figure 6.4) did not show consistent formation of the intermediate layer at the steel-CBPC interface. The corrosion performance in high pH environments was not further evaluated.

Much of the CBPC testing dealt with its performance in atmospheric environments. Results from limited outdoor exposures at South Florida inland and beach test sites were described. On a positive note, no severe corrosion of the steel substrates occurred during the 8-month outdoor exposures. The ceramic coating remained largely intact despite material loss, and no indication of rust bleed-out or coating blistering was observed, although significant surface oxidation occurred. Furthermore, corrosion at the scribe defect was minimal and no indication of rust undercutting the coating edge was observed. In terms of long-term durability and corrosion mitigation, one possible issue of concern relates to the compromise of coating integrity as shown by material loss even after relatively short outdoor exposure periods. Loss of material of a coating that evidently allows sufficient oxygen and moisture penetration would not provide good barrier coating performance. Indeed, enhanced undercoating surface oxidation that increased with time was apparent.

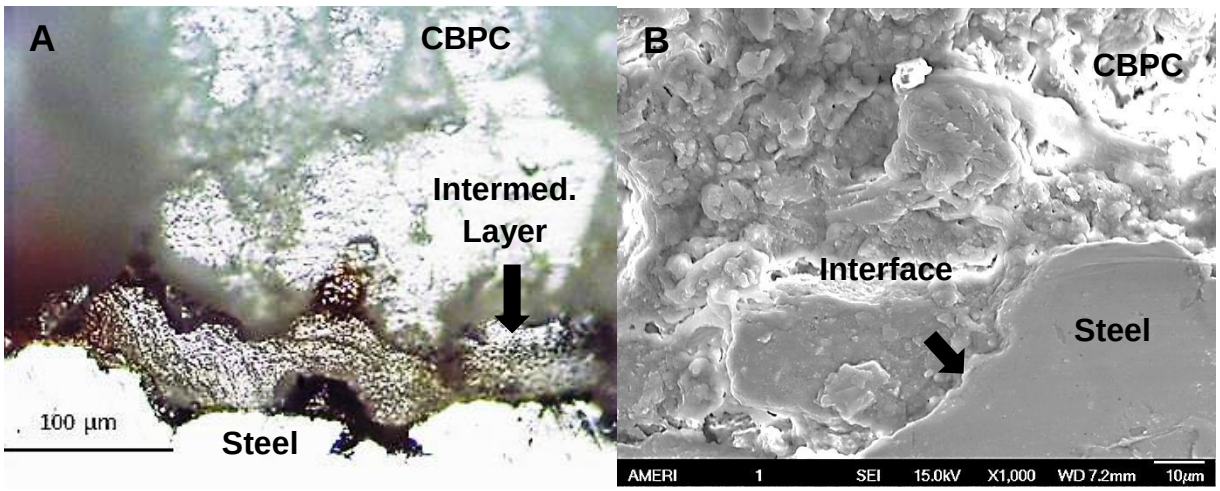


**Figure: 6.4 Optical and SEM Image of CBPC after Salt-Fog Exposure.**
A) Optical micrograph. B) SEM micrograph.

Aggressive accelerated testing of CBPC samples in salt-fog and immersion where high levels of moisture were available showed great propensity for the ceramic coating to deteriorate. In the salt-fog environment, the cohesive strength of the ceramic material was greatly degraded. In immersion testing, the coating was observed to crack and exfoliate from the substrate. It was apparent that the coating deterioration of the as-received samples that occurred during the aggressive salt-fog exposure and immersion testing could exacerbate the extent of undercoating surface corrosion (Figure 6.4a).

Interesting results relating to the intentional defect (scribed) sites exposing the substrate were observed. Corrosion at the defect sites on samples placed in outdoor and salt-fog exposure did not increase with time yet significant undercoating surface oxidation (similar to non-scribed samples) occurred throughout the samples. In immersion testing with salt solution however, corrosion at the defect site did form but surface oxidation appeared minimized. Comparable testing with non-scribed samples showed undercoating surface oxidation. Apparent pore resistance resolved from EIS testing of the scribed samples placed in salt solution, where the behavior at the defect site may be dominant, showed an increase with time. This was thought to be related to blocking of the scribe with corrosion product. Pore resistance for non-scribed samples placed in salt solution showed a constant to slow increase with time. Physical interpretation of these results is more elusive. The results may be explained by the fact that coating thickness loss and rust accumulation both occurred and would result in diverging trends. Further analysis of the impedance response by the equivalent circuit fitting detailed in Chapter 3 is needed to elucidate those findings.

In aqueous conditions where electrochemical polarization can be extended on the metal surface, it was thought that some form of galvanic coupling of the anodic site at the defect may have provided some beneficial cathodic polarization to surrounding locations. Similar extended effects at local sites on the metal interface (depending on the amount of available moisture) could be possible for non-immersed exposure conditions. Further testing to elucidate this behavior and the role of any intermediate alloy layers is needed.

From the findings to date in the preliminary study, an important issue for further evaluation, concerning long-term durability and corrosion protection by CBPC coatings, would be to address the reactions and processes that lead to the deterioration of the ceramic coating. It was observed that the as-received material has very poor compatibility with alkaline solution at pH 13. Freshly cast concrete pore water may cause early degradation of the coating. It was observed that conditions with high moisture availability and wetting and drying conditions could degrade the material as well. Environments where excessive water accumulation can occur or where there is direct exposure to water could cause early degradation of the coating. In atmospheric exposure, some coating degradation may occur, but early indicators seem to show that this rate can be reduced. The rather short-term outdoor exposures gave some promising results, but the level of undercoating surface oxidation may compromise long-term durability, as seen after 5800 hours in salt-fog exposure where rust bleed-out through the coating occurred. The expected intermediate alloy layer was not consistently identified (Figure 6.4b) and its role in corrosion mitigation has not been elucidated.

Conventional three-coat systems were tested in part for benchmark comparison with CBPC in the proposed testing. Generally speaking, the three-coat system performed well and the only point of contention was the significant rust bleed-out from scribed locations after 5800 hours of aggressive salt-fog exposure. Severe steel corrosion of CBPC generally did not occur except for rust bleed-through at non-scribed locations after 5800 hours exposure in aggressive salt-fog exposure. Comparison of electrochemical corrosion testing results of CBPC and three-coat in neutral pH solution with 3.5% NaCl are shown in Figure 6.5. As expected, more active potentials were initially measured for the three-coat system due to the presence of the zinc particles. Those potentials fluctuated to more positive potentials indicative of passive-like conditions. Correspondingly, the corrosion current there decreased with time. Fairly negative potentials were measured for CBPC as well ($E_{Corr}$ < -500 $mV_{SCE}$). Corrosion currents were significantly higher for CBPC than for the three-coat samples. This was thought to be due to the greater active surface area for CBPC due in part to coating degradation and the porous condition of the coating.

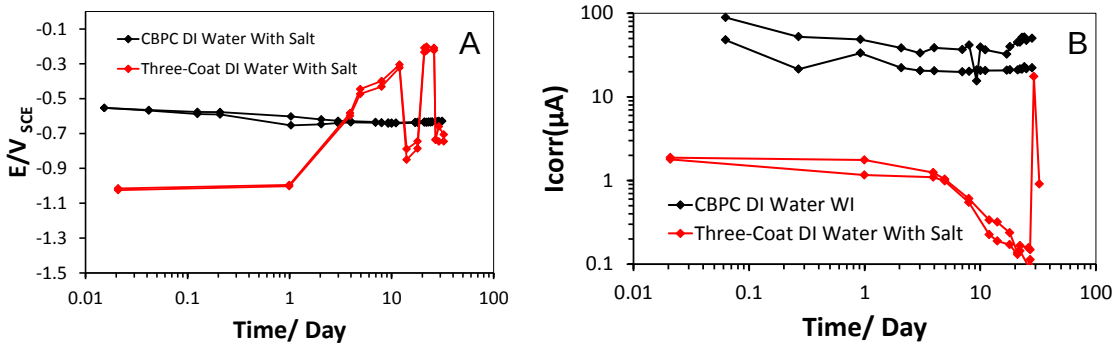


**Figure: 6.5 Corrosion Electrochemical Parameters of CBPC and Three-Coat**
A) Open circuit potential. B) Corrosion current.

### *6.1.2 Thermal Diffusion Galvanizing*

TDG-coated steel coupons subjected to outdoor exposure for up to 8 months generally showed positive results. No indication of steel rust development was observed. Of note however, changes in coating thickness and cases with significant degradation of the TDG (including observation of significant TDG layer cracking) were observed. Cross sections of some coated TDG samples after 8 month outdoor exposure are shown in Figures 6.6 and 6.7. The causes and significance of cracking in the TDG layer and ramifications on long-term durability were not studied. As described earlier, variations in topcoats result in varying coating performance. There was indication of increased pull-off strengths for coated samples whose post-exposure coating thickness tended to be below the mean as-received coating thickness. These data may indicate that exposure removed weaker surfaces or regions of the coating, leaving a stronger coating surface for the pull-off fixture to mount to, resulting in higher pull-off strengths.

Contrastingly, three-month salt-fog testing showed major iron corrosion product accumulation on plain TDG samples. The accumulated rust resulted in greater coating thicknesses and reduced pull-off strengths. This rust had been suggested by the manufacturer to be caused by iron within the TDG coating and topcoats were suggested to mitigate the aesthetics concerns. However, there remains concern about coating durability in the presence of local defects where localized iron corrosion products may impact the whole coating system. Indeed, pull-off testing of plain TDG samples with rust accumulation indicated poor adhesion of the surface rusts. In the 8-month salt-fog testing of coated TDG, no significant iron corrosion products developed locally in the scribed defects exposing the metal substrate. There, activity of the zinc alloy layers was apparent. Significant corrosion products sometimes formed at other sites where there were local defects in the topcoat. The durability of the topcoat is important for the overall durability of the coated system. Validation of long-term topcoat performance requires additional testing.

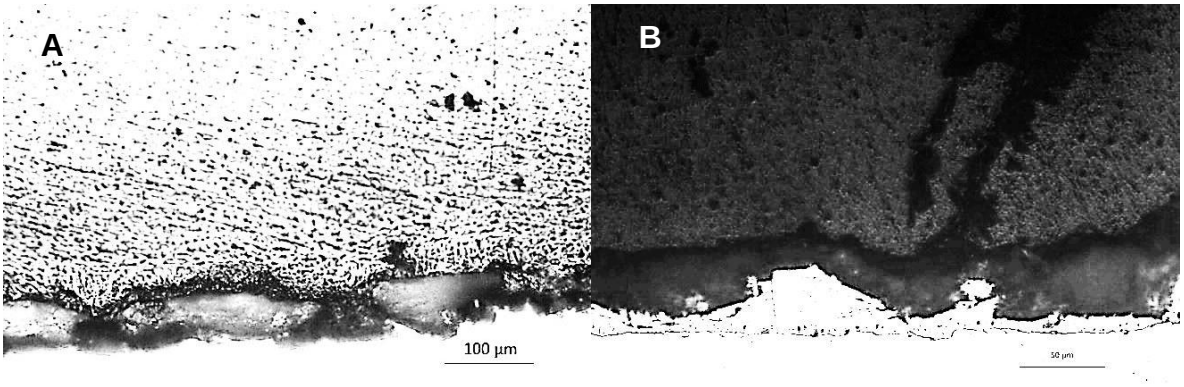


Front Face

Back Face

**Figure: 6.6 TDG Coating with Topcoat A after 8-Month Outdoor Inland Exposure Micrograph.**

A) Front face coating degradation. B) Back face coating degradation.

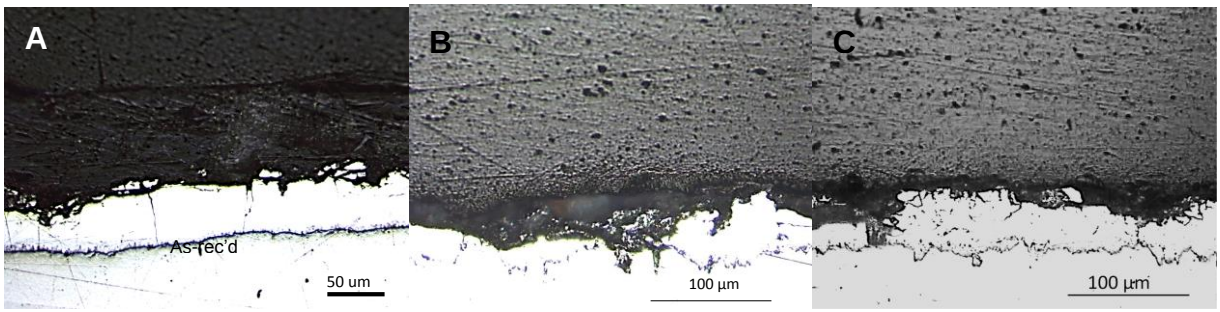


**Figure: 6.7 TDG Coating with Topcoat A+B after 8-Month Outdoor Inland Exposure Micrograph.**

A) As-received coating. B) Coating degradation. C) Coating degradation.

Although there was indication of zinc corrosion activity and some degradation of the topcoat (specifically Topcoat B in alkaline solution) after ~40 day immersion in solution, the level of degradation to TDG was not as severe as in outdoor and salt-fog exposure, where significant degradation to the topcoat and TDG were apparent. This discrepancy in observation has yet to be elucidated and factors such as time of exposure, moisture content, wetting and drying cycles, chloride buildup, oxygen and $CO_2$ availability, and the effects on zinc passivation require further attention. It is still envisioned that moisture accumulation and pooling can create aggressive conditions, especially in regions where bridge detailing may provide crevice environments. Defects exposing the steel substrate may still be of concern, but the initial results show that the TDG is promising as a corrosion resistant coating for structural steel.

Results indicated the importance of the choice of topcoat and quality of its application for TDG-coated steel in aggressive environments. However, the tested topcoats showed varying performance and indications of possible early degradation in outdoor and salt-fog exposures. Also, early degradation of Topcoat B was observed in alkaline solution immersion tests.

Electrochemical impedance spectroscopy (as described in Chapter 3) was used to provide an indication of coating condition. Resolved pore resistance trends with time were consistent with visual observations of coating degradation and measured corrosion behavior. Degradation of the topcoat resulted in enhanced activity of the TDG immersed in alkaline solution. In neutral solution including with 3.5% NaCl, the TDG exhibited near-passive conditions.

No significant corrosion of the base steel substrate was observed for any of the TDG coating conditions in any of the exposure environments. No preferential or localized steel corrosion was observed for scribed lines that exposed the steel substrate.

Although no severe steel corrosion was observed for TDG in outdoor exposure, degradation of the topcoat when present, and subsequent consumption of the TDG would result in shorter service life of the coating for corrosion mitigation. Electrochemical testing of TDG in neutral pH chloride and chloride-free solutions indicated a decrease in corrosion rates with time. The open circuit potential (-600 $mV_{SCE}$ and -900 $mV_{SCE}$ for chloride and chloride-free conditions, respectively) was fairly negative and indicative of zinc activity. The decrease in corrosion rates would then be indicative of conditions for zinc to approach passive-like conditions. Exposure in solution would be representative of an extreme case and could prevent any possible beneficial reaction by drying to form any protection oxide. In any case, significant deterioration of the topcoat and oxidation of the TDG were apparent in some outdoor exposure cases and would show that significant zinc consumption can occur quickly in ambient conditions. Furthermore, salt-fog testing showed that wet conditions with chloride

presence would cause severe surface oxidation and appropriate topcoats are needed in very aggressive environments. The variability in the amount of zinc consumed in testing is likely reflective of the wide variability in the as-received coating thicknesses of the materials used in testing here. The findings suggest that sufficient application of the TDG and robust topcoats are required for long-term durability.

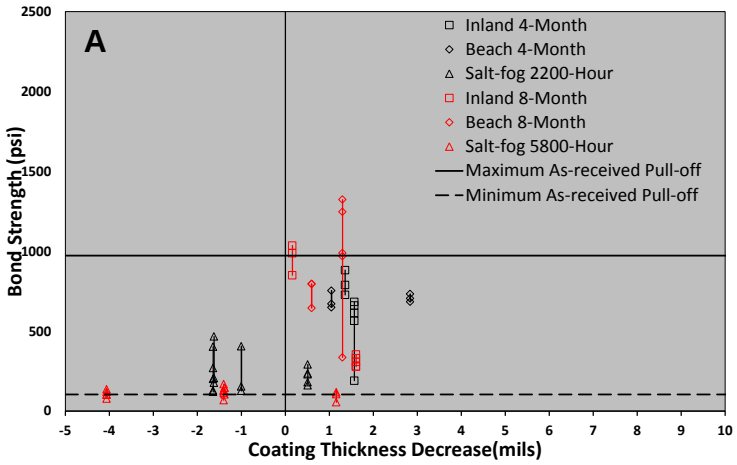


Metallizing

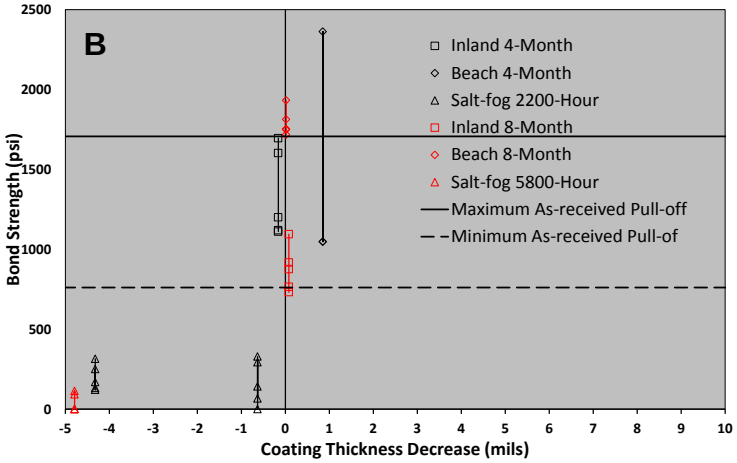


Plain TDG

**Figure: 6.8 TDG and Metallized Steel Coating Degradation (cont.).**
A) Metallizing. B) Plain TDG.

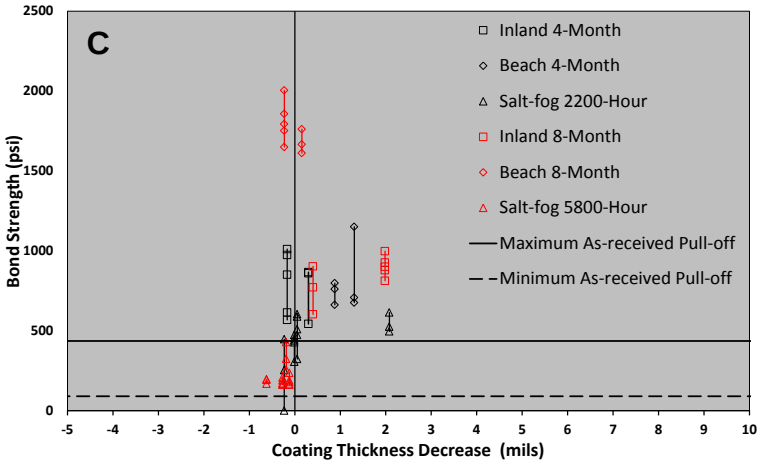


TDG Topcoat A+B

**Continuation of Figure: 6.8 TDG and Metallized Steel Coating Degradation**

C) TDG with topcoat A+B.

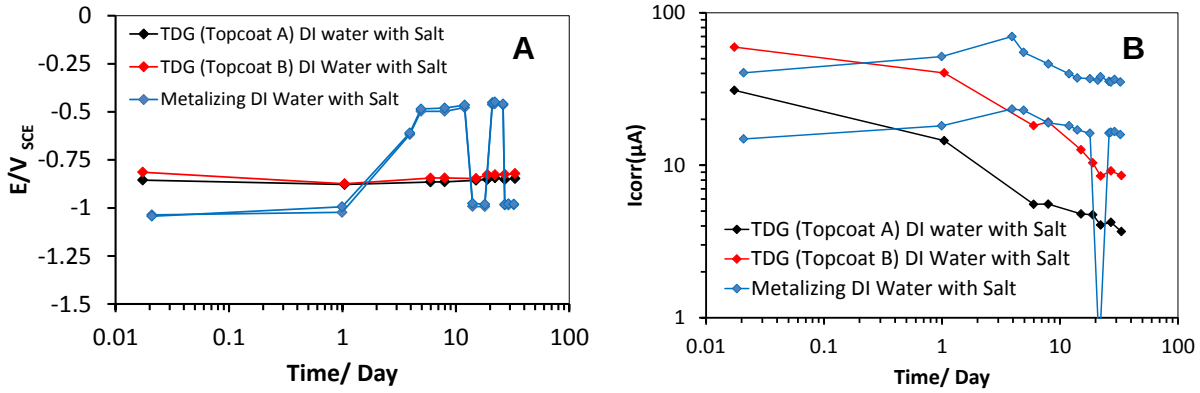


**Figure: 6.9 Corrosion Electrochemical Parameters of Metallized Steel and TDG.**

A) Open circuit potential. B) Corrosion current.

Metallized steel was tested in the research for benchmark comparison with TDG. Generally, coating degradation and corrosion behavior were similar except for the severe surface iron oxidation that was observed on Plain TDG in salt-fog exposure and at some local defect sites on topcoated TDG. Figure 6.8 shows graphs correlating the coating degradation parameters of pull-off strength $\sigma_{po}$ and coating thickness loss $t_d$ for metallized steel and TDG. It can be seen that general coating degradation trends for metallized steel and Plain TDG were similar. For both materials, zinc consumption resulting in net thickness loss can occur during early exposure in ambient outdoor exposures. Also in aggressive environments, surface oxides can form and (for testing purposes) can reduce pull-off strengths. As shown in Figure 6.9, similar behavior of metallized steel and TDG with Topcoat A and Topcoat B was observed in electrochemical testing. Potentials remained negative indicating zinc activity. High

corrosion currents were maintained throughout the testing, but a trend to lower values was observed for the TDG samples.

## 6.2 CONCLUSIONS AND RECOMMENDATIONS

**CBPC:**

High pH Environments:

- CBPC coating can severely deteriorate when immersed in high pH SPS solution (pH 13.3).
- Corrosion mitigation of steel in presence of salt in high pH solution was observed and was thought to be related to presence of intermediate CBPC layer.
- Appropriate consideration of CBPC application in reinforced concrete is needed due to severe coating degradation in high pH solutions representative of concrete pore water during early cement hydration and early concrete service. Further research is needed to determine degradation mechanism of the ceramic.
- Further research on the galvanic interactions of the intermediate CBPC layer is needed to elucidate its role in the observed corrosion mitigation.
- Research is needed to validate mechanical performance of CBPC in reinforced concrete applications (i.e. development length, coating flexibility, etc.).

Atmospheric Conditions:

- Poor coating adhesive and cohesive strengths were observed in as-received and exposed conditions.
- CBPC coating degraded due to wet/dry exposures.
- Degradation of the CBPC coating resulted in poor barrier protection.
- Undetected undercoating surface corrosion occurred regardless of extent of visual coating material loss.
- Extended undercoating surface corrosion occurred in immersed conditions (pH 7) regardless of chloride content. However, corrosion was localized to scribed regions when present.
- Short term outdoor testing (up to 8 months) showed no severe corrosion of steel substrate.
- The formation of intermediate layer was inconsistent along the length of steel interface.
- Although conventional 3-coat systems showed less propensity for coating degradation, the severity of the corrosion of the steel substrate at defect sites was greater than that with CBPC.
- Bridge locations with high moisture presence should be avoided to reduce CBPC coating degradation.

- The influence of galvanic coupling of intermediate layer and steel substrate (and in presence of exposed steel) should be further studied to identify possible corrosion mitigation.
- Compatibility of CBPC surface repair and recoating should be addressed.

**TDG:**

High pH Environments

- TDG showed passive-like behavior in neutral pH solutions but showed active corrosion in high pH solutions.
- No steel corrosion was observed in high pH solution in presence of 3.5% NaCl and exposure to steel substrate.
- Only TDG with topcoats were evaluated in high pH solution. However, those topcoats showed visible deterioration. Verification of performance without topcoat should be made.

Atmospheric Conditions

- Robust topcoats are needed due to the visual oxidation of iron present in the TDG coating.
- No severe steel corrosion was observed in the short-term outdoor exposure and good corrosion behavior was observed in salt-fog testing up to 5800 hours for TDG with topcoats.
- No preferential localized corrosion occurred at exposed steel locations in the immersion testing, outdoor exposures and salt-fog testing.
- Significant loss of topcoat and zinc layers can occur in aggressive exposure conditions.
- Comparable corrosion performance between TDG and metallized steel was observed in the time and conditions of the testing.
- Appropriate repair procedures for TDG after zinc consumption should be developed.

**REFERENCES**

AASHTO R-31. “Standard Practice for Evaluation of Coating Systems for Structural Steel,” *AASHTO Book of Standards*.

ArmorGalv, 2013. Environmental Friendly Thermal Diffusion Zinc. Retrieved May 27, 2013. http://www.armorgalv.com/armorgalv/ArmorGalv_HOME.html

ASTM A 1059-08. (2008). “Standard Specification for Zinc Alloy Thermo-Diffusion Coatings (TDC) on Steel Fasteners, Hardware, and Other Products1,” *ASTM Book of Standards*.

ASTM B 117-03. “Standard Practice for Operating Salt Spray (Fog) Apparatus,” *ASTM Book of Standards*.

ASTM D522 / D522M-13. “Standard Test Methods for Mandrel Bend Test of Attached Organic Coatings,” *ASTM Book of Standards.*

ASTM D523-08. “Standard Test Method for Specular Gloss,” *ASTM Book of Standards.*

ASTM D610-08(2012). “Standard Practice for Evaluating Degree of Rusting on Painted Steel Surfaces,” *ASTM Book of Standards.*

ASTM D714-02(2009). “Standard Test Method for Evaluating Degree of Blistering of Paints,” *ASTM Book of Standards.*

ASTM D1654-08. “Standard Test Method for Evaluation of Painted or Coated Specimens Subjected to Corrosive Environments,” *ASTM Book of Standards.*

ASTM D2244-11. “, Standard Practice for Calculation of Color Tolerances and Color Differences from Instrumentally Measured Color Coordinates,” *ASTM Book of Standards.*

ASTM D2794-93(2010). “,Standard Test Method for Resistance of Organic Coatings to the Effects of Rapid Deformation (Impact),” *ASTM Book of Standards.*

ASTM D3359-09. “Standard Test Methods for Measuring Adhesion by Tape Test,” *ASTM Book of Standards.*

ASTM D4541-09. “Standard Test Method for Pull-Off Strength of Coatings Using Portable Adhesion Testers,” ASTM Book of Standards.

ASTM G7 / G7M-11. “Standard Practice for Atmospheric Environmental Exposure Testing of Nonmetallic Materials,” *ASTM Book of Standards.*

Barsoukov, E. and Macdonald, J. R., *Impedance Spectroscopy: Theory, Experiment, and Applications*, 2nd ed. (Hoboken, NJ: Wiley Interscience, 2005).

Bernecki, T., Clement, K., Cox, E. Kogler, R., Lovelance, C., Peart, J., and Verma, I. “Bridge Maintenance Coatings.” FHWA Study Tour for Bridge Maintenance Coatings. January 1997.

Bogi, J. and Macmillan, R. “Phosphate Conversion Coatings on Steel,” Journal of Materials Science 12, (1977): pp.2235-2240.

Brigham, S.j. and Watkinson, C. “Understanding and Use of Glass Flake”. Trade publication. Paint & Coating Industry. March , 2009. V. 25. I. 3. Pp.22

Byram, K. “Florida Department of Transportation Specification Modification Justification and Details for Structural Coating Application and Coating Materials Acceptance,” Tri-Service Corrosion Conference, (2005).

Calla, E. and Modi S. C. “Long Life Corrosion Protection of Steel by Zinc-Aluminium Coating Formed by Thermal Spray Process”. Corrosion its Mitigation and Preventive Maintenance, CORCON – 2000. Mumbai, India.

Cantrell, K.J. and Westsik, J. H. “Secondary Waste Form Down Selection Data Package – Ceramicrete.” DE-AC05-76RL01830. Pacific Northwest National Laboratory, August 2011.

Castro, P., Sagues, A.A., Moreno, E.I., Maldonado, L., Genesca, J. “Characterization of Activated Titanium Solid Reference Electrodes for Corrosion Testing of Steel in Concrete,” Corrosion Science 52, 8 (1992): pp. 609-617.

Chang, L.M. and Chung, S. “Steel Bridge Protection Policy: Evaluation of Bridge Coating System for INDOT Steel Bridges.” FHWA/IN/JTRP-98/21. Indiana DOT and Purdue University. West Lafayette, IN. May 1999.

Chang, L.M. and Georgy, M. “Metallization of Steel Bridges: Research and Practice.” Final Report to Indiana DOT. FHWA/IN/JTRP-98/21. Indiana DOT and Purdue University. West Lafayette, IN. May 1999.

Chang, L. M., Zayed, T., and Fricker, J.D. “Steel Bridge Protection Policy: Evaluation of Bridge Coating System for INDOT Steel Bridges.” FHWA/IN/JTRP-98/21. Indiana DOT and Purdue University. West Lafayette, IN. May 1999.

Chong, S.L. and Yao, Y. “Are Two Coats As Effective As Three?” FHWA-HRT-2006-006. September/October 2006.

Dallin, G.W. Galvoinfo center. “ Continuous hot dip galvanizing – process and products”. August, 2012. Available Online: www.galvinfo.com

El-Mahdy, G. A., Nishikata, A., Tsuru, T. “AC Impedance Study on Corrosion of 55% Al-Zn Alloy-Coated Steel Under Thin Electrolyte Layers,” Corrosion Science 42, 9 (2000): pp. 1509-1521.

FDOT 2013a, Standard Specification for Road and Bridge Construction-2013.Section 975. “Structural Coating Materials”.

FDOT 2013b. Report. “Evaluation of ArmorGalv® under Salt Fog Exposure and Partial Immersion in Saltwater.” Florida Department of Transportation. May 2013. Available Online: http://www.armorgalv.com/armorgalv/Downloads_files/Florida%20DOT%20Armorgalv%20evaluation%20Final.pdf

Fontana, M., Greene, N., *Corrosion Engineering*, 3rd ed. (New York, NY: McGraw Hill, 1986).

Grundmeier, G., Schmidt , W., Stratmann, M. “Corrosion Protection by Organic Coatings: Electrochemical Mechanism and Novel Methods of Investigation,” Electrochimica Acta 45, 15-16 (2000): pp. 2515-2533.

Jalili, M.M., Moradian, S. and Hosseinpour, D. “The use of inorganic conversion coatings to enhance the corrosion resistance of reinforcement and the bond strength at the rebar/concrete.” Construction and Building Materials. V.23. Pp.233-8. 2009.

Jegannathan, S. Narayanan, S. Ravichandran, K., and Rajeswari, S. “Evaluation of the corrosion resistance of phosphate coatings obtained by anodic electrochemical treatment.” Progress in Organic Coatings. V. 57. Pp.392-99. 2006.

Kalendova, A. “Effects of particle sizes and shapes of zinc metal on the properties of anticorrosive coatings, Progress in Organic Coatings, V. 46, I. 4, June 2003. Pp. 324–332”

Kline, E. “Durable Bridge Coatings.” Modern Steel Construction. November 2009.
Kodumuri, P. and Lee, S. K. “Federal Highway Administration 100-Year Coating Study.” FHWA-HRT-12-044. November 2012.

Koger, R.A., Brydl, D., and Highsmith, C. “Recent FHWA Experience in Testing and Implementing Metallized Coatings for Steel Bridges.” Corrosion/98. Paper 499 NACE Int. Houston, TX. 1998.

Lau, K., Sagues, A. A. “Corrosion of Epoxy - and Polymer/Zinc-Coated Rebar in Simulated Concrete Pore Solution,” Corrosion Science 65, 10 (2009): pp. 681-694.

Mahdavian, M., Attar, M.M. “Another Approach in Analysis of Paint Coatings with EIS Measurement: Phase Angle at High Frequencies,” Corrosion Science 48, 12 (2006): pp. 4152-4157.

Marchebois, H., Joiret, S., Savall, C., Bernard, J.and Touzain, S. “Characterization of zinc-rich powder coatings by EIS and Raman spectroscopy, Surface and Coatings Technology, V.157. I. 2–3. 22 August 2002, Pp. 151–161

Materials Performance. “Corrosion Costs and Preventive Strategies in the United States.” July 2002. NACE International, Houston, TX.

Materials Performance. “Inorganic Ceramic Coating Shows Resistance to Corrosion.” Vol. 50, No. 10. October 2011. NACE International, Houston, TX.

Molnár & Liszi, J.“Protective properties of zinc-rich paints”. Joint International Meeting - the 200th Meeting of the Electrochemical Society, Inc. and the 52nd Annual Meeting of the International Society of Electrochemistry - San Francisco, California. September 2-7, 2001

Murray, J. N. “Electrochemical Test Methods for Evaluating Organic Coatings on Metals: An Update. Part III: Multiple Test Parameter Measurements,” Progress in Organic Coating 31, 4 (1997): pp. 375-391.

Myers, J.J., Zheng, W., and Washer, G. “Structural Steel Coatings for Corrosion Mitigation.” Report for Missouri Department of Transportation. TRyy0911. Missouri Department of Transportation. Jefferson City, MO. October 2010.

Narayanan, T.S.N. S., Jegannathan, S. and Ravichandran, K. “Corrosion Resistance of Phosphate Coatings Obtained by Cathodic Electrochemical treatment: Role of Anode–graphite Versus Steel,” Progress in Organic Coatings 55, (2006): pp. 355-362

Orazem, M., Tribollet, B., *Electrochemical Impedance spectroscopy*, (Hoboken, NJ: Wiley Interscience, 2008).

Pouliotte, J. Presentation.“ FDOT New Directions in Steel Corrosion Protection”. Retrieved May 27, 2013.http://www.pavementvideo.org/2012_SEBPP/PDF/10%20-%20FDOT%20New%20Directions%20in%20FDOT%20Steel%20Corrosion%20Protection%20-%20Jeff%20Pouliotte.pdf

Rust-anode, 2013. Cold Galvanizing Coating. Retrieved May 27, 2013. http://www.rustanode.com

Sommer, A.J. and Leidheiser, H. “Effect of alkali metal hydroxides on the dissolution behavior of a zinc phosphate conversion coating on steel and pertinence to cathodic delamination.”Corrosion. V.37. p.28. 1987.

Vetter, K., *Electrochemical Kinetics: Theoretical and Experimental Aspects*, (New York, NY: Academic Press, 1967).

Wagh, A.S. and Jeong, S.Y. “Chemically Bonded Phosphate Cermamics:I, A Dissolution Model of Formation.” J. Am. Ceram. Soc. V. 86. Pp.1838-44. 2003.

Wagh, A., Strain, R., Jeong, S., Reed, D., Krouse T., and Singh, D. “Stabilization of Rocky Flats Pu-Contaminated Ash within Chemically Bonded Phosphate Ceramics,” J. Nucl. Mater., 265, (1999): pp. 295-307.

Wagh, A.S. Advances in Ceramic Matrix Composites X: Proceedings of the 106th Annual Meeting of the American Ceramic Society, V. 165. 2005.

Yao, Y., Kodumuri, P., and Lee, S.K. “Performance Evaluation of One-Coat Systems for New Steel Bridges.” Report to FHWA. FHWA-HRT-11-046. SES Group and Associates, Chesapeake City, MD. June 2011.

Zhmurkin, D. Technical Paper. Tyco Electronics. “ Corrosion Resistance of Bolt Coatings”. July 23, 2009.

## APPENDIX A: SUMMARY

Table A.1. Summary of the All Tested Samples

| Exposure | Duration | Property | CBPC | | Three-Coat | | Plain TDG | TDG with Topcoat A | TDG with Topcoat B | TDG with Topcoat A+B | | Metalizing | |
|---|---|---|---|---|---|---|---|---|---|---|---|---|---|
| | | | US[1] | S[2] | US | S | S | S | S | US | S | US | S |
| Outdoor | 4-Month | Coating Degradation | N | N | N | N | N | N | N | N | N | N | N |
| | | Thickness (mils) | 2.0-8.0 | | 0.5-6.0 | | 0.2-2.0 | -1.5 -1.5 | -1.5 -0.5 | 0.1-7.0 | | 0.5-10.0 | |
| | | Pull-off Strength (psi) | <200 (B[4],C[5]) | | <1600 (C) | | >1000 (B) | <2000 (B) | <2000 (A[3],B) | <2000 (A,B) | | <1000 (C) | |
| | | Steel Corrosion | Y | Y | N | N | N | N | N | N | N | N | N |
| | | Zinc Corrosion | na | na | N | N | N | N | N | N | N | Y | Y |
| | | Surface Rust | N | N | N | N | N | N | N | N | N | Y | Y |
| | 8-Month | Coating Degradation | Y | Y | N | N | Y | Y | Y | N | N | Y | Y |
| | | Thickness (mils) | 0-6 | | -0.5 -6.0 | | 0-4.0 | 0-1.5 | 1.0-2.0 | -0.2-6.0 | | 0-7.5 | |
| | | Pull-off Strength (psi) | <500 (C) | | <2200 (A,B) | | <2000 (B) | <1000 (A) | <1000 (B) | <2500 (A) | | <1500 (C) | |
| | | Steel Corrosion | Y | Y | N | N | N | N | N | N | N | N | N |
| | | Zinc Corrosion | na | na | N | N | Y | N | N | Y | Y | Y | Y |
| | | Surface Rust | N | N | N | N | Y | N | N | Y | Y | Y | Y |
| Salt-Fog | 2200-Hrs | Coating Degradation | Y | Y | N | N | Y | na | na | Y | Y | N | N |
| | | Thickness (mils) | -2.0-2.0 | | -3.0-6.5 | | -4.0 -1.5 | na | na | -0.2-2.0 | | -2.0-3.0 | |

Continuation of Table A.1. Summary of the All Tested Samples

| Exposure | Duration | Property | CBPC | | Three-Coat | | Plain TDG | TDG with Topcoat A | TDG with Topcoat B | TDG with Topcoat A+B | | Metalizing | |
|---|---|---|---|---|---|---|---|---|---|---|---|---|---|
| | | | US[1] | S[2] | US | S | S | S | S | US | S | US | S |
| | 2200-Hrs | Pull-off Strength (psi) | <350 (B,C) | | <700 (A) | | <1000 (B) | na | na | <1000 (A) | | <500 (B) | |
| | | Steel Corrosion | Y | Y | N | N | Y | na | na | N | N | N | N |
| | | Zinc Corrosion | na | na | N | N | Y | na | na | Y | Y | Y | Y |
| | | Surface Rust | Y | Y | N | N | Y | na | na | N | N | N | N |
| | 5800-Hrs | Coating Degradation | Y | Y | Y | Y | Y | na | na | Y | Y | Y | Y |
| | | Thickness change (mils) | -2.0 - 0.10 | | 0-7.0 | | -5.0 - 0.5 | na | na | -1.0 - (-0.1) | | -4.0 - 1.0 | |
| | | Pull-off Strength (psi) | <150 (B) | | <1000 (A) | | <100 (B) | na | na | <1000 (B) | | <500 (B) | |
| | | Steel Corrosion | Y | Y | N | Y | Y | na | na | N | N | N | N |
| | | Zinc Corrosion | na | na | N | N | Y | na | na | Y | Y | Y | Y |
| | | Surface Rust | Y | Y | N | N | Y | na | na | Y | Y | Y | Y |
| Immersion | pH 7 w/o Cl(~30 Days) | Coating Degradation | Y | Y | na | na | na | Y | Y | na | na | na | na |
| | | Steel Corrosion | Y | N | na | na | na | N | N | na | na | na | na |
| | | Ecorr (mV) | -530 to -290 | -500 to -2[illegible] | na | na | na | -615 to -460 | -615 to -460 | na | na | na | na |
| | | Icorr (µA) | 20 to 5 | 10 to 6 | na | na | na | 1.28 to 1.33 | 2.4 to 2.3 | na | na | na | na |

Continuation of Table A.1. Summary of the All Tested Samples

| Exposure | Duration | Property | CBPC | | Three-Coat | | Plain TDG | TDG with Topcoat A | TDG with Topcoat B | TDG with Topcoat A+B | | Metalizing | |
|---|---|---|---|---|---|---|---|---|---|---|---|---|---|
| | | | US[1] | S[2] | US | S | S | S | S | US | S | US | S |
| Immersion | pH 7 with Cl(~30 Days) | Coating Degradation | Y | Y | na | na | na | Y | Y | na | na | na | na |
| | | Steel Corrosion | Y | Y | na | na | na | N | N | na | na | na | na |
| | | Ecorr (mV) | -475 to -700 | -600 to -700 | na | na | na | -875 to -832 | -875 to -832 | na | na | na | na |
| | | Icorr (µA) | 120 to 80 | 90 to 50 | na | na | na | 8.3 to 2.3 | 29.79 to 2.3 | na | na | na | na |
| | pH 13.3 w/o $Cl^-$(~30 Days) | Coating Degradation | Y | Y | na | na | na | Y | Y | na | na | na | na |
| | | Steel Corrosion | na | N | na | na | na | N | N | na | na | na | na |
| | | Ecorr (mV) | -550 to -230 | -500 to -250 | na | na | na | -1113 to -1118 | -818 to 1200 | na | na | na | na |
| | | Icorr (µA) | 25 to 0.5 | 22 to 2 | na | na | na | 14.21 to 130 | 14.21 to 131 | na | na | na | na |
| | pH 13.3 with $Cl^-$ (~30Days) | Coating Degradation | Y | Y | na | na | na | Y | Y | na | na | na | na |
| | | Steel Corrosion | na | Y | na | na | na | N | N | na | na | na | na |

Continuation of Table A.1. Summary of the All Tested Samples

| Exposure | Duration | Property | CBPC | | Three-Coat | | Plain TDG | TDG with Topcoat A | TDG with Topcoat B | TDG with Topcoat A+B | | Metalizing | |
|---|---|---|---|---|---|---|---|---|---|---|---|---|---|
| | | | US[1] | S[2] | US | S | S | S | S | US | S | US | S |
| Immersion | pH 13.3 with $Cl^-$ (~30Days) | Ecorr (mV) | -530 to -450 | -600 to 500 | na | na | na | -876 to -832 | -818 to -1107 | na | na | na | na |
| | | Icorr (µA) | 22 to 8 | 21 to 8 | na | na | na | 56 to 9 | 8 to 106 | na | na | na | na |

1. Un-scribed
2. Scribed
3. Glue failure
4. Partial coating failure
5. Total coating failure

## APPENDIX B: SAMPLE PICTURES

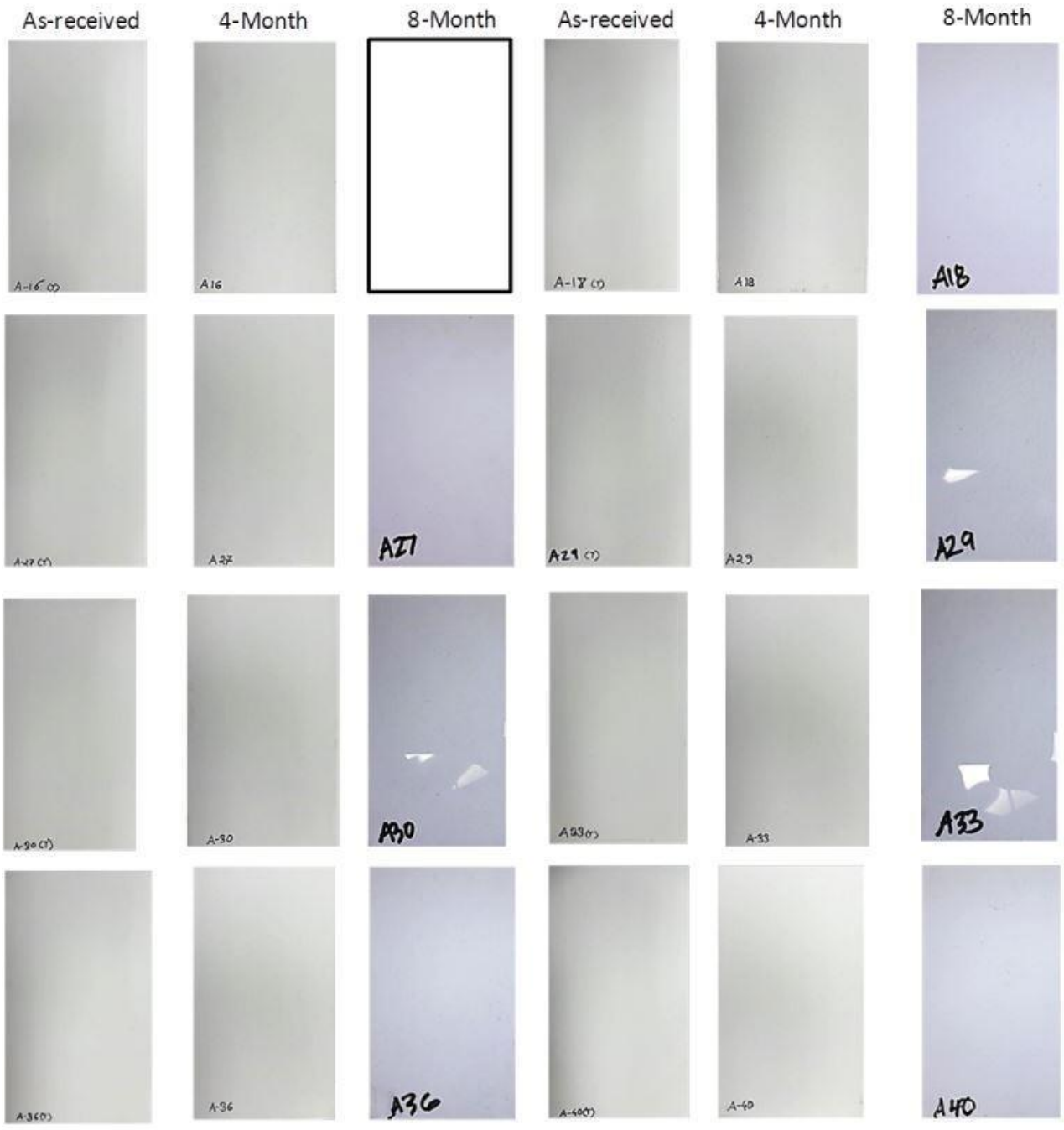


**Figure: B.1 CPBC (Non-scribed) Samples Installed at Inland Test Site**


**Figure: B.2 CPBC (Scribed) Samples Installed at Inland Test Site**

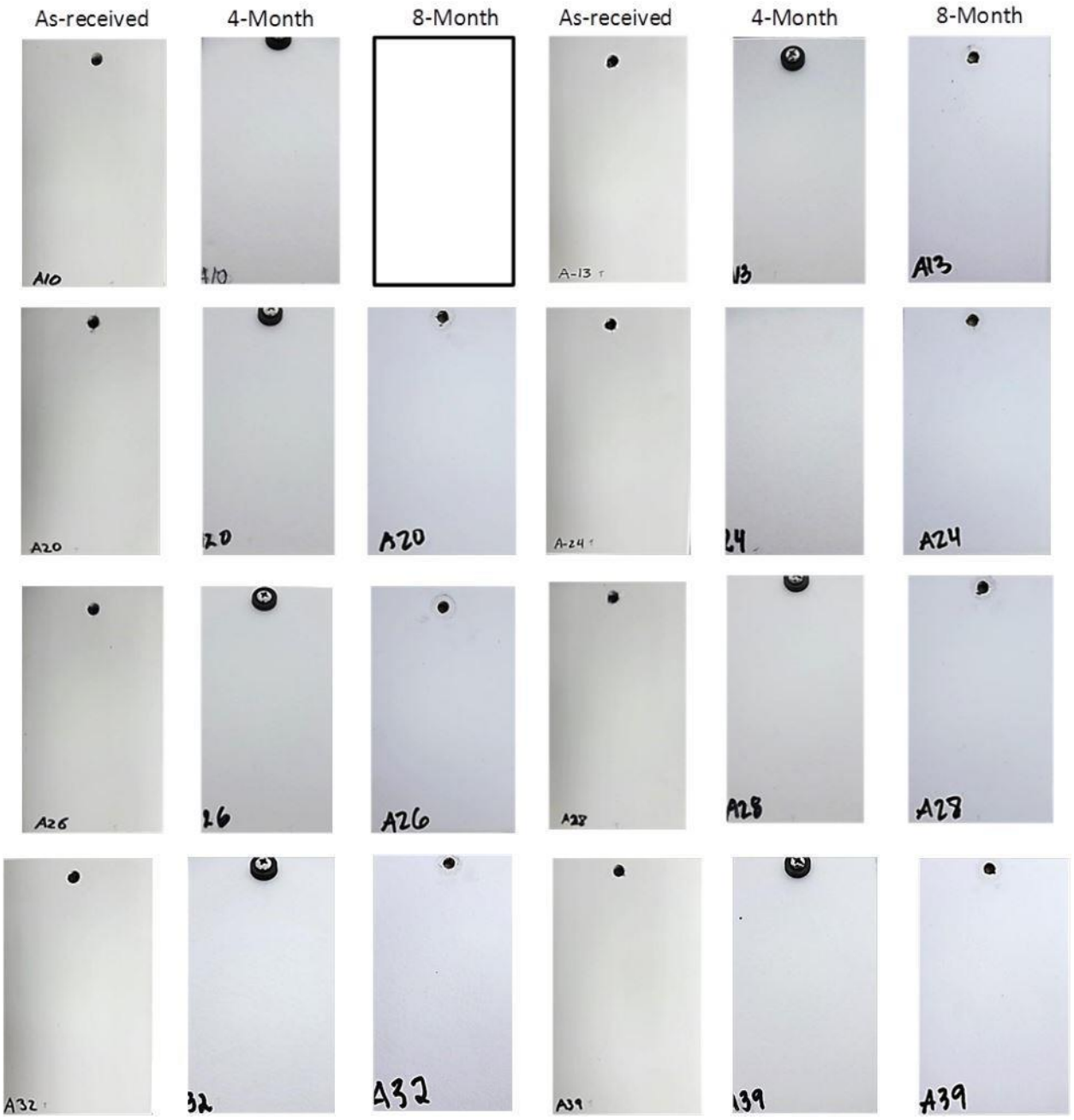


**Figure: B.3 CPBC (Non-scribed) Samples Installed at Beach Test Site**

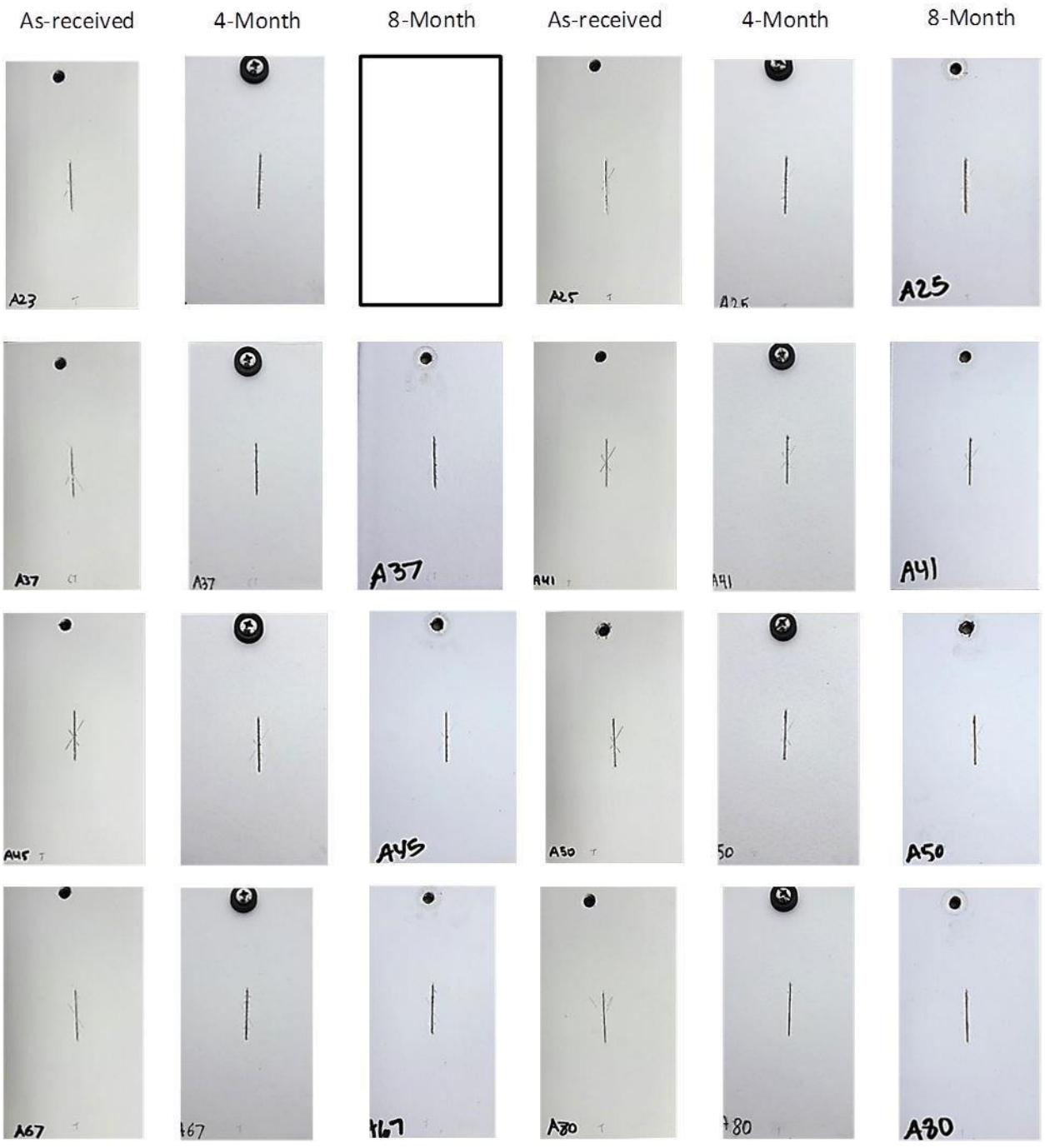


**Figure: B.4 CPBC (Scribed) Samples Installed at Beach Test Site**

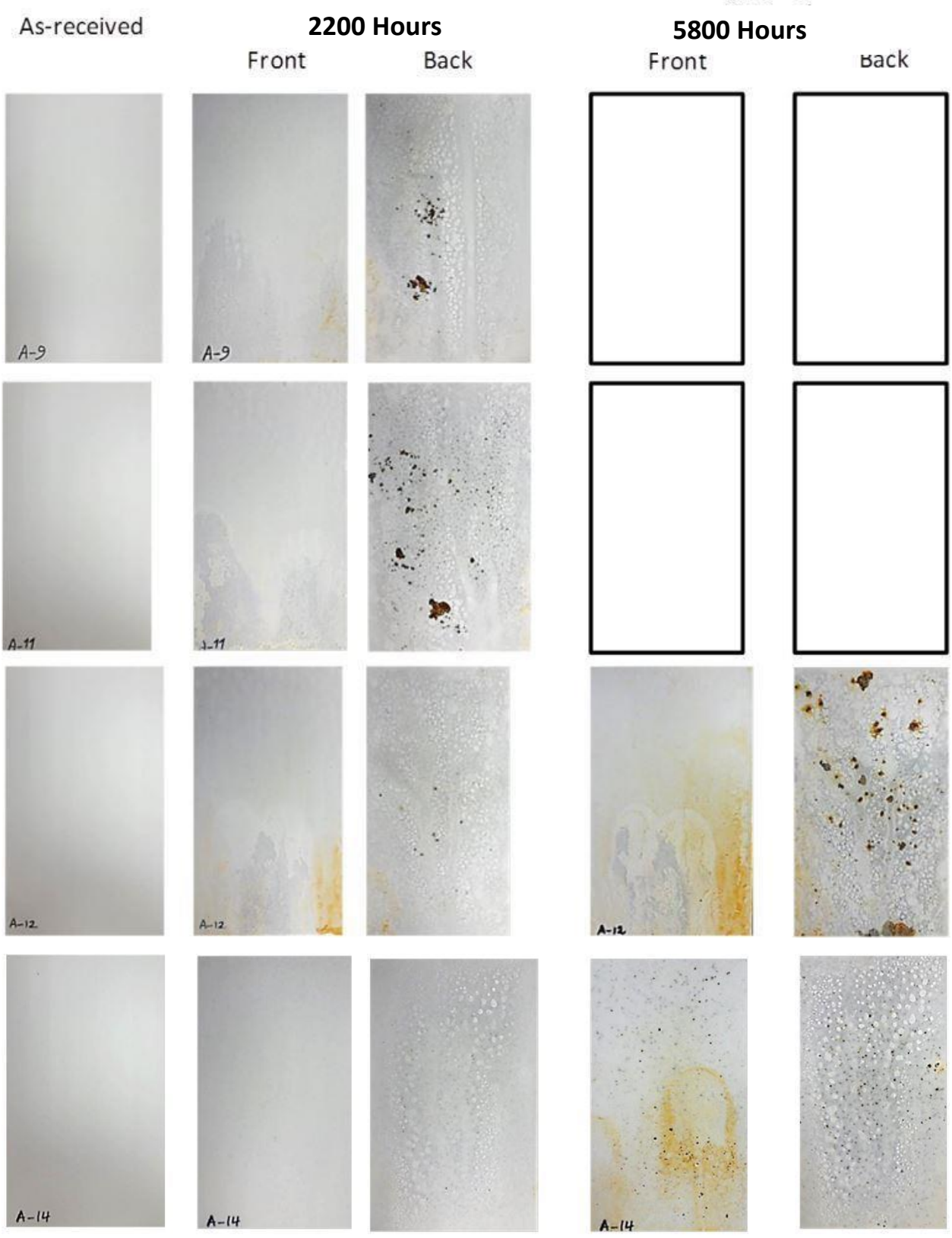


**Figure: B.5 CPBC (Non-scribed) Samples Installed in Salt-Fog Chamber (cont.)**

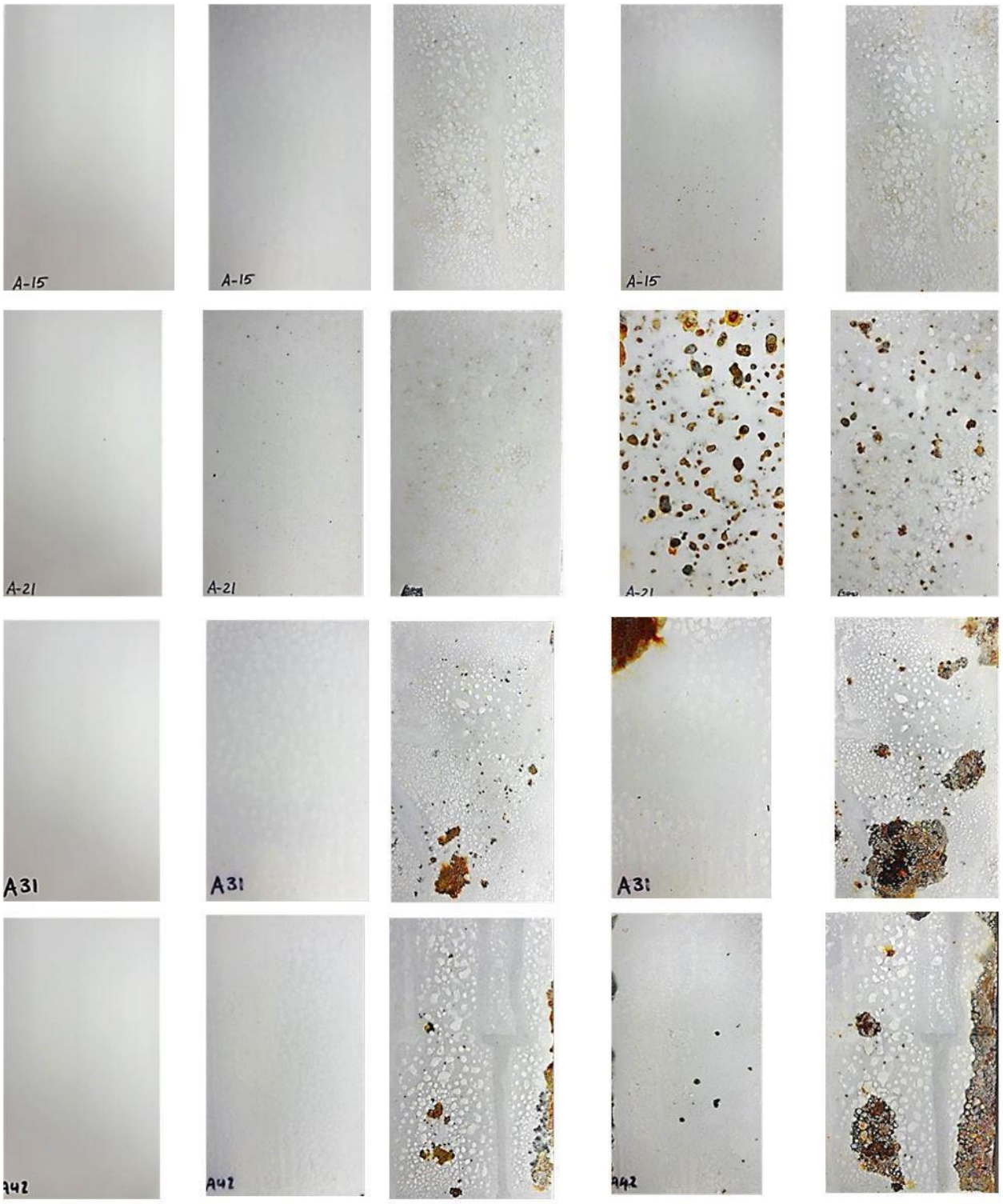


**Continuation of Figure: B.5 CPBC (Non-scribed) Samples Installed in Salt-Fog Chamber (cont.)**

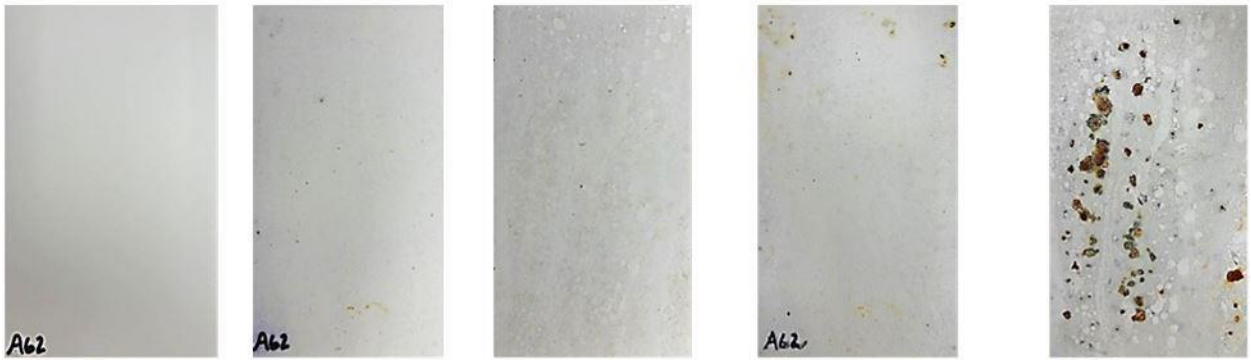


**Continuation of Figure: B.5 CPBC (Non-scribed) Samples Installed in Salt-Fog Chamber**

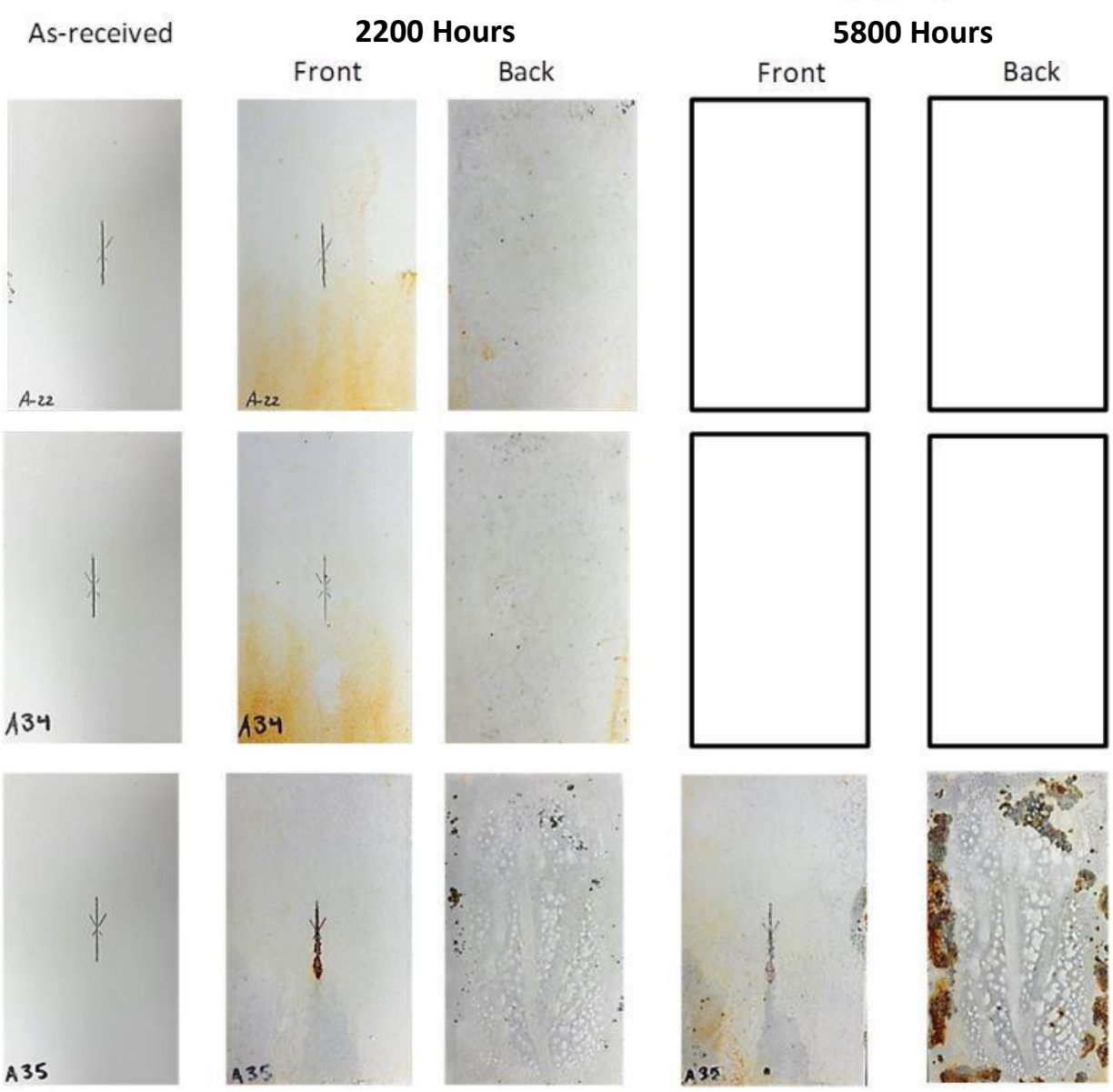


**Figure B.6: CPBC (Scribed) Samples Installed in Salt-Fog Chamber (cont.)**

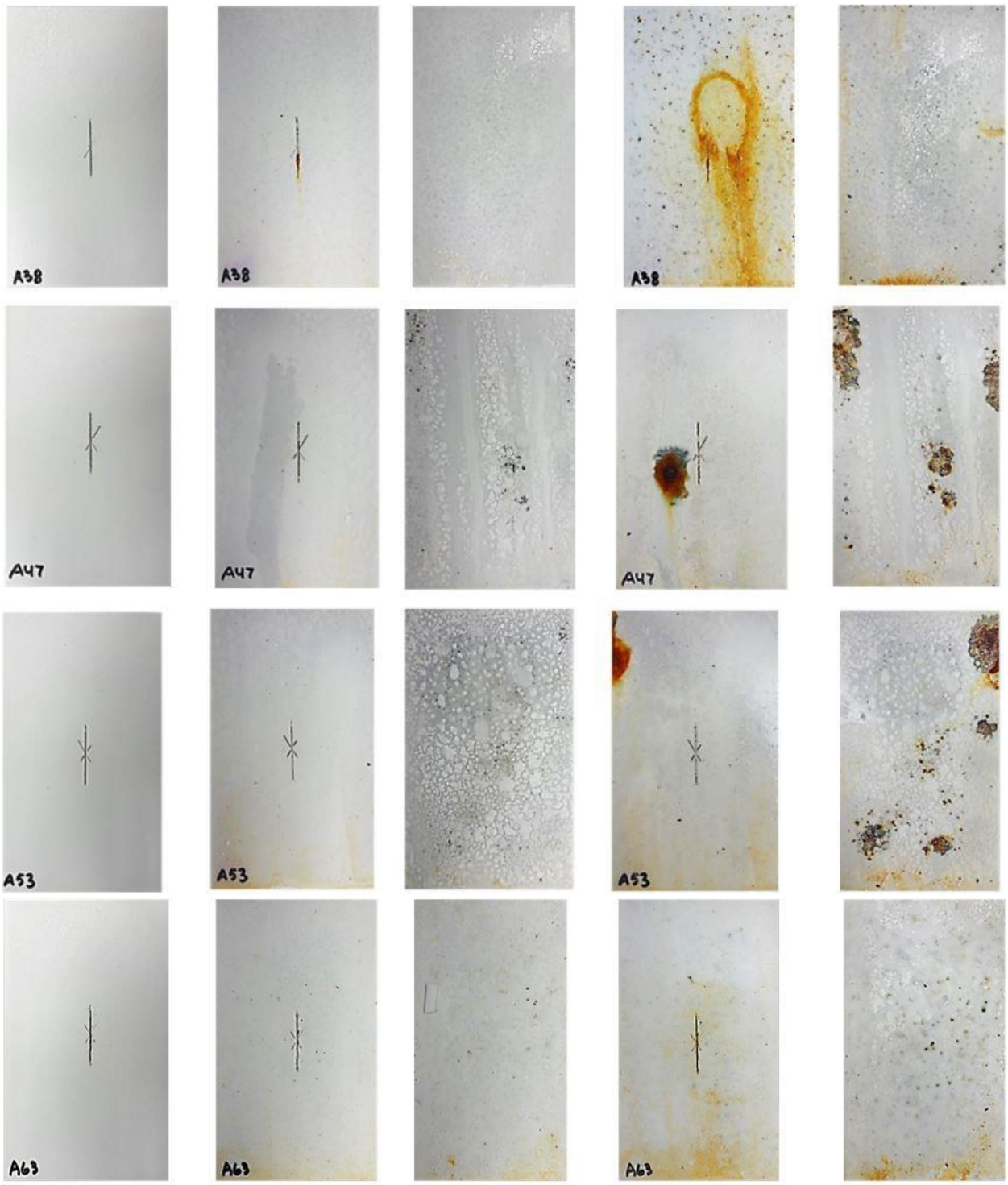


**Continuation of Figure: B.6 CPBC (Scribed) Samples Installed in Salt-Fog Chamber (cont.)**

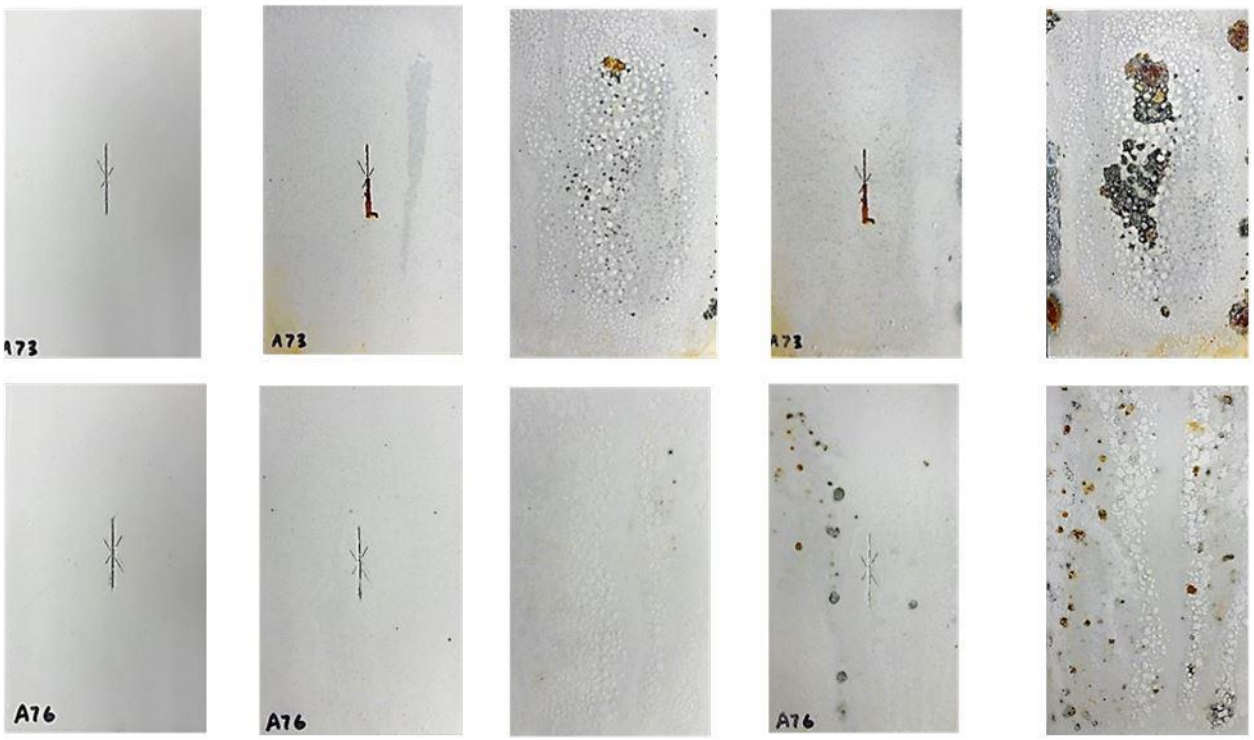


**Continuation of Figure: B.6 CPBC (Scribed) Samples Installed in Salt-Fog Chamber**

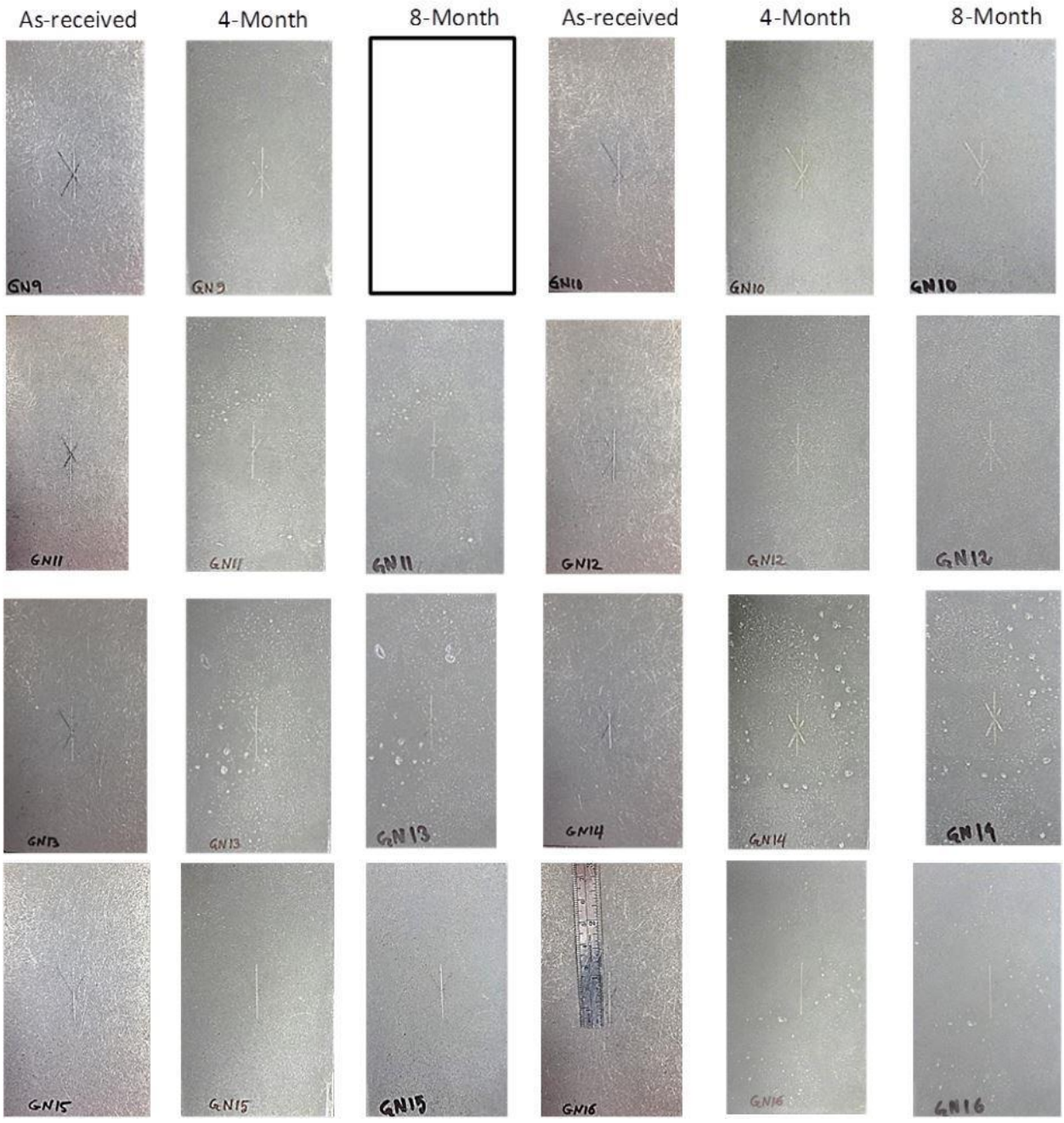


**Figure: B.7 Plain TDG (Scribed) Samples Installed at Inland Test Site**

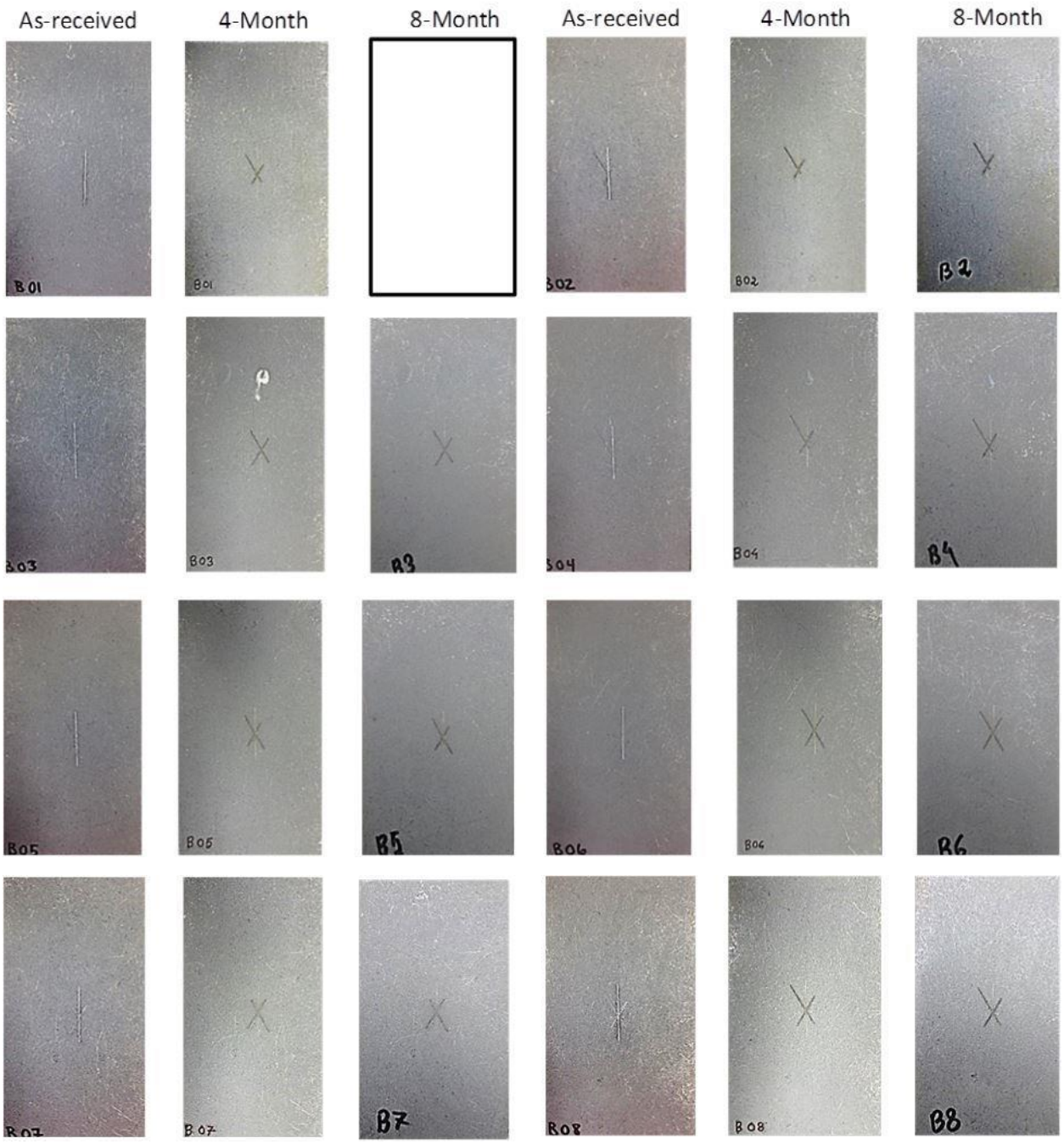


**Figure: B.8 TDG (Topcoat A, Scribed) Samples Installed at Inland Test Site**

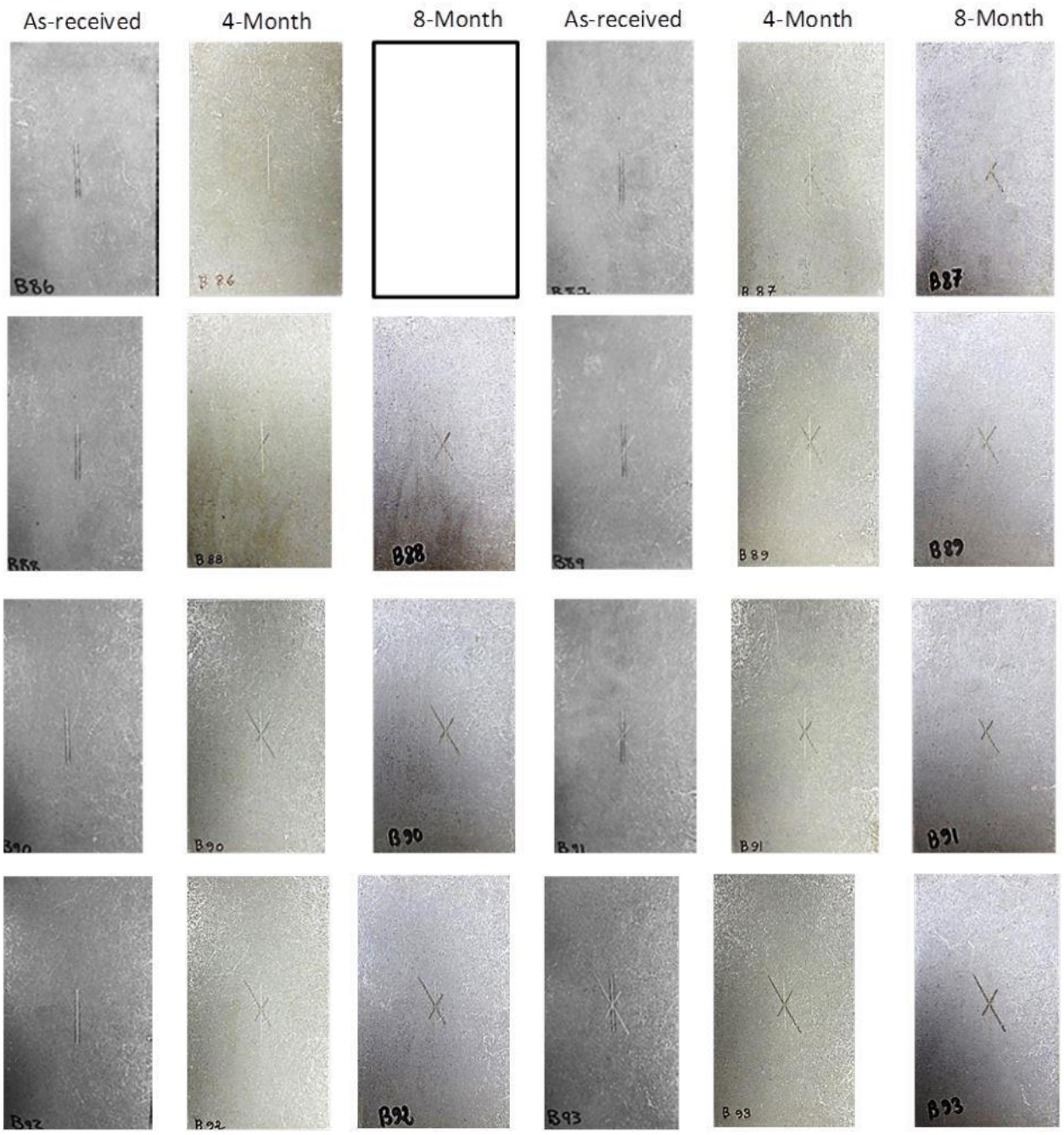


**Figure: B.9 TDG (Topcoat B, Scribed) Samples Installed at Inland Test Site**

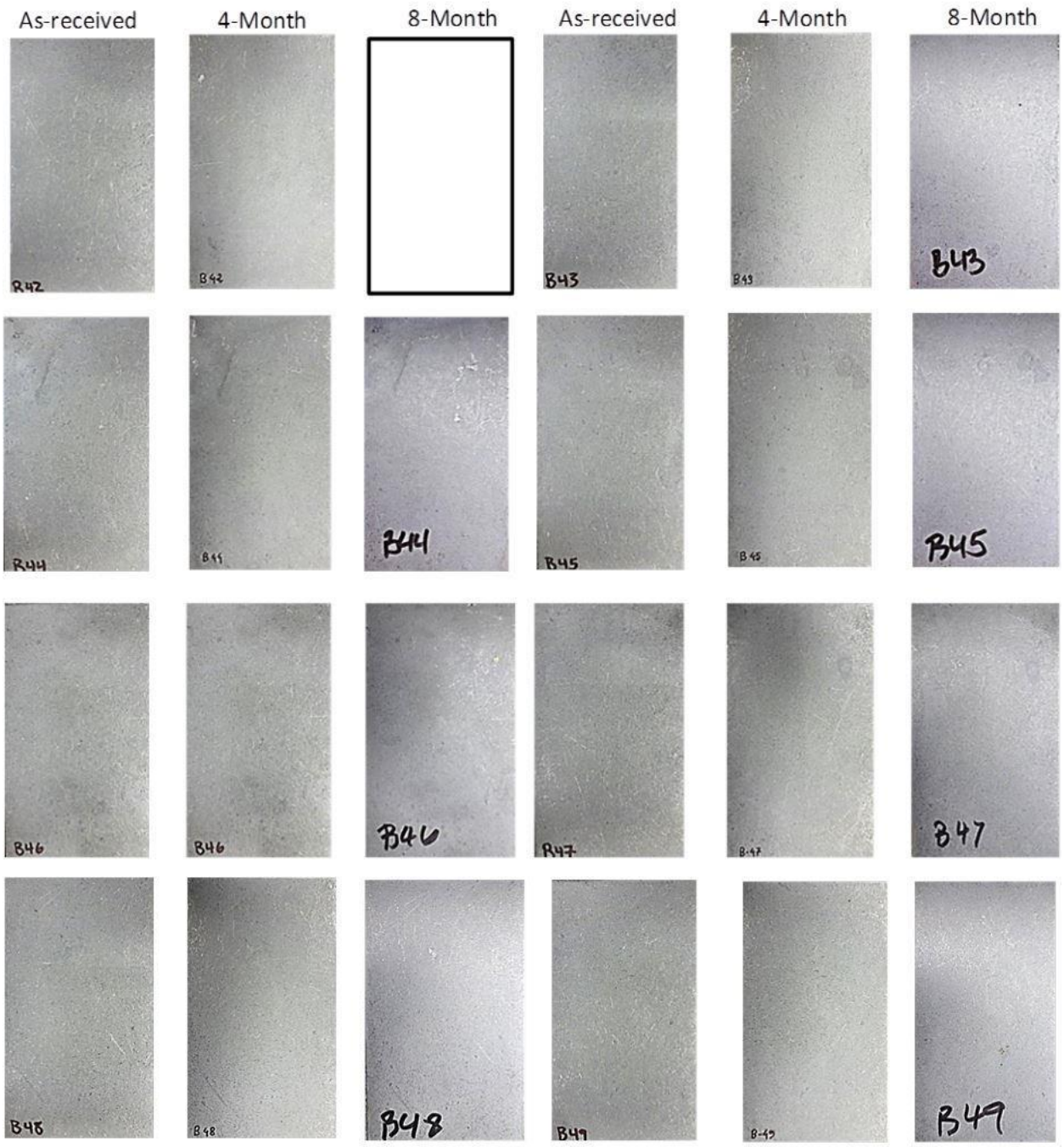


**Figure: B.10 TDG (Topcoat A+ B, Non- scribed) Samples Installed at Inland Test Site**

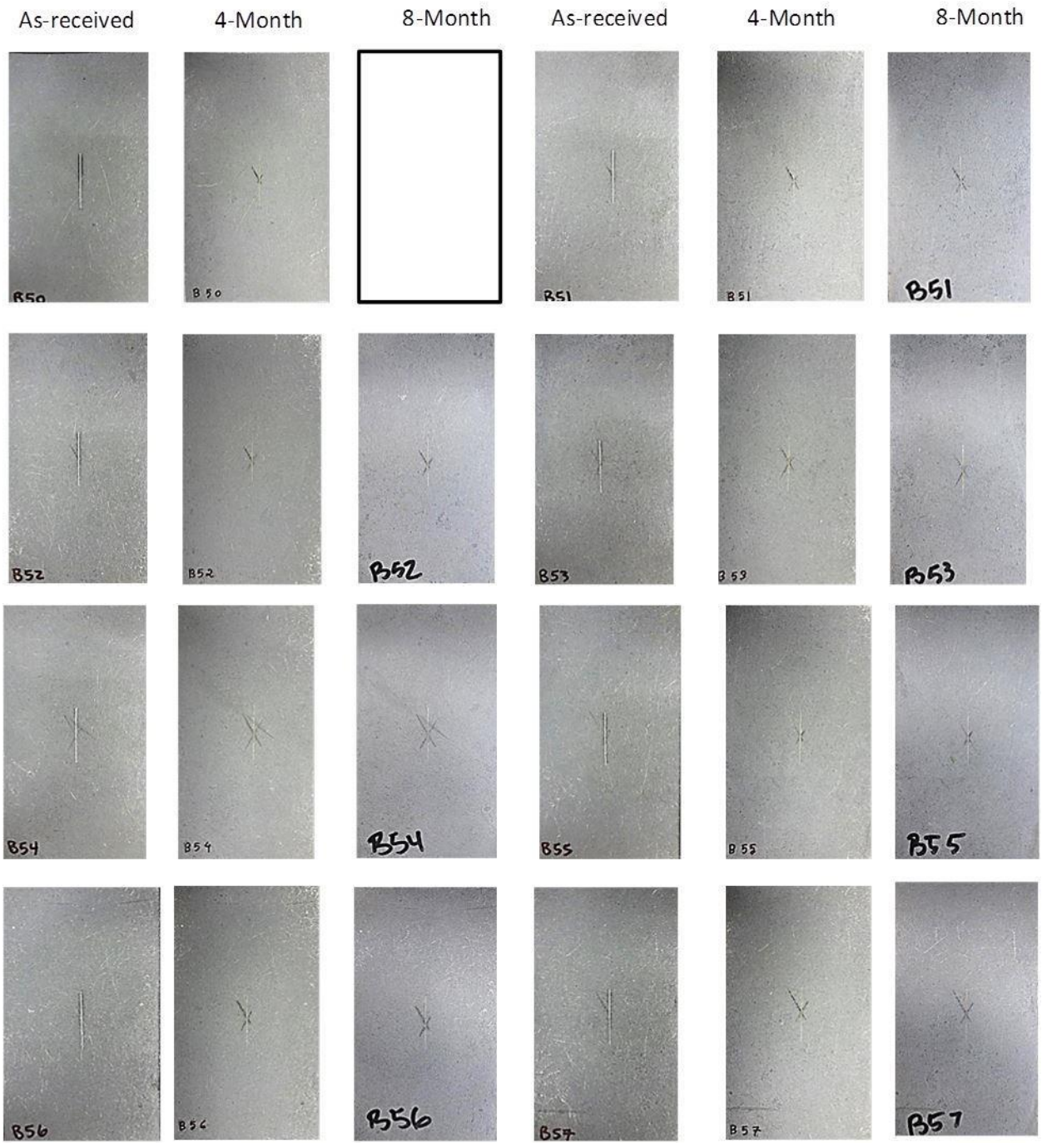


**Figure: B.11 TDG (Topcoat A+ B, Scribed) Samples Installed at Inland Test Site**

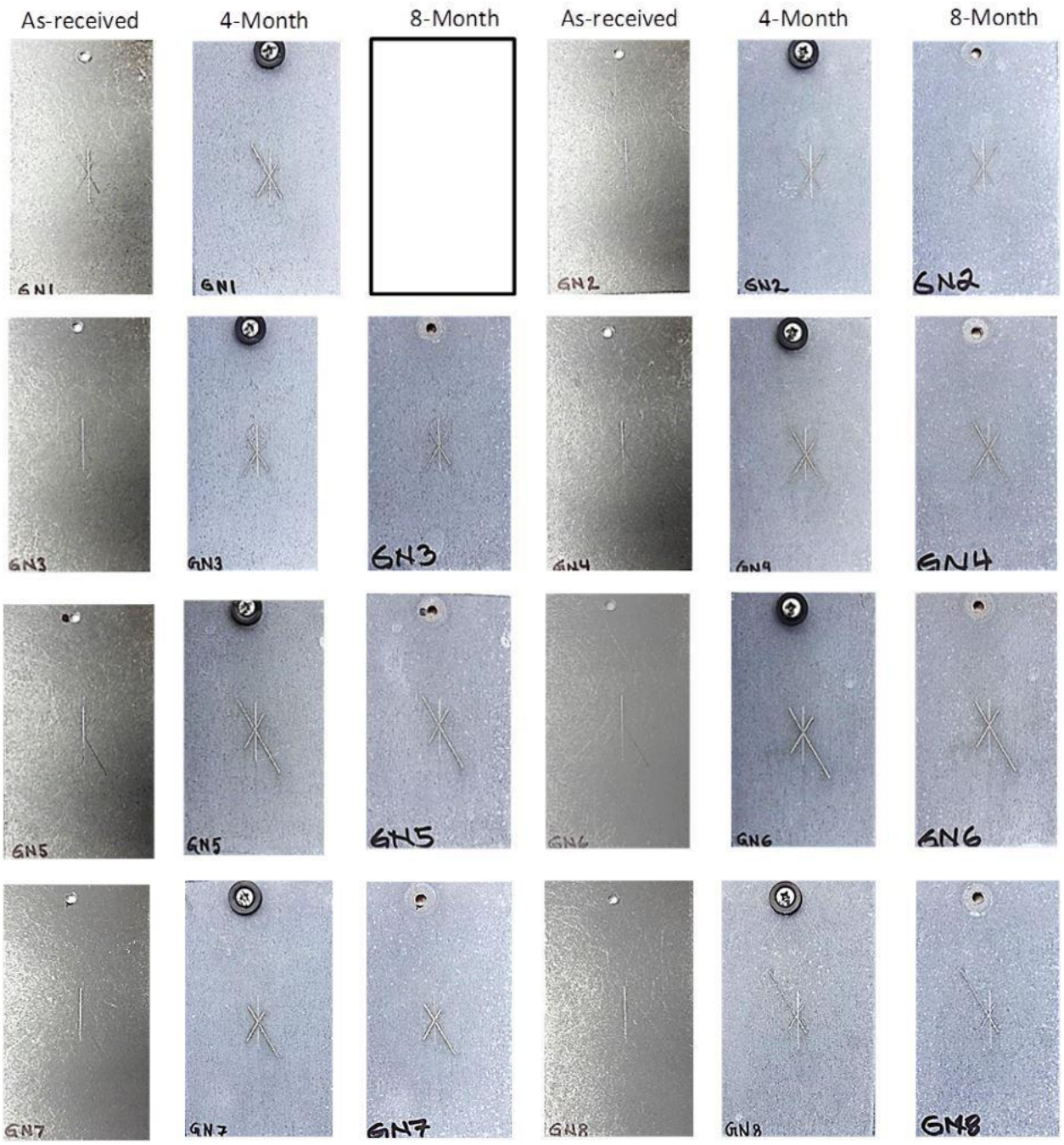


**Figure: B.12 Plain TDG (Scribed) Samples Installed at Beach Test Site**

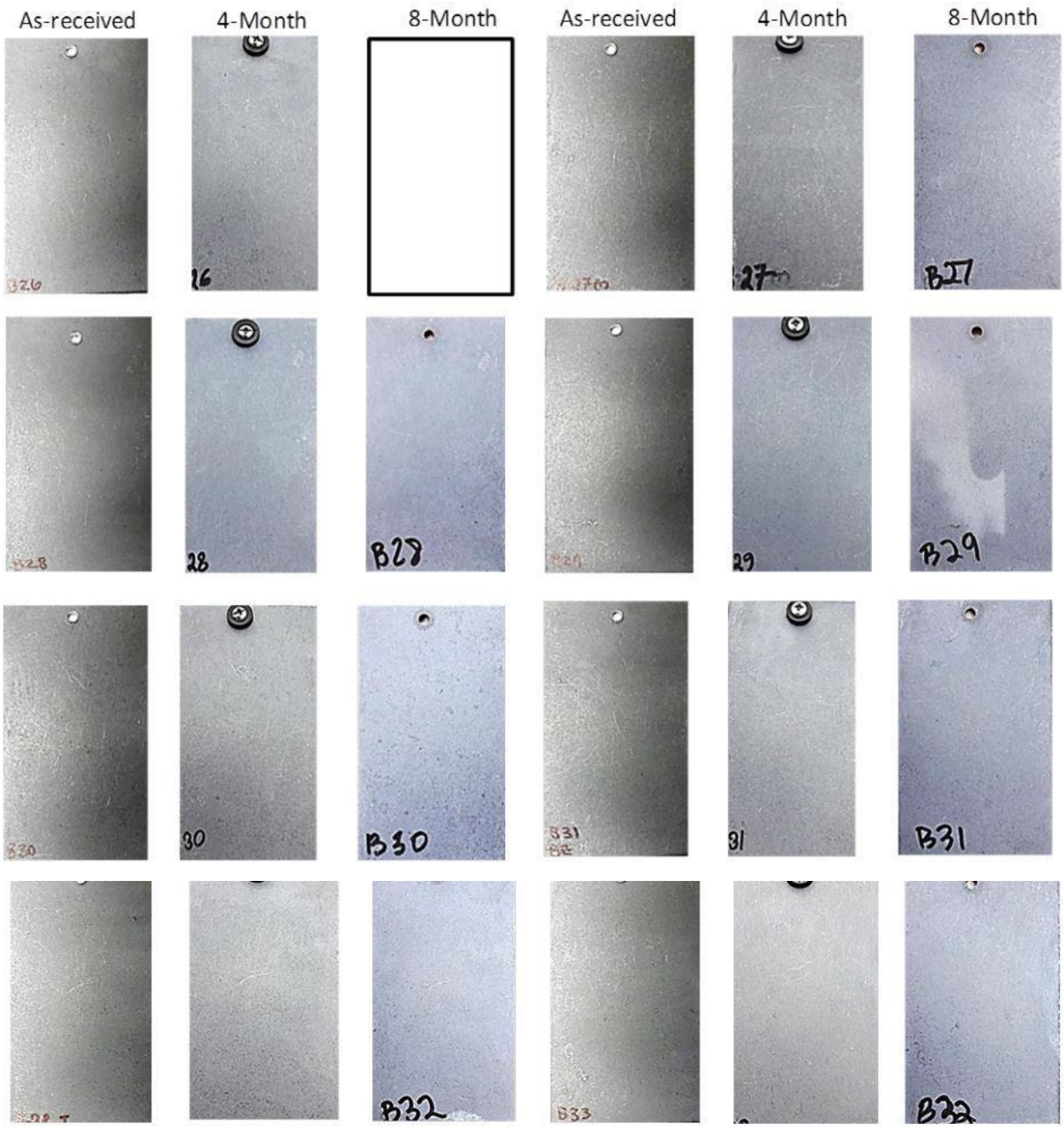


**Figure: B.13 TDG (Topcoat A+ B, Non- scribed) Samples Installed at Beach Test Site**

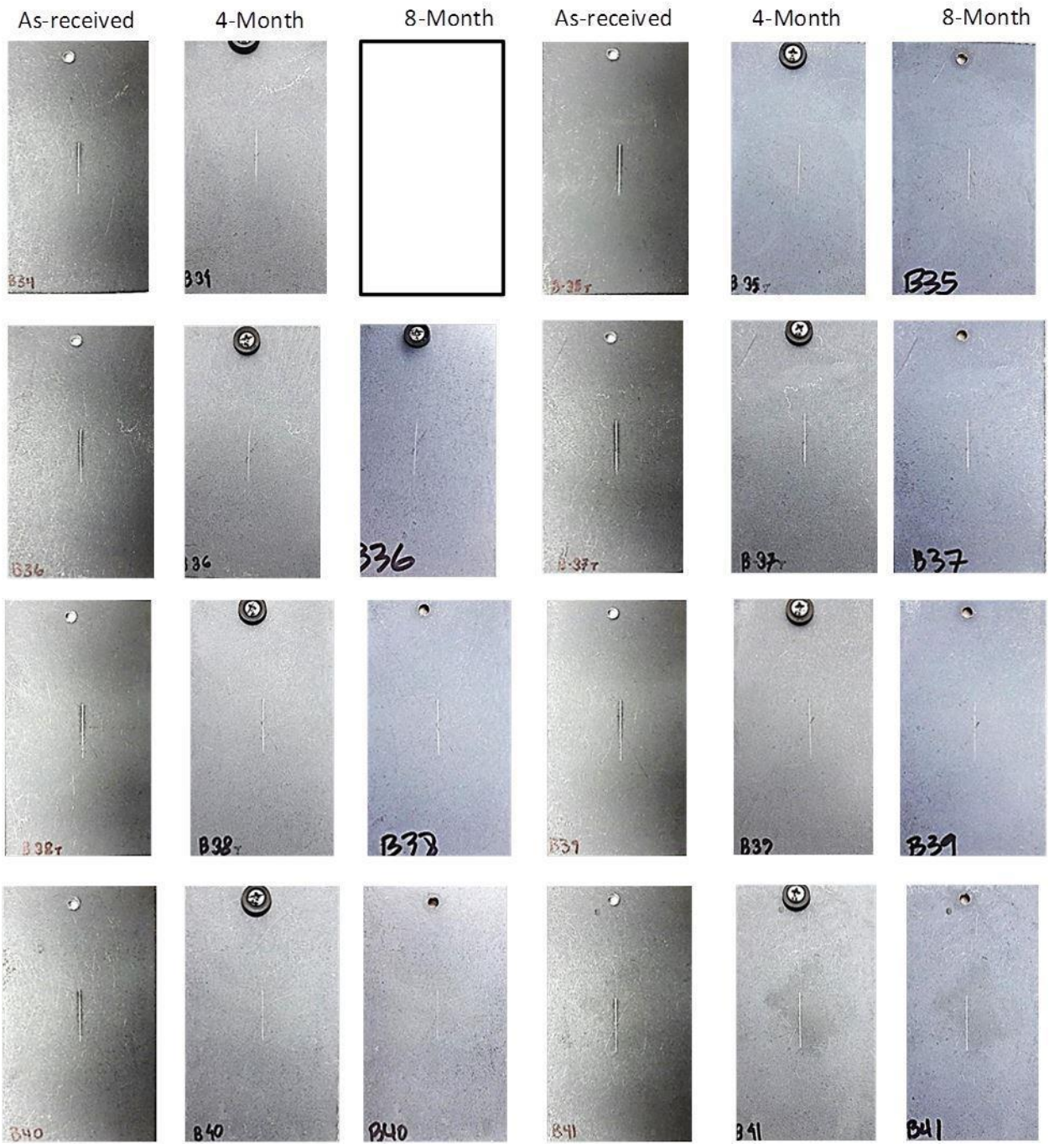


**Figure: B.14 TDG (Topcoat A+ B, Scribed) Samples Installed at Beach Test Site**

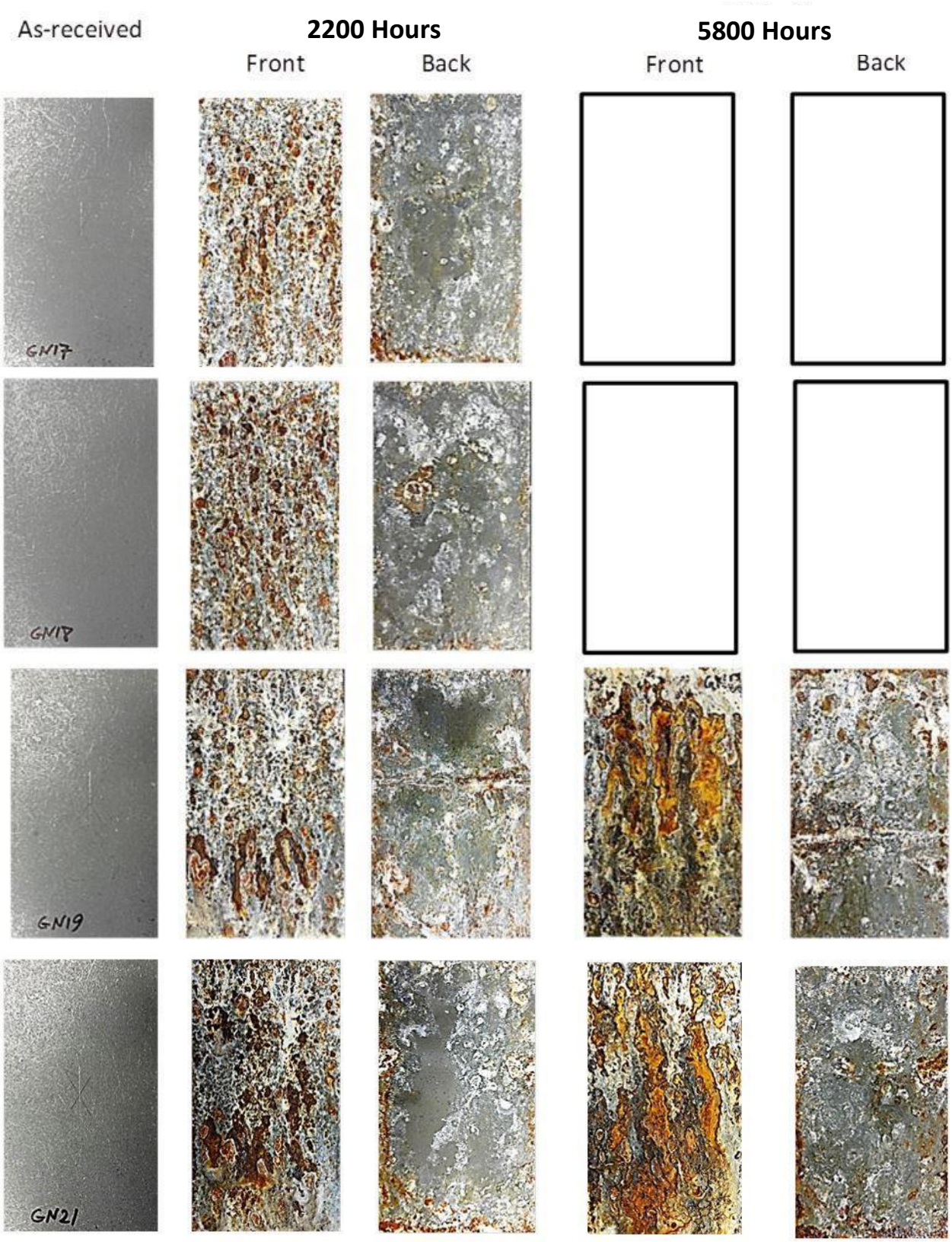


**Figure: B.15 Plain TDG (Scribed) Samples Installed in Salt-Fog Chamber (cont.)**

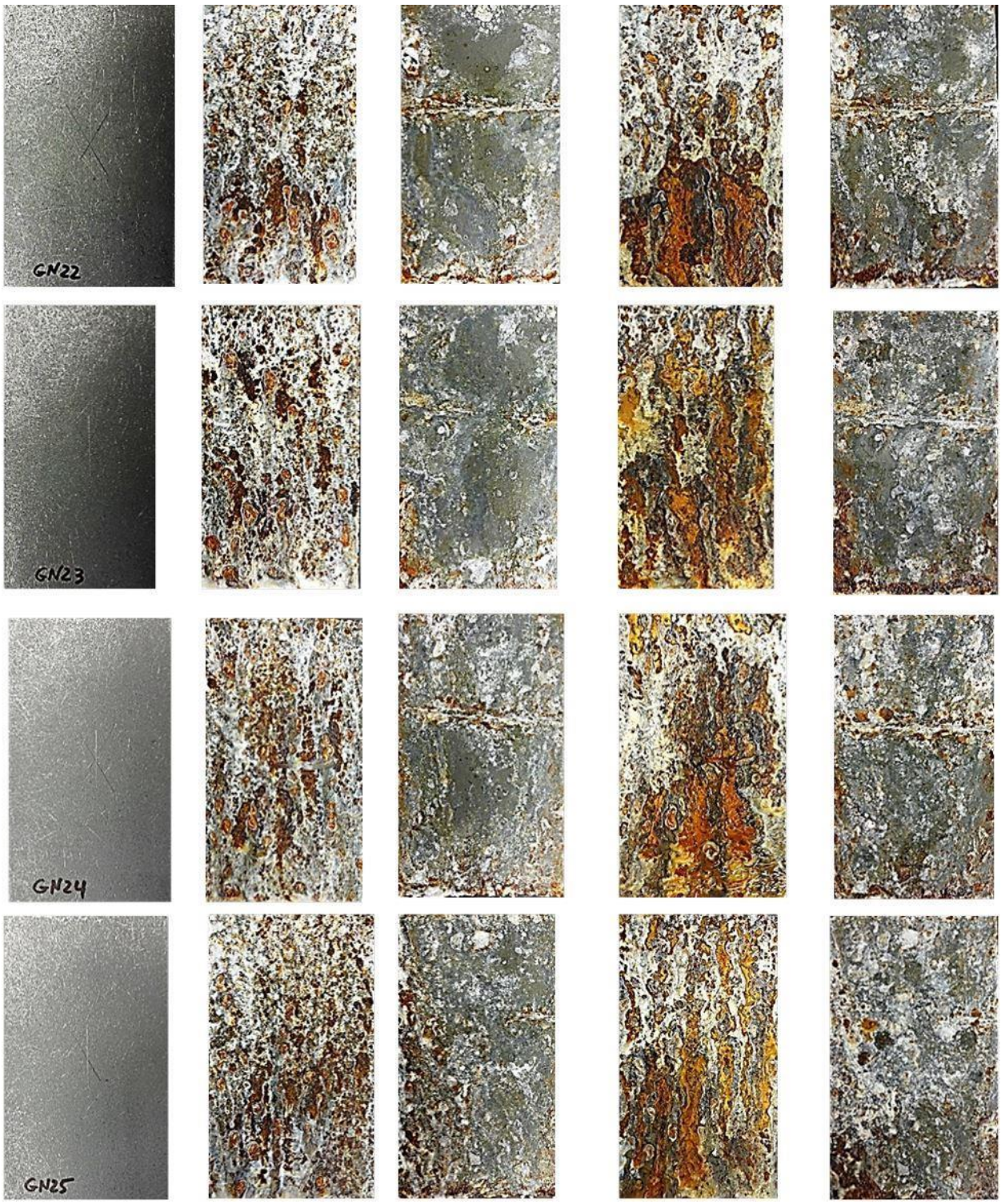


**Continuation of Figure: B.15 Plain TDG (Scribed) Samples Installed in Salt-Fog Chamber**

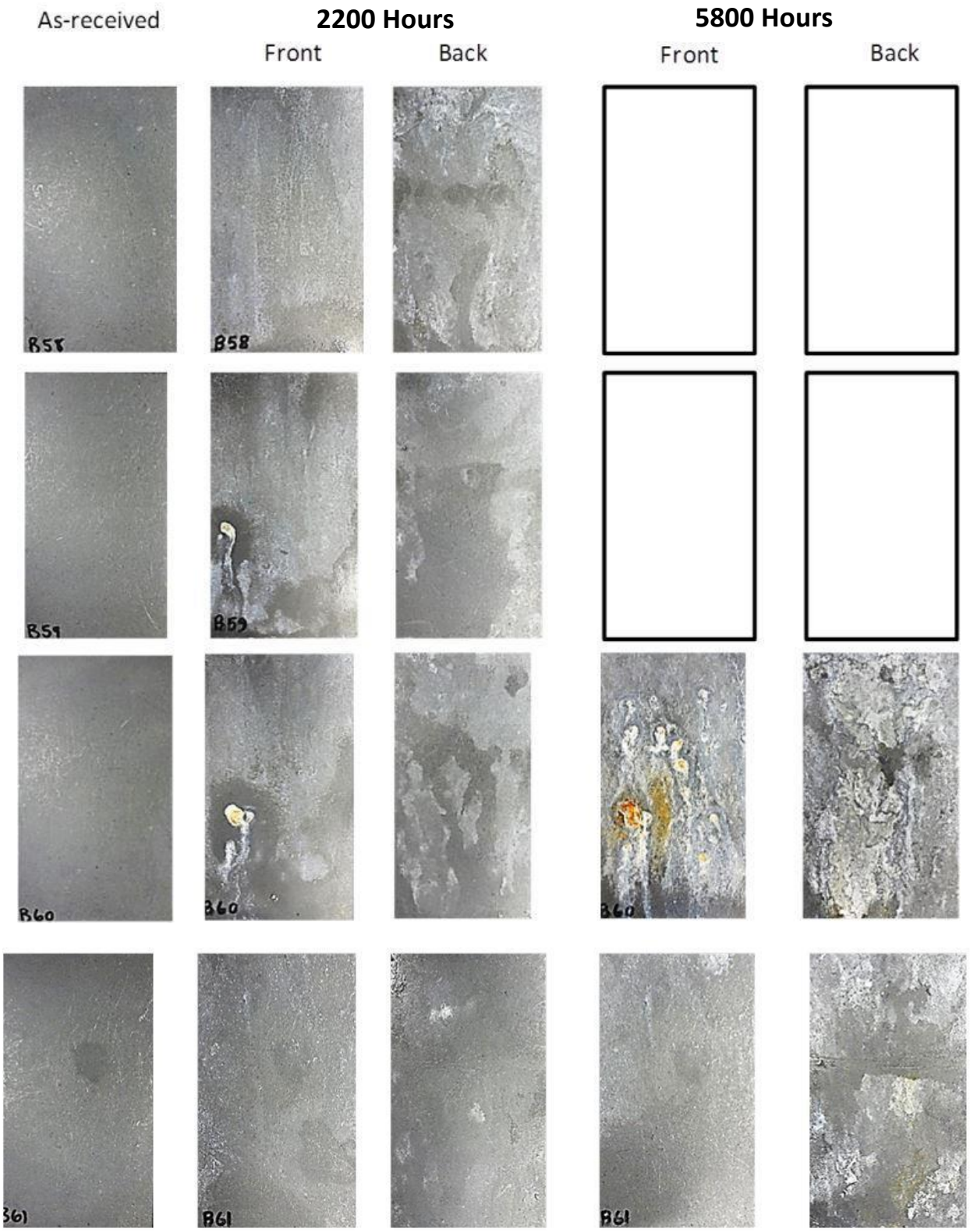


**Figure: B.16 TDG (Topcoat A+B, Non-scribed) Samples Installed in Salt-Fog Chamber (cont.)**

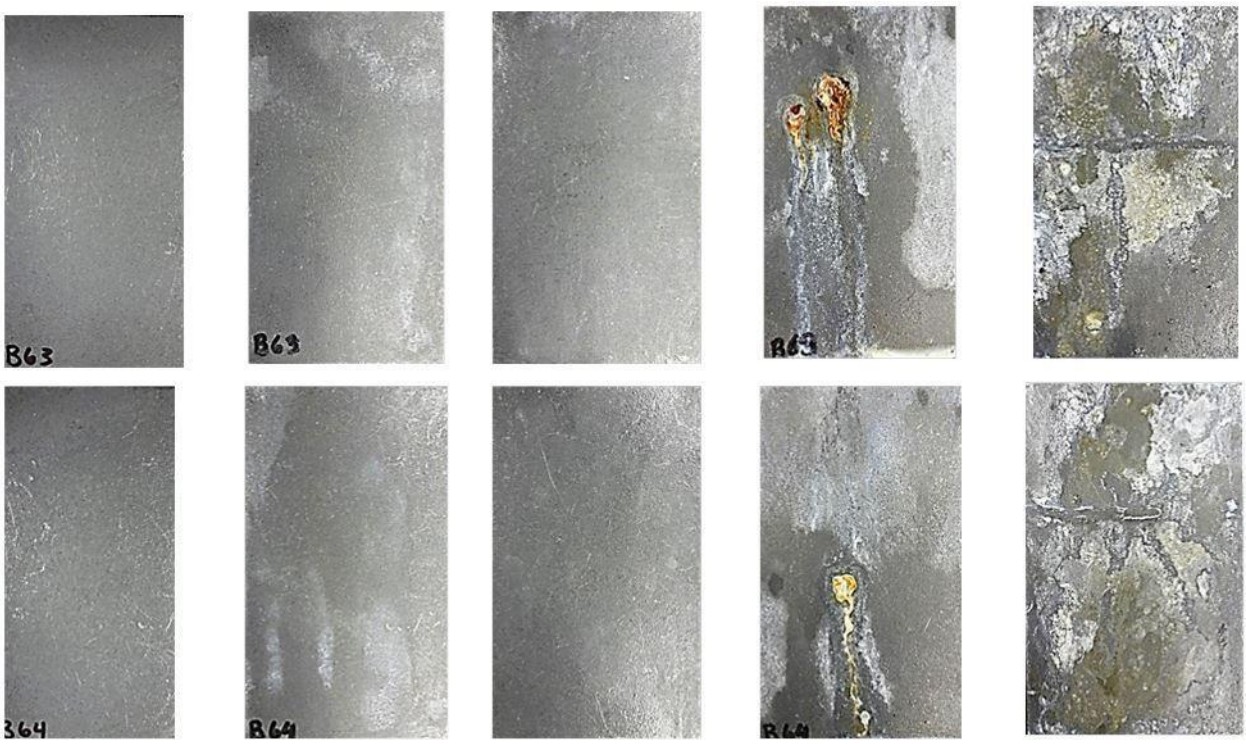


**Continuation of Figure: B.16 TDG (Topcoat A+B, Non-scribed) Samples Installed in Salt-Fog Chamber**

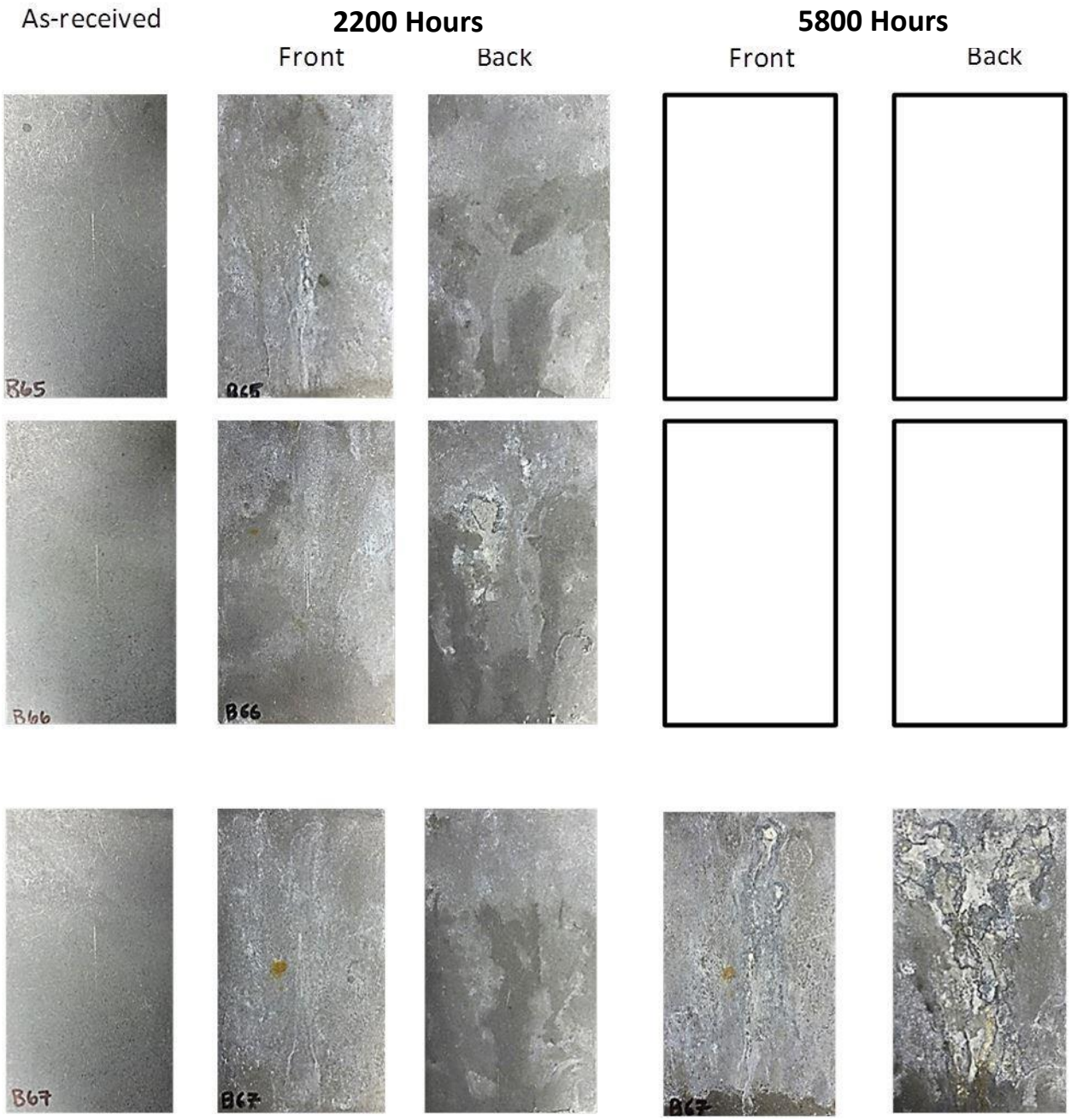


**Figure: B.17 TDG (Topcoat A+B, Scribed) Samples Installed in Salt-Fog Chamber (cont.)**

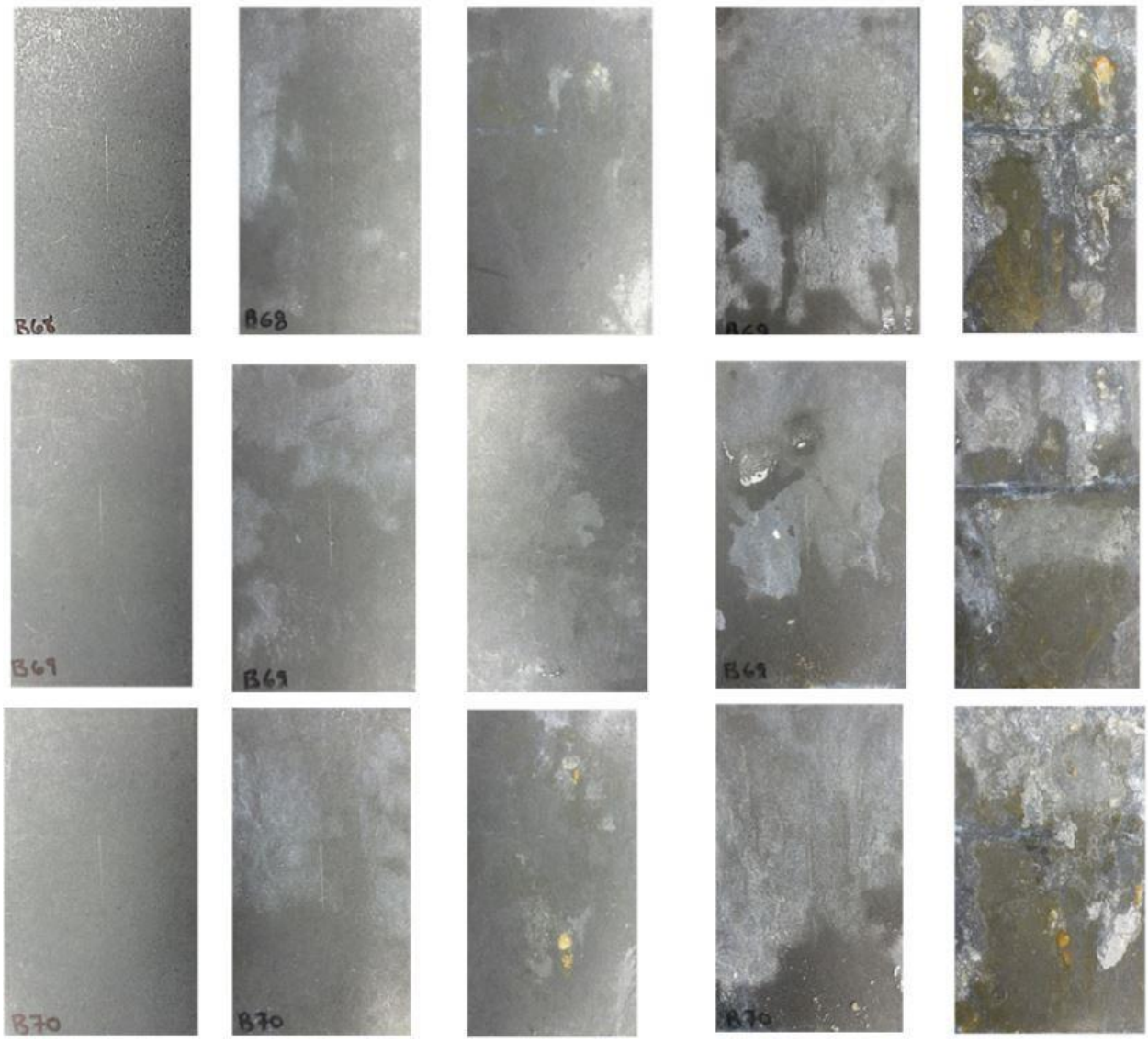


**Continuation of Figure: B.17 TDG (Topcoat A+B, Scribed) Samples Installed in Salt-Fog Chamber**

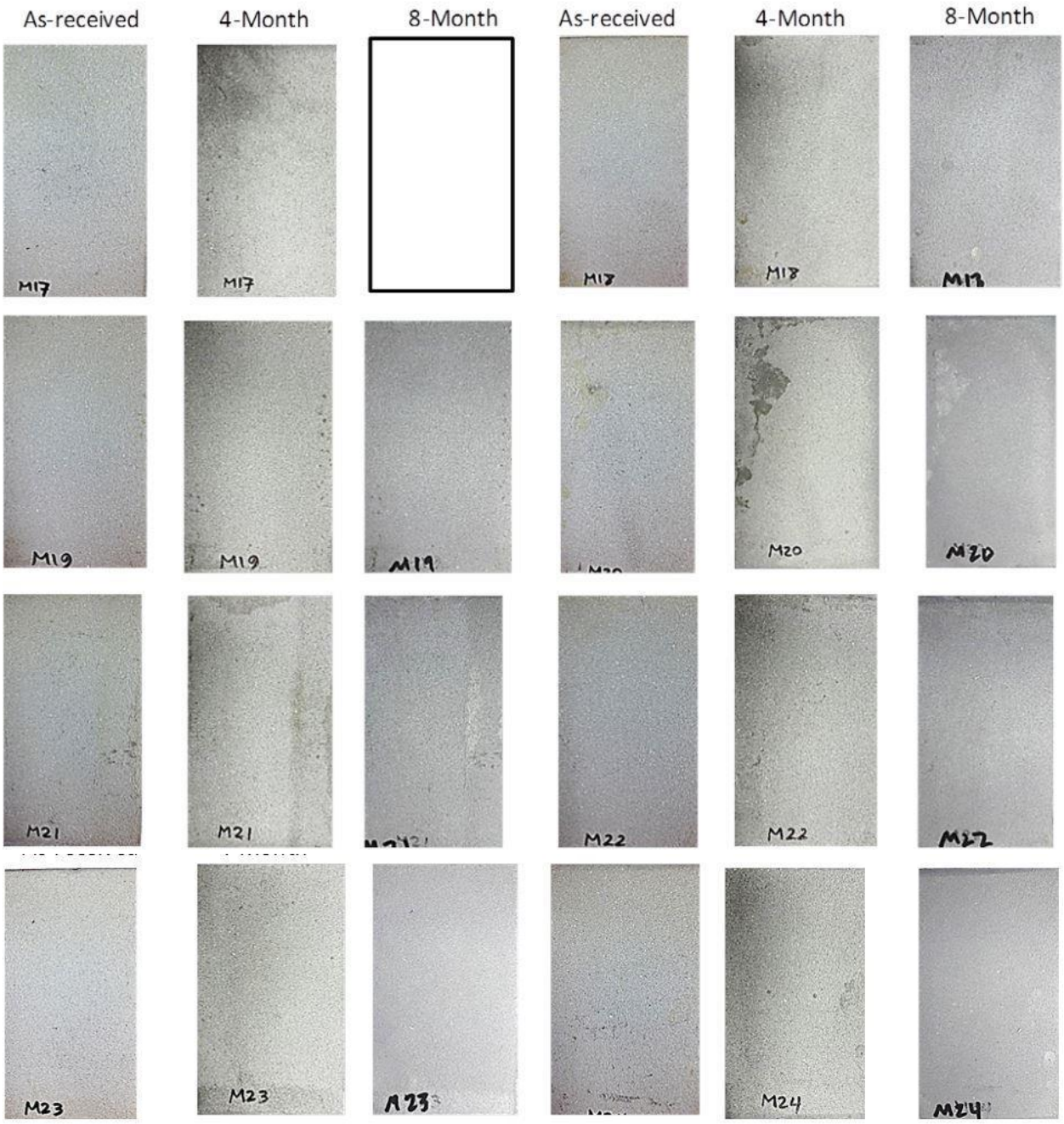


**Figure: B.18 Metalizing (Non-scribed) Samples Installed at Inland Test Site**

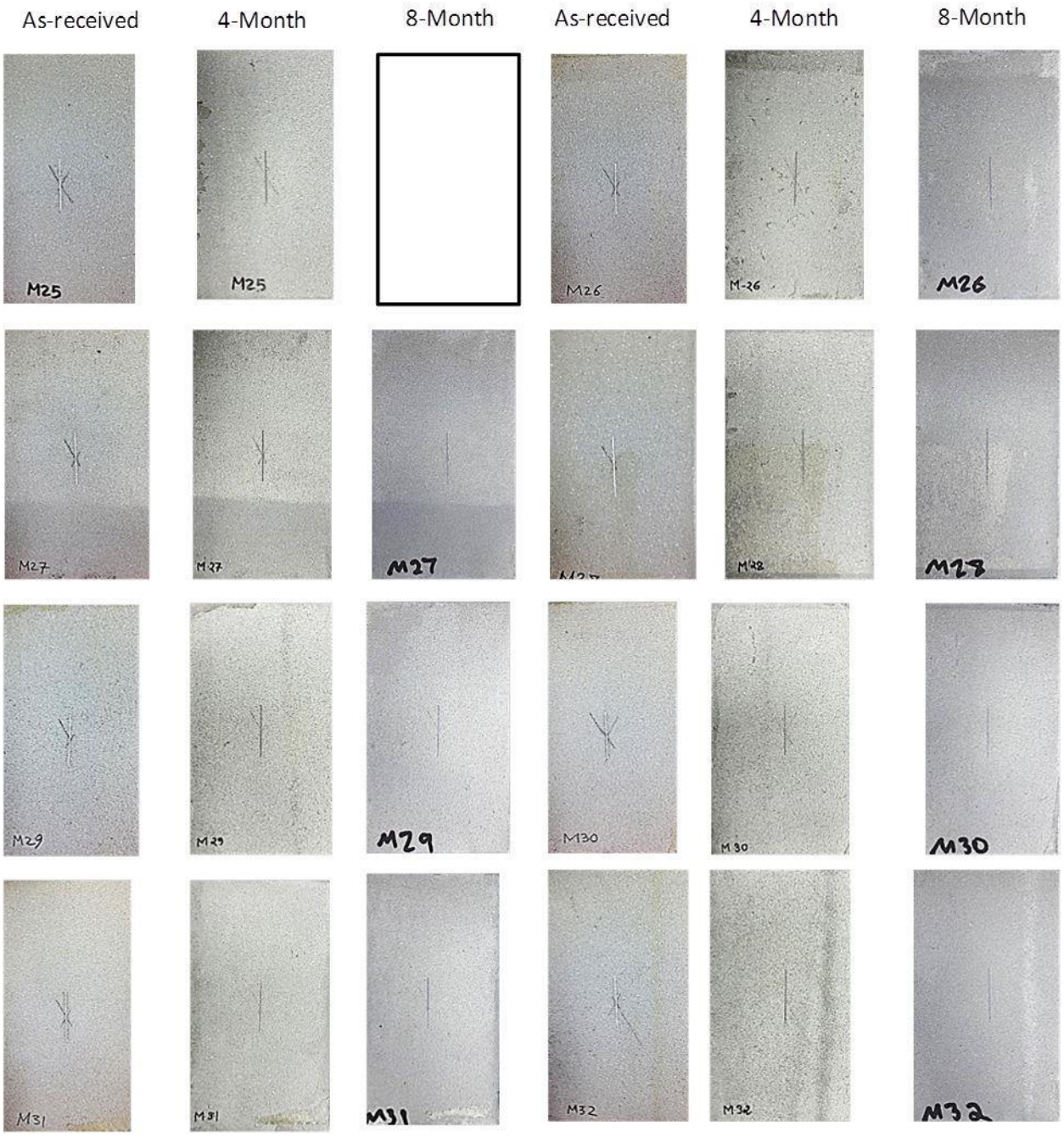


**Figure: B.19 Metalizing (Scribed) Samples Installed at Inland Test Site**


**Figure: B.20 Metalizing (Non-scribed) Samples Installed at Beach Test Site**


**Figure: B.21 Metalizing (Scribed) Samples Installed at Beach Test Site**

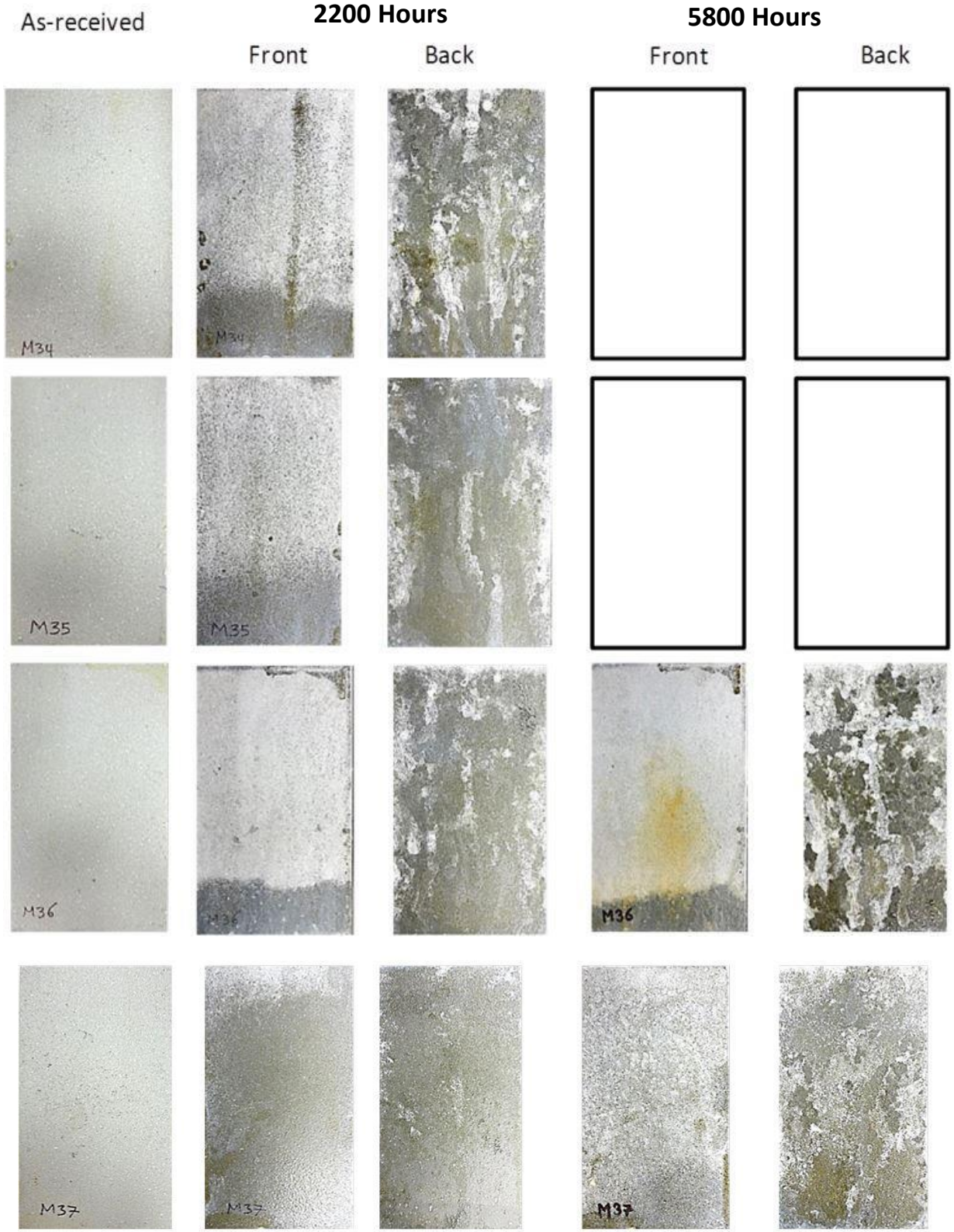


**Figure: B.22 Metalizing (Non-scribed) Samples Installed in Salt-Fog Chamber (cont.)**

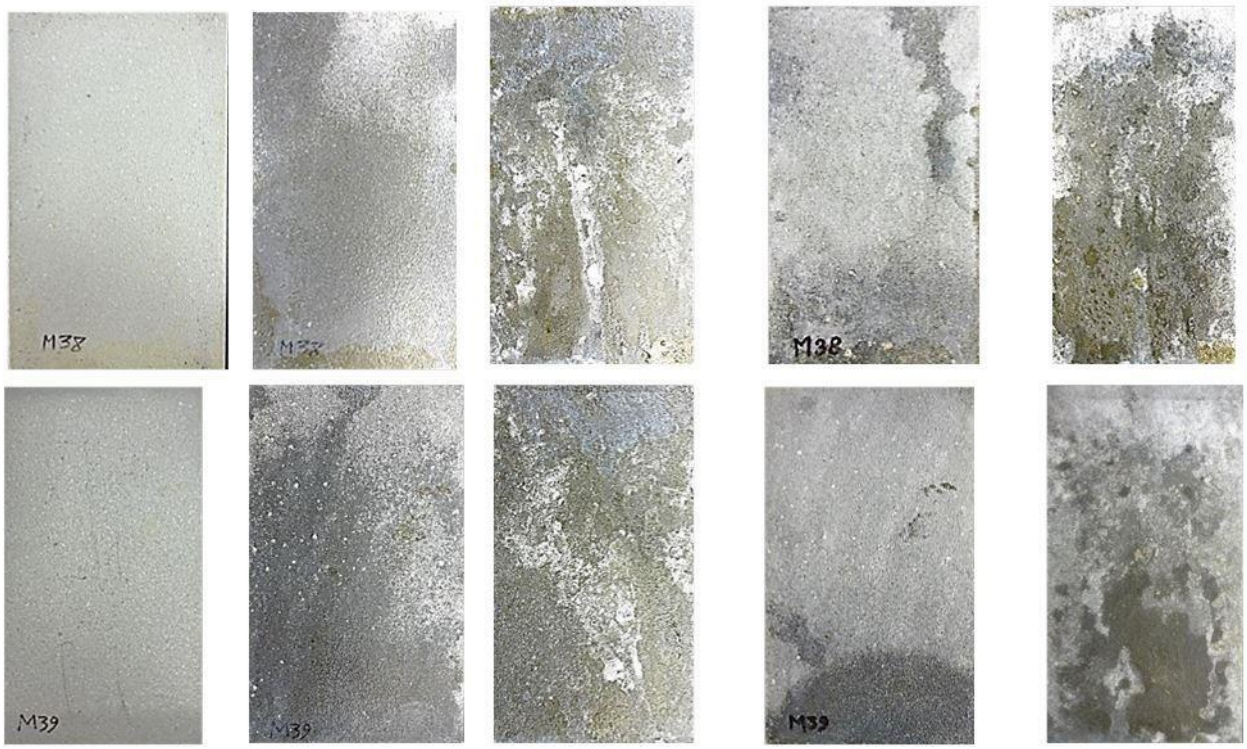


**Continuation of Figure: B.22 Metalizing (Non-scribed) Samples Installed in Salt-Fog Chamber**

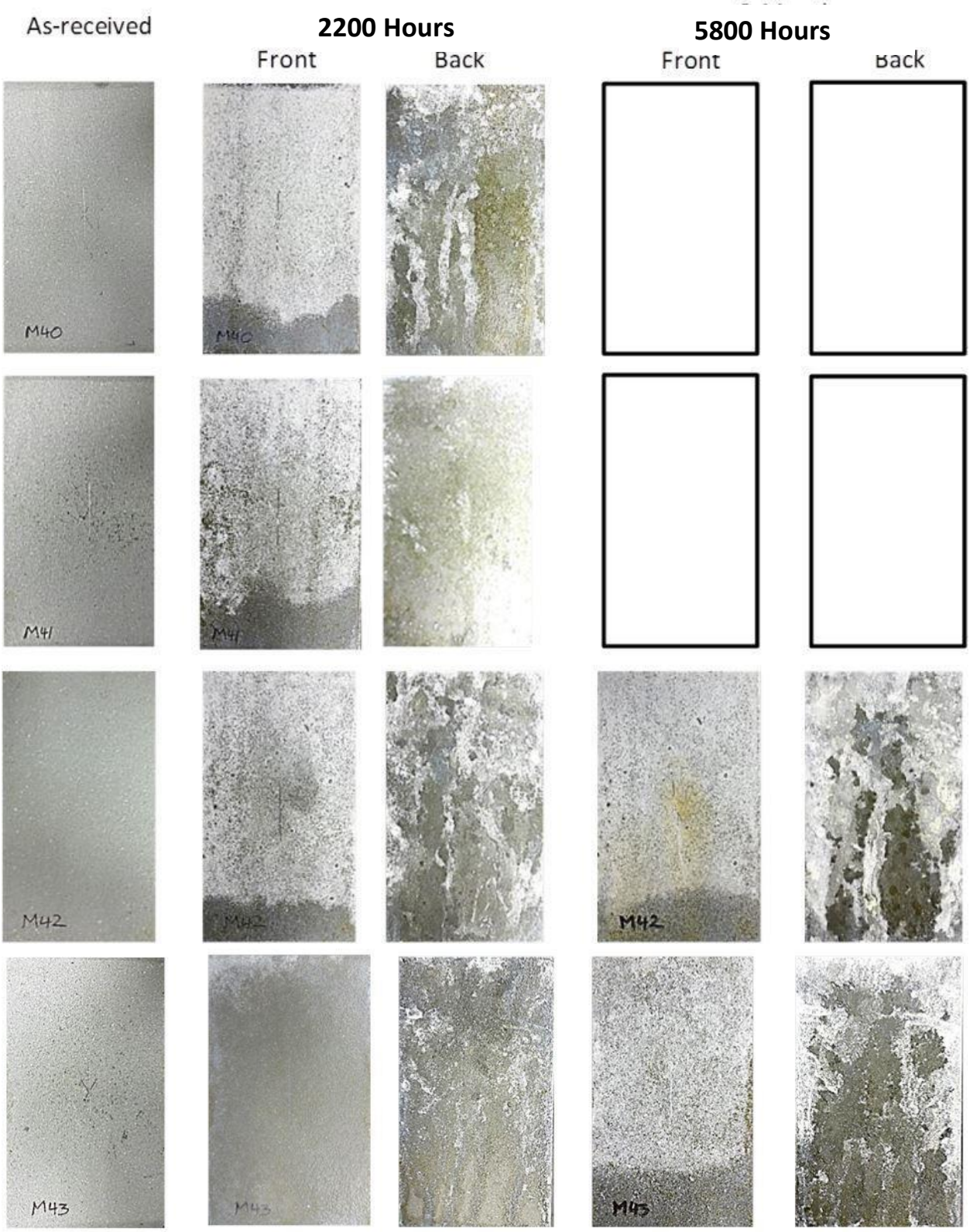


**Figure: B.23 Metalizing (Scribed) Samples Installed in Salt-Fog Chamber (cont.)**

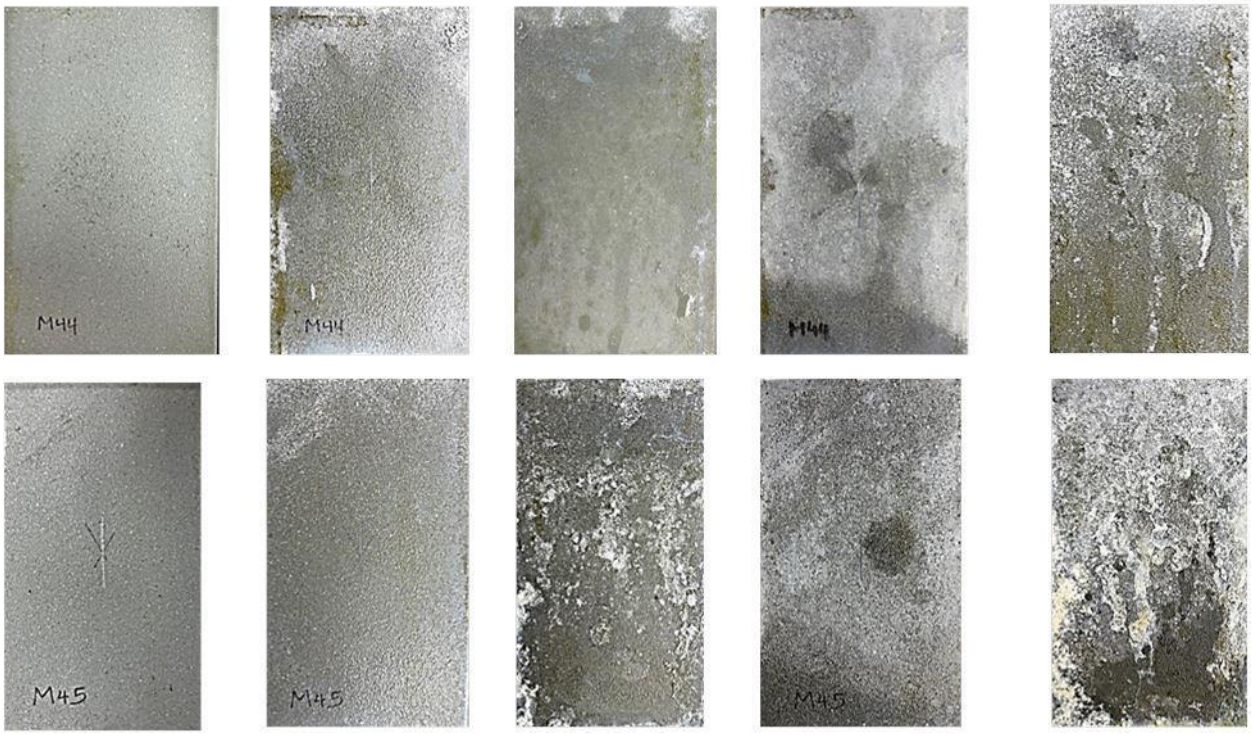


**Continuation of Figure: B.23 Metalizing (Scribed) Samples Installed in Salt-Fog Chamber**

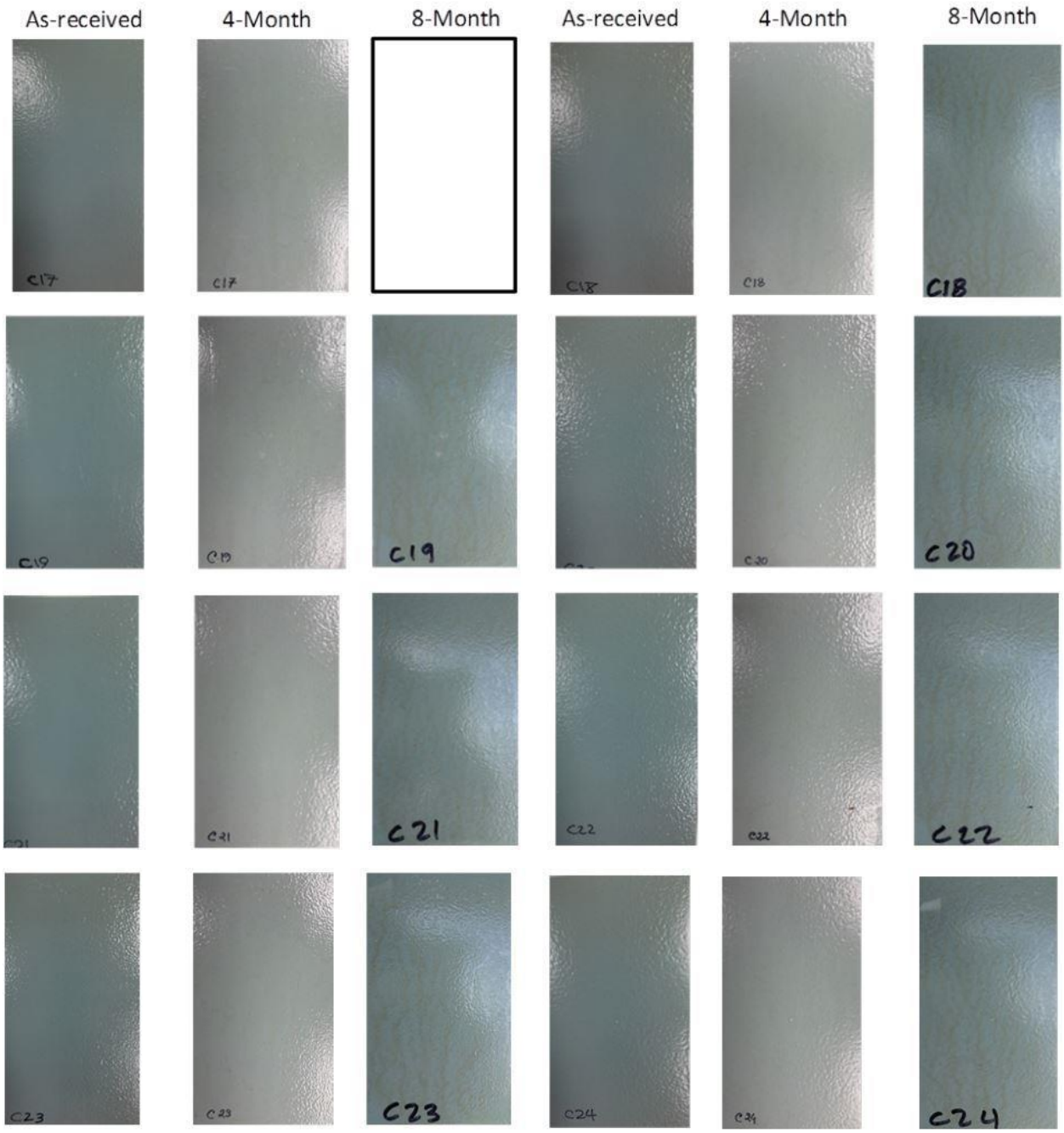


**Figure: B.24 Three-Coat (Non-scribed) Samples Installed at Inland Test Site**

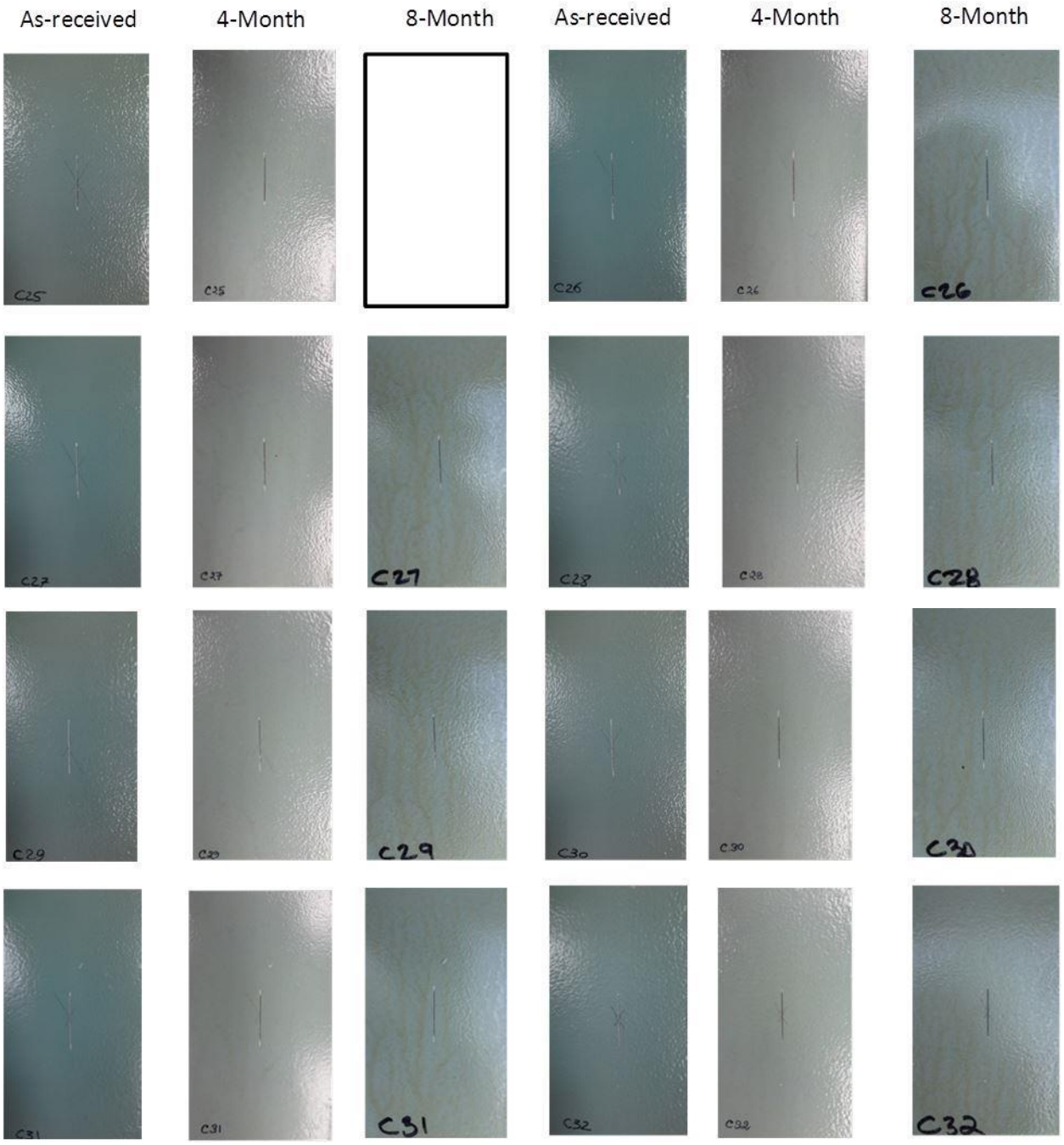


**Figure: B.25 Three-Coat (Scribed) Samples Installed at Inland Test Site**


**Figure: B.26 Three-Coat (Non-scribed) Samples Installed at Beach Test Site**


**Figure: B.27 Three-Coat (Scribed) Samples Installed at Beach Test Site**

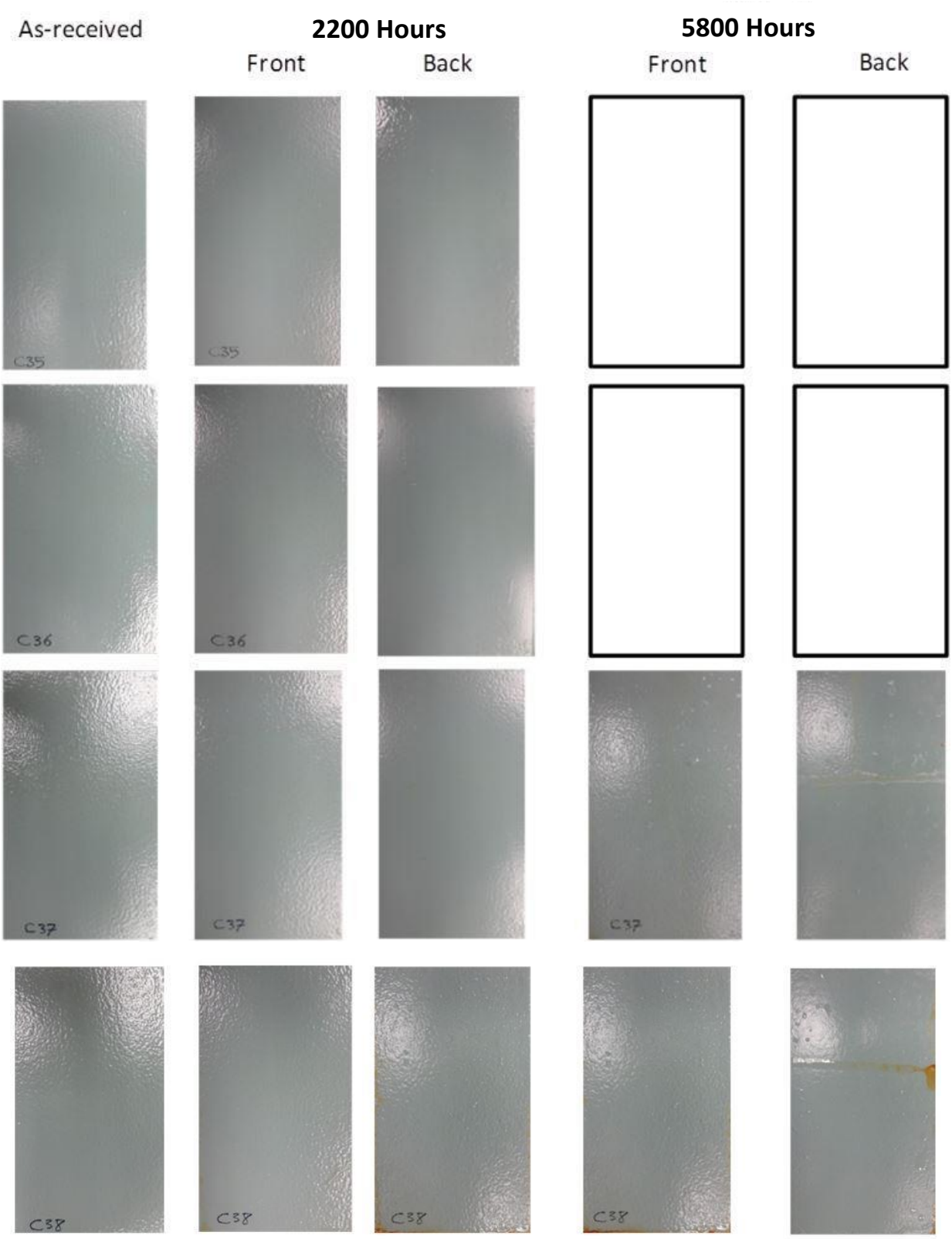


**Figure: B.28 Three-Coat (Non-scribed) Samples Installed in Salt-Fog Chamber (cont.)**

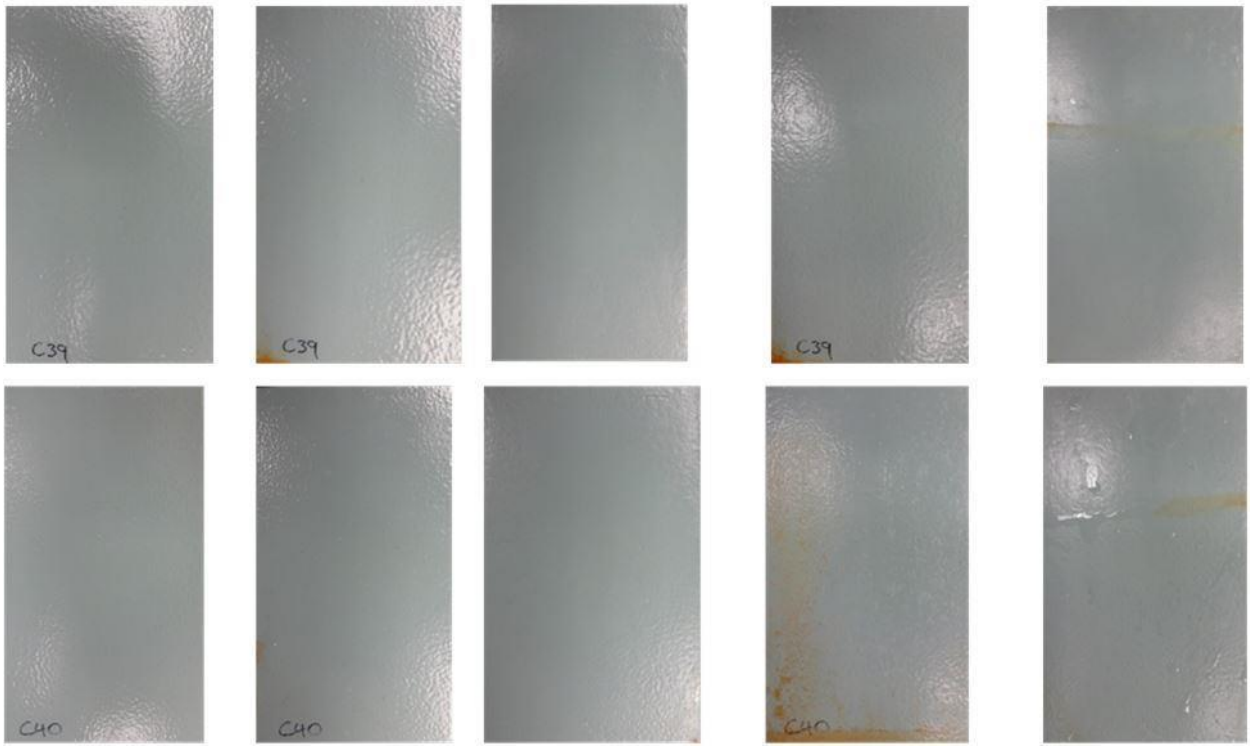


**Continuation of Figure: B.28 Three-Coat (Non-scribed) Samples Installed in Salt-Fog Chamber**

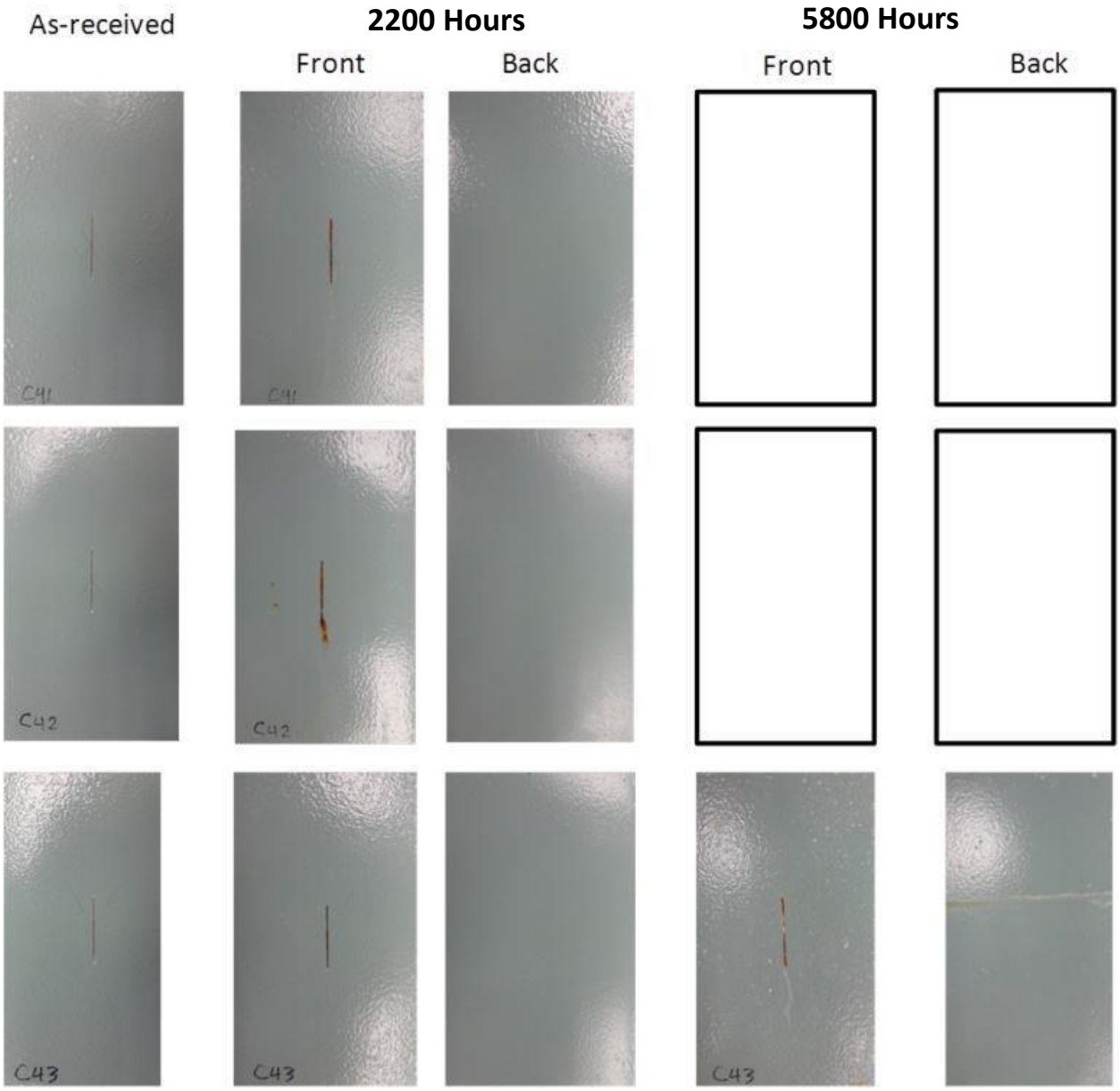


**Figure: B.29 Three-Coat (Scribed) Samples Installed in Salt-Fog Chamber (cont.)**

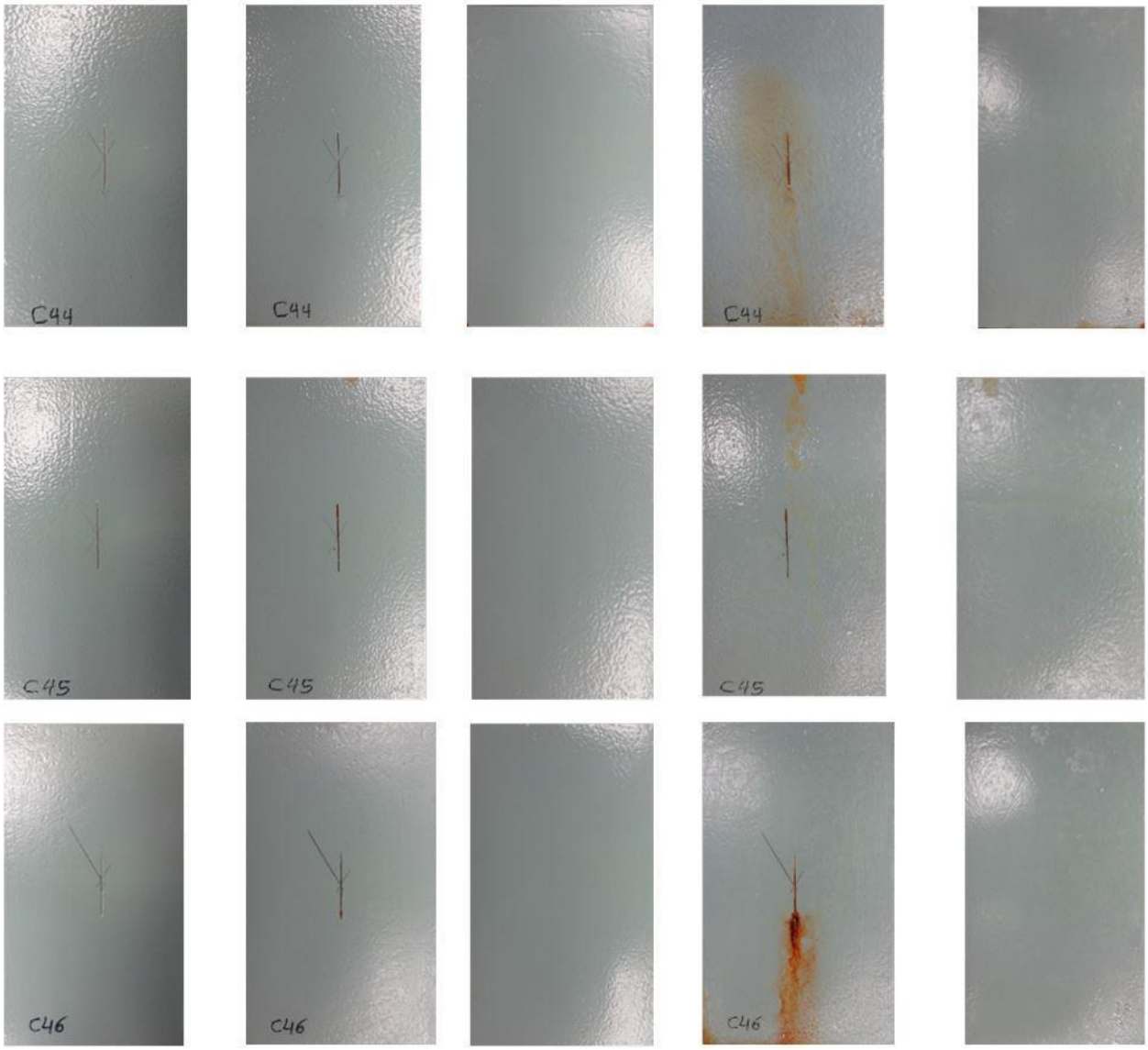


**Continuation of Figure: B.29 Three-Coat (Scribed) Samples Installed in Salt-Fog Chamber**